INSTITUT POLYTECHNIQUE DE PARIS

NNT : 2026IPPAX020

Thèse de doctorat

Geometry Driven Discretization of Differential Operators

Thèse de doctorat de l'Institut Polytechnique de Paris
préparée à Ecole Polytechnique

École doctorale n°636 École doctorale de l'Institut Polytechnique de Paris (EDIPP)
Spécialité de doctorat : Informatique

Thèse présentée et soutenue à Palaiseau, le 28 Avril 2026, par

THEO FRIEDRICH BRAUNE

Composition du Jury :

David Coeurjolly Directeur de Recherche, CNRS, LIRIS	Président
Anil Hirani Professor, University of Illinois at Urbana-Champaign	Rapporteur
Jacques-Olivier Lachaud Professor, Université de Savoie Mont Blanc	Rapporteur
Francesca Rapetti Professor, Université de Cote d'Azur	Examinateur
Jean-Marc Thiery Senior Research Scientist, Adobe Research	Examinateur
Mathieu Desbrun Directeur de Recherche, Inria	Directeur de thèse

Abstract

Discrete Exterior Calculus (DEC) has emerged as a key tool for the structure-preserving discretization of differential forms, proving vital in fields such as computational fluid dynamics, electromagnetism, and geometry processing. By maintaining the underlying geometric and topological properties of physical systems, DEC ensures numerical and physical fidelity. However, traditional DEC is restricted to scalar-valued forms. This limitation is significant, as many fundamental theories in physics and geometry, including general relativity, non-linear elasticity, and Yang-Mills gauge theories, are naturally formulated using bundle-valued differential forms and their associated covariant operators.

This thesis bridges that gap by extending the DEC framework to the bundle-valued setting. In the first part, we investigate the special case of connections on simplicial 2-manifolds, addressing the challenge of representing curvature and torsion consistently in a discrete environment. We introduce a modified discrete Levi-Civita connection and a corresponding discrete representation of the torsion 2-form, demonstrating their utility within a geometry processing pipeline.
In the second part, we develop a general framework for discrete bundle-valued exterior calculus. A central contribution is the formalization of integration for bundle-valued forms by leveraging the interplay between connections and retractions. This theoretical foundation enables a rigorous discretization scheme that induces discrete bundle-valued forms directly from their smooth counterparts. Building on this integration theory, we introduce a novel discrete exterior covariant derivative. We demonstrate that this operator converges to its continuous counterpart under mesh refinement, overcoming limitations in prior research. Furthermore, we show that the Bianchi identities are satisfied in an exact combinatorial sense and hold true in the limit. In addition, we establish that core properties of the continuous theory, such as naturality and Whitney interpolation, are preserved within our framework. Finally, we demonstrate that the presented constructions are not limited to simplicial complexes, but extend to a broader class of non-simplicial cells.

Resumé

Le calcul extérieur discret (DEC) s'est imposé au cours des deux dernières décennies comme un cadre fondamental pour la discrétisation structure-préservante des formes différentielles. En s'appuyant sur une correspondance précise entre les structures combinatoires et les structures différentielles, le DEC permet de préserver au niveau discret des identités topologiques essentielles – telles que l'identité $d^2 = 0$ et le théorème de Stokes –, garantissant ainsi la fidélité géométrique et physique. Ces propriétés structurelles en font un outil central dans des domaines tels que la méchanique des fluides numérique, l'électromagnétisme et la géométrie différentielle discrète. Cependant, le DEC traditionnel est limité aux formes à valeurs scalaires. Cette restriction constitue une limitation majeure, car de nombreuses théories fondamentales en physique et en géométrie — notamment la relativité générale, l'élasticité non linéaire et les théories de jauge de Yang-Mills — sont naturellement formulées à l'aide de formes différentielles à valeurs dans un fibré vectoriel, muni d'une connexion et d'une dérivée extérieure covariante. L'absence d'un cadre discret cohérent pour ces objets empêche une discrétisation géométriquement fidèle de ces théories.

Cette thèse comble cette lacune en étendant le DEC au cadre des fibrés vectoriels. Dans la première partie, nous étudions le cas particulier des connexions sur les variétés simpliciales de dimension deux, en abordant le défi que constitue la représentation cohérente de la courbure et de la torsion dans un cadre discret. Nous présentons une version discrète modifiée de la connexion de Levi-Civita sur des maillages, qui constitue une meilleure approximation de la connexion de Levi-Civita de la variété lisse sous raffinement du maillage. La torsion d'une connexion est une 2-forme à valeurs dans le fibré tangent. Pour traiter la torsion de manière discrète, nous exploitons le fait que, sur les variétés de dimension deux, il existe des isomorphismes explicites entre les 2-formes différentielles à valeurs dans le fibré tangent, les champs vectoriels et les 1-formes scalaires. Nous utilisons ensuite un calcul extérieur discret scalaire appliqué aux 1-formes pour analyser et contrôler la torsion et la courbure d'une connexion de manière systématique. Nous analysons le comportement numérique de ces constructions, qui sont intégrées dans un pipeline de traitement géométrique pour des applications telles que la conception de champs de directions, la génération de motifs à rayures ainsi que des méthodes telles que la méthode de la chaleur vectorielle.

Dans la deuxième partie de cette thèse, nous développons un cadre général pour le calcul extérieur discret à valeurs dans un fibré. Nous commençons par donner un aperçu de la théorie continue des formes différentielles à valeurs dans un fibré vectoriel. Nous présentons ensuite un schéma combinatoire pour les formes différentielles discrètes à valeurs dans un fibré vectoriel. Nous mettons ensuite cette description abstraite en relation avec les formes différentielles continues définies sur un fibré vectoriel. L'étape décisive consiste à formaliser une notion d'intégration adaptée aux formes à valeurs dans un fibré. Contrairement au cas scalaire, l'intégration de telles formes nécessite un mécanisme permettant de comparer différentes fibres. Nous montrons que cette comparaison peut

être effectuée de manière naturelle en utilisant l'interaction entre les connexions et les rétractions. Cette construction fournit un principe canonique qui permet de déduire des cochaînes discrètes directement à partir de formes différentielles lisses à valeurs dans un fibré vectoriel. Sur cette base, nous introduisons une nouvelle dérivée extérieure covariante discrète. Nous montrons que cet opérateur converge vers son homologue continu sous raffinement du maillage, résolvant ainsi les problèmes de cohérence observés dans les approches antérieures. Nous établissons également que la courbure discrète obtenue à partir de cette dérivée est compatible, au sens de la convergence, avec la courbure lisse associée à la connexion continue sous-jacente. Un résultat central de cette deuxième partie est la satisfaction exacte des identités de Bianchi au niveau combinatoire. Nous montrons que ces identités, formulées dans le cadre discret, sont vérifiées exactement. De plus, nous prouvons que l'identité algébrique de Bianchi reste valable à la limite lorsque l'on affine le maillage. Par ailleurs, nous démontrons que les propriétés structurelles fondamentales de la théorie continue – telles que la naturalité, la compatibilité avec les morphismes de fibrés et l'interpolation de Whitney – sont préservées dans notre cadre discret.

Enfin, nous démontrons que nos constructions ne se limitent pas aux complexes simpliciaux, mais s'étendent à une classe plus large de complexes cellulaires non simpliciaux, élargissant ainsi le champ d'application du cadre proposé.

Acknowledgements

A PhD takes a great deal of time and energy, but looking back, I see a journey I enjoyed so much. The road was not always easy, yet it was one along which I grew as a person and had a lot of fun. This deeply rewarding experience was made possible by a number of remarkable people. First and foremost, I want to thank my supervisor, Mathieu, for his guidance and support throughout these years. I enjoyed working with you enormously, and I am extremely grateful for everything you taught me in computer science, graphics, mathematics and beyond. It has been a privilege to learn from you, both as a scientist and as a person. I also want to thank Yiying for co-advising me. The countless times we were completely stuck and you saw, within minutes, a creative and elegant way out will never stop amazing me. A giant thank you goes to Mark as well. It was such a privilege and so much fun to work with you and to learn from you. Thank you for your kindness and your patience and for teaching me so many invaluable things: beautiful mathematics, how to write good C++, how to make beautiful illustrations and presentations, and so much more. I want to thank my jury members Anil Hirani, Jacques-Olivier Lachaud, David Coeurjolly, Francesca Rapetti, and Jean-Marc Thiery. I want to thank François for working out bundle-valued DEC with us. I want to thank Ulrich, Felix, and Oliver from TU Berlin for helping me build my foundations as an undergraduate and for getting me interested in (discrete) differential geometry in the first place. A great deal was also learned during an internship at Adobe. A big thanks to Jean-Marc for mentoring me and showing me a new angle on graphics and numerics and to Jérémie for teaching me to turn beautiful ideas into robust and efficient software. I want to thank Pooran for the many rounds of TDs in geometric modelling. Those sessions taught also me a great deal in many ways. Beyond that, thank you for your kindness and for believing in me. I want to thank the people from the Geomerix and Vista labs who accompanied me along this way and made it so enjoyable. Thank you Jiong, Nissim, Julie, Jingyi, Damien, Wei, Jiayi, Tara, Amandine, Rodrigo, Julia, Pierre, Lucas, Xavier, Vicky, Ramana, Weizhou and Aude. Thank you for your empathy and for the wonderful environment you created. Outside the plateau, I want to thank Kian, Soheil, Parimah, Fatemeh, Mariya, Marjan, Philipp, Julia, Cynthia, Sri, Juan, Thais, Sanu, Nasim, Felix, Valon and Ferdinand for all your support –whereever you are right now– and the good moments along the way. I want to thank my family Christine, Martin, and Sophie for always being there for me, believing in me, and supporting me throughout the PhD and in every other part of life. And I want to thank you, Fatemeh. Thank you for being so curious to explore so many new things with me. Thank you for all the incredible dishes you made for me along this path. Thank you for being there for me, and for your love and support.

List of Symbols

Smooth Manifolds

Symbol	Description
$\mathcal{M}$	A smooth manifold.
$\Omega^k(\mathcal{M})$	The space of smooth, scalar-valued differential k-forms on $\mathcal{M}$.
d	Exterior derivative for scalar-valued forms.
$\wedge$	Wedge product for scalar-valued forms.
σ^k	k-dimensional simplex.
s	A region in the smooth manifold M diffeomorphic to simplex σ.
ψ	Diffeomorphism mapping reference simplex into $\mathcal{M}$.
c_s, c_m	Center of mass of a simplex s or a face m.

Smooth Vector Bundles and Connections

Symbol	Description
$\pi : E \to \mathcal{M}$	Smooth vector bundle over $\mathcal{M}$.
E_p	Fiber at $p \in \mathcal{M}$.
$\Gamma(E)$	The space of smooth global sections of the bundle E.
$\Omega^k(\mathcal{M}, E)$	The space of vector bundle-valued k-forms (taking values in E).
$\Omega^k(\mathcal{M}, \mathrm{End}(E))$	The space of endomorphism-valued k-forms (taking values in $\mathrm{End}(E)$).
∇	Connection on the vector bundle E.
d^∇	Smooth exterior covariant derivative induced by ∇.
ω	Smooth connection 1-form, representing ∇ locally in a chosen frame.
Ω^∇	Smooth curvature 2-form.
P_γ	The continuous parallel transport operator along a curve γ.

List of Symbols

Discrete Bundle-Valued Calculus

Symbol	Description
$\mathcal{R}_{ij}$	Discrete parallel transport mapping $E_{v_j} \to E_{v_i}$.
R_{ij}	Matrix representation of $\mathbb{R}_{ij}$.
ω_{ij}	Discrete connection 1-form ($R_{ij} - \mathrm{Id}$).
$\boldsymbol{\Omega}^{\nabla}$	Discrete curvature 2-form on σ at v_0.
σ, v_0	Reference simplex and its specified base vertex.
f^{∇, v_0}	Parallel-Propagated Frame (PPF) at v_0.
R^{∇, v_0}	Gauge transformation into the PPF at v_0.
α^{∇, v_0}	Coordinate representation of α in the PPF at v_0.
${}^{\nabla}_{\varphi_v}\!\!\int$	Connection-dependent integral with a retraction onto v.
$\mathfrak{d}^{\nabla}$	Sided discrete exterior covariant derivative.
Alt^{∇}	Alternation operator for combinatorial averaging.
d^{∇}	Alternated discrete exterior covariant derivative ($\mathrm{Alt}^{\nabla}\mathfrak{d}^{\nabla}$).

Table of Contents

1 | Introduction

Many problems in geometry processing, computational physics, and applied geometry require the discretization of differential operators on curved domains. Typical examples include the computation of fluxes, circulations, and conservation laws on surfaces or volumetric meshes. In the smooth setting, such quantities are naturally expressed in a coordinate-free way using differential forms and their exterior derivative. Preserving their structure in a discretization is essential for numerical robustness, stability, and physical fidelity [MR02].

Discrete exterior calculus (DEC) [Hir03, DKT08] has emerged as a principled framework for achieving this goal. By representing differential forms through integrals over mesh elements and defining discrete differentiation via incidence relations, DEC reproduces Stokes' theorem and the algebraic structure of the de Rham complex exactly at the discrete level [Bos98] This structure-preserving property has led to a wide range of successful applications in geometry processing [?] and computational physics, where discrete operators inherit conservation laws and topological invariants from their smooth counterparts.

However, to date, far less attention has been dedicated to the discretization of *differential forms with values in a vector bundle* — even if Cartan's original work [Car23] made extensive use of such bundle-valued forms. One obvious difficulty is that bundle-valued forms do not seamlessly admit a simple discretization: indeed, the mere pointwise expression of a bundle-valued form requires a pointwise fiber, making it difficult to properly define a discrete counterpart to the exterior covariant derivative where the integration over a domain can only be achieved in a common fiber. An exception is the case of discrete connections on two-dimensional surfaces, which has garnered significant interest in vector field processing [CDS10, DGBD20] to define parallel transport and connection curvature for instance; but this 2D case can be handled with connections that are seen as angle-valued forms (since 2D rotations are commutative) once a section of the frame bundle has been chosen, while the general case requires the use of discrete forms with values in the group of rotation matrices, bringing significant difficulties due in part to their non-commutativity.

Yet, the use of connection curvature is key in fields such as Yang-Mills theory and relativity [Ein16] in computational physics, since it provides an invariant, frame-independent measure. It is therefore natural to hope that the development of structure-preserving discretizations of the exterior calculus of bundle-valued forms can be beneficial for a wide range of numerical endeavors. At present, there is no general formal, readily-computable, discrete analogue of this construction that both preserves the underlying geometric structure and converges under mesh refinement.

The aim of this thesis is to address this gap. We develop a discrete exterior calculus for bundle-valued differential forms that extends the structure-preserving philosophy of DEC beyond the scalar valued setting. Our focus lies on simplicial meshes and operators that admit a clear geometric interpretation, integrate naturally into geometry processing pipelines, and provably converge to their smooth counterparts.

In the first part of this thesis, we review the mathematical foundations of vector bundles, smooth exterior calculus, and discrete exterior calculus. Building on this background, we then investigate torsion and curvature for discrete connections on surfaces. This work was carried out in collaboration with Mark Gillespie, Yiying Tong, and Mathieu Desbrun, and was published in ACM Transactions on Graphics [BGTD25]. In the second part, we introduce a general framework for discrete bundle-valued exterior calculus. This framework was developed in collaboration with François Gay-Balmaz, Yiying Tong, and Mathieu Desbrun, and is publicly available on arXiv [BTGBD25].

1.1 Differential Forms as Measurements

We begin by recalling the interpretation of differential forms as measurements on oriented geometric objects, emphasizing the perspective that underlies discrete exterior calculus. We refer to [AMR88] as a reference for the following review of exterior calculus.

Work in a Force Field along a Path

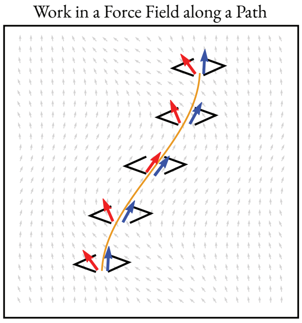

Covector Field / Differential 1-Form

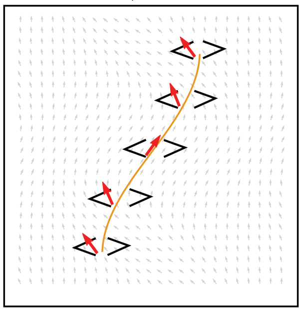

Let us consider a classical problem from mechanics. Suppose that $\mathcal{M}$ is a smooth manifold and that we are given a vector field V on $\mathcal{M}$. Formally a vector field is a smooth section of the *tangent bundle* $T\mathcal{M} = \bigsqcup_{p\in\mathcal{M}} T_p\mathcal{M}$, the disjoint union of all tangent planes at points in $p \in \mathcal{M}$, that is, an assignment $p \mapsto V_p \in T_p\mathcal{M}$ varying smoothly with p. We write $V \in \Gamma T\mathcal{M}$.

What is the work performed by V when moving an object along a smooth curve $\gamma\colon [0,1] \to \mathcal{M}$? Assuming we are given a metric $\langle\cdot,\cdot\rangle$ on $T\mathcal{M}$, the work can be expressed as

$$W(\gamma) = \int_\gamma \langle V(\gamma), \dot{\gamma}\rangle.$$

A closer inspection reveals that, at each point $\gamma(t)$, the primary object of interest is not $V(\gamma(t))$, but rather the action that this vector has on the current tangent direction, i.e $\langle V(\gamma(t)), \cdot\rangle$. Mathematically, the (linear) action of a vector on another vector is given by an element in the dual space.

Mathematically, the linear action of a vector on another vector is given by an element in the dual space — for each point $p \in \mathcal{M}$, the cotangent space $T_p^*\mathcal{M}$ is defined as the dual of the tangent space $T_p\mathcal{M}$, that is, the space of linear maps $T_p\mathcal{M} \to \mathbb{R}$. Collecting these spaces across $\mathcal{M}$ yields the *cotangent bundle* $T^*\mathcal{M} = \bigsqcup_{p\in\mathcal{M}}$.

This observation reflects a general principle in physics: for vector fields such as velocity fields, force fields, or electric fields, what matters is how the field acts on an object moving through the space (or more generally spacetime), rather than the vector alone.

This perspective suggests a reformulation: Instead of assigning to each point $p \in \mathcal{M}$ a vector $V_p \in T_p\mathcal{M}$, we may equivalently consider the associated *covector*, this is what we refer to as a *differential 1-form*.

Definition 1.1 (Differential 1-form and Musical Isomorphism)**.** *Let $\mathcal{M}$ be a smooth manifold. We call a section $\alpha \in \Gamma T^*\mathcal{M}$ through the cotangent bundle a* differential 1-form*. We denote the space of differential 1-forms on $\mathcal{M}$ with $\Omega^1(\mathcal{M})$. In addition, if we are given a metric g, it induces the canonical isomorphisms*

$$^\flat\colon T\mathcal{M} \to \Omega^1(\mathcal{M})\colon v \mapsto g(v,\cdot), \text{ and } ^\sharp\colon \Omega^1(\mathcal{M}) \to T\mathcal{M}\colon \alpha = v^\flat \mapsto v,$$

which we refer to as the musical isomorphisms.

Any differential 1-form $\alpha \in \Omega^1(\mathcal{M})$ introduces a measurement on curves. Given any (piecewise) smooth curve $\gamma \in \mathcal{C}^1(\mathcal{M})$, we can define the action of the differential form on γ via

$$\alpha\colon \mathcal{C}^1(\mathcal{M}) \to \mathbb{R}\colon \gamma \to \int_\gamma \alpha = \int_{[0,1]} \alpha_{\gamma(t)}[\dot\gamma(t)]\mathrm{d}t.$$

We note that when we concatenate two curves, the action on the two curves is summed. Similarly, when reversing the orientation of a curve, we simply flip the sign of the induced action.

Formally a differential form of degree k is defined as follows:

Definition 1.2 (Differential k-forms)**.** *Let $k \geq 0$. The k*-th exterior power *$\Lambda^k V^*$ of a vector space V is the space of alternating k-linear maps*

$$\omega\colon \underbrace{V \times \cdots \times V}_{k \text{ times}} \to \mathbb{R}.$$

A differential k-form *on a smooth manifold $\mathcal{M}$ is a smooth section of the bundle $\Lambda^k T^*\mathcal{M}$. We denote the space of differential k-forms by $\Omega^k(M)$. Given an evaluation point $p \in \mathcal{M}$ and an ordered set of tangent vectors fields $s = [v_0, \dots, v_k \in T_pM]$, we denote by $\omega_p[s] = \omega_p[v_0, \dots, v_k]$ the evaluation of ω on the stencil $s = [v_0, \dots, v_k]$.*

The wedge product. The wedge product is a bilinear operation that combines differential forms while enforcing antisymmetry. For 1-forms $\alpha, \beta \in \Omega^1(M)$, the wedge product $\alpha \wedge \beta \in \Omega^2(M)$ is defined pointwise by

$$(\alpha \wedge \beta)(v_1, v_2) = \alpha(v_1)\beta(v_2) - \alpha(v_2)\beta(v_1),$$

for all tangent vectors v_1, v_2.

More generally, the wedge product of a k-form and an ℓ-form yields a $(k+\ell)$-form that is multilinear and alternating: given $\alpha \in \Omega^k(M)$ and $\beta \in \Omega^\ell(M)$, the $(k+\ell)$-form $\alpha \wedge \beta \in \Omega^{k+\ell}(M)$ is the antisymmetrization of the tensor product of the two forms, i.e., for all $X_1,\dots,X_{k+\ell} \in \Gamma(TM)$,

$$\begin{aligned}\alpha \wedge \beta(X_1,\dots,X_{k+\ell}) &= \frac{1}{(k+\ell)!}\mathrm{Alt}(\alpha\otimes\beta)(X_1,\dots,X_{k+\ell}) \\ &= \frac{1}{(k+\ell)!}\sum_{\sigma\in S_{k+\ell}} \mathrm{sgn}(\sigma)\alpha(X_{\sigma(1)},\dots,X_{\sigma(k)})\beta(X_{\sigma(k+1)},\dots,X_{\sigma(k+\ell+1)}),\end{aligned} \tag{1.1.1}$$

where $S_{k+\ell}$ denotes the permutation of $(k+\ell)$ indices.

Local representation. If $\phi = (x_1,\dots,x_n)$ is a local coordinate chart on $\mathcal{M}$, then the differentials $(dx_1,\dots,dx_n)$ form a basis of the cotangent space T_p^*M at each point $p \in \mathcal{M}$. Any differential k-form $\alpha \in \Omega^k(\mathcal{M})$ can therefore be written locally as

$$\omega = \sum_{1\le i_1<\cdots<i_k\le n} \omega_{i_1\cdots i_k}\, dx^{i_1}\wedge\cdots\wedge dx^{i_k}.$$

Integration of differential k-forms We briefly recall the classical construction of integration for scalar-valued differential forms on smooth manifolds, in order to fix notation and provide a reference point for the bundle-valued generalization discussed later.

Definition 1.3. *Let $\mathcal{M}$ be a smooth n-dimensional manifold and let $\alpha \in \Omega^k(\mathcal{M})$. The* support *of α is defined as*

$$\mathrm{supp}(\alpha) = \{p \in \mathcal{M} \mid \alpha_p \neq 0\}.$$

Throughout this section, we restrict attention to compactly-supported differential forms. This is a mild assumption for our purposes, since most applications considered in this thesis involve differential forms defined on compact manifolds.

Given a compactly-supported differential form and a local coordinate chart, we may define the integral of the form locally as follows.

Definition and Theorem 1.4. *Let $\mathcal{M}$ be an n-dimensional manifold and let $\alpha \in \Omega^n(\mathcal{M})$ be a compactly supported differential form. Let $U \subset \mathbb{R}^n$ and $V \subset \mathcal{M}$ be open sets such that there exists a coordinate chart $\phi = (x_1,\dots,x_n)\colon U \to V$. Denote by $(\partial x_1,\dots,\partial x_n)$ the induced local frame of the tangent bundle.*

The integral of α over V is defined by

$$\int_V \alpha = \int_U \alpha_{\phi(p)}\Big[\partial x_1(p),\dots,\partial x_n(p)\Big]\, d\mu_{\mathbb{R}^n}(p).$$

This definition is independent of the chosen coordinate chart: if $\psi = (y_1,\dots,y_n)\colon U \to V$ is another coordinate chart, then

$$\int_U \alpha_{\phi(p)}\Big[\partial x_1(p),\dots,\partial x_n(p)\Big]\, d\mu_{\mathbb{R}^n}(p) = \int_U \alpha_{\psi(p)}\Big[\partial y_1(p),\dots,\partial y_n(p)\Big]\, d\mu_{\mathbb{R}^n}(p). \tag{1.1.2}$$

Proof. See [AMR88, Proposition 7.5]. □

The above construction defines integration locally in a single chart. To extend this definition to the entire manifold, we employ partitions of unity.

Definition 1.5. *Let $\mathcal{M}$ be a smooth n-dimensional manifold. An* atlas *of $\mathcal{M}$ is a collection of charts $\mathcal{A} = \{\phi_i : U_i \to V_i\}$ such that*

$$\mathcal{M} = \bigcup_i V_i.$$

Definition 1.6. *A* partition of unity *on a smooth manifold $\mathcal{M}$ consists of a family $\{(V_i, g_i)\}$ such that:*

1. *$\{V_i\}$ is a locally finite open covering of $\mathcal{M}$,*
2. *$g_i \in \mathcal{C}^\infty(\mathcal{M})$, with $g_i \geq 0$ and $\operatorname{supp}(g_i) \subset V_i$,*
3. *for all $p \in \mathcal{M}$, it holds that $\sum_i g_i(p) = 1$.*

If $\mathcal{A} = \{(V_j, \phi_j)\}$ is an atlas of $\mathcal{M}$, a partition of unity $\{(V_i', g_i)\}$ is said to be subordinate *to $\mathcal{A}$ if for each V_i' there exists $V_j \in \mathcal{A}$ such that $V_i' \subset V_j$. A manifold is said to* admit a partition of unity *if every atlas admits a subordinate partition of unity.*

With these notions in place, the global integral of a compactly-supported differential form is defined as follows.

Definition 1.7. *Let $\mathcal{M}$ be a smooth n-dimensional manifold admitting a partition of unity $\{(V_i, g_i)\}$. Let $\alpha \in \Omega^n(\mathcal{M})$ be a compactly supported differential form. The integral of α over $\mathcal{M}$ is defined by*

$$\int_{\mathcal{M}} \alpha = \sum_i \int_{V_i} g_i \alpha.$$

For a detailed proof that this definition is well defined and independent of the chosen partition of unity, see [AMR88, Proposition 7.1.6].

Differential Forms as Measurements In the discussion above, we recalled that differential 1-forms can be interpreted as linear functionals acting on tangent vectors and, upon integration, as measurements of work performed along oriented curves. This interpretation naturally extends to differential forms of higher degree.

For instance, in fluid mechanics one is often interested in the *flux* of a velocity field through an oriented surface patch. Unlike the work done along a curve, such a quantity depends on two independent tangent directions at each point and changes sign when the orientation of the surface is reversed. Consequently, flux is naturally modeled by a differential 2-form, whose evaluation encodes both magnitude and orientation. More generally, given an oriented, embedded

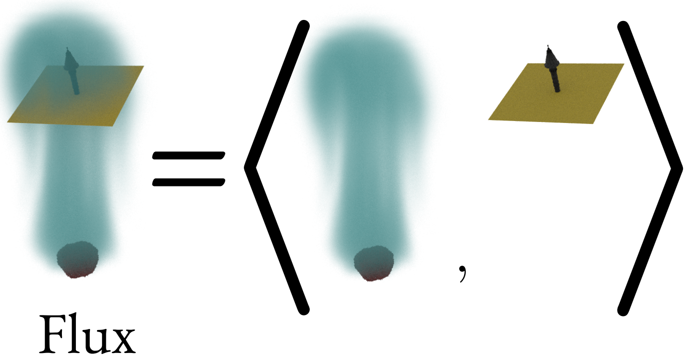

Figure 1.1: **Flux as Scalar Valued Differential Form.** A vector field V induces a measurement on oriented surface patches by evaluating the flux of V through the patch. This measurement is naturally modeled by a differential 2-form, whose evaluation encodes both magnitude and orientation.

k-dimensional manifold $\sigma \subset \mathcal{M}$, a differential k-form $\omega \in \Omega^k(\mathcal{M})$ can be integrated over σ, yielding a scalar quantity that depends only on the oriented geometry of σ. From this perspective, differential k-forms may be viewed as measurements of oriented k-dimensional content.

This viewpoint is particularly well suited for discretization: k-forms naturally pair with k-dimensional geometric objects, such as edges, faces, and volumes, and their integrals represent intrinsic quantities associated with these oriented elements. As such, differential forms provide a natural language for describing measurements on both smooth and discrete domains.

1.2 Exterior Derivative and Stokes' Theorem

Having interpreted differential forms as measurements on oriented domains, a natural question arises: how do such measurements change? In physical terms, this corresponds to questions such as: how does the circulation of a vector field vary across a surface, or how does the flux through a surface change within a volume? In classical vector calculus, these questions are answered by operators such as the gradient, curl, and divergence.

The exterior derivative provides a unified and coordinate-free generalization of these notions. Rather than introducing separate differential operators for each type of quantity, the exterior derivative acts uniformly on differential forms of arbitrary degree.

Definition 1.8 (Exterior derivative)**.** *Let $\mathcal{M}$ be a smooth manifold. The* exterior derivative *is a linear operator*

$$d\colon \Omega^k(\mathcal{M}) \to \Omega^{k+1}(\mathcal{M}),$$

defined for all $k \geq 0$, which satisfies the following properties:

1. *For a smooth function $f \in \Omega^0(\mathcal{M})$, the exterior derivative df coincides with the differ-*

ential of f.

2. *d is graded linear and obeys the graded Leibniz rule*

$$d(\alpha \wedge \beta) = d\alpha \wedge \beta + (-1)^k \alpha \wedge d\beta, \quad \alpha \in \Omega^k(\mathcal{M}).$$

3. $d^2 = 0$.

The action of the exterior derivative can be interpreted as follows. If a differential k-form measures oriented k-dimensional content, then its exterior derivative measures how this content accumulates on the boundary of a $(k+1)$-dimensional region. In this sense, the exterior derivative relates measurements on a domain to measurements on its boundary.

Theorem 1.9 (Stokes' theorem)**.** *Let M be an oriented smooth manifold and let $\Omega \subset M$ be a compact, oriented $(k+1)$-dimensional submanifold with boundary $\partial\Omega$. For any differential k-form $\omega \in \Omega^k(M)$, the following identity holds:*

$$\int_\Omega d\omega = \int_{\partial\Omega} \omega.$$

Stokes' theorem subsumes many classical integral theorems of vector calculus as special cases, including the fundamental theorem of calculus, Green's theorem, the classical Stokes theorem, and the divergence theorem.

The exterior derivative organizes differential forms into a sequence of linear spaces connected by structure-preserving operators. Together with the property $d^2 = 0$, this yields the *de Rham complex*

$$0 \longrightarrow \Omega^0(\mathcal{M}) \xrightarrow{d} \Omega^1(\mathcal{M}) \xrightarrow{d} \Omega^2(\mathcal{M}) \xrightarrow{d} \cdots \xrightarrow{d} \Omega^n(\mathcal{M}) \longrightarrow 0, \tag{1.2.1}$$

where $n = \dim \mathcal{M}$. The exactness properties of this complex encode fundamental topological information about the manifold and underlie many conservation laws in physics. From the perspective adopted here, the de Rham complex expresses a compatibility between integration, differentiation, and orientation that is entirely independent of coordinates.

1.3 Discrete Exterior Calculus

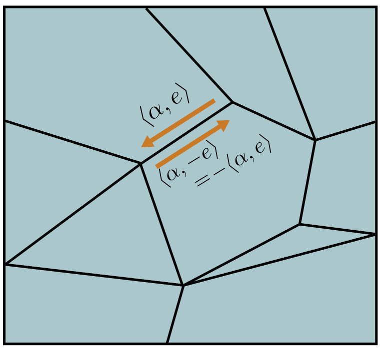

We now review the core ideas of discrete exterior calculus, focusing on the aspects that will later be extended to bundle-valued forms. A key feature of differential forms is that they induce an action on oriented domains through integration. This observation suggests a natural discretization strategy: rather than discretizing pointwise values of fields, one may discretize the *integrals* of differential forms over a finite collection of domains. This approach is particularly well suited to triangulated manifolds, where the geometry is represented by a finite set of simplices of varying dimension.

Let M be an oriented cellular complex. We denote by $\mathcal{C}_k(M)$ the vector space of formal linear combinations of oriented k-cells, called *k-chains*. The boundary operator

$$\partial\colon \mathcal{C}_k(M) \to \mathcal{C}_{k-1}(M)$$

maps each oriented $k-$cell to the alternating sum of its oriented boundary $(k-1)$-cells. A fundamental property of the boundary operator is that $\partial^2 = 0$, reflecting the fact that the boundary of a boundary vanishes.

Discrete differential forms arise naturally as linear functionals on chains.

Definition 1.10 (Discrete differential forms)**.** *A* discrete k-form *on M is a linear map*

$$\omega\colon \mathcal{C}_k(M) \to \mathbb{R}.$$

The space of discrete k-forms is therefore the dual space

$$\mathcal{C}^k(M) := \mathrm{Hom}(\mathcal{C}_k(M), \mathbb{R}),$$

whose elements are referred to as k-cochains*.*

Equivalently, a discrete k-form assigns a single scalar value to each oriented k-simplex. This value may be interpreted as the integral of an underlying smooth k-form over that simplex. Reversing the orientation of the simplex changes the sign of the assigned value, mirroring the orientation dependence of smooth differential forms.

The discrete analogue of the exterior derivative is defined by duality with the boundary operator.

Definition 1.11 (Coboundary operator)**.** *The* coboundary operator

$$\mathrm{d}\colon \mathcal{C}^k(M) \to \mathcal{C}^{k+1}(M)$$

is defined by

$$\langle \mathrm{d}\omega, c\rangle := \langle \omega, \partial c\rangle \quad \textit{for all } c \in \mathcal{C}_{k+1}(M),$$

where $\langle\cdot,\cdot\rangle$ denotes the natural pairing between chains and cochains.

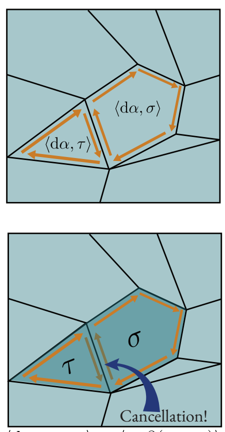

$\langle \mathrm{d}\alpha, \tau+\sigma\rangle = \langle \alpha, \partial(\tau+\sigma)\rangle$

This definition immediately implies two fundamental properties. First, the coboundary operator satisfies

$$\mathrm{d}^2 = 0,$$

since $\partial^2 = 0$. Thus, discrete differential forms assemble into the *discrete de Rham complex*

$$0 \longrightarrow \mathcal{C}^0(M) \xrightarrow{\mathrm{d}} \mathcal{C}^1(M) \xrightarrow{\mathrm{d}} \mathcal{C}^2(M) \xrightarrow{\mathrm{d}} \cdots \xrightarrow{\mathrm{d}} \mathcal{C}^n(M) \longrightarrow 0. \tag{1.3.1}$$

Second, the defining relation of d_h is precisely a discrete form of Stokes' theorem: the integral of a discrete $(k+1)$-form over a

$(k+1)$-simplex is equal to the sum of the integrals of the corresponding k-form over its oriented boundary faces. In this sense, the fundamental compatibility between differentiation and integration is preserved exactly at the discrete level.

This summary of DEC is by far not complete. For a detailed discusson of discrete wedge products, Lie derivative or Hodge Star operators we refer to [Hir03, DHLM05].

1.4 Bundle-Valued Differential Forms

Up to this point, we have restricted our attention to differential forms that take values in the real numbers. This scalar-valued setting already captures a wide range of geometric and physical quantities, such as work along curves or flux through surfaces, and it is precisely the regime in which discrete exterior calculus has proven most successful. However, many fundamental objects in geometry and physics are not scalar-valued. In Cartan's original formulation of differential geometry, differential forms are frequently *bundle-valued*, taking values in a vector bundle rather than in $\mathbb{R}$.

A first example arises in continuum mechanics. In elasticity, the stress exerted by a deforming body can be probed by considering an oriented surface element and asking for the force acting across it. Reversing the orientation of the surface reverses the sign of the force, yet the quantity being measured is a vector rather than a scalar. Such objects are naturally modeled as *vector-valued*

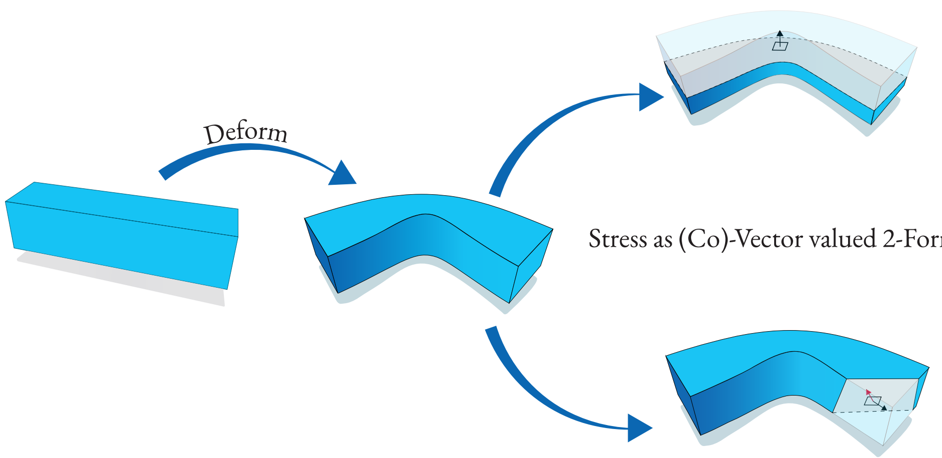

Figure 1.2: **Stress as a Vector-Valued Differential Form.** The stress generated by a deforming body can be probed by selecting an oriented surface element and measuring the force transmitted across it. This measurement is naturally modeled by a vector-valued differential 2-form, whose evaluation on an oriented surface element encodes both the magnitude and the direction of the transmitted force. In this example, the displacement field corresponds to the third nontrivial eigenmode of a linear elasticity energy defined on the body. For the test parallelogram shown in the top right, no force is transmitted across the surface, and the stress form therefore evaluates to zero on this stencil. In contrast, for the test parallelogram in the bottom right, a nonzero component of force acts across the surface. We visualize the unit normal of the test surface in black and the value of the stress 2-form in red.

differential 2-forms, a viewpoint that has been adopted in several geometric formulations of elasticity [KAT+07, WNC23, RBC+23]. This example already illustrates a fundamental departure from the scalar setting: measurements now take values in a vector space that varies from point to point.

An even more intrinsic example is provided by the *solder form*. On a smooth manifold M, the solder form is a canonical 1-form defined on the tangent bundle and taking values in the tangent bundle itself. At each point, it acts by

$$\theta(X) = X,$$

that is, it identifies a tangent vector with itself. While this definition appears tautological at first glance, the importance of the solder form lies in its role within Cartan's calculus, where it mediates between abstract differential forms and geometric directions on the manifold. Unlike scalar-valued forms, the solder form takes values in the tangent bundle, and any attempt to differentiate it necessarily involves comparing vectors that live in different tangent spaces.

This observation marks a fundamental departure from the scalar setting. Whereas the exterior derivative of a scalar-valued form is defined intrinsically, the differentiation of a bundle-valued form requires additional geometric structure specifying how values in different fibers are related. Only once such a rule is prescribed does differentiation become meaningful. In the smooth theory, this leads to the exterior covariant derivative, and geometric quantities such as torsion arise naturally from this construction.

These considerations highlight the limitations of scalar discrete exterior calculus and motivate the development of a discrete theory for bundle-valued differential forms. Before addressing the discrete setting, we first review the corresponding smooth geometric framework, emphasizing the structures and identities that will later guide our discretization.

1.5 Smooth Theory of Connections

To prepare for a discrete extension, we next review the smooth theory of bundle-valued differential forms and connections. We begin by first reviewing the geometric concepts that we will discretize, highlighting the properties we wish to preserve in the discrete realm.

1.5.1 Preliminaries

In the study of an n-dimensional manifold $\mathcal{M}$, we often encounter a vector bundle $\pi : E \to \mathcal{M}$, and a local trivialization $\phi : E|_U \to U \times \mathbb{R}^r$ with $U \subset \mathcal{M}$ being an open subset. This provides us with a local frame field $\{f_1, ..., f_r\}$ on U associated with the canonical basis $\{e_1, ..., e_r\}$ of $\mathbb{R}^r$ given by $f_a(x) = \phi^{-1}(x, e_a)$ for each point $x \in U$. If we switch to another local trivialization $\widetilde{\phi} : \pi^{-1}(\widetilde{U}) = E|_{\widetilde{U}} \to \widetilde{U} \times \mathbb{R}^r$ (where $\widetilde{U}$ is another open subset of $\mathcal{M}$), the resulting local frame $\{\widetilde{f_a}\}$ relates to the local frame $\{f_a\}$ via a matrix of change of bases $A : U \cap \widetilde{U} \to GL(r)$. Using the Einstein summation convention, we have

$$f_a = \widetilde{f}_b A^b_a. \tag{1.5.1}$$

For a section $s \in \Gamma(E)$ of the vector bundle (i.e., an assignment for each point $p \in \mathcal{M}$ of a vector $s(p)$ in the point's fiber $\pi^{-1}(p)$), which we can express locally as $s = f_a s^a = \widetilde{f}_a \widetilde{s}^a$, the components

s^a and $\widetilde{s}^a$ are, instead, related through

$$\widetilde{s}^a = A^a_b s^b.$$

Connection. Given a vector bundle $\pi : E \to \mathcal{M}$, a connection ∇ is a bilinear map $\nabla : \Gamma(T\mathcal{M}) \times \Gamma(E) \to \Gamma(E)$ such that for $g \in C^\infty(M)$, $s \in \Gamma(E)$, and $X \in \Gamma(T\mathcal{M})$, we have

(i) $\nabla_X(gs) = g\nabla_X\, s + dg(X)\, s$ (i.e., it satisfies Leibniz Rule)

(ii) $\nabla_{(gX)}\, s = g\nabla_X\, s.$ (i.e., it is tensorial in X)

In local frames, where $s = f_a s^a$, we can write $\nabla s = f_a \otimes (ds^a + \omega^a_b s^b)$, i.e.,

$$\nabla_X s = f_a(ds^a(X) + \omega^a_b(X)s^b), \tag{1.5.2}$$

for all $X \in \Gamma(T\mathcal{M})$, where $\omega \in \Omega^1(U, \mathfrak{gl}(r))$ is the *local connection* 1*−form* given by $\nabla f_a = f_b \omega^b_a$. Here $\mathfrak{gl}$ denotes the Lie algebra of the Lie group $GL(r)$. Using Equation (1.5.1) we can express the change of the local connection $1-$form $\widetilde{\omega}$ for another local trivialization through the *gauge transformation*:

$$\omega = A^{-1}\widetilde{\omega}A + A^{-1}\mathrm{d}A \quad \Leftrightarrow \quad \widetilde{\omega} = A\omega A^{-1} - \mathrm{d}A\, A^{-1}. \tag{1.5.3}$$

This relationship between the local connection one-forms is central to the understanding of the behavior of the connection under changes of local trivializations.

A connection ∇ on the vector bundle $\pi : E \to M$ naturally induces a connection ∇^{End} on the endomorphism bundle $\mathrm{End}(E) \to \mathcal{M}$, whose fiber at p is the space $\mathrm{End}(E_p) = \mathrm{Hom}(E_p, E_p)$ of endomorphisms of E_p. It is defined by enforcing the Leibniz rule on $L(x)$,

$$\left(\nabla^{\mathrm{End}}_X L\right)(s) := \nabla_X(L(s)) - L(\nabla_X s), \tag{1.5.4}$$

for all $L \in \Gamma(\mathrm{End}(E))$.

Pullback connection. Given a smooth map $\Psi : \mathcal{M} \to \mathcal{N}$ between two manifolds and a vector bundle $\pi : E \to \mathcal{N}$ over $\mathcal{N}$, we can define the *pullback bundle* as $\pi' : \Psi^*E \to \mathcal{M}$, $(\Psi^*E)_p := E_{\Psi(p)}$. Given a connection ∇ on E, we want to equip the pullback bundle with a pullback connection $\Psi^*\nabla$ such that, for any given section $s \in \Gamma E$, we have

$$(\Psi^*\nabla)\Psi^*s = \Psi^*(\nabla s).$$

Such a connection exists and is called the *pullback connection*. We refer the reader to [MS74] for the proof of its existence and uniqueness.

Parallel transport. Parallel transport is a fundamental concept in differential geometry and plays a key role in understanding the geometry of manifolds. Given a curve $\gamma : [0,1] \to \mathcal{M}$ and a vector $v_0 \in E_{\gamma(0)}$ in the fiber at $\gamma(0)$, parallel transport along γ is the process of transporting v_0 to $\gamma(t)$ while maintaining its direction in the vector bundle.

The resulting vector at $\gamma(t)$ is denoted by $v(t)$ and is a solution to the differential equation

$$D_t v(t) = 0 \quad \text{and} \quad v(0) = v_0, \qquad (1.5.5)$$

where $D_t v$ is the covariant time derivative of curves $v(t) \in E$ associated to a connection ∇ on E, given locally by

$$D_t v = f_a(\partial_t v^a + \omega^a_b(\dot{\gamma})v^b). \qquad (1.5.6)$$

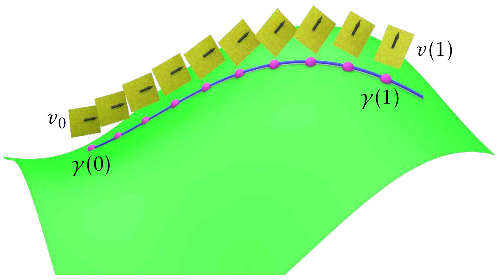

Here, v^a are the components of v in a local frame f_a for the fiber, and ω^a_b are the connection coefficients associated with ∇ in f_a.

The unique solution to the initial value problem Equation 1.5.5 along γ yields a one-parameter family of parallel transport maps

$$\mathcal{R}_{\gamma,t} \colon E_{\gamma(t)} \to E_{\gamma(0)},$$

which is an intrinsic object. We will simply write $\mathcal{R}_t$ the parallel transport maps, when the choice of the curve γ is obvious from the context. If we consider a local frame field $f_a(x)$ in a neighborhood of the curve, the linear map can be represented by a matrix $(R_t)^a_b$, via $\mathcal{R}_t f_a(\gamma(t)) = f_b(\gamma(0))(R_t)^b_a$. Moreover, according to Equation 1.5.3, the matrix R_t is the solution to $\frac{d}{dt}R_t = R_t\omega_{\gamma(t)}(\dot{\gamma}(t))$.

The solution to this last equation can be written as the path-ordered matrix exponential

$$P\left(\exp \int_0^t \omega_{\gamma(\tau)}(\dot{\gamma}(\tau))d\tau\right).$$

As ω is applied to the right of R, we order the terms with larger τ to the right. For instance, the second-order term in the power series of the matrix exponential is

$$P\,\frac{1}{2}\left(\int_0^t \omega_{\gamma(\tau)}(\dot{\gamma}(\tau))\,d\tau\right)^2 = \int_{\tau_2=0}^{t}\int_{\tau_1=0}^{\tau_2} \omega_{\gamma(\tau_1)}(\dot{\gamma}(\tau_1))\,\omega_{\gamma(\tau_2)}(\dot{\gamma}(\tau_2))\,d\tau_1 d\tau_2.$$

By utilizing the parallel transport matrices associated with (f_a) along γ as a gauge field, we can derive a new frame field

$$\widetilde{f_a}(\gamma(t)) = f_b(\gamma(t))(R_t^{-1})^b_a.$$

Consequently, in this new frame, $\tilde{\omega}(\dot{\gamma}) = 0$ by construction, and a constant $\widetilde{v} \in \mathbb{R}^r$ along the curve satisfies the initial value problem Equation (1.5.5), i.e., $\widetilde{v} = R_t v(t) = v_0$. Alternatively, in the original frame f_a, the parallel transport is given by $v(t) = R_t^{-1}v_0$.

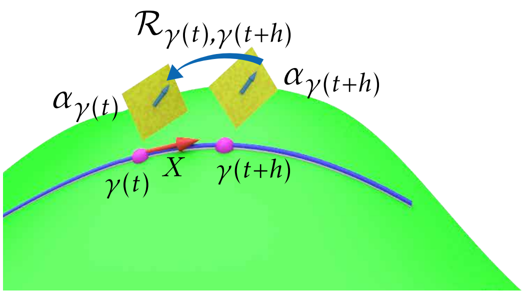

If $X = \dot{\gamma}(0) \in T_{\gamma(0)}\mathcal{M}$ and $\alpha \in \Gamma(E)$ is a section of E, then the parallel transport map $\mathcal{R}_t$ can be used to define the covariant derivative of α with respect to X at $\gamma(0)$ as

$$(\nabla_X\alpha)_{\gamma(0)} = \lim_{t\to 0}\frac{\mathcal{R}_t\alpha_{\gamma(t)} - \alpha_{\gamma(0)}}{t} = \frac{d}{dt}\bigg|_{t=0}\mathcal{R}_t\alpha_{\gamma(t)}. \qquad (1.5.7)$$

1.5.2 Operators and their properties

We end this section with a review of the basic operators (and their properties) for which we will provide discrete equivalents in the remainder of this paper.

Wedge product. We defined the wedge product for scalar valued differential forms in Equation (1.1.1). This notion can be similarly extended to forms that take values in vector bundles: the wedge product $\wedge$ between bundle-valued forms and scalar-valued forms can be defined as:

$$\wedge\colon \Omega^k(\mathcal{M},E)\times\Omega^\ell(\mathcal{M})\to\Omega^{k+\ell}(\mathcal{M},E)\colon (\alpha,\beta)\mapsto \alpha\wedge\beta=\frac{(k+\ell)!}{k!\ell!}\mathrm{Alt}(\alpha\otimes\beta),$$

where the tensor product applied to $(k+\ell)$ vectors $X_1,\dots,X_{k+\ell}\in\Gamma(T\mathcal{M})$ is

$$\alpha\otimes\beta(X_1,\dots,X_{k+\ell})=\alpha(X_1,\dots,X_k)\beta(X_{k+1},\dots,X_{k+\ell}).$$

Exterior covariant derivative. The exterior covariant derivative is a natural extension of the standard exterior derivative of scalar-valued forms to forms that take values in a vector bundle. In particular, given a connection ∇ on $\pi: E\to\mathcal{M}$, the exterior covariant derivative $d^\nabla:\Omega^k(\mathcal{M},E)\to\Omega^{k+1}(\mathcal{M},E)$ obeys

$$d^\nabla(\alpha\otimes s)=d\alpha\otimes s+(-1)^k\alpha\wedge\nabla s,\quad \forall\alpha\in\Omega^k(\mathcal{M}),\forall s\in\Gamma(E),\tag{1.5.8}$$

where $\otimes$ denotes the tensor product of differential forms and sections of the bundle E. Here, we view $\nabla_{(\cdot)}s$ as an $E-$valued 1-form. In local coordinates, Equation (1.5.8) is expressed as

$$(d^\nabla\gamma)^a=d\gamma^a+\omega^a_b\wedge\gamma^b,\tag{1.5.9}$$

where $\gamma=f_a\gamma^a\in\Omega^k(U,E)$ in a given local frame field $\{f_a\}$ of E, while the associated local connection $1-$form for this frame field has components ω^a_b.

Note that given a smooth map $\Psi\colon\mathcal{M}\to\mathcal{N}$ between two manifolds, and a vector bundle $\pi: E\to\mathcal{N}$ with connection ∇, the exterior covariant derivative commutes with the pullback: given a form $\alpha\in\Omega^k(\mathcal{N},E)$ one has

$$d^{\Psi^*\nabla}(\Psi^*\alpha)=\Psi^*(d^\nabla\alpha).\tag{1.5.10}$$

Additionally, given a bundle-valued form $\alpha\in\Omega^k(\mathcal{M},E)$ and a scalar-valued form $\lambda\in\Omega^\ell(\mathcal{M})$, the *Leibniz rule* between the wedge product and the exterior covariant derivative holds, i.e.,

$$d^\nabla(\alpha\wedge\lambda)=\mathrm{d}^\nabla\alpha\wedge\lambda+(-1)^k\alpha\wedge d\lambda.$$

For a proof of these last two properties, see [Mar18] for instance.

Curvature two-form and Bianchi identities. Connections are geometric structures that capture the idea of parallel transport along curves, and are an essential tool in the study of fiber bundles.

One important geometric invariant of connections is the *curvature* 2*–form* $\Omega^\nabla\in\Omega^2(\mathcal{M},\mathrm{End}(E))$, which measures the failure of a connection to be flat, i.e., the impossibility of endowing the base manifold with a Euclidean structure. This skew-symmetric tensor is useful in geometry and physics in areas such as general relativity, gauge theory, and topological quantum field theory. It quantifies the noncommutativity of parallel transport around closed loops and encodes the infinitesimal holonomy of the connection, also known as Ambrose-Singer theorem [AS53]. The *curvature 2−form* is defined as

$$\Omega^{\nabla}(X,Y)s := d^{\nabla}(d^{\nabla}s)(X,Y), \quad s \in \Gamma(E),\ X,Y \in \Gamma(T\mathcal{M}).$$

If we are given a local frame field, it can be shown that we have the local formula

$$\Omega^a_b = d\omega^a_b + \omega^a_c \wedge \omega^c_b = (d\omega + \omega \wedge \omega)^a_b. \tag{1.5.11}$$

This local formula is also sometimes written abusively as $\Omega^{\nabla} = d^{\nabla}\omega$, to be understood as applying the exterior covariant derivative for vector-valued forms to the columns of the connection $1-$form ω in the local frame. One can then show that the following general equation holds:

$$d^{\nabla}d^{\nabla}\alpha = \Omega^{\nabla}(\cdot,\cdot) \wedge \alpha, \quad \forall \alpha \in \Omega^k(\mathcal{M}, E), \tag{1.5.12}$$

a property proving that unlike the exterior derivative d of scalar-valued differential forms, the operator d^{∇} is *not* nilpotent in general. Note that this property is often referred to as the *algebraic Bianchi identity*.

Another important property is what is often referred to as the *differential Bianchi identity*, a consequence of the Leibniz rule and antisymmetry of the exterior covariant derivative: it states that

$$d^{\nabla^{\mathrm{End}}}\Omega^{\nabla} = 0, \tag{1.5.13}$$

where ∇^{End} is the induced connection on the endomorphism bundle $\mathrm{End}(E) \to \mathcal{M}$. More generally it can be shown that for the induced connection on the endomorphism bundle, Eq. Equation (1.5.12) can be expressed as

$$d^{\nabla^{\mathrm{End}}}d^{\nabla^{\mathrm{End}}}\beta = [\Omega^{\nabla} \wedge \beta], \quad \forall \beta \in \Omega^k(M, \mathrm{End}(E)), \tag{1.5.14}$$

where $[\cdot \wedge \cdot]$ is the commutator using the wedge product.

Another usual identity linking curvature tensor and covariant derivatives is that, given a connection ∇ on a vector bundle $\pi : E \to M$ and for any 0-form $s \in \Gamma(E)$, one has:

$$\Omega^{\nabla}(X,Y)s = \nabla_X\nabla_Y s - \nabla_Y\nabla_X s - \nabla_{[X,Y]}s, \quad \forall X,Y \in \Gamma(TM), \tag{1.5.15}$$

where $[X,Y] = XY - YX$ denotes the Lie-bracket between vector fields.

The curvature 2−form and its two associated Bianchi identities are central geometric notions in the study of connections as they are independent of the choice of local trivializations of the associated vector bundle E. Consequently, we will ensure that our discretization respects these important properties.

Remark 1.12. The curvature is *gauge covariant*. This means that given two local frame fields $\{f_a\}$ and $\{\tilde{f}_a\}$, related via a matrix of change of bases as $f_a = \tilde{f}_b A^b_a$ (see Equation (1.5.1)) with associated local connection $1-$form ω and $\tilde{\omega}$, then the components of the matrix-valued curvature in both frame are related as

$$\widetilde{\Omega}^{\nabla} = d\tilde{\omega} + \tilde{\omega} \wedge \tilde{\omega} = A(d\omega + \omega \wedge \omega)A^{-1} = A\Omega^{\nabla}A^{-1}.$$

That is, a change of basis in the fiber only amounts to a change of basis for the representation matrix of the curvature endomorphism, see [CCL99, Eq. (1.29), page 108].

Riemannian connections. Given a smooth manifold $\mathcal{M}$, we call $\mathcal{M}$ a *Riemannian manifold* if the tangent bundle possesses a Riemannian metric, i.e., a section $g \in \Gamma(\mathrm{Sym}^2(T\mathcal{M}))$ such that $g_x : T_x\mathcal{M} \times T_x\mathcal{M} \to \mathbb{R}$ is a scalar product for each fiber space. A connection ∇ on the tangent bundle is said to be compatible with the metric if it preserves the metric structure, which is a natural condition in Riemannian geometry. In other words, ∇ is compatible with the metric if the covariant derivative of the metric with respect to a vector field X can be expressed in terms of the metric and ∇ as

$$d\Big(g(s_1, s_2)\Big)(X) = g(\nabla_X s_1, s_2) + g(s_1, \nabla_X s_2) \quad \forall s_1, s_2 \in \Gamma(T\mathcal{M}), X \in \Gamma(T\mathcal{M}). \tag{1.5.16}$$

If the connection is compatible with the metric, for any two vectors $v, w \in T_x\mathcal{M}$, the inner product $g(R_t v, R_t w)$ is preserved along parallel transport, where R_t denotes the parallel transport map associated with the connection ∇. In a local orthonormal frame, this implies that the local expressions of R_t belong to the special orthogonal group $SO(n)$. This compatibility of the connection with the metric structure is a fundamental requirement in Riemannian geometry: it plays a major role in the definition of the Levi-Civita connection, which is the unique connection that is both compatible with the metric *and* torsion-free — see the next paragraph for a definition of torsion.

Solder form and torsion. For the special case where $E = T\mathcal{M}$, the tautological $1-$form θ, or *solder form*, is a bundle-valued $1-$form defined as $\theta(X) = X$ for any vector field X on $\mathcal{M}$. For a connection ∇, the *torsion* $2-$*form* is derived from the solder form through

$$\Theta^\nabla = d^\nabla \theta = d\theta + \omega \wedge \theta \ \in \Omega^2(\mathcal{M}, T\mathcal{M}), \tag{1.5.17}$$

where the last equality holds only locally. While the curvature $2-$form Ω^∇ measures the deviation of the covariant derivative from the exterior derivative, the torsion $2-$form Θ, on the other hand, measures the deviation of the covariant derivative from the Lie derivative, meaning that it measures the failure of the connection to preserve the Lie bracket of vector fields under parallel transport. Specifically, given a connection ∇, the torsion $2-$form Θ is also expressed through

$$\Theta^\nabla(X, Y) = d^\nabla \theta(X, Y) = \nabla_X Y - \nabla_Y X - [X, Y]$$

for vector fields X and Y on M.

The *algebraic Bianchi identity* often refers to the differential identity from Equation (1.5.12) specifically applied to the solder form; it relates the exterior derivative of the torsion $2-$form to the curvature $2-$form and the solder form through

$$d^\nabla \Theta^\nabla = d^\nabla d^\nabla \theta = \Omega^\nabla \wedge \theta. \tag{1.5.18}$$

Remark 1.13 (Bianchi Identities in (Pseudo) Riemannian Geometry)**.** Suppose we consider the special case of a Riemannian manifold and $E = T\mathcal{M}$. Let ∇ be the Levi-Civita connection, i.e., the unique torsion free connection compatible with the metric. In this case we usually write $\Omega^\nabla(X, Y)Z = R(X, Y)Z$, with R the Riemann curvature $(1, 3)$-tensor, i.e., $R \in T\mathcal{M}^* \otimes T\mathcal{M}^* \otimes T\mathcal{M}^* \otimes T\mathcal{M}$. We have

$$\mathrm{d}^{\nabla^{\mathrm{End}}} \Omega^\nabla = 0 \ \Leftrightarrow \ \nabla_X R(Y, Z) + \nabla_Y R(Z, X) + \nabla_Z R(X, Y) = 0$$

and
$$0 = d^\nabla d^\nabla \theta = \Omega^\nabla \wedge \theta \;\Leftrightarrow\; R(X,Y)Z + R(Y,Z)X + R(Z,X)Y = 0,$$

which are the familiar Bianchi identities as formulated in (pseudo)-Riemannian geometry. A common form found in literature uses tensor notation. Let $(\partial_1, \ldots, \partial_n)$ be a local coordinate frame of $T\mathcal{M}$. Let $(dx^1, \ldots, dx^n)$ the associated dual frame. Using the Einstein sum convention the coordinates of the Riemannian curvature tensor can be expressed as the components of the curvature 2−form as
$$[\Omega^\nabla]^\mu_\nu = R^\mu_{\nu,\alpha,\beta} dx^\alpha \wedge dx^\beta,$$
where
$$R^\mu_{\nu,\alpha,\beta} = dx^\mu \Big(R(\partial_\alpha, \partial_\beta)\partial_\nu \Big).$$
The algebraic Bianchi identity then reads
$$0 = R^\mu_{\nu\alpha\beta} + R^\mu_{\alpha\beta\nu} + R^\mu_{\beta\nu\alpha}.$$
As for the endomorphism-valued case, the definition for the covariant derivative of a tensor field this time becomes:
$$R^\mu_{\nu\alpha\beta;\lambda} = \partial_\lambda R^\mu_{\nu\alpha\beta} + R^\kappa_{\nu\alpha\beta}\omega^\mu_{\lambda\kappa} - R^\mu_{\kappa\alpha\beta}\omega^\kappa_{\lambda\nu} - R^\mu_{\nu\kappa\beta}\omega^\kappa_{\lambda\alpha} - R^\mu_{\nu\alpha\kappa}\omega^\kappa_{\lambda\beta}.$$
Using this definition of covariant tensor derivative, the differential Bianchi identity for the Levi-Civita connection reads
$$0 = R^\mu_{\nu\alpha\beta;\lambda} + R^\mu_{\nu\lambda\alpha;\beta} + R^\mu_{\nu\beta\lambda;\alpha}.$$
For a detailed derivation of these formulas from Equation (1.5.13) and Equation (1.5.18), see [Fra11] p.298-301.

The preceding discussion highlights that extending discrete exterior calculus to bundle-valued differential forms requires substantially more structure than in the scalar case. While the smooth theory provides a clear conceptual framework through Cartan's calculus, its discrete counterpart must address how bundle-valued quantities are represented, transported, and differentiated on a mesh, while preserving the underlying geometric identities.

Before developing a general discrete exterior calculus for bundle-valued forms, it is instructive to study a concrete example. Connections on two-dimensional surfaces provide such a setting. In particular, torsion arises naturally as a vector-valued 2-form, that cannot be straightforwardly investigated with the standard tools from scalar-valued DEC, making it a suitable test case for discretizing bundle-valued exterior calculus.

2 | Discrete Torsion Of Connections On Surfaces

In the previous chapter, we developed a general framework for differential forms with values in a vector bundle, and discussed the geometric structures that must be preserved when discretizing such objects. Before turning to the full generality of bundle-valued exterior calculus, we now focus on a concrete and particularly instructive special case: connections on two-dimensional surfaces.

Many tasks in geometry processing involve comparing directions across a surface: transporting vectors, designing smooth direction fields, or aligning patterns along a mesh. Such comparisons require a rule for relating tangent directions at nearby points. In differential geometry, this role is played by a connection. Accordingly, discrete connections have become a fundamental tool in geometry processing, appearing in applications ranging from vector field and stripe pattern design [CDS10, KCPS15, LTGD16], to vectorization of 2D sketches [GHB$^+$23], and design tools for several forms of fabrication [MMDH$^+$23, MMWC23, MJBHC24]. In the smooth setting, connections on surfaces can be studied using Cartan's method of *moving frames*, where they are characterized by two quantities: their scalar-valued *curvature*, and their vector-valued *torsion*. However, existing work on connections focuses almost exclusively on curvature, neglecting torsion entirely.

2.1 Connections On Surfaces: A Two-Dimensional Specialization

We briefly recall the basic notions of moving frames, connections, curvature, and torsion in the surface setting, reformulated in a concrete and geometric way that will guide our discrete construction.

2.1.1 Vector Fields and Moving Frames

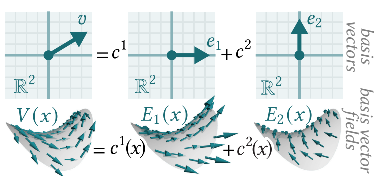

Vector field design is ubiquitous in geometry processing [dGDT16, VCD$^+$17]. The method of moving frames provides a convenient way of calculating with vector fields on smooth surfaces, and arises naturally in applications such as parameterization [CC23], shape deformation [Cor24], and hexahedral meshing [CC19, FHTB23]. We have discussed in Section 1.5.1 that given a local trivialization, we can express sections, in particular vector fields, through scalar-valued functions associated to this trivialization.

In the two-dimensional case, just as one can express a vector v in the plane as a linear combination of basis vectors e_1 and e_2, one can express a *vector field* $V(x)$ on a surface patch as a linear combination of *basis vector fields* $E_1(x)$ and $E_2(x)$, *i.e.*

$$V(x) = c^1(x)E_1(x) + c^2(x)E_2(x), \tag{2.1.1}$$

where $c^1(x)$ and $c^2(x)$ are scalar-valued coefficient functions. The basis fields E_1 and E_2 are often thought of as the columns of a single spatially-varying matrix $E(x)$, referred to as a *moving frame*. This is precisely a local trivialization of the tangent bundle $T\mathcal{M}$, in the sense of the general bundle-theoretic framework introduced earlier. For simplicity, we will always assume that E is an *orthonormal* frame. Note that it may be impossible to find a globally-defined moving frame—or even a single nonvanishing vector field (see the Poincaré–Hopf theorem). Hence, basis fields are usually defined locally: one can perform any desired calculation using different basis fields on each small patch, stitching the results together to obtain global results on the whole surface.

2.1.2 Connections and Parallel Transport on Surfaces

While the directional derivative $D_X f$ of a scalar function f simply measures the rate of change of f as one moves along a tangential direction X, *directional derivatives of vector fields on surfaces* are more involved: vectors at different points on the surface belong to different tangent spaces, and *a priori* cannot be compared directly. A *connection* is a choice of operator $\nabla_X V$ acting as a directional derivative of a tangent vector field V in direction X; unlike the case of scalar functions, there are infinitely many meaningful connections.

Connections in a moving frame If we pick a moving frame $E(x)$ to express our vector field $V(x)$ using its coefficient functions $c^1(x)$ and $c^2(x)$, then any connection can be written in the form

$$\nabla_X \begin{pmatrix} c^1(x) \\ c^2(x) \end{pmatrix} = \begin{pmatrix} D_X c^1(x) \\ D_X c^2(x) \end{pmatrix} + \begin{pmatrix} \omega^1_1(X) & \omega^1_2(X) \\ \omega^2_1(X) & \omega^2_2(X) \end{pmatrix} \begin{pmatrix} c^1(x) \\ c^2(x) \end{pmatrix}, \tag{2.1.2}$$

$$\nabla = d + \omega, \tag{2.1.3}$$

where d is the componentwise exterior derivative, and ω is understood as a matrix-valued 1-form, known as the *connection 1-form*. In the language of Section 1.5, the matrix-valued 1-form ω corresponds to the local connection 1-form ω^a_b expressed in the moving frame E.

A connection allows us to *parallel transport* vectors along curves: if we have a vector V at point x, and a curve γ connecting x to another point y, we obtain a transported vector at y by taking the unique extension of V along γ whose directional derivative in the direction of γ stays identically zero.

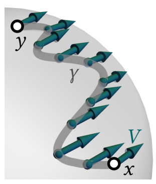

The 1-form ω which we use to write our connection depends crucially on the choice of frame E: if we pick a new frame, we have to use a different connection 1-form to describe the exact same connection. These ω values are only meaningful locally, and do not fit together into a globally-defined matrix-valued 1-form on the whole surface. However, the *difference* between two connections is always a globally-defined 1-form. Indeed, connections form an *affine space*: starting from a connection ∇, we can write any other connection as the sum of ∇ and a globally-defined 1-form.

Metric-compatible connections We introduced prior in Equation 1.5.16 the notion of metric-compatibility for connections on general Riemannian manifolds. In the special case of surfaces, this condition has a particularly simple expression in terms of the connection 1-form ω.

A connection ∇ is *metric compatible* if parallel transport preserves the lengths of vectors. This means the parallel transport map between any two tangent spaces is an isometry — an element of the orthogonal group $O(n)$ rather than the full general linear group $GL(n)$. At the infinitesimal level, this constraint has a direct algebraic interpretation. If we choose an orthonormal frame $E(x)$ with respect to the underlying Riemannian metric, the connection 1-form ω must take values in the Lie algebra of the orthogonal group, $\mathfrak{so}(n)$— the space of skew-symmetric matrices. So $\omega(X)$ is skew-symmetric for every tangent vector X, encoding the infinitesimal rotation that the connection induces along X. Therefore the connection 1-form ω is of the form

$$\omega(X) = \begin{pmatrix} 0 & -\alpha(X) \\ \alpha(X) & 0 \end{pmatrix}, \tag{2.1.4}$$

for some scalar-valued 1-form α. We restrict attention to metric connections, and often use the identification between matrix-valued connection 1-forms ω and the equivalent scalar-valued 1-forms α such that $\omega = \mathbb{J}\alpha$, where $\mathbb{J}$ denotes the matrix $\left(\begin{smallmatrix} 0 & -1 \\ 1 & 0 \end{smallmatrix}\right)$. This identification allows us to represent metric connections using only a single scalar-valued 1-form α. This reduction to a single scalar-valued 1-form α is a peculiarity of the two-dimensional setting, where the structure group $SO(2)$ of orthogonal transformations is abelian. In higher dimensions, connection 1-forms of metric preserving connections necessarily take values in the Lie-algebra of orthogonal transformation, denoted as $\mathfrak{so}(n)$, and such a simplification is no longer possible.

Curvature and torsion As observed by Cartan, one can picture parallel transport as a description of the motion of a surface as it locally rolls around on the tangent plane of some point [Car23, Sha97]. Curvature and torsion capture two key features of this rolling behavior: curvature measures how much the surface rotates when rolled along an infinitesimal loop, while torsion measures how far it translates. Both curvature and torsion have simple expressions in the language of differential forms. If our connection is encoded by a connection 1-form ω in moving frame E, we have seen in Equation 1.5.11 that the curvature of our connection is the matrix-valued 2-form $\Omega^\nabla = d\omega + \omega \wedge \omega$. For metric connections on surfaces, $\omega \wedge \omega = 0$, so the curvature is just

$$\Omega^\nabla = d\omega = \mathbb{J}d\alpha. \tag{2.1.5}$$

For any pair of tangent vectors X, Y at some point p, the matrix $\Omega^\nabla(X, Y)$ describes the rotation applied to the tangent plane at p when the surface is rolled along the infinitesimal parallelogram spanned by X and Y. The component $d\alpha$ measures the rotation angle, and acts as a scalar measurement of curvature, generalizing the Gaussian curvature of a surface to arbitrary metric connections. We have seen previously seen in Equation 1.5.17 that the torsion of our connection is the vector-valued 2-form Θ^∇, with

$$\Theta^\nabla = d\theta + \omega \wedge \theta. \tag{2.1.6}$$

Here θ is the *dual frame* associated to our moving frame E, which takes in a tangent vector and returns the components of that tangent vector in the basis E. We denote its components by $\theta(x) = (E^1(x), E^2(x))$. Unlike the connection 1-form ω, which is only defined relative to a choice of frame $E(x)$ in a local neighborhood, the curvature and torsion yield well-defined *global* 2-forms, meaningful in any coordinates on the surface.

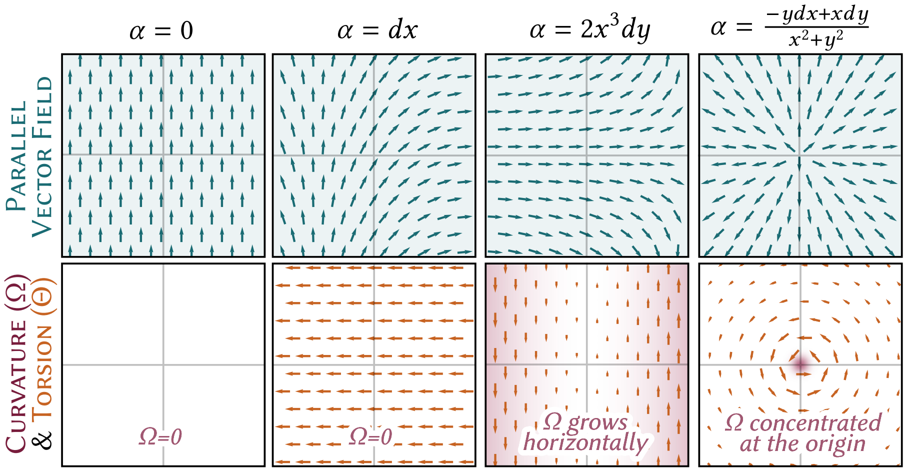

Figure 2.1: **Metric-compatible connections.** Even in $\mathbb{R}^2$ equipped with the standard metric and standard basis, parallel transport of vectors by a metric connection may look very different from a simple translation. Here we consider four connection 1-forms α, and plot parallel vector fields for each connection *(top row)*, as well as the curvature *(bottom row, scalar density)* and torsion *(bottom row, vector field)* of each connection. All four connections are compatible with the standard metric—as their parallel fields are unit vector fields—but the rotations and singularities present in their parallel-transported vector fields can become arbitrarily complicated.

Compatibility conditions between curvature and torsion Starting from a given connection ∇ and for any globally-defined 1-form $\alpha = \alpha_1 E^1 + \alpha_2 E^2$, we can define a new connection as $\widetilde{\nabla} = \nabla + \mathbb{J}\alpha$. Note that

$$\mathbb{J}\alpha \wedge \theta = \alpha \wedge \mathbb{J}\begin{pmatrix} E^1 \\ E^2 \end{pmatrix} = \alpha \wedge \begin{pmatrix} -E^2 \\ E^1 \end{pmatrix} = -\begin{pmatrix} \alpha_1 \\ \alpha_2 \end{pmatrix} E^1 \wedge E^2. \tag{2.1.7}$$

Thus, the changes in curvature and torsion between the new and the old connections are given by

$$\Omega^{\widetilde{\nabla}} - \Omega^{\nabla} = \mathbb{J} d\alpha, \quad \text{and} \quad \Theta^{\widetilde{\nabla}} - \Theta^{\nabla} = -\alpha^\sharp \, dA, \tag{2.1.8}$$

which implies that these changes are linked: *the change in exact part of the change in torsion*.

The Levi-Civita connection For any metric on a manifold, there is a unique metric connection with zero torsion. This connection, called the Levi-Civita connection $\nabla^{\text{LC}} = d + \mathbb{J}\alpha^{\text{LC}}$ encodes the geometry of the surface in important ways: for instance, the curvature of the Levi-Civita connection gives the surface's Gaussian curvature $\kappa = -d\alpha^{\text{LC}}$. And once you know the Levi-Civita connection, the calculation of curvature and torsion for all other connections also simplifies: 2.1.8 shows that the curvature tensor of a connection $\widetilde{\nabla} = \nabla^{\text{LC}} + \mathbb{J}\alpha$ is $\mathbb{J}(d\alpha - \kappa dA)$, and the torsion $\Theta^{\widetilde{\nabla}}$ is

$$\Theta^{\widetilde{\nabla}} = -\alpha^\sharp \, dA. \tag{2.1.9}$$

This notion of torsion as a deviation from the Levi-Civita connection will be leveraged in this chapter.

It is important to emphasize that the Levi-Civita connection is just one of many connections compatible with a given surface metric. While a metric connection preserves the lengths of vectors, it may not encode the surface geometry like the Levi-Civita connection does. For instance, the curvature of a metric connection may be completely different from the Gaussian curvature defined by the metric (Figure 2.1). The only relationship between them is that on closed surfaces, the connection curvature must obey the Gauss-Bonnet theorem: just like the ordinary Gaussian curvature, it must sum to 2π times the surface's Euler characteristic.

2.1.3 Connections on Discrete Surfaces

Most existing works using connections on triangle meshes follows the basic strategy of [CDS10] (or its dual variant), where one picks an arbitrary basis to encode tangent vectors in each face and then encodes the connection using an angle-valued dual 1-form giving the angle by which a vector must be rotated when parallel transporting it from one face to an adjacent one. These tangent bases on each face act as a globally-defined moving frame, allowing the connection to be represented as a discrete globally-defined 1-form, without the need to use locally-defined frames on surface patches. The curvature of a discrete connection at a primal mesh vertex is then obtained by summing up the connection angles on the dual loop around that vertex. This curvature depends linearly on the connection 1-form, so is easy to find connections with any desired set of curvatures—such as trivial connections with only a few non-zero curvatures.

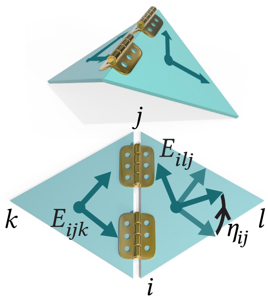

However, while this strategy suffices to discretize curvature, no discrete notion of torsion was ever proposed. A canonical connection on triangle meshes, that was leveraged by [CDS10] and which we will call the *hinge connection* η, is found by unfolding the hinge between two faces and measuring the angle η_{ij} between the chosen frames on these two faces (see inset, where the rotation angle η_{ij} aligns frame E_{ijk} with frame E_{ijl}). Crane et al. refer to this connection as "the discrete Levi-Civita connection", since its parallel transport is locally a translation in the isometric hinge map and its curvature is the usual discrete Gaussian curvature. Indeed, the hinge connection is exactly the Levi-Civita connection of the mesh, viewed as a polyhedral surface with piecewise-flat metric. Our approach also singles out this hinge map as a convenient "reference" connection from which we can encode other connections through dual 1-forms, but we also introduce a new discrete Levi-Civita connection which offers lower torsion (seen as the deviation from the Levi-Civita connection of an underlying smooth surface) by spreading vertex curvatures over dual faces. This spreading of curvature is reminiscent of the primal as-Levi-Civita-as-possible connection of [LTGD16], which spreads curvature over primal faces, but Liu et al. use a more complex parameterization of vector fields, considering tangent vectors which may lie on mesh vertices, edges, or faces.

In the remainder of this chapter, we present a practical approach to torsion processing on surface meshes. First, we introduce a new discrete Levi-Civita connection which views a mesh not as a polyhedral surface with curvature concentrated at singularities, but as an approximation to a smooth surface with locally-constant curvature. We then describe how the discrete notion of torsion of a connection can be defined to mirror the continuous definition from Equation 2.1.9, i.e., we consider the discrete torsion of a connection as *the* discrete dual 1-form *by which a connection deviates from the discrete Levi-Civita connection*. This choice makes little difference in the continuous world, where the spaces of vector-valued 2-forms, vector fields, and 1-forms are all isomorphic. However, in our discrete setting, this discretization offers a practical and robust computational framework for torsion manipulation: we can trivially control the torsion of a connection while keeping its curvatures, and vice-versa as shown on several geometry processing applications in Section 2.3.

2.2 Torsion on Discrete Surfaces

In this section, we first outline our notation in Section 2.2.1, and introduce a new discrete Levi-Civita connection which distributes curvature smoothly over dual faces in Section 2.2.2. From this low-torsion "reference" connection, we introduce a discrete notion of torsion modeled after Equation 2.1.9, *i.e.*, we define the torsion of a connection as the discrete dual 1-form by which it deviates from the discrete Levi-Civita connection. In Section 2.2.3, we review the various ways to prescribe torsion, with or without preserving curvatures.

2.2.1 Notation and Conventions

Surface mesh and quantities We work on a manifold triangle mesh $M = (\mathcal{V}, \mathcal{E}, \mathcal{F})$ with vertices $i \in \mathcal{V}$, edges $ij \in \mathcal{E}$, and faces $ijk \in \mathcal{F}$. We use $\overrightarrow{ij}$ to denote an oriented halfedge from i to j. A value u_i denotes a quantity u at vertex i, and similarly for edges and faces (see inset), while a value u_i^{jk} denotes a quantity at the corner of face ijk incident on vertex i, and a value $u_{\overrightarrow{ij}}$ denotes a quantity at halfedge $\overrightarrow{ij}$. For instance, the position of vertex i is $p_i \in \mathbb{R}^3$, the length of edge ij is $\ell_{ij} \in \mathbb{R}$, the area of face ijk is $A_{ijk} \in R$, and the angle at corner i of face ijk is $\varphi_i^{jk} \in [0, \pi)$.

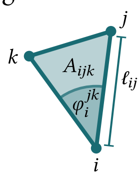

Frame fields. A discrete frame field consists of a choice of frame per face of our mesh. These frames can be written explicitly as matrices $E_{ijk} \in \mathbb{R}^{3\times 2}$ associated to each face ijk, where the two columns of E_{ijk} are orthonormal vectors in $\mathbb{R}^3$ tangent to face ijk. One can also store frames intrinsically as 2×2 matrices, interpreting the columns as tangent vectors in a fixed basis on face ijk. As mentioned in Section 2.1.2, we use $\mathbb{J}$ to denote $90°$ rotation matrix $\begin{pmatrix} 0 & -1 \\ 1 & 0 \end{pmatrix}$.

We will also make use of *local* frame fields defined on the 1-rings of the mesh vertices. We will denote the value of such a local field on face ijk as E_i^{jk} to indicate that the frame is associated with vertex i.

Dual mesh and orientations. We also consider the dual of M, which has a face $*i$ corresponding to each vertex of M, and edge $*ij$ corresponding to each edge of M, and a vertex $*ijk$ corresponding to each face of M. Our algorithm works with any choice of dual (*e.g.* circumcentric or barycentric), but we find that circumcentric duals can perform poorly on low-quality meshes (Section 2.3.4). As on the primal mesh, we denote value u on dual edge $*ij$ as u_{*ij}, *etc.* We also use $*\overrightarrow{ij}$ to denote the oriented halfedge running along dual edge $*ij$, picking the orientation that places $*\overrightarrow{ij}$ counterclockwise of $\overrightarrow{ij}$.

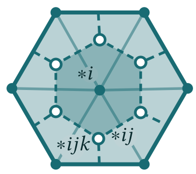

Discrete connections A discrete metric connection provides a rotation angle $\alpha_{*\overrightarrow{ij}}$ on each halfedge describing how the coordinates of a vector v_{ilj} written in the frame of the right-hand face should be transformed to obtain a parallel-transported vector v_{ijk} in the frame of the left-hand face (see inset).

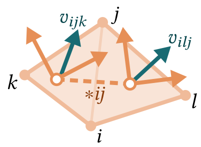

As in the smooth setting, the angles α depend on the choice of frames, but once we write any connection α^0 in these frames, every other connection can be expressed as the sum of α^0 with a discrete dual 1-form. We follow [CDS10] and write our connections as offsets from the hinge connection η, but one could equally well pick any other connection to start from.

2.2.2 A New Discrete Levi-Civita Connection

As mentioned in Section 2.1.3, the hinge map is the exact Levi-Civita connection of a triangle mesh, viewed as a polyhedral surface with curvature concentrated at its vertices (see inset). However, this singular geometry differs in many ways from the geometry of the smooth surface which the mesh is supposed to approximate. We instead introduce a new connection $\omega^{\mathrm{LC}} = \mathbb{J}\alpha^{\mathrm{LC}}$ derived by spreading the curvature to be constant on each 1-ring instead. We find that this constant-curvature local approximation of the surface yields a connection with consistently lower error than the hinge map compared to the continuous Levi-Civita connection (Figure 2.6) without much added complexity.

To derive this formula we will in a first step calculate the Levi-Civita connection of a surface with constant curvature.

Constant-Curvature Levi-Civita Connection. We begin by constructing a local frame field by leveraging the geodesic polar map of the one-ring [WW94]. We define geodesic polar coordinates in the neighborhood of each vertex i. That is, we pick some arbitrary reference edge ij to act as the positive x-axis, and then define polar coordinates $(r, \overline{\varphi})$, where the radius r measures the distance to vertex i, and the normalized angle $\overline{\varphi}$ measures the angle along the surface to edge ij, normalized by a factor of $\frac{2\pi}{\Phi_i}$ so that the angles around i sum up to a full 2π (rather than summing to the discrete tip angle sum Φ_i). At any point x in face ijk, $x \neq p_i$, we define our frame by first computing polar basis unit vectors $e_r = (x - p_i)/\|x - p_i\| \in \mathbb{R}^3$ and $e_\varphi = N_{ijk} \times e_r$, and then expressing our frame as

$$E_x = \begin{pmatrix} e_r & e_\varphi \end{pmatrix} \begin{pmatrix} \cos\overline{\varphi} & \sin\overline{\varphi} \\ -\sin\overline{\varphi} & \cos\overline{\varphi} \end{pmatrix}. \tag{2.2.1}$$

If we index the neighboring vertices as $j_0, \ldots, j_n$, the geodesic polar coordinates can be evaluated in closed form at the circumcenter of each neighboring face $i j_k j_{k+1}$ as

$$\begin{cases} r_{ij_kj_{k+1}} = \dfrac{\ell_{j_kj_{k+1}}}{2\sin\varphi_i^{j_kj_{k+1}}}, \\ \overline{\varphi}_{ij_kj_{j+1}} = \dfrac{2\pi}{\Phi_i}\left(\dfrac{\pi}{2} - \varphi_{j_{k+1}}^{ij_k} + \displaystyle\sum_{s=0}^{k-1} \varphi_i^{j_sj_{s+1}}\right). \end{cases} \tag{2.2.2}$$

Piecewise-flat metric. The geodesic polar map is easy to visualize: imagine the one-ring made of paper, and bend that into a cone with its discrete Gaussian curvature κ_i. Projecting the cone

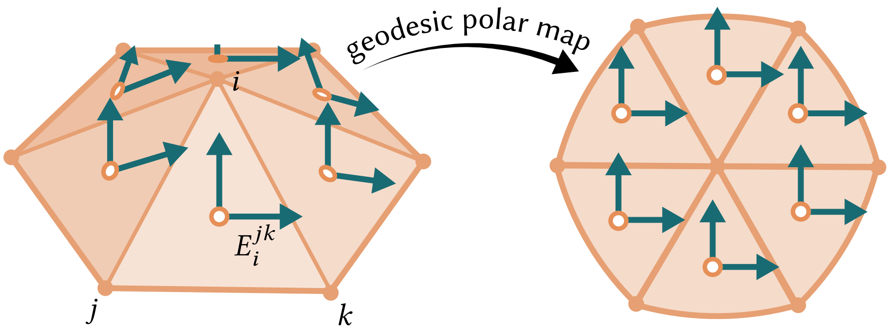

Figure 2.2: **Local One-ring Frame.** We construct for every one-ring neighborhood a *geodesic polar frame* field which is constant per each face *(left)*. This frame is constructed from a geodesic polar map of the 1-ring, *i.e.*, a planar parameterization where radial edge lengths are unchanged and the tip angles around vertex i are scaled by a constant to sum to 2π *(right)*.

along the direction of the axis of the cone, we have the geodesic polar map $(r, \bar{\varphi})$ with the origin at the center vertex. The solder form is precisely

$$\theta = \begin{pmatrix} du + \sin\bar{\varphi}\frac{\kappa_i}{2\pi} r d\bar{\varphi} \\ dv - \cos\bar{\varphi}\frac{\kappa_i}{2\pi} r d\bar{\varphi} \end{pmatrix} \tag{2.2.3}$$

where $(u, v) = r(\cos\bar{\varphi}, \sin\bar{\varphi})$. One may verify that $\alpha^{\mathrm{LC}} = -\kappa_i/(2\pi) d\bar{\varphi}$ precisely satisfies $d\theta + \alpha \mathbb{J} \wedge \theta$.

The discrete connection values are given as integrals along dual edges:

$$\int_{*i} d\theta = \int_{\partial *i} \frac{\kappa_i}{2\pi}(v, -u)^T d\bar{\varphi},$$

which is the angle weighted average of the boundary coordinates rotated by 90°, rescaled by $\frac{\kappa_i}{2\pi}$.

If calculated in the true geodesic polar frame, the hinge connection actually provides the correct integral of $\tau_{*\vec{ij}} = \int_{\vec{ij}} \alpha^{\mathrm{LC}}$. One can see this by assuming the difference in the angles formed at the vertex in the mesh $\Delta\varphi$ will be the rotation angle for parallel transport in the hinge map, the corresponding rotation in the two frames of the geodesic polar frame would be $\Delta\bar{\varphi}$, the difference provides $\tau_{*\vec{ij}} = -\kappa_i/(2\pi)\Delta\bar{\varphi}$.

Constant-curvature metric. For a metric of constant Gaussian curvature K, the normalized 1-form in the $d\bar{\varphi}$ direction is:

$$e^{\bar{\varphi}} = r\sin\left(\sqrt{K}r\right)/\sqrt{K} d\bar{\varphi}, \tag{2.2.4}$$

which also works in the case $K < 0$, since $\sin$ can be turned into $\sinh$ when applied to imaginary numbers. To simplify the derivation, we still use the expansion $\sin(x) = x - x^3/6$. Then

$$d\theta = \frac{1}{2}K\begin{pmatrix} v \\ -u \end{pmatrix} du \wedge dv, \tag{2.2.5}$$

i.e., the integral will be the barycenter coordinates rescaled by half of the pointwise Gaussian curvature. The analytic expression of the Levi-Civita connection is thus $\alpha^{\mathrm{LC}} = -\frac{1}{2}Kr^2 d\bar{\varphi}$.

Consider now the frames at two neighboring dual vertices $*imj$ and $*ijk$. The hinge map would unfold triangles imj and ijk in the plane, and simply translate the frame from $*imj$ to $*ijk$. Due to the angle scaling of the polar map, our geodesic polar frame introduces an extra rotation of $\left(\frac{2\pi}{\Phi_i}-1\right)\varphi_{*ij}$. Hence, in our frame field, the value of the hinge connection along $*ij$ is precisely (if K_i denotes the discrete (integrated) Gaussian curvature))

$$\eta_{*ij}=\left(1-\tfrac{2\pi}{\Phi_i}\right)\varphi_{*ij}=-\tfrac{K_i}{\Phi_i}\varphi_{*ij}. \tag{2.2.6}$$

Since the geodesic polar map scales angles by $\frac{2\pi}{\Phi_i}$, the 1-form $d\overline{\varphi}$ is equal to $\frac{\Phi_i}{2\pi}$ times the ordinary angular 1-form $d\varphi$ in the plane. Moreover, the integral of $\frac{1}{2}r^2 d\varphi$ along a plane curve γ is simply equal to the area of the region formed by connecting the endpoints of γ to the origin. Therefore, the integral of the constant-curvature Levi-Civita connection along a dual edge $*ij$ is equal to $\kappa\frac{\Phi_i}{2\pi}$ times the area of the region in the geodesic polar plane formed by connecting the endpoints of $*ij$ to the origin. Since the polar map has constant Jacobian determinant $\frac{2\pi}{\Phi_i}$, we can compute this area as κ times the area formed on the original mesh by connecting the endpoint of $*ij$ to vertex i. Thus, the integral of the constant-curvature Levi-Civita connection along a dual edge $*ij$ in our geodesic polar frame is simply $-\frac{K_i}{A_i}A_{*ij}$, where A_i denotes the area of the dual cell associated to vertex i. For a primal edge ij let $\lozenge_{ij}$ be its associated diamond area.

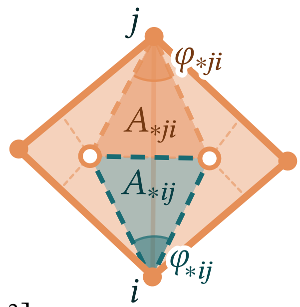

Unfortunately, these values do not define a valid connection on our mesh, since they generally define incompatible rotations along the two sides of dual edge $*ij$. Writing down the compatibility conditions explicitly may seem nontrivial, but they can easily be expressed by observing that because the set of valid connections is an affine space, every connection can be written as the hinge map plus a discrete dual 1-form. Explicitly, if $\alpha_{*ij}=\eta_{*ij}+\mathring{\alpha}_{*ij}$, then α_{*ji} must be equal to $\eta_{*ji}-\mathring{\alpha}_{*ij}$. A natural way of reconciling the desired Levi-Civita integrals along the two sides of dual edge $*ij$ is to minimize the area-weighted error

$$\mathcal{E}(\mathring{\alpha})=\sum_{ij}\left[\tfrac{1}{2}A_{*ij}\left(\eta_{*ij}+\mathring{\alpha}_{*ij}+\tfrac{K_i}{A_i}A_{*ij}\right)^2+\tfrac{1}{2}A_{*ji}\left(\eta_{*ji}-\mathring{\alpha}_{*ij}+\tfrac{K_j}{A_j}A_{*ji}\right)^2\right]. \tag{2.2.7}$$

The energy is minimized by setting

$$\mathring{\alpha}_{*ij}=\tfrac{1}{A_{*ij}+A_{*ji}}\left(A_{*ji}\left(\eta_{*ji}+\tfrac{K_j}{A_j}A_{*ji}\right)-A_{*ij}\left(\eta_{*ij}+\tfrac{K_i}{A_i}A_{*ij}\right)\right). \tag{2.2.8}$$

Substituting the values of η_{*ij} from Equation 2.2.6 yields for us the formula

$$\alpha_{ij}^{\mathrm{LC}}=\eta_{ij}+\tfrac{1}{\lozenge_{ij}}\left(K_iA_{*ij}\left(\frac{A_{*ij}}{A_i}-\frac{\varphi_{*ij}}{\Phi_i}\right)-K_jA_{*ji}\left(\frac{A_{*ji}}{A_j}-\frac{\varphi_{*ji}}{\Phi_j}\right)\right), \tag{2.2.9}$$

Note that in the case of a local region of the triangulation with only equilateral triangles, the ratios A_{*ij}/A_i and φ_{*ij}/Φ_i are all precisely $\frac{1}{6}$, and this connection reduces back to the hinge map. But in irregular regions, the two will generally differ.

2.2.3 Discrete Torsion of a Connection

Once we have a discrete Levi-Civita 1-form $\omega^{\mathrm{LC}}=\mathbb{J}\alpha^{\mathrm{LC}}$, we can understand torsion in the discrete realm via Equation 2.1.9: in the continuous case, the torsion of a connection measures its deviation from the Levi-Civita connection. We thus define the discrete torsion of a discrete connection $\omega = \mathbb{J}\alpha$ as the dual 1-form

$$\tau := \alpha - \alpha^{\mathrm{LC}}. \qquad (2.2.10)$$

This definition exactly parallels the continuous definition and provides a simple and straightforward way not only to define torsion, but also to enable torsion processing on connections through Hodge decomposition [CdGDS13] of this dual 1-form by controlling its curl, divergence, and harmonic components as we described next.

Curl-constrained assignment of torsion. Since the curl of any change of torsion corresponds to a change in curvature (Equation 2.1.8), we can modify a connection $\omega = \mathbb{J}\alpha$ while keeping its curvature fixed by solving for a new connection whose torsion has the same curl. Explicitly, we maintain the connection's holonomy around collapsible dual cycles if and only if we add to α a harmonic dual 1-form, a dual gradient field $d_1^T f$ (where f is a dual 0-form, *i.e.*, a set of values on the mesh faces) — or both. Note that adding a harmonic form will affect the holonomy of each homology generator of the surface; so the higher the genus of a surface, the more ways the torsion can be edited, which can potentially be useful in applications such as quadrangulation, *e.g.*, with holonomy of multiples of $\pi/2$.

Divergence-constrained assignment of torsion. Conversely, given a discrete connection $\omega = \mathbb{J}\alpha$, one can preserve the divergence of its torsion by adding $\star_1 d_0 p$ for a scalar potential p defined on vertices. As the additional connection is the $90°$–rotated gradient of p, it is divergence-free, and will not alter the above-mentioned gradient component of torsion $d_1^T f$. In other words, such a perturbation is the minimal change needed to modify the connection's curvature.

We show examples of torsion editing in Section 2.3 to emphasize how torsion affects the notion of parallel transport in various geometry processing applications.

2.2.4 Trivial Connections

[CDS10] proposed to design tangent n-vector fields over a given mesh by prescribing their singularities and associated indices. They solve for a metric connection — dubbed a trivial connection — with zero holonomy around all mesh vertices and around the generators if the genus is non-trivial, except on each of the singularities where the holonomy is set based on the singularity index. These constraints amount to a set of linear equations fixing the curvature around each vertex and the holonomy about each homology generator. Since these linear constraints are less numerous than the number of dual edges, the authors proposed taking the solution with the minimal L^2 norm, reasoning that this choice ensures that the connection is as close to the original hinge connection, and thus perturbs the notion of parallel transport the least. The final vector field with prescribed singularities is then constructed from an arbitrary unit vector on a face that is parallel-transported throughout the mesh via this new connection. Since the connection is compatible with the metric, this construction generates a unit vector field.

Our discrete theory of torsion introduces a new interpretation of this optimization problem: the L^2 norm that Crane et al. minimize is akin to our Equation 2.2.10, except that it measures the distance to the hinge map rather than the distance to our new discrete Levi-Civita connection.

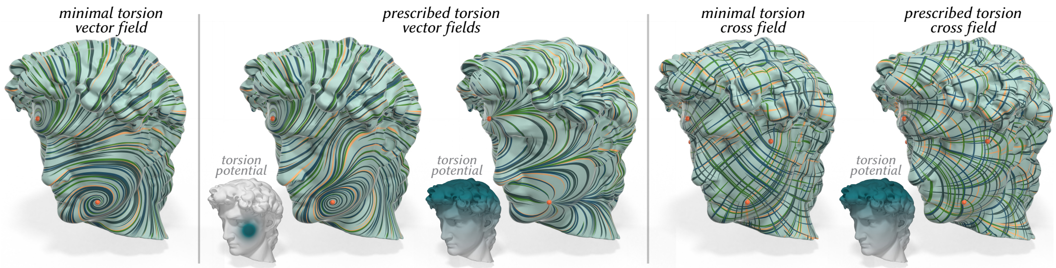

Figure 2.3: **Torsion-controlled trivial connections.** Here we explore the impact of torsion on vector field design: a parallel vector field for a minimal-torsion trivial connection with prescribed singularities is shown on the left, while parallel fields for trivial connections with additional gradient components in their torsion are shown in the center, along with the prescribed scalar potentials. A compact potential changes the field locally *(center left)*, while a globally-supported potential causes larger-scale changes *(center right)*. Torsion can also be incorporated into the design of n-vector fields such as cross fields *(right)*.

Moreover, we obtain a new geometric interpretation of the space of trivial connections with prescribed singularities—these are precisely the connections whose torsion 1-forms have a fixed curl. Inside this space, we can move beyond the idea of minimizing torsion to explore the effects of prescribing different torsions. As discussed in Section 2.2.3, we can easily ensure that our new torsion obeys the curl constraints as long as we only modify it by adding the gradient of a scalar potential. As Figure 2.3 demonstrates, this alteration of the trivial connection may have a substantial impact.

2.3 Evaluation and Results

Now we explore the effect of torsion prescription in scenarios like n-vector field design (Section 2.3.1), connection Laplacians (Section 2.3.2), before moving on to discuss convergence to ground-truth analytic connections in several scenarios (Section 2.3.3), and discussing the choice of dual mesh (Section 2.3.4).

2.3.1 N–Vector Field Design

As observed by [CDS10], one can use a connection to design tangent vector fields on a surface: if we have a connection, we can obtain a vector field by picking one vector at an arbitrary point, and parallel transporting that vector to all other points of the surface. The resulting vector field will be continuous if and only if the connection is *trivial*—meaning that its curvature at every vertex is a multiple of 2π, as its holonomy around every loop.

As discussed in Section 2.2.4, imposing these curvature constraints fixes the curl and harmonic components of the torsion, leaving exactly the torsion's gradient component free to prescribe. In Figure 2.3 we show several vector fields generated from different trivial connections all sharing the same curvature constraints. In general, modifying the torsion by the differential $d_1^T f$ of a potential function f will introduce a twist into the parallel vector fields, with more twist in regions where the magnitude of f is greater.

The case of n-vector field design is no different: setting singularities with indices being multi-

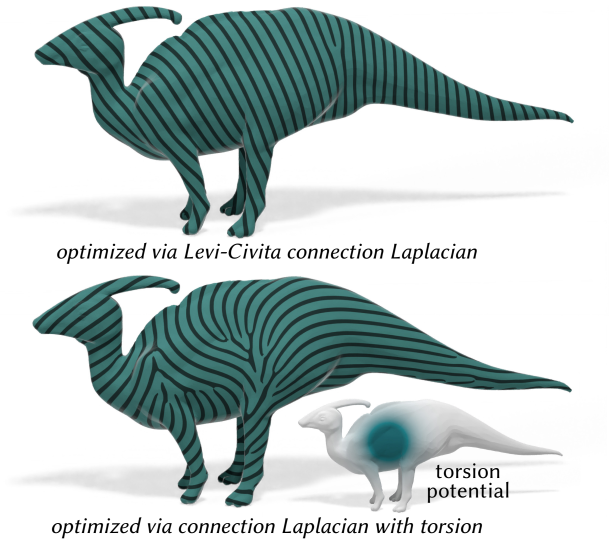

Figure 2.4: **Optimal vector fields for different connections.** Just as the ordinary Laplacian measures the smoothness of scalar functions, the connection Laplacian defines a notion of smoothness for vector fields. Computing an optimal vector field in the sense of [KCPS13] using the discrete Levi-Civita connection to build the connection Laplacian yields a field whose streamlines are as straight as possible in 3D space *(top)*, whereas using a connection with a nontrivial torsion (here, the gradient of a potential) introduces twists into the streamlines *(bottom)*.

ple of $2\pi/n$ will generate tangent direction fields that are smooth up to local rotations by multiples of $2\pi/n$, such as cross fields for instance for $n = 4$ (Figure 2.3, *right*).

2.3.2 Connection Laplacians

A connection on a surface can also be used to define a *connection Laplacian*, which measures the smoothness of vector fields just as the ordinary Laplacian measures the smoothness of scalar functions. This connection Laplacian thus plays an important role in algorithms throughout geometry processing [KCPS13, LTGD16, SSC19], and our connections can be directly used to construct more general dual connection Laplacians for face-based vector fields. In the primal setting, it is also easy to add a primal 1-form to any choice of connection to obtain a primal connection Laplacian with torsion. Figure 2.5 illustrates the impact of torsion on the vector heat method of [SSC19], where the (primal) connection Laplacian is used to solve a discrete vector diffusion problem, approximating parallel transport of vectors along shortest paths. As pointed out by [SSC19, §6.1.3] using a connection Laplacian for a new connection then approximates parallel transport using your new connection. Sharp et al. show that one can apply vector diffusion to a pair of vector fields to compute a *logarithmic map*, approximating the distance and direction from a single source vertex to all other vertices. By modifying one of the diffusion equations to use a connection with torsion, we can effectively "twist" the polar parameterization.

As another example, [KCPS13] proposed an algorithm to compute smooth direction fields as eigenfunctions of a connection Laplacian. Using a connection Laplacian with torsion encourages a similar twisting behavior in direction fields, creating interesting branching patterns if the direction fields are visualized using the stripe pattern algorithm of [KCPS15], see Figure 2.4.

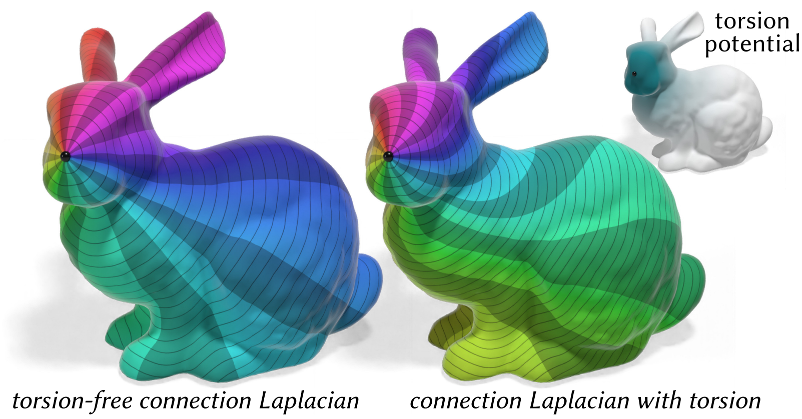

Figure 2.5: **Torsion-controlled vector heat method.** The connection Laplacian used in the vector heat method of [SSC19] can be formed for any connection. In this example, we compute a logarithmic map—a sort of global polar parameterization—using the connection Laplacian of an ordinary torsion-free connection *(left)*, and using a connection with prescribed non-zero torsion equal to the gradient of a torsion potential *(right)*, which introduces a distinct twist into the radial lines of the parameterization.

Relation to the Affine Heat Method. As illustrated in Figure 2.5, the modification of the connection laplacian with an additional torsion potential can introduce a twist in the arising UV map. Recently, Soliman and Sharp [YS25] proposed a different technique —the *affine heat method*— to improve the quality of UV maps arising from vector heat diffusion. The affine heat method constructs UV maps via a different mechanism: it augments the bundle to $TM \oplus \mathbb{R}$ and performs diffusion with an affine (homogeneous) connection Laplacian whose sections carry both a tangent component and a homogeneous coordinate. After dehomogenization, the recovered tangent-plane quantities behave like *displacements* rather than unit directions, i.e., their magnitudes vary and can encode translational information. This additional degree of freedom is precisely what enables their method to produce low-distortion parameterizations in challenging settings. From this perspective, while both approaches influence UV maps by altering the Laplacian used for heat flow, they do so at different levels: we alter the connection on TM through a scalar torsion perturbation, whereas the affine heat method changes the *representation space* itself to explicitly include translations.

2.3.3 Convergence

In this section, we measure the convergence of our discrete connections to analytic solutions under mesh refinement.

Convergence of our discrete Levi-Civita connection. In Figure 2.6, we plot the L^2 errors of the hinge map and our discrete Levi-Civita connection compared to the true Levi-Civita connection on smooth surfaces of the form $z = \lambda_1 x^2 + \lambda_2 y^2$. These examples are universal, in the sense that locally, any smooth surface can be approximated up to second order by a quadratic surface $z = ax^2 + bxy + cy^2$, and moreover any such quadratic form can be diagonalized by a simple rotation of the xy-plane, reducing to the simple quadratic surfaces which we consider. We gen-

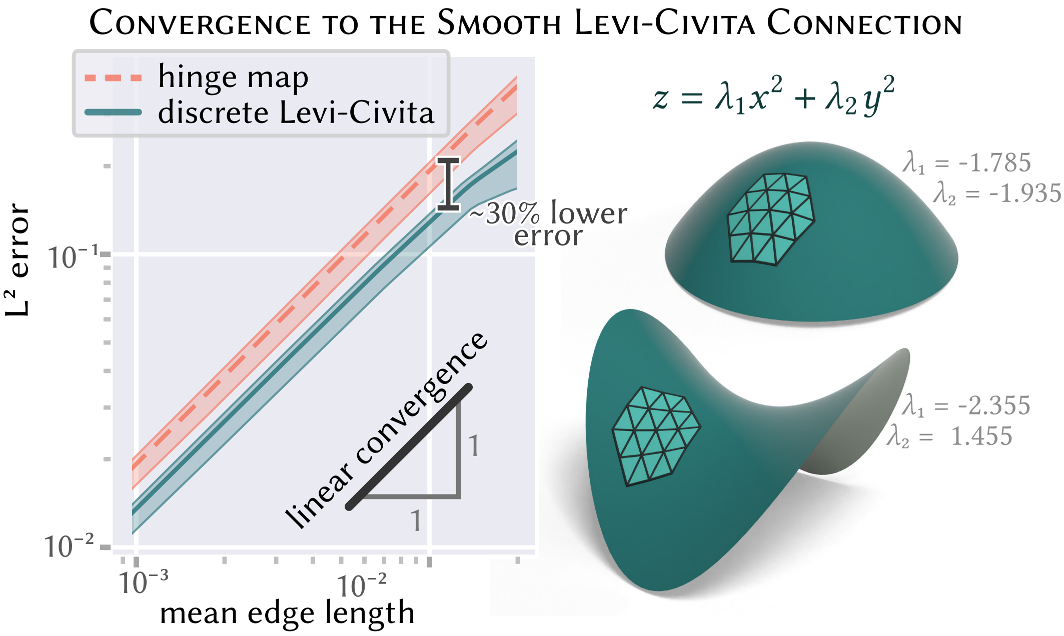

Figure 2.6: **Convergence test.** Here we plot the L^2 errors of the hinge map vs. our discrete Levi-Civita connection compared to the smooth Levi-Civita connection on several hundred randomly generated quadratic surfaces. The plotted lines show the average error across all experiments, while shaded envelopes show the maximum and minimum errors. Both discrete connections converge at the same linear rate, but our discrete Levi-Civita connection offers lower error in every case. Two sample surfaces are shown on the right

erated 500 random quadratic surfaces with values of λ_1 and λ_2 chosen uniformly at random in the range of $[-2.5, 2.5]$. As expected, both discrete connections converge linearly under refinement, but our discrete Levi-Civita connection has consistently lower error than the hinge map — around 30% lower in this particular example. To ensure that we compare the accuracy of the two connections over the whole surface, rather than merely along dual edges, we measure the error in each vertex one-ring by fitting a linear 1-form to the discrete connection values on the adjacent dual edges, and compute the L^2 distance to a 2nd-order-accurate approximation to the smooth Levi-Civita connection within this region—we provide a derivation of the reference solution in Section 2 of the supplemental material.

Convergence of trivial connections. Our identification of torsion with deviation from the Levi-Civita connection allows us to derive closed form expressions for trivial connections with prescribed singularities on smooth surfaces. In App. A we derive an analytic expression for minimal-torsion trivial connections on the sphere, and in Figure 2.7, we plot the L^∞ error of trivial connections on the sphere computed starting from our discrete Levi-Civita connection, and from the hinge map, compared to an analytic reference solution with minimal torsion and one with nonzero prescribed torsion. Because the ground truth trivial connection blows up near the singularities, we measure the error on a small surface patch away from the singularities. Note that the prescribed torsion arising from the potential is captured almost perfectly by the discretization, so both trivial connections have near-identical errors.

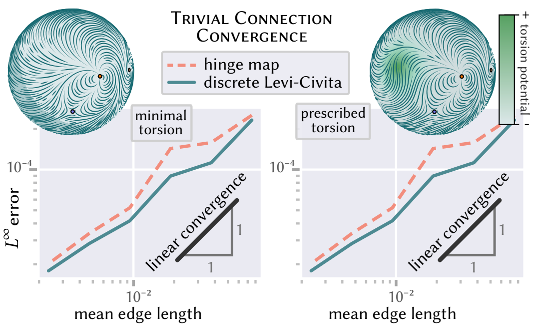

Figure 2.7: **Convergence to trivial connections.** Here we plot the L^∞ error of a discrete trivial connections compared to an analytic reference solution with minimal torsion *(left)* and with prescribed torsion *(right)*. Since the solutions blow up around singularities, we measure the error on a patch of the sphere away from the singularities.

2.3.4 Sensitivity to Dual Mesh

We finally point out that the choice of dual mesh can have an impact on the robustness of our discrete Levi-Civita connection. The use of the circumcentric dual simplifies many expressions (*e.g.*, the half-diamond areas A_{*ij} and A_{*ji} in Equation 2.2.9 become equal, to each other on the circumcentric dual, and the angle φ_{*ij} subtended by a dual edge can be written explicitly in terms of the corner angles opposite edge ij as $\pi - \varphi_k^{ij} - \varphi_m^{ji}$).

However, using the circumcentric dual may lead to flipped dual edges (even on otherwise high-quality meshes), which may lead to large numerical errors. In practice, we find that implementing our method using the barycentric dual mesh leads to significantly less sensitivity to triangle quality without requiring a large increase in implementation complexity or degrading solution quality on well-conditioned meshes. Other choices, such as the hybrid approach of [MDSB03], may be adopted instead.

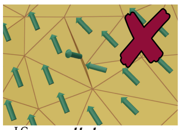

α^{LC}-parallel transport (circumcentric dual)

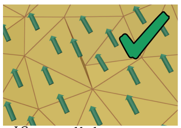

α^{LC}-parallel transport (barycentric dual)

Conclusion In this chapter we introduced a discrete notion of torsion for connections on the tangent bundle of surfaces. This construction served as a concrete and accessible instance of a bundle-valued differential form in a discrete setting, and illustrated how parallel transport, covariant differentiation, and structure-preserving identities can be realized on a mesh.

The surface case benefits from several dimension-specific simplifications. On a two-dimensional manifold, vector-valued differential 2-forms are naturally isomorphic to vector fields, which in turn can be identified with scalar-valued differential 1-forms through the surface metric. Moreover, metric-compatible connections on surfaces admit a scalar representation through a single dual 1-form. These identifications significantly simplify both the representation and the discretization of curvature and torsion.

Beyond surfaces, however, these simplifications no longer apply. For general vector bundles or the tangent bundle of higher-dimensional manifolds, metric-compatible connections cannot be encoded using scalar-valued forms alone. Curvature becomes a genuinely matrix-valued 2-form, and torsion remains an intrinsically vector-valued 2-form.

This increased algebraic complexity already manifests itself in existing work on volumetric meshes, where connections are represented by matrix-valued quantities and curvature control leads to nonlinear formulations (e.g., [CC19]). These observations indicate that the two-dimensional construction developed here cannot simply be extended by analogy. While parallel transport was already present in the preceding setting, it effectively reduced to a scalar-valued framework with trivial fiber interactions. For general vector bundles, however, transport becomes an essential and nontrivial operation: it is required even to relate quantities in different fibers, and its path dependence introduces fundamentally new structure. A systematic treatment therefore calls for a reformulation of discrete exterior calculus itself.

3 Discrete Exterior Calculus of Bundle-Valued Forms

Moving from scalar- to bundle-valued differential forms raises a number of foundational questions.

- How should discrete forms be represented when their values live in different fibers?
- How can discrete exterior differentiation be defined in a way that accounts for parallel transport?
- Which algebraic identities of Cartan's calculus—such as Leibniz rules, Bianchi identities, or Stokes-type relations—should be preserved exactly, and which can only be expected to hold under mesh refinement?

While recent combinatorial approaches [Sch18, BEHS21] have addressed aspects of these questions, these approaches did not analyze thoroughly the relation of discrete bundle-valued formsto continuous bundle-valued forms. Indeed, these approaches assumed that discrete forms were given. One of the major contributions of our work is to propose a discretization scheme to obtain such discrete forms from smooth ones

The purpose of this chapter is to provide such a systematic framework. Building on the smooth theory developed earlier in chapter 1, we formulate a discrete exterior calculus for bundle-valued differential forms on simplicial meshes. We define discrete forms, their covariant exterior derivatives, and the associated curvature and torsion operators. Finally, we establish that the resulting structure preserves the essential geometric identities of the smooth theory and converges under mesh refinement.

3.1 Discrete Connections and Bundle-valued Differential Forms

We now discuss our discretization of bundle-valued forms and connections, for which related operators will be derived in the next section. Throughout this section and for the remainder of this paper, we consider an arbitrary discrete manifold M represented by a *simplicial complex* embedded in $\mathbb{R}^n$. In addition to the mesh notation introduced in Section 2.2.1, we denote the 3D cells of the mesh by $\mathcal{C}^3 = \{c_{ijkl}\}$, etc. More generally, we will also refer to the set of all k−cells of M as $\mathcal{C}^k$ (or $\mathcal{C}^k(M)$). In this chapter we will restrict our attention to the case that all cells are simplicial.

In Chapter 4 we will discuss how we can extend the construction to a larger family of nonsimplicial cells. For simplicity of exposition, we will assume that the manifold is *oriented*, which is a negligible constraint given the local nature of this theory.

3.1.1 Discrete Vector Bundles, Frame Bundles, and Connections

In our discrete setup, a number of discrete notions of continuous definitions are rather natural to define as a collection of discrete objects on M, representing a discretization of their respective continuous notions. While these definitions alone are not sufficient (in particular, no notion of bundle topology will be defined yet), we will complete the discrete picture in the upcoming sections.

Definition 3.1 (Discrete Vector Bundle)**.** *A discrete vector bundle of rank r over a discrete orientable manifold M is simply defined as a collection of vector spaces $\{\mathbf{E}_{v_i}\}_{v_i \in \mathcal{V}} := \mathbf{E}(M)$ (i.e., one vector space per vertex), with $\dim(\mathbf{E}_{v_i}) = r$.*

We can then equip each of these vertex-based vector spaces with a frame to form a *discrete analog of a local section of the frame bundle* over M.

Definition 3.2 (Section of Discrete Frame Bundle)**.** *A section of the* discrete frame bundle *of the rank-r vector bundle $\mathbf{E}(M)$ consists in a collection of frames $\{\mathbf{F}_{v_i}\}_{v_i \in \mathcal{V}} := \mathbf{F}(M)$ defining an arbitrary choice of frame for each vector space $\mathbf{E}_{v_i}$.*

We can now define a *discrete connection* $\boldsymbol{\nabla}$ as a collection of maps between the extremities of each edge of M.

Definition 3.3 (Discrete Connection)**.** *A discrete connection $\boldsymbol{\nabla}$ is defined as an assignment, for each edge e_{ij} of the discrete orientable manifold M, of an invertible linear map $\mathcal{R}_{ij} : \mathbf{E}_{v_j} \to \mathbf{E}_{v_i}$, with $\mathcal{R}_{ij} \circ \mathcal{R}_{ji} = \mathbf{Id}_{v_i}$ representing the parallel transport induced by a continuous connection ∇ along e_{ij}, see Figure 3.1.*

These maps $\{\mathcal{R}_{ij}\}_{e_{ij} \in \mathcal{E}}$ can be thought of as discrete parallel transport maps along edges, where the continuous definition from Equation (3.2.1) is integrated along an edge to define a map between two adjacent vertices. In practice, one can express each linear map $\mathcal{R}_{ij}$ of a connection through a matrix $R_{ij} \in GL(r)$, stored on vertex v_i, using a discrete frame field $\mathbf{F}(M)$. Note that a number of properties in the continuous case apply to these discrete equivalents. For instance, if each of the fibers $\mathbf{E}_{v_i}$ possesses an inner product $\langle \cdot, \cdot \rangle_{\mathbf{E}_{v_i}}$, we say that the discrete connection is *compatible with the metric* if the maps $\mathcal{R}_{ij} : (\mathbf{E}_{v_j}, \langle \cdot, \cdot \rangle_{v_j}) \to (\mathbf{E}_{v_i}, \langle \cdot, \cdot \rangle_{v_i})$ are orthonormal.

When each frame $\mathbf{F}_{v_i}$ is orthonormal, this implies $R_{ij} \in \mathrm{SO}(r)$: a frame at a vertex is naturally parallel-transported along an edge through a pure rotation.

Given two discrete manifolds M, N and a discrete vector bundle $\mathbf{E}$ over N, with a discrete connection $\boldsymbol{\nabla}$, we can finally define the notion of *discrete pullback bundle*. An abstract simplicial map $f : M \to N$ is a map that maps any vertex $v \in \mathcal{C}^0(M)$ to a vertex $\tilde{v} \in \mathcal{C}^0(N)$ and satisfies in addition for $\sigma \in \mathcal{C}^k(M)$ that there exists any $\tilde{k}$-simplex $\tilde{\sigma}$ in $\mathcal{C}^{\tilde{k}}(N)$ such that $f(\sigma) = \tilde{\sigma}$. Given an abstract simplicial map $f : M \to N$, the pullback bundle $f^*\mathbf{E}$ over M is naturally defined as $(f^*\mathbf{E})_{v_i} = \mathbf{E}_{f(v_i)}, \forall v_i \in \mathcal{V}$. We then follow [BEHS21] for the definition of the *pullback connection*.

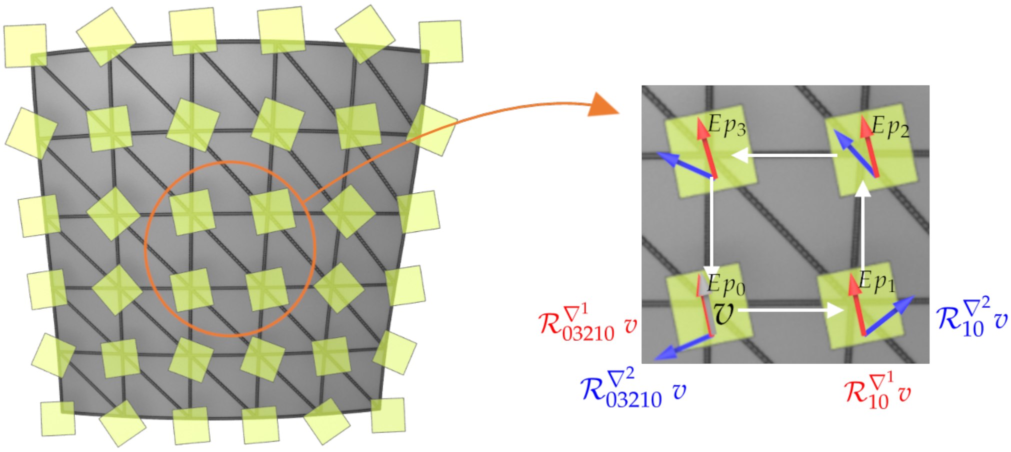

Figure 3.1: **Discrete Connections.** A discrete vector bundle $\boldsymbol{E}$ assigns a vector space to each vertex on a mesh. To compare quantities in different fibers, we need to encode how the individual fibers are *connected*. A connection consists of a collection of linear maps between neighboring fibers. In the figure, each box represents a frame for each fiber space over a vertex. The right part of the figure visualizes the local action of two different discrete connections. Starting with an initial vector $v \in \boldsymbol{E}_{p_0}$ (gray), we illustrate the different parallel transports induced by two different connections, ∇^1 and ∇^2. Different connections on the same vector bundle result in distinct notions of parallel transport and curvature.

Definition 3.4 (Pullback Connection [BEHS21]). *Let $f: M \to N$ be a simplicial map and $\mathbf{E}$ a discrete vector bundle over N with discrete connection $\boldsymbol{\nabla}$. A pullback connection $f^*\boldsymbol{\nabla}$ is defined as a collection of linear maps $\{\mathcal{R}_{ij}: \mathbf{E}_{f(j)} \to \mathbf{E}_{f(i)}\}_{e_{ij}\in\mathcal{E}(M)}$ with:*

$$\mathcal{R}_{ij} := \begin{cases} \mathcal{R}_{f(v_i)f(v_j)} & \text{if } e_{f(v_i),f(v_j)} \in \mathcal{E}(N) \\ \mathrm{Id}_{\mathbf{E}_{f(v_i)}} = \mathrm{Id}_{\mathbf{E}_{f(v_j)}} & \text{otherwise, } f(v_i) = f(v_j). \end{cases}$$

3.1.2 Discrete Bundle-Valued Differential Forms

Given a discrete vector bundle $\mathbf{E}$ over a discrete manifold M, we now define the notion of *discrete bundle-valued ℓ–form* as, for now, a collection of abstract maps. How these maps relate to the continuous case will be elucidated later (see Section 3.2) in order to guarantee proper convergence to continuous forms for increasing mesh resolution.

Definition 3.5 (Discrete (1,0)-tensor-valued ℓ–form). *A discrete vector-valued ℓ–form $\boldsymbol{\alpha}$ on M is a collection of maps which, for each ℓ–simplex σ and one of its vertices v, returns a vector in $\mathbf{E}_v$, i.e.,*

$$\boldsymbol{\alpha}: \ \sigma \in \mathcal{M}^\ell, v \in \sigma \subset \mathcal{C}^0 \mapsto \boldsymbol{\alpha}(\sigma, v) \in \mathbf{E}_v, \tag{3.1.1}$$

such that if $\bar{\sigma}$ is the simplex σ with reversed orientation, one has $\boldsymbol{\alpha}(\bar{\sigma}, v) = -\boldsymbol{\alpha}(\sigma, v)$ for all

$v \in \sigma$.

Note that this definition means that in contrast to the discretization of scalar-valued forms in FEEC or DEC, discrete bundle-valued differential forms are *not* to be understood as a linear space of cochains, but rather as *maps for simplex-vertex pairs*: bundle-valued $\ell-$forms should be regarded as abstract "sided" maps (as they are attached to a particular vertex of the simplex) for now. Moreover, we will assume *for now* that a discrete bundle-valued $\ell-$form is defined through its values on all simplex-vertex pairs (σ, v) for σ is an $\ell-$simplex and v is one of its vertices: later on (see Sec 3.2.2), once we precisely define how a discrete bundle-valued form is sampled from a continuous form, we will restrict this definition to only **one vector value per $\ell-$simplex**, like in existing finite-dimensional (scalar-valued) exterior calculus frameworks.

We also define the notion of *discrete* $(1,1)$*-tensor-valued $\ell-$forms* (or *discrete homomorphism-valued $\ell-$*forms). Given a vector bundle $\pi : E \to M$ with connection ∇, we consider the bundle $\mathrm{End}(E) \to M$ with induced connection ∇^{End}. One can equivalently describe it as the bundle of $(1,1)$-tensors of E. This latter description allows for a more flexible representation, preserving the underlying structure of endomorphism forms by considering separate evaluation and input fibers for each cell.

Definition 3.6 (Discrete $(1,1)$-tensor-valued $\ell-$form)**.** *A discrete* $(1,1)$*-tensor-valued $\ell-$form $\boldsymbol{\beta}$ on M is a collection of maps which, for each $\ell-$simplex σ and two of its vertices (w, the input [or 'cut'] fiber, and v, the output (or* evaluation*) fiber), returns a homomorphism between $\mathbf{E}_w$ and $\mathbf{E}_v$, i.e.,*

$$\boldsymbol{\beta} \colon \sigma \in \mathcal{C}^{\ell}, v \in \sigma, w \in \sigma \mapsto \boldsymbol{\beta}(\sigma, v, w) \in \mathrm{Hom}(\mathbf{E}_w, \mathbf{E}_v), \tag{3.1.2}$$

such that if $\bar{\sigma}$ is the simplex σ with reversed orientation, one has $\boldsymbol{\beta}(\bar{\sigma}, v, w) = -\boldsymbol{\beta}(\sigma, v, w)$ for all $v, w \in \sigma$.

Remark 3.7. The discrete curvature $\boldsymbol{\Omega}^{\nabla}$ defined in Definition 3.12 with evaluation and cut fibers at two different vertices is an example of a discrete endomorphism-valued $2-$form. Note that we could trivially extend these previous definitions to (p,q)-tensor-valued discrete forms using p input vertices and q output vertices; but we will not explore this extension in this work.

Following [BEHS21] we can finally define the notion of *pullback of a discrete bundle-valued form* as follows:

Definition 3.8 (Pullback of a Discrete Vector-Valued Form [BEHS21])**.** *Given a simplicial map $f : M \to N$ and a discrete vector bundle $\mathbf{E}$ over N, let $\boldsymbol{\alpha}$ be an $\mathbf{E}-$valued discrete $\ell-$form. We define the $f^*\mathbf{E}-$valued pullback form $f^*\boldsymbol{\alpha}$ on M as*

$$f^*\boldsymbol{\alpha}(\underbrace{s := [v_0, \ldots, v_\ell]}_{\in \mathcal{C}^{\ell}(M)}, v_0) = \begin{cases} \boldsymbol{\alpha}([f(v_0), \ldots, f(v_\ell)], f(v_0)) & \textit{if } [f(v_0), \ldots, f(v_\ell)] \in \mathcal{C}^{\ell}(N), \\ 0 & \textit{otherwise.} \end{cases}$$

A similar definition for *discrete endomorphism-/homomorphism-valued forms* holds trivially.

3.1.3 Discrete Connection One-Form

Recall that in the smooth theory, once we are given a trivialization of the smooth vector bundle $E \to \mathcal{M}$, we can treat the fibers as vector spaces of rank r (say, copies of $\mathbb{R}^r$). The local connection $1-$form ω associated with a given connection ∇ is then defined as $\nabla s^a = ds^a + \omega^a_b s^b$, where ω measures how much the connection deviates from the exterior derivative d (applied to coordinates); so if $\omega = 0$, i.e., $\nabla = d$ in a given frame field, then the matrix representation of parallel transport in this frame field satisfies $R_{ij} = \mathrm{Id}_{\mathbb{R}^r}$.

We thus formulate the definition of a *discrete connection* $1-$*form* as follows:

Definition 3.9. *Let M be a discrete manifold with discrete vector bundle $\mathbf{E}(M)$ of rank r and let $\mathbf{F}(M)$ be a section of the discrete frame bundle. For a given discrete connection $\boldsymbol{\nabla}$ defined by a set of edge matrices R_{ij} when expressed in $\mathbf{F}$, we define its associated discrete local connection $1-$form $\boldsymbol{\omega}$ as the collection of $r \times r$ matrices $\boldsymbol{\omega}_{ij}$ (one per edge $e_{ij} \in M$) with*

$$\boldsymbol{\omega}_{ij} := R_{ij} - \mathrm{Id}_{\mathbb{R}^{r\times r}} \in \mathbb{R}^{r\times r}. \tag{3.1.3}$$

Note that a discrete local connection $1-$form thus also measures how much the discrete connection-induced parallel transport locally deviates from the identity, mimicking the continuous definition $\nabla s^a = ds^a + \omega^a_b s^b$. And just like in the smooth case, the realizations of the per-coordinate exterior derivative and the connection $1-$form for a given connection change depending on the chosen frame field $\mathbf{F}$. We will, in fact, exploit this property in our work.

Remark 3.10. We can also regard Equation (3.1.3) as a linear approximation of the smooth case: if each parallel-transport edge matrix R_{ij} comes from the integration of a continuous $1-$form ω over the edge e_{ij}, then it is given by $R_{ij} = P\exp\left(\int_{e_{ij}} \omega\right)$. The first-order Taylor expansion of this path-ordered matrix exponential is $\mathrm{Id}_{v_i} + \int_{e_{ij}} \omega$, ensuring consistency with the continuous case. One could instead define $\boldsymbol{\omega}_{ij}$ as the integrated value of the continuous connection $1-$form ω, and then linearize the exponential map by setting $R_{ij} := \mathrm{Id}_{v_i} + \boldsymbol{\omega}_{ij}$; but given the central role of parallel transport in our work, we find this second way to discretize connection and parallel transport less appealing.

Remark 3.11. In the context of this discretization approach, we presume the continuity of the underlying local frame field. However, this assumption encounters limitations due to the globally assigned frame per vertex. Notably, the applicability of a continuous local frame encounters constraints, as illustrated by the hairy ball theorem, which prohibits the existence of a global frame for the tangent bundle on a sphere. Extending this notion to bundles with potentially nontrivial characteristic classes, even for a seemingly straightforward base manifold like a tetrahedron, it may become infeasible to employ a single bundle chart to parametrize the bundle on the cell. Our work specifically focuses on scenarios where *a local setup* suffices, and a single chart is adequate to parametrize the bundle. In this case, we point out that the parametrization of the bundle is independent of the chart. However, in cases involving multiple charts, a need arises for compatibility conditions between them to meet global topology constraints. Further exploration of these conditions remains a direction for future research.

3.1.4 Discrete Curvature Two-Form

Given a discrete connection $\boldsymbol{\nabla}$, we now design a notion of *discrete connection curvature* akin to the continuous definition of Ω^{∇}. Since the Ambrose-Singer theorem links the curvature of the connection to the holonomy of an infinitesimal loop, it is tempting to define the discrete curvature 2–form $\boldsymbol{\Omega}^{\boldsymbol{\nabla}}$ on a triangle $\sigma = [v_0, v_1, v_2]$ on, say, fiber $\mathbf{E}_{v_0}$ through the difference between the integrated connection 1–form over the triangle edges and the identity at the evaluation fiber via

$$\boldsymbol{\Omega}^{\boldsymbol{\nabla}}(\sigma, v_0) := \mathcal{R}_{01} \cdot \mathcal{R}_{12} \cdot \mathcal{R}_{20} - \mathrm{Id}_0 \in \mathrm{End}(\mathbf{E}_{v_0}). \tag{3.1.4}$$

However, Equation (3.1.4) is not a constructive definition: one cannot meaningfully *sum* this definition over two triangles, even if they share the same evaluation vertex v_i. In other words, since this curvature is associated with a loop instead of a simple chain, we cannot use the summability of chains to induce a notion of curvature integral over a larger region. We need to leverage the underlying algebraic structure of chains instead.

Inspired by synthetic geometry for infinitesimal cells [Koc97] and the definition proposed in [Sch18, BEHS21], we propose not to use parallel transport along triangle boundary loops, but instead, to *compare parallel transport along two 1–chains whose difference forms a triangle boundary loop*. This change, which amounts to comparing the integration of the connection form over two 1–chains — and each time parallel-transporting the result back to fiber $\mathbf{E}_{v_0}$ — may seem tautological, but it will allow us to define a notion of addition of the curvature 2–form over two 2–chains sharing a 1-chain. Note that it now casts the curvature two-form on M as a discrete *homomorphism-valued 2–form*.

Definition 3.12. *Let M be a discrete orientable manifold equipped with a discrete vector bundle $\mathbf{E}(M)$ and connection $\boldsymbol{\nabla} = \{\mathcal{R}_{ij}\}_{e_{ij} \in \mathcal{E}}$. Let $\sigma = [v_0, v_1, v_2] \in \mathcal{C}^2$ be a triangle of M. For the evaluation fiber $\mathbf{E}_{v_0}$ at v_0, the three expressions for the discrete curvature 2–form $\boldsymbol{\Omega}^{\boldsymbol{\nabla}}$ depending on whether we use v_1, v_2, or v_0 as the cut vertex (comparing respectively parallel-transports over the oriented 1–chains e_{01} vs. $e_{02}e_{21}$, $e_{01}e_{12}$ vs. e_{02}, and $e_{01}e_{12}e_{20}$ vs. $\varnothing$, see Figure 3.2) are:*

$$\boldsymbol{\Omega}^{\boldsymbol{\nabla}}(\sigma, v_0, v_1) = \mathcal{R}_{01} - \mathcal{R}_{02}\mathcal{R}_{21} \in \mathrm{Hom}(\mathbf{E}_{v_1}, \mathbf{E}_{v_0}), \tag{3.1.5}$$

$$\boldsymbol{\Omega}^{\boldsymbol{\nabla}}(\sigma, v_0, v_2) = \mathcal{R}_{01}\mathcal{R}_{12} - \mathcal{R}_{02} \in \mathrm{Hom}(\mathbf{E}_{v_2}, \mathbf{E}_{v_0}), \tag{3.1.6}$$

$$\boldsymbol{\Omega}^{\boldsymbol{\nabla}}(\sigma, v_0, v_0) = \mathcal{R}_{01}\mathcal{R}_{12}\mathcal{R}_{20} - \mathrm{Id}_0 \in \mathrm{Hom}(\mathbf{E}_{v_0}, \mathbf{E}_{v_0}). \tag{3.1.7}$$

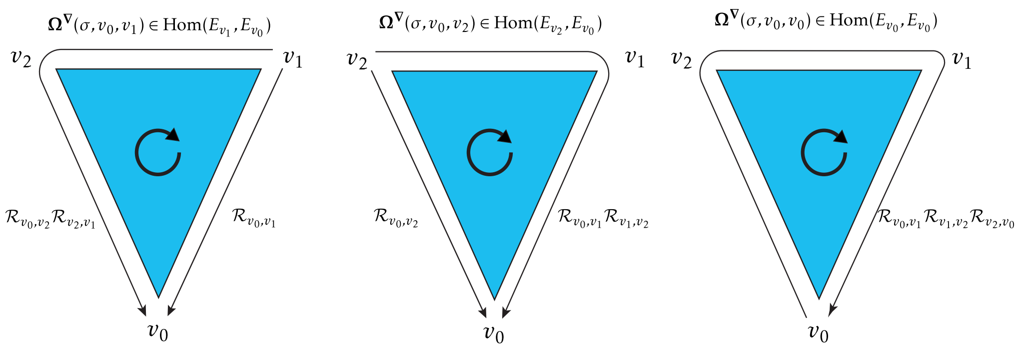

Figure 3.2: **Curvatures.** Illustration of the discrete curvatures for different cut vertices.

From this definition, the meaning of "*evaluation fiber*" and "*cut fiber*" should become clear: instead of measuring the traditional holonomy of the loop starting at v_0 through $\mathbf{\Omega}^{\nabla}(\sigma, v_0)$, we instead compare transport along two paths, both from the evaluation fiber to the cut fiber but on opposite sides of the triangle, with the path difference being the original triangle boundary.

Remark 3.13. Given a *non-simplicial* 2-cell with a discrete vector bundle and connection, we can easily extend the definition of the discrete curvature similarly through a difference of parallel transports along two paths following the boundary of the cell from the evaluation vertex to the cut vertex.

Equation (3.1.7) matches the discrete holonomy expression from Equation (3.1.4). In fact, all three expressions listed in Def. 3.12 are trivial extensions of the definition in Equation (3.1.4): since $\mathcal{R}_{ij} \circ \mathcal{R}_{ji} = \mathrm{Id}_{v_i}$, they are all equivalent up to post-multiplication. Similarly, changing the evaluation fiber to another vertex than v_0 would simply require a pre-multiplication by the accumulated parallel transport from v_0 to the new evaluation fiber. Despite its apparent redundancy, the value of this encoding is in its *summability*: the curvature $2-$form for two adjacent simplices can be summed if their evaluation and cut fibers are the same, resulting in an expression of the curvature on the (now non-simplicial) union still representing the difference in integration of the connection form over two $1-$chains evaluated at the evaluation fiber. Moreover, we will see in the next section that the expressions we propose actually correspond to a particular choice of integration of the curvature $2-$form over $2-$simplices using an ordering induced by a canonical retraction, *putting on a formal footing these seemingly arbitrary expressions*.

3.2 Discrete Bundle-Valued Exterior Calculus

In the preceding chapters, we reviewed the theory and discretization of connections and introduced a combinatorial description of discrete vector bundles and bundle-valued differential forms. While this framework provides a natural discrete analog of the smooth theory, it remains unclear how these discrete objects relate to their continuous counterparts in a manner suitable for analysis and computation.

The first objective of this chapter is therefore to establish a notion of *integration* for bundle-valued differential forms. Unlike the scalar-valued case, the definition of such integrals involves both a choice of connection and a retraction that identifies nearby fibers. For numerical evaluation, these integrals must be expressed in a frame field. However, the resulting values depend sensitively on this choice. A central contribution of this chapter is to show that, for a distinguished class of frame fields, the bundle-valued integral admits a dual formulation that yields a canonical *guidance frame* for discretization.

Along the way, we highlight several fundamental differences between the discrete calculus of scalar-valued forms and its bundle-valued counterpart, stemming from the need to perform fiber-dependent evaluations and parallel transport.

3.2.1 Integration of Bundle-valued forms

We reviewed in Equation 1.5.7 that given a connection ∇ and a path γ, introduces a parallel transport map along between the start and end fiber of the curve. Using these parallel transport maps, we can define a *connection-dependent integration of a bundle-valued* $1-$*form* quite naturally.

Definition 3.14. *Let $\pi : E \to \mathcal{M}$ be a vector bundle over a smooth manifold with connection ∇ and let $\alpha \in \Omega^1(\mathcal{M}; E)$ be a bundle-valued $1-$form. For a curve $\gamma \colon [0,1] \to \mathcal{M}$, we define:*

$$\overset{\nabla}{\underset{\gamma}{\int}} \alpha = \overset{\nabla}{\underset{[0,1]}{\int}} \gamma^* \alpha = \int_0^1 \mathcal{R}_{\gamma,t} \alpha_{\gamma(t)}(\dot{\gamma}(t))\, dt \in E_{\gamma(0)},$$

where $\mathcal{R}_{\gamma,t} \colon E_{\gamma(t)} \to E_{\gamma(0)}$ denotes the parallel transport along γ for a fixed t. We note that the integral gives a vector in the fiber attached to the initial point of the curve γ.

We can further extend this notion of connection-dependent integral $\overset{\nabla}{\int}$ to an arbitrary k-form over a retractable region $S \subset M$: the existence of a connection allows us to define a proper integration through parallel transport to bring the final value to a same "evaluation" vector space, as defined below.

Definition 3.15. *Let $\pi : E \to \mathcal{M}$ be a vector bundle with connection ∇ and let $\alpha \in \Omega^k(\mathcal{M}; E)$ be a bundle-valued k-form. For a region $S \subset \mathcal{M}$, with S homeomorphic to a closed k-dimensional ball, let $\varphi \colon S \to B_k(0) \subset \mathbb{R}^k$ be a homeomorphism from S to the unit k-dimensional ball centered at 0. Furthermore, let $\tilde{\gamma}_{\varphi(v),\varphi(p)} \colon [0,1] \to \varphi(S) = B_k(0)$ be the straight joining path from $\varphi(p)$ to a chosen point $\varphi(v)$ and let $\gamma_{v,p} := \varphi^{-1}(\tilde{\gamma}_{\varphi(v),\varphi(p)}) \colon [0,1] \to S$ be the induced curve in S. For $p \in S$ let*

$$\mathcal{R}_p^{\nabla,\varphi_v} \in \mathrm{Hom}(E_p, E_v) \tag{3.2.1}$$

be the parallel transport along $\gamma_{v,p}$. We denote by $\mathcal{R}^{\varphi_v}$ the induced transport field, i.e., a function mapping a point p to a linear map between E_p and E_v. We define the parameterization-induced connection-dependent integral as

$$\overset{\nabla}{\underset{S}{{}_{\varphi_v}\!\int}} \alpha = \int_S \mathcal{R}^{\nabla,\varphi_v} \alpha \in E_v.$$

If the choice of the parameterization is clear from context, we will suppress the parameterization φ in the notation for the integral and denote the parallel-transport field as $\mathcal{R}^{\nabla,v}$.

The connection-dependent integral can more generally be defined through a smooth strong deformation retraction $\varphi_v \colon [0,1] \times S \to S$ onto $v \in S$, with the path γ defined through $\gamma_p(t) = \varphi_v(1-t, p)$, since φ_v satisfies $\varphi_v(0,p) = p$, $\varphi_v(1,p) = v$, and $\varphi_v(t,v) = v$, see Figure 3.3.

While the above construction provides a well-defined notion of integration for bundle-valued forms, it is à priori unclear how it relates to exterior covariant differentiation. The discrete exterior derivative for scalar-valued forms finds a simple and exact discretization as the coboundary operator in numerical versions of exterior calculus by leveraging Stokes' theorem $\int_S d\cdot = \int_{\partial S} \cdot$, from which ensues a whole discrete de Rham complex [Bos98, DKT08, Arn18]. In our bundle-valued case, finding a discrete version of the exterior covariant derivative d^∇ is more difficult: for a bundle-valued form α, one has to define the discrete equivalent of — and eventually, numerically

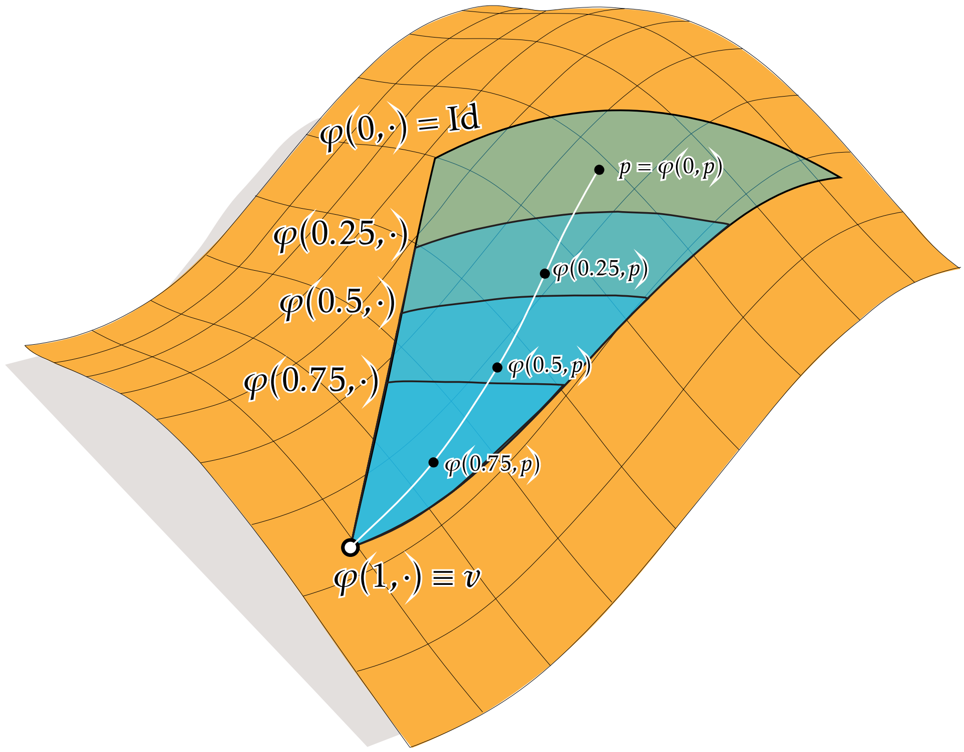

Figure 3.3: **Retraction.** In this illustration, we consider a domain s and demonstrate the retraction of s onto one of its boundary points $v \in s$. For any point $p \in s$, the aforementioned retraction induces radial joining paths from p to v, which can serve as paths for parallel transport from source point p to v. This parallel transport, defined along these paths, can be used subsequently to define the parallel-propagated frame based in v.

evaluate — integrals of the type:

$$\int_S d^\nabla \alpha = \int_S d\alpha + \int_S \omega \wedge \alpha = \int_{\partial S} \alpha + \int_S \omega \wedge \alpha. \tag{3.2.2}$$

Note that such integrals of bundle-valued forms necessitate a *chosen frame field* to be well defined, in contrast to the scalar-valued scenario. Moreover, while Stokes' theorem can be partially leveraged as indicated in Equation (3.2.2), the last term of this equation is particularly difficult to handle: it involves the integration of a wedge product which, even for scalar-based forms, endures severe limitations in the discrete realm [Kot08]. In order to deal with these two issues, we define a specific frame field that will enable a consistent framework for the discretization of bundle-valued exterior calculus with convergence guarantees.

We now present a possibility to define integrate discrete bundle-valued forms, offering a tool that allows us to turn smooth bundle-valued forms into discrete bundle-valued forms.

Designing gauge fields to simplify evaluations. Our approach relies on a simple, but key property afforded by gauge transformations: *there always exists a local frame field with respect to which the connection* $1-$*form is zero at some local point* (see Figure 3.4). As described for instance in [CCL99, Thm 2.1, page 107], given a local connection $1-$form ω, one can always construct a local frame field such that the connection $1-$form $\tilde{\omega}$ after gauge transformation (i.e., expressed in this new frame field) vanishes at a given point $c \in \mathcal{M}$. Therefore, an approach to discretizing expressions such as Equation (3.2.2) — and thus inducing the notion of a discrete (integrated) exterior covariant derivative — is to design an "as-parallel-as-possible" frame field which will render the connection $1-$form ω zero at a point in the simplex (we will use this point to be one of its vertices, or sometimes, its center of mass): indeed, assuming the connection $1-$form is Lipschitz continuous, the use of such a frame field will *bound the value of the last term of Equation (3.2.2)* by the diameter of the simplex — thus *guaranteeing its convergence to zero in the limit of mesh refinement*. Consequently, the integral of the exterior covariant derivative of a bundle-valued form over a simplex evaluated in a properly chosen frame field will be expressible, just like in the scalar-valued case, as *boundary integral values* only. This approach, which recovers Stokes' theorem for flat connections, will be key to *ensure correct numerical evaluation* in the limit of mesh refinement as it will allow us to recover actual continuous values of exterior covariant derivatives of bundle-valued forms.

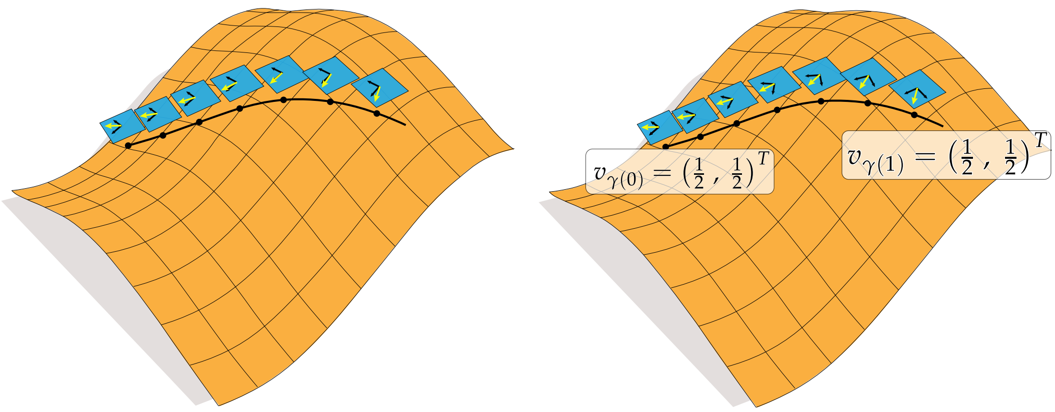

Figure 3.4: We investigate two distinct frame fields on the same vector bundle with an identical connection (E, ∇). The yellow vector is parallel transported by the same parallel transport rule ∇ along the curve. With a local frame construction facilitated by a rotation field R^∇, we can alter both the differential and the connection $1-$form. By employing a parallel-propagated frame field (right), we achieve $\omega^\nabla = 0$ along the curve. To see that, note that the coordinates of the parallel transported vector do not change along the curve. Therefore the matrix representation of the parallel transport is the identity matrix. Hence its logarithm, the connection $1-$form, is zero along the curve. In contrast, when using a non-parallel-propagated frame (left), the connection $1-$form does not vanish along the path. Intuitively, the parallel-propagated frame field on the right "follows" the transport rule. Consequently, $\tilde{\omega}$ vanishes along these radial lines. This behavior highlights the distinctive properties of the two frame fields in terms of their interaction with the bundle's connection.

Parallel-propagating frame fields. To explain more concretely how one can design a frame field that bounds the wedge-product term from Equation (3.2.2), let us go back temporarily to the continuous case, where we can formally construct a notion of parallel-propagated frame field and understand its impact on the evaluation of the integrated exterior covariant derivative. We now formalize this idea by introducing a specific class of frame fields.

Definition 3.16 (Continuous Parallel-Propagated Frame)**.** *Let $\pi : E \to \mathcal{M}$ be a vector bundle with connection ∇. Let $s = [v_0, \dots, v_\ell] \subset \mathcal{M}$ be a region in $\mathcal{M}$ for which there exists a diffeomorphism to an ℓ−simplex $\sigma = [w_0, \dots, w_\ell]$ where each point v_i are mapped to an associated vertex w_i of σ. Let f be a local, arbitrary frame field of E over this region s. For any given corner $v \in \{v_0, \dots, v_\ell\}$, we also define a (strong deformation) retraction $\varphi_v : [0,1] \times s \to s$ derived from a canonical retraction $\varphi_w^\sigma : [0,1] \times \sigma \to \sigma$ of the simplex σ through the aforementioned diffeomorphism, whose retracting paths are radially joining the vertex w associated to point v (see Figure 3.3 for an illustration in 2D); i.e.,*

$$\begin{aligned} \varphi_w^\sigma \colon [0,1] \times \sigma &\to \sigma \\ (t,p) &\mapsto t\,w + (1-t)\,p. \end{aligned} \tag{3.2.3}$$

Moreover, for any point $p \in \sigma$, we denote by $\mathcal{R}^{\nabla,v}(p) \colon E_p \to E_v$ the ∇−induced parallel transport map from E_v to E_p along the path induced by the retraction φ_v and $R^{\nabla,v} \colon \mathbb{R}^r \to \mathbb{R}^r$ the matrix field representing $\mathcal{R}^{\nabla,v}(.)$ in the coordinate frame f.

A frame field $\{f_a^{\nabla,v}\}$ over region s is now called ***parallel-propagated frame field*** *from $v \in M$ if*

$$\mathcal{R}^{\nabla,v}(p) f_a^{\nabla,v}(p) = f_a(v), \quad \text{for all } p \in s, \text{for all } a = 1, \dots, r. \tag{3.2.4}$$

i.e., if the frame $f_a(v)$ at v has been parallel-transported throughout s via the connection ∇. Furthermore, we call $R^{\nabla,v}$ the gauge field *of the parallel-propagated frame field from $v \in M$, see Figure 3.5*

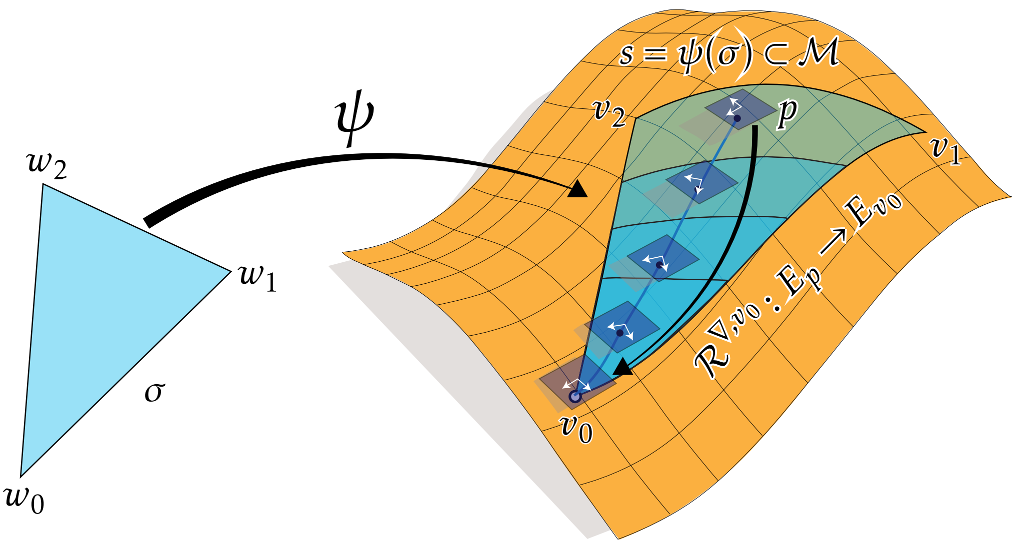

Figure 3.5: **Parallel-propagated frame field.** Given a simplex σ and a diffeomorphism ψ into $\mathcal{M}$, let $s = \psi(\sigma)$. Fix a frame of E at the base vertex v_0 and extend it over s by parallel transport with respect to the connection ∇ along the retraction-induced paths. By construction, transporting the frame at any point $p \in s$ back to v_0 recovers the original frame. The connection 1-form represented in this frame vanishes at the source point v_0.

With this notion of a parallel-propagated field (denoted PPF subsequently for short), we can now define how a form is expressed in such a PPF field:

Definition 3.17. *Using the same setting as in Def. 3.16 we denote the representation $\alpha^{\nabla,v}$ in the PPF from v of an E-valued ℓ−form $\alpha \in \Omega^{\ell}(\mathcal{M};E)$ through:*

$$f_a^{\nabla,v}(\alpha^{\nabla,v})^a = \alpha = f_a\alpha^a = \left(f_b^{\nabla,v}(R^{\nabla,v})_a^b\right)\alpha^a,$$

where α denotes at the same time the ℓ−form and its local expression with respect to the local frame f. We have

$$\alpha^{\nabla,v} = R^{\nabla,v}\alpha. \tag{3.2.5}$$

Similarly, we denote the representation of the local connection 1−form ω (associated with the connection ∇) in the PPF from v undergoing the gauge transformation by

$$\omega^{\nabla,v} = R^{\nabla,v}(\omega - (R^{\nabla,v})^{-1}dR^{\nabla,v})(R^{\nabla,v})^{-1},$$

see Equation (1.5.3).

Remark 3.18. Let us note that a connection-dependent integral can be written in terms of the frames as

$$\underset{s}{\overset{\nabla}{\underset{\varphi_v}{\int}}} \alpha = \int_s \mathcal{R}^{\nabla,v}\alpha = \int_s \mathcal{R}^{\nabla,v}(\alpha^{\nabla,v})^a f_a^{\nabla,v}(p) = \int_s (\alpha^{\nabla,v})^a f_a(v) \in E_v,$$

where we used Equation (3.2.4). Because of the last expression, in our development below, this E_v−valued integral will be often identified with the $\mathbb{R}^r$−valued integral of the local expression $\alpha^{\nabla,v}$, namely, with

$$\int_s \alpha^{\nabla,v} = \int_s R^{\nabla,v}\alpha,$$

see Equation (3.2.5). Here $R^{\nabla,v}$ the matrix of $\mathcal{R}^{\nabla,v}$ with respect to the frame $\{f_a\}$. One passes from one to the other representation by using the frame $\{f_a\}$ at the point v.

Note that with the change of frame field from $\{f_a\}$ to $\{f_a^{\nabla,v}\}$, forms are not the only entities changing: the differential d also changes its coordinate-based expression in the PPF frame accordingly.

It is now a trivial exercise to check that $\omega^{\nabla,v}(v) = 0$, i.e., $\omega^{\nabla,v}$ vanishes at the point v, by construction. Assuming that the curvature 2−form admits a Lipschitz bound, we can thus deduce that $\|\omega^{\nabla,v}\| = \mathcal{O}(h)$ on s, where h is the diameter of the simplicial region s. If we now express the exterior covariant derivative in this novel frame field $\{f_a^{\nabla,v}\}$, as explained in Section 1.5.2, Equation 1.5.9, we obtain with this choice of coordinates the following connection-dependent expression:

$$\left(d^{\nabla}\alpha\right)^{\nabla,v} = d\alpha^{\nabla,v} + \omega^{\nabla,v} \wedge \alpha^{\nabla,v}.$$

We now recall from Def. 3.15 that the connection dependent integral is given by

$$\underset{s}{\overset{\nabla}{\underset{\varphi_v}{\int}}} d^{\nabla}\alpha := \int_s \mathcal{R}^{\nabla,v} d^{\nabla}\alpha \in E_v.$$

As commented above, this E_v−valued integral can be identified with the $\mathbb{R}^r$−valued integral $\int_s (d^{\nabla}\alpha)^{\nabla,v}$, which yields

$$\begin{aligned}\int_s (d^\nabla \alpha)^{\nabla,v} &= \int_s d\alpha^{\nabla,v} + \omega^{\nabla,v} \wedge \alpha^{\nabla,v} = \int_{\partial s} \alpha^{\nabla,v} + \int_s \omega^{\nabla,v} \wedge \alpha^{\nabla,v} \\ &= \int_{\partial s} R^{\nabla,v}\alpha + \int_s \omega^{\nabla,v} \wedge \alpha^{\nabla,v}. \end{aligned} \tag{3.2.6}$$

Given that the volume of s is of order $h^{\ell+1}$, the last term $\int_s \omega^{\nabla,v} \wedge R^{\nabla,v}\alpha$ is of order $\mathcal{O}(h^{\ell+2})$ due to our choice of frame field — thus negligible when analyzing the convergence under refinement of the integrated exterior covariant derivative of the bundle-valued form α. Only the boundary integral term is of order $\mathcal{O}(h^{\ell+1})$ and thus dominates under refinement. It holds

$$\int_s (d^\nabla \alpha)^{\nabla,v} = \int_{\partial s} \alpha^{\nabla,v} + \mathcal{O}(h^{\ell+2}). \tag{3.2.7}$$

Remark 3.19. We introduced in Section 2.2.2 the notion of a geodesic polar map that we used to construct a frame (e_0, e_1). This construction amounts exactly to a parallel-propagated frame based at the vertex of the evaluation domain.

Consequences. From Equation (3.2.6), we notice that we can define a discrete bundle-valued exterior calculus built out of discrete forms which are the integrals of their continuous counterparts evaluated using parallel-propagated frames: once the high-order wedge product term is neglected, we get that the PPF-evaluated integral of the exterior covariant derivative of a form α over a simplex s can be well approximated by PPF-evaluated integrals of the form α over the boundary faces of s — a simple extension of the regular discrete exterior derivative for scalar-based forms defined via Stokes' theorem. The remainder of this paper describes this approach in detail; we will even show that notions that we proposed previously, like the discrete curvature two-form for example, can also be understood in light of this PPF-based calculus, providing a formal link between discrete and continuous calculus.

3.2.2 Revisiting the Discretization of Bundle-valued Forms

While Def. 3.5 formalized a discrete bundle-valued differential form as a collection of abstract maps, we can now express what these maps are in relation to the continuous case. Once this discretization (often referred to the de Rham map for scalar-based discrete exterior calculus [TKB99]) is defined, we can then define a notion of reconstruction which provides a differential form interpolating the discrete mesh values (referred to as the Whitney map in scalar-based discrete exterior calculus [TKB99]).

De Rham map for bundle-valued forms. Based on the continuous retraction explained in Section 3.2.1, the value of a discrete form evaluated on a simplex σ at a vertex v could be defined as the PPF-induced integration of its continuous counterpart form, where a simplicial region s of a continuous manifold is approximated as the simplex σ, i.e.,

$$\boldsymbol{\alpha}(\sigma, v) := \int_s \mathcal{R}^{\nabla,v}\alpha \in E_v. \tag{3.2.8}$$

However, having to store values for each pair of simplex σ and corner vertex v grows rapidly with the dimension of the simplex, and it does not match the number of degrees of freedom of the scalar case of discrete or finite-element exterior calculus.

Instead, we propose to use a *barycenter-based PPF* per simplex, leading to a single value per $\ell-$simplex for an $\ell-$form as conventional discretizations of exterior calculus of scalar-based forms [Bos98, DKT08, Arn18]. Corner evaluations for this simplex can then be achieved through parallel transport $\mathcal{R}_{v,c_s}$ from its barycenter c_s to one of its corners v — which is either evaluated using the continuous parallel transport or approximated using the discrete $1-$connection (through the integral of a least-squares estimate of a linear ω within the simplex or the use of Whitney basis $1-$forms); in this case, the discretization of a bundle-valued form evaluated on a simplex σ at a vertex v becomes:

$$\boldsymbol{\alpha}(\sigma, v) = \mathcal{R}_{v,c_s} \int_s \mathcal{R}^{\nabla,c_s} \alpha \in E_v. \tag{3.2.9}$$

In practice, one could store directly the barycenter-based value, or just one of its derived corner values per simplex σ as all other corner values can be recovered through parallel transport. While these two definitions exactly match for $1-$forms as parallel transport along edges is known (while it has to be interpolated from edge values for higher-order simplices), they differ by $\mathcal{O}(h^{\ell+3})$ for a general $\ell-$dimensional simplicial region s. Note that both definitions are frame-dependent: they rely on a canonical frame field, the PPF. This is a specificity of bundle-valued forms on non-flat manifolds as it involves non-commutative compositions of parallel transport: discretization must account for a particular choice of a local frame field to even make sense. Once these initial simplex values are established via the resulting de Rham maps we just described, the actual continuous manifold can be forgotten as all computations of our discrete calculus will solely use these values of discrete forms.

Whitney map for bundle-valued forms. Given the definition of the de Rham map described above, constructing a Whitney map (mapping all the barycenter-based values of all $\ell-$simplices of a discrete bundle-valued $\ell-$form $\boldsymbol{\alpha}$ to a differential bundle-valued form $\tilde{\alpha}$) is rather simple.

In the scalar valued case, we recall that if we are given a simplex $\tau = [v_0, \ldots, v_m]$ of dimension $m \geq \ell$, we can for a vertex $v_i \in \tau$ define barycentric coordinate functions $\phi_{v_i} : \tau \to [0,1]$ (or Whitney-0-forms) as the unique affine function that is 1 at the vertex v_i and zero at any other vertex. Following [Whi57], we can define the Whitney $\ell-$form associated to the $\ell-$simplex $\sigma = [w_0, \ldots, w_\ell] \subset \tau$ as follows:

$$\phi_\sigma = \ell! \sum_{i=0}^{\ell} (-1)^i \phi_{w_i} \, d\phi_{v_0} \wedge \ldots \wedge \widehat{d\phi_{v_i}} \wedge \ldots \wedge d\phi_{v_\ell}.$$

For a simplex τ of dimension $\dim(\tau) \geq \ell$, let t be the simplicial region that is the image of τ under a diffeomorphism following the conventions in Def. 3.16. Let $\sigma^\ell(\tau)$ be the set of all simplices of dimension ℓ included in τ. The reconstruction of a differential $\ell-$form $\tilde{\alpha}$ expressed in the barycenter-based PPF of τ can be achieved through the weighted sum of the discrete bundle-valued forms for all $\ell-$dimensional simplices $\sigma \in \sigma^\ell(\tau)$. The pointwise evaluation of $\tilde{\alpha}$ for a given point p then depends on the lowest-dimensional simplex τ that contains p: the evaluation of the bundle-valued $\ell-$form $\tilde{\alpha}$ on τ at point $p \in \tau$ given by

$$\tilde{\alpha}_{|_\tau}(p) = \mathcal{R}^{\nabla, c_\tau}(p)^{-1} \sum_{\sigma \in \sigma^\ell(\tau)} \mathcal{R}_{c_\tau, c_\sigma}\, \phi_\sigma(p)\, \boldsymbol{\alpha}(\sigma, c_\sigma) \; \in \Omega^\ell(\tau, E), \tag{3.2.10}$$

where ϕ_σ is the Whitney $\ell-$form associated with σ within τ, and $\mathcal{R}_{c_\tau, c_\sigma}$ is barycenter-to-barycenter parallel transport constructed based on the discrete $1-$form connection. One can check that the de Rham map of a Whitney map of a discrete bundled-valued form is the identity, providing a proper link between continuous and discrete bundle-valued forms: indeed, for a given $\ell-$cell η, the Whitney map for any point p inside η is given by

$$\tilde{\alpha}_p = \mathcal{R}^{\nabla, c_\eta}(p)^{-1} \sum_{\sigma \in \sigma^\ell(\eta)} \mathcal{R}_{c_\eta, c_\sigma}\, \phi_\sigma(p)\, \boldsymbol{\alpha}(\sigma, c_\sigma) = \mathcal{R}^{\nabla, c_\eta}(p)^{-1} \mathcal{R}_{c_\eta, c_\eta}\, \phi_\eta(p)\, \boldsymbol{\alpha}(\eta, c_\eta),$$

since the set of all $\ell-$simplices $\sigma^\ell(\eta)$ is reduced to η for any $p \in \eta$. Therefore, the re-discretization of the Whitney map through the integral in the parallel-propagated frame field yields back the original discrete form.

Remark 3.20. Note that we provide, through Equation 3.2.10, a piecewise expression of the Whitney map to convert the discrete values of $\ell-$simplices into a differential form. This should not be surprising as transitioning between simplices of different dimensions means that the local frame field changes. Consequently, the coordinate representation of the form's evaluation may exhibit jumps across simplices. While readers may find this behavior perplexing, it mirrors the jumping behavior already observed in scalar-valued Whitney forms when changing cells, as only tangential continuity is enforced. Moreover, in our case, we must now also accommodate the varying frame fields, leaving no choice but to use a piecewise definition.

Remark 3.21. It is possible to construct a PPF for any small neighborhood containing multiple simplices with an arbitrary initial local frame field. Indeed, we may consider a geodesic graph with edges connecting the barycenter of each simplex to the barycenter of each of its incident simplices. Picking a seed center c_{σ_0}, we can parallel transport its frame to all the barycenters in the neighborhood through a minimum spanning tree. We then parallel-transport the frames at each barycenter to all the points within the interior of its associated simplex. In this PPF covering the neighborhood (we can make it smooth through convolution with a mollifier if the frame field needs to be continuous), the integral of any $\ell-$form can be assembled through $\mathcal{R}_{c_{\sigma_0}, c_\sigma}\, \alpha(\sigma, c_\sigma)$ with an error of $\mathcal{O}(h^{\ell+2})$ under the assumption of bounded curvature. This allows bundle-valued $\ell-$forms to be locally treated as a vector-valued $\ell-$cochain through integration over an oriented local $\ell-$submanifold discretized as an $\ell-$chain. However, one should note that it is path-dependent on the choice of parallel transport (through a minimum spanning tree in our example), and will not result in a discrete version of Stokes' theorem, as expected from the continuous theory.

3.2.3 Discrete Exterior Covariant Derivative for Bundle-valued Forms

In this section, we formally define our discrete operator for the exterior covariant derivative, in two steps to highlight the similarities and differences with previous work.

Sided Exterior Covariant Derivative. Guided by Equation (3.2.6), Equation (3.2.7) and our meaning of a discrete form from Equation (3.2.8), we first define a discrete operator $\mathfrak{d}^{\boldsymbol{\nabla}}$ which approximates the exterior covariant derivative.

Definition 3.22 (PPF-induced Exterior Covariant Derivative)**.** *Let M be a discrete manifold and $\mathbf{E} \to M$ be a discrete vector bundle with connection $\boldsymbol{\nabla} = \{\mathcal{R}_{ij}\}$. Let $\sigma = [v_0, \dots, v_{\ell+1}]$ be an $(\ell+1)$-simplex and $\boldsymbol{\alpha}$ a discrete $\mathbf{E}$–valued ℓ–form. We define the* sided *discrete exterior derivative of the form $\boldsymbol{\alpha}$ as*

$$\mathfrak{d}^{\boldsymbol{\nabla}}\boldsymbol{\alpha}([v_0, \dots, v_{\ell+1}], v_0) = \mathcal{R}_{0,1}\ \boldsymbol{\alpha}([v_1, \dots, v_{\ell+1}], v_1) + \sum_{i=1}^{\ell+1} (-1)^i \boldsymbol{\alpha}([v_0, \dots, \hat{v}_i, \dots, v_{\ell+1}], v_0). \tag{3.2.11}$$

Remark 3.23. The operator $\mathfrak{d}^{\boldsymbol{\nabla}}$ was already introduced in an equivalent form in [BEHS21] as *the* exterior covariant derivative. One of our contributions is to show that if the discrete form $\boldsymbol{\alpha}$ arises through integration in a vertex-based PPF and the discrete connection $\boldsymbol{\nabla}$ arises through integration from a smooth connection ∇, then this operator approximates the integral in Equation (3.2.6) with

$$\mathfrak{d}^{\boldsymbol{\nabla}}\boldsymbol{\alpha}([v_0, \dots, v_{\ell+1}], v_0) = \int_s \mathcal{R}^{\nabla, v_0}\ d^{\nabla}\alpha + \mathcal{O}(h^{\ell+2})$$

and, thus, converges under refinement. To see this, consider the case of a one-form α and a triangle $\sigma := [v_a, v_b, v_c] \subset M$. From Equation (3.2.6), we know that the integral over σ of the exterior covariant derivative in the PPF based at v_a turns into

$$\int_\sigma R^{\nabla, v_a} d^{\nabla}\alpha = \int_{[v_a, v_b]} R^{\nabla, v_a}\alpha + \int_{[v_b, v_c]} R^{\nabla, v_a}\alpha + \int_{[v_c, v_a]} R^{\nabla, v_a}\alpha + \mathcal{O}(h^3),$$

see Remark 3.18. Def. 3.22 tells us that $\mathfrak{d}^{\boldsymbol{\nabla}}\boldsymbol{\alpha}([v_a, v_b, v_c], v_a) := \mathcal{R}_{v_a v_b}\boldsymbol{\alpha}([v_b, v_c], v_b) - \boldsymbol{\alpha}([v_a, v_c], v_a) + \boldsymbol{\alpha}([v_a, v_b], v_a)$. Since our values from the discrete form $\boldsymbol{\alpha}$ were induced from a v_a–centered PPF, we have

$$\int_{[v_a, v_b]} \mathcal{R}^{\nabla, v_a}\alpha = \boldsymbol{\alpha}([v_a, v_b], v_a) \quad \text{and} \quad \int_{[v_c, v_a]} \mathcal{R}^{\nabla, v_a}\alpha = -\boldsymbol{\alpha}([v_a, v_c], v_a),$$

hence the continuous and discrete definitions match if we can prove that:

$$\mathcal{R}_{v_a, v_b}\boldsymbol{\alpha}([v_b, v_c], v_b) - \int_{[v_b, v_c]} \mathcal{R}^{\nabla, v_a}\alpha = \mathcal{O}(h^3).$$

Indeed, one has:

$$\mathcal{R}_{v_a, v_b}\int_{[v_b, v_c]} \mathcal{R}^{\nabla, v_b}\alpha - \int_{[v_b, v_c]} \mathcal{R}^{\nabla, v_a}\alpha = \int_{[v_b, v_c]} \left(\mathcal{R}_{v_a, v_b}\mathcal{R}^{\nabla, v_b} - \mathcal{R}^{\nabla, v_a}\right)\alpha, \tag{3.2.12}$$

and since for any point p in σ we can build an auxiliary simplex $[v_a, v_b, p]$ such that Equation (3.2.12) turns into an integral of evaluations of discrete curvature expression in the sense of Def. 3.12, we get

$$\left(\mathcal{R}_{v_a, v_b}\mathcal{R}^{\nabla, v_b} - \mathcal{R}^{\nabla, v_a}\right)(p) = \boldsymbol{\Omega}^{\boldsymbol{\nabla}}([v_a, v_b, p], v_a, p)\ \sim\ \mathcal{O}(h^2).$$

Below, we will delve into further detail regarding how the discrete curvature, defined as the difference of parallel transport, accurately approximates the sampled smooth curvature up to order $\mathcal{O}(h^3)$. This analysis will provide justification for the estimation $\mathbf{\Omega}^{\nabla}([v_a, v_b, p], v_a, p) \sim \mathcal{O}(h^2)$.

Hence, the discrete operator $\mathfrak{d}^{\nabla}$ will converge in the limit to the correct pointwise value of the exterior covariant derivative. Note that this argument holds for a form of arbitrary order ℓ: each time, it is the opposite face to the evaluation vertex that needs to be examined to prove the equivalence between discrete and continuous definitions up to $\mathcal{O}(h^{\ell+2})$.

Averaging Derivatives. While we proved the convergence of $\mathfrak{d}^{\nabla}$ to its continuous equivalence, one may note that the order of accuracy is not sufficient to ensure that two consecutive applications of this operator ($\mathfrak{d}^{\nabla} \circ \mathfrak{d}^{\nabla}$) will still converge, which is the real obstacle to establishing the Bianchi identities (Equation (1.5.12) and Equation (1.5.13)). We thus further alter our discrete exterior covariant derivative operator to gain one additional order of accuracy through local averaging, with an operator we denote as the *alternation operator*.

Definition 3.24 (Alternation Operator for Discrete Bundle-Valued Forms)**.** *Let* $\mathbf{E}$ *be a discrete vector bundle with connection* $\nabla = \{\mathcal{R}_{ij}\}_{(ij)\in\mathcal{E}}$ *over a discrete manifold* M*. Let* $\sigma = [v_0, \ldots, v_\ell] \in M$ *be an* ℓ*–simplex. For a discrete* $\mathbf{E}$ *valued* ℓ*–form* $\boldsymbol{\alpha}$ *we define its "alternated" form* $\mathrm{Alt}^{\nabla}(\boldsymbol{\alpha})$ *on* σ *evaluated at* v_0 *via*

$$\mathrm{Alt}^{\nabla}(\boldsymbol{\alpha})([v_0, \ldots, v_\ell], v_0) = \frac{1}{(\ell+1)!} \sum_{\pi \in S_{\ell+1}} \mathrm{sgn}(\pi) \mathcal{R}_{v_0, v_{\pi(0)}} \boldsymbol{\alpha}([v_{\pi(0)}, \ldots, v_{\pi(\ell)}], v_{\pi(0)}).$$

where $S_{\ell+1}$ *is the set of all permutations* π *of the* $(\ell+1)$ *vertices of* σ*.*

Remark 3.25. Note that this operator allows us to transform $\mathfrak{d}^{\nabla}$ so that the second vertex singled out in Equation (3.2.11) of Def. 3.22 no longer plays a distinguished role: the alternation averages all the analogous sided exterior covariant derivative estimates obtained from the remaining vertices. It is worth emphasizing that the alternation operator is purely combinatorial and remains well-defined as a map on abstract bundle-valued forms, requiring neither a metric nor a parallel-propagated frame. When the discrete forms do arise through integration in an appropriate PPF, it is precisely this reshuffling of the sided derivative that secures the improved convergence order under refinement. Moreover, one readily checks that the connection 1-form is stable under this alternation operator.

Remark 3.26. Note that the *alternation of a discrete bundle-valued form* requires a connection to allow for the averaging to be performed in a common fiber, in contrast to the direct symmetrization of the smooth case. It is thus easy to show that in general, $\mathrm{Alt}^{\nabla}(\mathrm{Alt}^{\nabla}(\boldsymbol{\alpha}))(\sigma, v_0) \neq \mathrm{Alt}^{\nabla}(\boldsymbol{\alpha})(\sigma, v_0)$, i.e., the alternation operator is not a projector. However, we preserve the fact that the alternation operator commutes with the pullback of a simplicial map in the sense that $\mathrm{Alt}^{f^*\nabla}(f^*\boldsymbol{\alpha})(\sigma, v_0) = \mathrm{Alt}^{\nabla}(\boldsymbol{\alpha})(f(\sigma), f(v_0))$.

Discrete Exterior Covariant Derivative. We now propose to change the formula of the exterior derivative as follows.

Definition 3.27 (Discrete Bundle-valued Exterior Covariant Derivative)**.** *Let* $\mathbf{E}$ *be a discrete vector bundle with connection* $\boldsymbol{\nabla}$ *over a discrete manifold* M. *Let* $\sigma \subset M$ *with* $\sigma = [v_0, \ldots, v_{\ell+1}]$ *be a* $(\ell+1)$*-simplex. For a discrete vector-valued differential* ℓ*–form* $\boldsymbol{\alpha}$ *we define the discrete exterior covariant derivative with the alternation from Def. 3.24 as*

$$\boldsymbol{d}^{\boldsymbol{\nabla}}\boldsymbol{\alpha}([v_0,\ldots,v_{\ell+1}],v_0) = \mathrm{Alt}^{\boldsymbol{\nabla}}\mathfrak{d}^{\boldsymbol{\nabla}}(\boldsymbol{\alpha})([v_0,\ldots,v_{\ell+1}],v_0).$$

Applying the alternation operator after $\mathfrak{d}^{\boldsymbol{\nabla}}$ removes the arbitrariness of picking the second vertex in the simplex σ in Equation (3.2.11), thus in effect averaging various *sided* exterior covariant derivative estimates of equal approximation order $\mathcal{O}(h^{\ell+2})$. Through the averaging, the resulting discrete exterior covariant derivative gains one order of accuracy, becoming accurate to $\mathcal{O}(h^{\ell+3})$. This accuracy improvement is akin to the accuracy gain one obtains when using centered vs. sided finite difference approximations of derivatives. More precisely, we will show in the convergence proof in Theorem 3.43 that if $\alpha \in \Omega^{\ell}(M,E)$ and $\boldsymbol{\alpha}$ is the associated discrete form as defined in Equation (3.2.8), then the following holds

$$\boldsymbol{d}^{\boldsymbol{\nabla}}\boldsymbol{\alpha}([v_0,\ldots,v_{\ell+1}],v_0) = \mathcal{R}_{v_0,c_s}\int_s \mathcal{R}^{\nabla,c_s}\, d^{\nabla}\alpha + \mathcal{O}(h^{\ell+3}),$$

where c denotes the barycenter of a region. The quantity on the left hand side is still a discrete bundle valued form in the sense of Definition 3.5, however this result shows that if the discrete form $\boldsymbol{\alpha}$ is obtained through discretization in a PPF, the alternation of the sided covariant exterior derivative approximates up to order $\mathcal{O}(h^{\ell+3})$, the integral of the *continuous* covariant exterior derivative in a barycenter-based PPF, transported back to v_0.

3.2.4 Discrete Endomorphism-valued Exterior Covariant Derivative

After defining a discrete exterior covariant derivative applicable to bundle-valued forms in Section 3.2.3, we need to extend this operator to discrete endomorphism-valued forms as well in order to be able to apply it, for instance, to discrete curvatures.

Definition 3.28. *(PPF-induced discrete exterior covariant derivative for endomorphism-valued forms) Let* $\mathbf{E}$ *be a discrete vector bundle over a discrete manifold* M *with connection* $\boldsymbol{\nabla} = \{\mathcal{R}_{ij}\}$. *Let* $\sigma = [v_0,\ldots,v_{\ell+1}] \subset M$ *be a* $(\ell+1)$*-simplex and* $\boldsymbol{\beta}$ *be a discrete* $(1,1)$*-tensor valued* ℓ*–form. Finally, for* $v \in \sigma$, *let* $\sigma_v = [v_0,\ldots,\hat{v},\ldots,v_{\ell+1}]$ *be the simplicial face of* σ *opposite to vertex* v. *We define the PPF-induced discrete exterior covariant derivative on simplex* σ *for* $(1,1)$*-tensor valued forms given an evaluation fiber* $\mathbf{E}_{v_0}$ *and a cut fiber* $\mathbf{E}_{v_{\ell+1}}$ *through:*

$$\begin{aligned}\mathfrak{d}^{\boldsymbol{\nabla}}\boldsymbol{\beta}(\sigma,v_0,v_{\ell+1}) =& \mathcal{R}_{01}\boldsymbol{\beta}(\sigma_{v_0},v_1,v_{\ell+1}) + \sum_{i=1}^{\ell}(-1)^i\boldsymbol{\beta}(\sigma_{v_i},v_0,v_{\ell+1})\\ &+ (-1)^{\ell+1}\boldsymbol{\beta}(\sigma_{v_{\ell+1}},v_0,v_{\ell})\mathcal{R}_{\ell,\ell+1}.\end{aligned}$$

This new definition is simply a variant of Def. 3.22 to account for the two-prong nature of discrete endomorphism-valued forms. It was already proposed, as is, in [BEHS21]; but for the same convergence issues discussed earlier, we must complement this sided definition with a post-alternation to make it useful numerically, which also requires a new definition for the case of $(1,1)$-tensor-valued forms, as given below.

Definition 3.29. *(Alternation Operator for Discrete* $(1,1)$*-tensor-valued Forms) Let* $\mathbf{E}$ *be a discrete vector bundle with connection* $\nabla = \{\mathcal{R}_{ij}\}_{(ij)\in\mathcal{E}}$ *over a discrete manifold* M*. Let* $\sigma = [v_0, \dots, v_\ell] \in M$ *be an* ℓ*–simplex. For a discrete* $(1,1)$*-tensor valued* ℓ*–form* β *we define its "alternated" form* $\mathrm{Alt}^{\nabla}(\beta)$ *for an* ℓ*–form* β *on the simplex* σ *evaluated in* v_0 *with input in* v_ℓ *through*

$$\begin{aligned}
&\mathrm{Alt}^{\nabla}\beta([v_0,\dots,v_\ell],v_0,v_\ell)\\
&\quad= \frac{1}{(\ell+1)!}\sum_{\pi\in S_{\ell+1}}\Bigg(\frac{1+\mathrm{sgn}(\pi)}{2}\mathcal{R}_{v_0,v_{\pi(0)}}\beta([v_{\pi(0)},\dots,v_{\pi(\ell)}],v_{\pi(0)},v_{\pi(\ell)})\mathcal{R}_{v_{\pi(\ell)},v_\ell}\\
&\qquad+\frac{\mathrm{sgn}(\pi)-1}{2}\mathcal{R}_{v_0,v_{\pi(0)}}\beta([v_{\pi(0)},\dots,v_{\pi(\ell)}],v_{\pi(0)},v_{\pi(\ell)})\mathcal{R}_{v_{\pi(\ell)},v_{\pi(\ell-1)}}\mathcal{R}_{v_{\pi(\ell-1)},v_\ell}\Bigg).
\end{aligned}$$

Remark 3.30 (Invariance of the alternation for the curvature form)**.** Note that the curvature form is stable under this definition of the alternation of $(1,1)$-tensor valued forms: for a simplicial cell $\sigma = [abc]$, one can directly check that

$$\begin{aligned}
\mathrm{Alt}^{\nabla}\mathbf{\Omega}^{\nabla}([abc],a,c) &= \frac{1}{6}\Big(\mathbf{\Omega}^{\nabla}([abc],a,c)+R_{ab}\mathbf{\Omega}^{\nabla}([bca],b,a)R_{ac}+R_{ac}\mathbf{\Omega}^{\nabla}([cab],c,b)R_{bc}\\
&\quad-\mathbf{\Omega}^{\nabla}([acb],a,b)R_{bc}-R_{ab}\mathbf{\Omega}^{\nabla}([bac],b,c)-R_{ac}\mathbf{\Omega}^{\nabla}([cba],c,a)R_{ab}R_{bc}\Big)\\
&= \mathbf{\Omega}^{\nabla}([abc],a,c).
\end{aligned}$$

This property would not have held if an average with pre- and post- composition along a joining edge had been used.

From the two operators above, we can now define our discrete exterior covariant derivative for endomorphism-valued forms.

Definition 3.31 (Discrete endomorphism-valued exterior covariant derivative)**.** *Let* $\mathbf{E}$ *be a discrete vector bundle over a discrete manifold* M *with connection* $\nabla = \{\mathcal{R}_{ij}\}$.
Let $\sigma = [v_0,\dots,v_{\ell+1}] \subset M$ *be a* $(\ell+1)$*-simplex and* β *be a discrete* $(1,1)$*-tensor valued* ℓ*–form. We define the discrete exterior covariant derivative on simplex* σ *for* $(1,1)$*-tensor valued forms given an evaluation fiber* $\mathbf{E}_{v_0}$ *and a cut fiber* $\mathbf{E}_{v_{\ell+1}}$ *through:*

$$\boldsymbol{d}^{\nabla}\beta([v_0,\dots,v_{\ell+1}],v_0,v_{\ell+1}) = \mathrm{Alt}^{\nabla}\mathfrak{d}^{\nabla}\beta([v_0,\dots,v_{\ell+1}],v_0,v_{\ell+1}).$$

As we will discuss at length in Section 3.3.2 when we provide numerical tests, our proposed operator for endomorphism-valued forms satisfies our initial goals of proper accuracy order and consistency with the vector-valued case (so that we obtain a discrete algebraic Bianchi identity). However, it is *not* the only definition with these properties: while we average over all possible permutations, one could pick only a subset of permutations (which, in practice, improves the efficiency of the computations). In this case, not all combinatorial properties will be fulfilled. However, the improved order of convergence in the limit can still be maintained.

Remark 3.32. In the smooth setting, d^{∇} for endomorphism valued forms is induced from d^{∇} for vector valued forms by enforcing the Leibniz rule. The discrete $\mathfrak{d}^{\nabla}$ operator of [BEHS21] satisfies this property. We do not explore this relationship further in this work and leave it for future research.

3.2.5 Revisiting Discrete Curvature

The earlier definition of the discrete curvature two-form $\mathbf{\Omega}^{\boldsymbol{\nabla}}$ in Section 3.1.4 was *postulated* directly from a discrete connection $\boldsymbol{\nabla}$ (and its associated connection one-form $\boldsymbol{\omega}$, see Section 3.1.3) as an early example of discrete (1,1)-tensor-valued form: it was obtained by extending the notion of holonomy-based curvature by measuring the difference of parallel transport on two different paths between a "cut" and an "evaluation" fiber. Now that the link between discrete bundle-valued forms and continuous ones through PPF-dependent integration has been established, we revisit this key notion to show that it mirrors the continuous definition of the curvature two-form after a specific contraction-based integration.

Continuous case. We consider a *contractible* two-dimensional region C (assumed, without loss of generality, to be a disk of a smooth manifold M and a vector bundle $\pi : E \to M$ with connection ∇. Given a local frame field $F = \{f_a\}$, the connection can be expressed with the local connection 1−form ω, and the curvature 2−form is locally given as $\Omega^\nabla = d\omega + \omega \wedge \omega$, see Equation (1.5.11). Let us select two points, v and w, on the boundary ∂C of C. The point v corresponds to the evaluation vertex discussed above in the discrete case, while w corresponds to the cut vertex. We denote by $\gamma_{v,w} \subset \partial C$ the path joining v and w along the boundary of C with positive orientation, and by $\gamma'_{v,w}$ the corresponding boundary path with negative orientation, such that $\gamma_{v,w} - \gamma'_{v,w} = \partial C$ (see inset) We proceed by generating a new frame field, denoted as $\{\tilde{f}_a\}$, through parallel transport. The initial frame, $f_a(v)$, situated at vertex v, is transported along two distinct paths: $\gamma_{v,w}$ and $\gamma'_{v,w}$. The discrepancy between the frames, which results at vertex w after the parallel transports, is intricately linked to the holonomy. Extending this frame construction to the interior of C involves a retraction corresponding to a 2D polar (ρ, θ) parametrization of the interior of C: in this parametrization, $\mathbf{e}_\rho$ aligns consistently with the retracted boundary, as depicted in Figure 3.6, with vertex w fixed. From this parametrization, we can construct a new frame field by parallel transporting the boundary frames along the $\mathbf{e}_y$ direction towards the interior of C. This process forms a new frame field, $\tilde{f}_b R^b_a = f_a$, where R denotes the rotation field responsible for adapting vector components from the local frame field $\{f_a\}$ into the new frame field $\tilde{F} = \{\tilde{f}_a\}$.

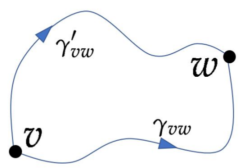

It now holds for the connection 1−form $\tilde{\omega}$ in this new frame field that $\tilde{\omega} = R\omega R^{-1} - (dR)R^{-1}$. Consequently, for any point $p \in C\backslash w$ in the punctured region, one has $\tilde{\omega}_p(e_\rho) = 0$. The curvature form $\tilde{\Omega}^\nabla$ in the new frame field becomes $\tilde{\Omega}^\nabla = R\Omega R^{-1}$ (see Section 1.5). With the components expressed in $\tilde{F}$, one has

$$\widetilde{\Omega}^\nabla = d\tilde{\omega} + \tilde{\omega} \wedge \tilde{\omega}.$$

However in the punctured region $C \setminus w$, $\tilde{\omega} \wedge \tilde{\omega} \equiv 0$, since $\tilde{\omega} \wedge \tilde{\omega}(e_\rho, e_\theta) = \tilde{\omega}(e_\rho)\tilde{\omega}(e_\theta) - \tilde{\omega}(e_\theta)\tilde{\omega}(e_\rho) = 0$ except at the singularity w. Thus, the integral of the curvature becomes:

$$\int_C R\Omega^\nabla R^{-1} = \int_C \widetilde{\Omega}^\nabla = \int_C d\tilde{\omega} + \tilde{\omega} \wedge \tilde{\omega} = \int_{\partial C} \tilde{\omega}. \tag{3.2.13}$$

In other words, the fact that we parallel-propagated the frame $f_a(v)$ at v through retraction proves that the mismatch at w when we parallel transport the frame along the two sides of the boundary from v (which was, in essence, the meaning of our discrete curvature evaluation) is exactly equal to this retraction-induced connection-dependent *integral of the curvature* 2*−form*.

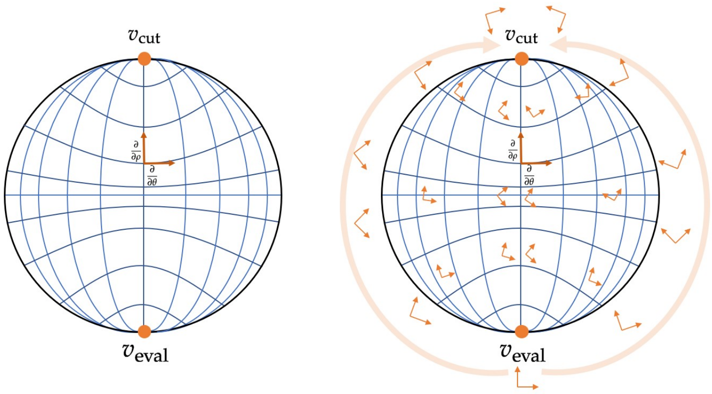

Figure 3.6: **Retraction-based parameterization.** (Left): a retraction of the disk defines a (ρ, θ) parameterization of the (punctured) disk, where the ρ direction is along the retraction direction, while the θ direction corresponds to a transversal direction. (Right): Starting from a parallel-transported frame field F_{eval} from v_{eval} along the boundary, we can parallel-propagate this boundary frame field towards the interior of the punctured disk along the curves corresponding to the y direction of this retraction-based parameterization. The curvature integral simplifies to the discrepancy between frames at v_{cut}, transported from v_{eval} via the retraction, and evaluated in $\mathrm{Hom}(\mathbf{E}_{v_{\mathrm{cut}}}, \mathbf{E}_{v_{\mathrm{eval}}})$.

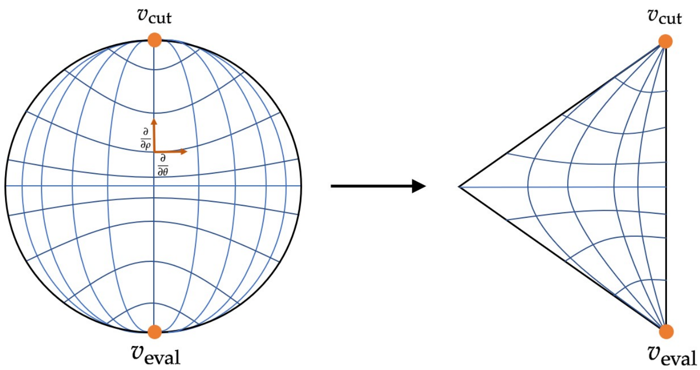

Figure 3.7: **Disk to Triangle.** A parallel-propagated frame over a disc induces a parameterization within the triangle once a homeomorphism to transform the disc into a triangle is defined. We illustrate the resulting parallel-transport paths as images under the homeomorphism map. The integrated curvature in this frame field precisely corresponds to the disparity in parallel transport along the two distinct boundary paths connecting the cut and evaluation fibers.

Consequences for the discrete curvature two-form. The interpretation of the frame mismatch described above brings a series of consequences. First and foremost, it puts our definition of the two-prong discrete curvature 2-form sketched in Section 3.1.4 on solid footing, as the continuous argument above remains valid on a 2-simplex $\sigma = [v, u, w]$. Additionally, it justifies the summability of this definition, in stark contrast to a holonomy-based notion of curvature: if one considers a second simplex $\sigma' = [w, z, v]$ sharing the edge $\{v, w\}$, then $\mathbf{\Omega}^{\nabla}(\sigma, v, w)$ and $\mathbf{\Omega}^{\nabla}(\sigma', v, w)$ can be summed to yield the discrete non-simplicial curvature $\mathbf{\Omega}^{\nabla}(\sigma \cup \sigma', v, w)$: the two canonical simplicial retractions combine into a retraction over their union, so the induced parallel-propagated frame field on each simplex coincides with the one obtained by applying the construction directly to the union cell (see Figure 3.8). Consequently, the two-prong discrete curvature extends without modification to non-simplicial contractible cells, and the sum of two curvatures over a region delimited by a discrete edge path between evaluation and cut vertices arises naturally, as the parallel transports along the shared edge cancel on both sides.

We now show that the two-prong discrete curvature agrees with the pointwise evaluation of the smooth curvature 2-form to order $\mathcal{O}(h^3)$. For a simplex $\sigma = [v_{\text{eval}}, w, v_{\text{cut}}]$, the curvature integral in the parallel-propagated frame reduces to the frame mismatch at v_{cut}:

$$\int_\sigma R\Omega^\nabla R^{-1} = \int_{\partial\sigma} \tilde{\omega} = R_{v_{\text{eval}}w}R_{wv_{\text{cut}}} - R_{v_{\text{eval}},v_{\text{cut}}}.$$

We relate the left-hand side to $\int_\sigma \Omega^\nabla$ by splitting:

$$\int_\sigma R\Omega^\nabla R^{-1} = \int_\sigma (R - \mathrm{Id})\Omega^\nabla R^{-1} + \int_\sigma \Omega^\nabla(R^{-1} - \mathrm{Id}) + \int_\sigma \Omega^\nabla.$$

By construction, $R(v_{\text{eval}}) = \mathrm{Id}$, so $R - \mathrm{Id}$ vanishes at v_{eval} and satisfies $R - \mathrm{Id} = -\tilde{\omega} + \mathcal{O}(h^2)$ via the first-order Taylor expansion of R. Since $\tilde{\omega} = \mathcal{O}(h)$ throughout σ by the PPF construction, and $\mathrm{vol}(\sigma) = \mathcal{O}(h^2)$, a Lipschitz bound on Ω^∇ and R gives:

$$\int_\sigma (R - \mathrm{Id})\Omega^\nabla R^{-1} \in \mathcal{O}(h^3).$$

For the second term, we use the fact that matrix inversion is smooth on $\mathrm{GL}(r)$, with differential

$$0 = d(R^{-1}R) = d(R^{-1})R + R^{-1}\,dR, \qquad \text{i.e.} \quad d(R^{-1}) = -R^{-1}(dR)R^{-1}.$$

Evaluating at the identity gives $d(R^{-1})|_{R=\mathrm{Id}} \cdot \delta R = -\delta R$, so by Taylor expansion:

$$R^{-1} = \mathrm{Id} - (R - \mathrm{Id}) + \mathcal{O}(\|R - \mathrm{Id}\|^2),$$

where the remainder is controlled uniformly for h small, since R remains in a compact neighborhood of Id in $\mathrm{GL}(r)$. Therefore:

$$R^{-1} - \mathrm{Id} = -(R - \mathrm{Id}) + \mathcal{O}(h^2) = \tilde{\omega} + \mathcal{O}(h^2),$$

and the same area-and-Lipschitz argument yields $\int_\sigma \Omega^\nabla(R^{-1} - \mathrm{Id}) \in \mathcal{O}(h^3)$. Hence:

$$\int_\sigma R\Omega^\nabla R^{-1} = \int_\sigma \Omega^\nabla + \mathcal{O}(h^3).$$

Sampling the integrand at v_{eval} then gives

$$\int_\sigma \Omega^\nabla = \Omega^\nabla_{v_{\text{eval}}}(v_{\text{cut}} - v_{\text{eval}}, w - v_{\text{eval}}) + \mathcal{O}(h^3),$$

and combining:

$$\boldsymbol{\Omega}^\nabla(\sigma, v_{\text{eval}}, v_{\text{cut}}) = R_{v_{\text{eval}}w}R_{wv_{\text{cut}}} - R_{v_{\text{eval}}v_{\text{cut}}} = \Omega^\nabla_{v_{\text{eval}}}(v_{\text{cut}} - v_{\text{eval}}, w - v_{\text{eval}}) + \mathcal{O}(h^3). \quad (3.2.14)$$

The $\mathcal{O}(h^3)$ accuracy is therefore a direct consequence of $\tilde{\omega} = \mathcal{O}(h)$ within the simplex. As we show next, switching to a center-based parallel-propagated frame improves $\tilde{\omega}$ to $\mathcal{O}(h^2)$, which propagates through the same argument to yield $\mathcal{O}(h^4)$ accuracy — consistent with the numerical convergence rates observed in Section 3.3.3. For the convergence proofs that follow, however, the key ingredient will be a pointwise bound on the curvature form compared to the parallel transport discrepancy.

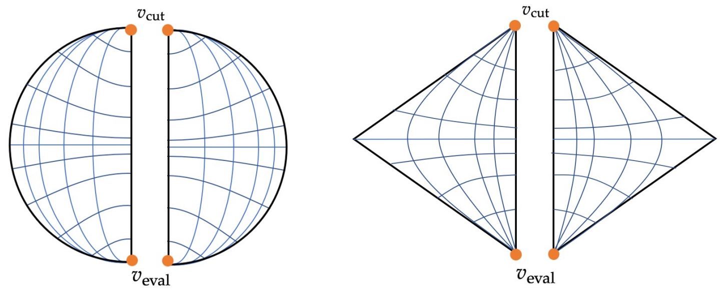

Figure 3.8: **Summing Curvatures.** For two triangles using the same two prongs $(v_{\text{cut}}, v_{\text{eval}})$, the curvature evaluated over their union will be the sum of the curvatures with the same two prongs because the parallel-propagated frames derived from these two prongs properly align.

PPF-induced Discrete Exterior Covariant Derivative for the Connection One Form. When computing the discrete exterior covariant derivative of a vector-valued form, only an evaluation fiber suffices for the definition of a parallel-propagated frame field. However, when dealing with the exterior covariant derivative of the connection 1−form, it becomes necessary to specify both a cut and evaluation fibers since the result is a curvature, i.e., a $(1,1)$-tensor in this particular case. Upon specifying these parameters, we obtain an induced parallel-propagated frame field, as illustrated in Figure 3.6. This reduction leads to the boundary integral:

$$\int_C R\Omega^\nabla R^{-1} = \int_C \widetilde{\Omega}^\nabla = \int_C d\tilde{\omega} + \tilde{\omega} \wedge \tilde{\omega} = \int_{\partial C} \tilde{\omega}.$$

To evaluate the Lie algebra integral, we can treat the columns of the connection 1−form as three independent vector valued 1−forms. This motivates the definition of the PPF-induced exterior covariant derivative, evaluated at v_{eval} and cut at v_{cut}:

$$\mathfrak{d}^\nabla \omega([v_{\text{eval}}, w, v_{\text{cut}}], v_{\text{eval}}, v_{\text{cut}}) := \omega_{v_{\text{eval}},w} + \mathcal{R}_{w,v_{\text{eval}}} \omega_{w,v_{\text{cut}}} - \omega_{v_{\text{eval}},v_{\text{cut}}},$$

for a given discrete connection $\boldsymbol{\nabla}$ with discrete connection form $\boldsymbol{\omega}$.

Note that this PPF-induced discrete exterior covariant derivative shares a resemblance with the vector-valued one, akin to the smooth case: by regarding the matrix of the discrete connection 1−form as a set of r vector-valued differential forms, the PPF-induced discrete exterior covariant derivative manifests as a vector-valued discrete exterior covariant derivative on these vector components. The case of the connection 1−form is, however, special: the exterior covariant derivative of the connection 1−form is not a Lie-algebra valued quantity anymore, but a $(1,1)$-tensor valued 2−form instead, necessitating in the discrete case the addition of a choice of "cut fiber". Using the definition of the discrete connection 1−form, see Equation (3.1.3), we obtain that indeed:

$$\begin{aligned}
&\mathfrak{d}^\nabla \omega([v_{\text{eval}}, w, v_{\text{cut}}], v_{\text{eval}}, v_{\text{cut}}) && (3.2.15)\\
&= (\mathcal{R}_{v_{\text{eval}},w} - \text{Id}) + \mathcal{R}_{v_{\text{eval}},w}(\mathcal{R}_{w,v_{\text{cut}}} - \text{Id}) - (\mathcal{R}_{v_{\text{eval}},v_{\text{cut}}} - \text{Id})\\
&= \mathcal{R}_{v_{\text{eval}},w}\mathcal{R}_{w,\text{cut}} - \mathcal{R}_{v_{\text{eval}},v_{\text{cut}}} = \boldsymbol{\Omega}^\nabla([v_{\text{eval}}, w, v_{\text{cut}}], v_{\text{eval}}, v_{\text{cut}}), && (3.2.16)
\end{aligned}$$

justifying, a posteriori, our definition of discrete curvature.

3.3 Properties and Convergence of our Discrete Operators

In the previous sections, we introduced a discrete calculus for discrete bundle-valued forms in a principled manner, based on parallel-propagated frames. We now shift our focus towards discussing the resulting properties of our discrete operators, before analyzing their convergence under refinement. We will then provide quantitative evidence through numerical tests to verify our claims, both in terms of properties and of convergence order.

3.3.1 Properties of the Discrete Exterior Derivative

The discrete exterior covariant derivative $\boldsymbol{d}^{\nabla}$ introduced in Def. 3.27 has several intrinsic properties, and as it differs from the operator introduced by [BEHS21] mostly through a post alternation, it also inherits combinatorial properties proven in [BEHS21]. We review them next.

Naturality of $\boldsymbol{d}^{\nabla}$. As mentioned in Equation (1.5.10), it is an important result in the theory of smooth exterior calculus that the pullback commutes with the exterior derivative. For the discrete operator $\boldsymbol{d}^{\nabla}$, a similar result holds true due to a lemma proven in [BEHS21].

Lemma 3.33 (Pullback commutes with $\mathfrak{d}^{\nabla}$, from [BEHS21])**.** *Given a simplicial map $f : M \to N$ between two discrete manifolds M and N, and a discrete vector bundle with connection $(\mathbf{E}, \boldsymbol{\nabla})$ over N, let $\boldsymbol{\alpha}$ be an $\mathbf{E}$–valued discrete ℓ–form. For a $(\ell+1)$-simplex $\sigma = [v_0, \ldots, v_{\ell+1}]$ of M, one has:*

$$f^*(\mathfrak{d}^{\nabla}\boldsymbol{\alpha})(\sigma, v_0) = \mathfrak{d}^{f^*\nabla} f^*\boldsymbol{\alpha}(f(\sigma), f(v_0))$$

Corollary 3.34 (Naturality of $\boldsymbol{d}^{\nabla}$)**.** *Given a simplicial map $f : M \to N$ between two discrete manifolds M and N, and a discrete vector bundle with connection $(\mathbf{E}, \boldsymbol{\nabla})$ over N, let α be an $\mathbf{E}$–valued discrete ℓ–form. For a $(\ell+1)$-simplex $\sigma = [v_0, \ldots, v_{\ell+1}]$ of M, one has:*

$$f^*(\boldsymbol{d}^{\nabla}\alpha)(\sigma, v_0) = \boldsymbol{d}^{f^*\nabla} f^*\alpha(f(\sigma), f(v_0))$$

Proof. This is a direct consequence of the previous lemma and the fact that the pullback commutes with the alternation operator as mentioned in Rem. 3.26. □

Antisymmetry of $\boldsymbol{d}^{\nabla}$. In the scalar-valued case, discrete differential forms are skew-symmetric maps, in the sense that permuting the vertices of an evaluation simplex leads to multiplication with the sign of the permutation. In the bundle-valued case, discrete differential forms are defined as abstract maps mapping into a vertex fiber of a given cell. Therefore, our operator is antisymmetric *as long as we keep the evaluation fiber fixed*, since any switch of two vertices will result in a sign flip in the evaluation of $\boldsymbol{d}^{\nabla}$ due to the alternation within its definition.

Differential Bianchi identity. The celebrated second Bianchi identity reviewed in Equation (1.5.13) holds exactly in the discrete setting.

Proposition 3.35 (Differential Bianchi identity)**.** *Let* $\mathbf{E}$ *be a discrete vector bundle with connection* ∇ *over a discrete manifold M. For any* 3*–simplex* $\sigma = [v_0, v_1, v_2, v_3] \subset M$*. One has:*

$$\boldsymbol{d}^{\nabla}\boldsymbol{\Omega}^{\nabla}(\sigma, v_0, v_3) = 0 \tag{3.3.1}$$

Proof. As proven in [BEHS21], we know that $\mathfrak{d}^{\nabla}\boldsymbol{\Omega}^{\nabla}(\sigma, v_0, v_3) = 0$. Therefore,

$$\boldsymbol{d}^{\nabla}\boldsymbol{\Omega}^{\nabla}(\sigma, v_0, v_3) = \mathrm{Alt}^{\nabla}\mathfrak{d}^{\nabla}\boldsymbol{\Omega}^{\nabla}(\sigma, v_0, v_3) = 0.$$

□

Algebraic Bianchi identity. The algebraic Bianchi identity, reviewed in Equation (1.5.18), also holds in our discrete calculus. While [BEHS21] showed that their exterior covariant derivative satisfies

$$\mathfrak{d}^{\nabla}\mathfrak{d}^{\nabla}\boldsymbol{\alpha}([v_0, \ldots, v_{\ell+2}], v_0) = \boldsymbol{\Omega}^{\nabla}([v_0, v_1, v_2], v_0, v_2)\, \boldsymbol{\alpha}([v_2, \ldots, v_{\ell+2}], v_2)$$

for any vector-valued form $\boldsymbol{\alpha}$, our discrete exterior covariant derivative satisfies the algebraic Bianchi identity for an implicitly-defined combinatorial wedge product.

Definition and Theorem 3.36 (Algebraic Bianchi Identity)**.** *Let M be a discrete manifold with a discrete bundle* $\mathbf{E}$ *and connection* ∇*. Further let* $\boldsymbol{\alpha}$ *be a discrete* $\mathbf{E}$*–valued* ℓ*–form and* $\sigma = [v_0, \ldots, v_{\ell+2}]$ *a* $(\ell+2)$*-simplex. In this case there exists a set* $K \subseteq C^2(\sigma) \times C^{\ell}(\sigma)$ *consisting of* 2*– and* ℓ*–subcells of* σ *such that for all* $(m, \kappa) \in K$ *with a shared vertex* $w_{m,\kappa}$ *we have*

$$\begin{aligned}\boldsymbol{d}^{\nabla}\boldsymbol{d}^{\nabla}\boldsymbol{\alpha}(\sigma, v_0) &= \frac{1}{(\ell+3)!\,(\ell+2)!}\sum_{(m,\kappa)\in K}\boldsymbol{\Omega}^{\nabla}(f, v_0, w_{m,\kappa})\,\boldsymbol{\alpha}(\kappa, w_{m,\kappa})\\ &=: \boldsymbol{\Omega}^{\nabla}\wedge\boldsymbol{\alpha}(s, v_0),\end{aligned}$$

where the sum defines implicitly a wedge product *between the curvature* 2*–form and* $\boldsymbol{\alpha}$*, reminiscent of scalar-based wedge products defined through cup products [Hir03]. Similarly, for any* $(1,1)$*-tensor-valued* ℓ*–form* $\boldsymbol{\beta}$*, two consecutive applications of our discrete exterior covariant derivative* $\mathbf{d}^{\nabla}$ *yield implicitly a discrete commutator:*

$$\boldsymbol{d}^{\nabla}\boldsymbol{d}^{\nabla}\boldsymbol{\beta} = [\boldsymbol{\Omega}^{\nabla}\wedge\boldsymbol{\beta}].$$

Proof. For discrete $(1,0)$-tensor valued forms, see App. B. The case of discrete $(1,1)$-tensor valued forms is similar — but for an evaluation fiber $\mathbf{E}_{v_0}$ and a cut fiber $\mathbf{E}_{v_{\ell+2}}$ one has:

$$\begin{aligned}&\mathfrak{d}^{\nabla}\mathfrak{d}^{\nabla}\boldsymbol{\beta}([v_0, \ldots, v_{\ell+2}], v_0, v_{\ell+2})\\ &= \boldsymbol{\Omega}^{\nabla}([v_0, v_1, v_2], v_0, v_2)\boldsymbol{\beta}([v_2, \ldots, v_{\ell+2}], v_2, v_{\ell+2})\\ &\qquad - \boldsymbol{\beta}([v_0, \ldots, v_{\ell}], v_0, v_{\ell})\boldsymbol{\Omega}^{\nabla}([v_{\ell}, v_{\ell+1}, v_{\ell+2}], v_{\ell}, v_{\ell+2}),\end{aligned}$$

hence the resulting commutator. □

Remark 3.37. In the realm of scalar-valued DEC, Kotiuga [Kot08] established theoretical limitations regarding the definition of a discrete scalar-valued wedge product. However, associativity of the wedge product is not an issue in our context, as there is no inherent product structure on the bundle; and graded anti-commutativity is irrelevant given the non-commutative nature of the underlying product for $(1, 1)$-tensors, and vectors.

Since the operator $\boldsymbol{d}^{\nabla}$ is a well defined map between the set of bundle valued differential ℓ-forms and $(\ell + 1)$-forms, its composition is associative, thus it holds

$$\boldsymbol{d}^{\nabla} \circ (\boldsymbol{d}^{\nabla} \circ \boldsymbol{d}^{\nabla}) = (\boldsymbol{d}^{\nabla} \circ \boldsymbol{d}^{\nabla}) \circ \boldsymbol{d}^{\nabla}.$$

By the implicit definition of the wedge product, this yields for any general discrete bundle valued form $\boldsymbol{\alpha}$

$$\boldsymbol{d}^{\nabla}(\boldsymbol{\Omega}^{\nabla} \wedge \boldsymbol{\alpha}) = \boldsymbol{\Omega}^{\nabla} \wedge \boldsymbol{d}^{\nabla}\boldsymbol{\alpha}. \tag{3.3.2}$$

We emphasize that the wedge product defined above is only defined for the curvature $2-$form and a vector valued $\ell-$form. It is not a general discrete wedge product, since it is defined implicitly by applying d^{∇} twice to a vector bundle valued ℓ-form. There are physical theories where a more general product is required. However the observation in Equation (3.3.2) shows us that the operator is structure preserving in the sense that it satisfies the Leibniz rule

$$\boldsymbol{d}^{\nabla}(\boldsymbol{\Omega}^{\nabla} \wedge \boldsymbol{\alpha}) = \underbrace{\boldsymbol{d}^{\nabla}\boldsymbol{\Omega}^{\nabla}}_{\substack{=\boldsymbol{0} \\ \text{differential Bianchi identity}}} \wedge \boldsymbol{\alpha} + (-1)^2 \boldsymbol{\Omega}^{\nabla} \wedge \boldsymbol{d}^{\nabla}\boldsymbol{\alpha} = \boldsymbol{\Omega}^{\nabla} \wedge \boldsymbol{d}^{\nabla}\boldsymbol{\alpha}.$$

However we will demonstrate, in Section 3.3.3 that our discrete wedge product converges under refinement toward the smooth wedge product when applied to the proper discretization of a smooth form — unlike the definition given in [BEHS21] as they did not properly relate discrete and continuous bundle-valued forms, see Figure 3.12.

Remark 3.38. Given a connection $\boldsymbol{\nabla} = \{\mathcal{R}_{ab}\}_{e_{ab} \in \mathcal{E}}$ and an arbitrary choice of frame field, the discrete connection $1-$form for the edge between vertices a and b is given by $\boldsymbol{\omega}_{ab} = R_{ab} - \mathrm{Id}$. Furthermore, we saw in Equation (3.2.16) that

$$\mathfrak{d}^{\nabla}\omega([abc], a, c) = \boldsymbol{\Omega}^{\nabla}([abc], a, c).$$

Hence, with our alternation operator for $(1, 1)$-tensor based forms and the stability of $\boldsymbol{\Omega}^{\nabla}$ under the Alt operator (see Rem. 3.30), it holds that

$$\boldsymbol{d}^{\nabla}\omega([abc], a, c) = \boldsymbol{\Omega}^{\nabla}([abc], a, c), \tag{3.3.3}$$

in an exact sense. However it should be noted that the use of $\boldsymbol{d}^{\nabla}$ above is slightly abusive: it is neither the discrete exterior covariant derivative of a $(1, 0)$-tensor valued form, nor of a $(1, 1)$-tensor valued form. Instead, it is made out of the composition of a PPF-induced exterior covariant derivative for $(1, 0)$-tensor valued form applied to ω, composed with the alternation operator for $(1, 1)$-tensor valued forms. This *hybrid* operator is specific to the connection $1-$form and reflects the special and local nature of the curvature form in the continuous case.

We should also mention here that our linearized version of the matrix logarithm used in the definition of the discrete connection $1-$form is crucial to ensure that this property holds (see

Rem. 3.10). Finally, we proved that $\boldsymbol{d}^{\nabla}\boldsymbol{d}^{\nabla} = \boldsymbol{\Omega}^{\nabla}\wedge$ for any vector-valued form, and one can check that indeed, for a discrete vector-valued $0-$form $\mathbf{z}$, we have:

$$\begin{aligned}
&\boldsymbol{d}^{\nabla}\boldsymbol{d}^{\nabla}\mathbf{z}([abc],a) \\
&\qquad = \frac{1}{6}\Big((R_{ab}R_{bc} - R_{ac})z_c + R_{ab}(R_{bc}R_{ca} - R_{ba})z_a + R_{ac}(R_{ca}R_{ab} - R_{cb})z_b \\
&\qquad\quad - (R_{ac}R_{cb} - R_{ab})z_b - R_{ab}(R_{ba}R_{ac} - R_{bc})z_c - R_{ac}(R_{cb}R_{ba} - R_{ca})z_a\Big).
\end{aligned}$$

Note that this wedge product between the curvature $2-$ form and a vector-valued $0-$form does *not* correspond to a simple pointwise product as in the continuous case: this property will only be valid in the limit of mesh refinement.

3.3.2 Convergence analysis

In Section 3.2.1, we introduced the use of parallel-propagated frame fields to simplify the high-order terms of the integral of the discrete exterior covariant derivative. In this section, we discuss how the order of approximation is affected by the location of the *origin* of the PPF being used: indeed, if we integrate the exterior derivative in a center-based parallel-propagated frame field, we achieve an even higher accuracy order than using a corner-based PPF.

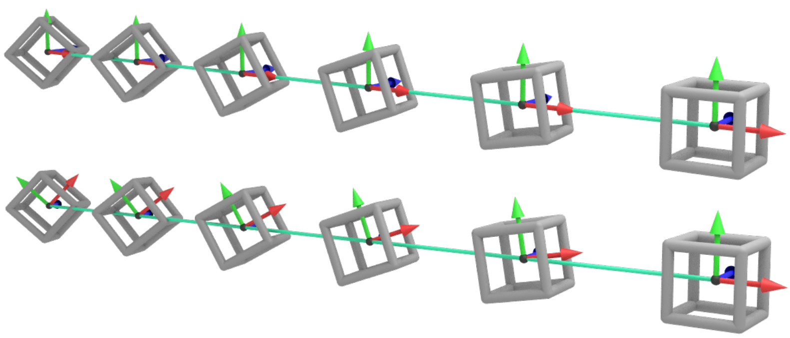

Figure 3.9: **Parallel-propagated frames.** Given a connection, we can use the parallel-propagated frame on TM (bottom) for integration; integration in some non-parallel-propagated/non-geometric frame (like the one on top) does not lead to convergence.

Theorem 3.39 (Improved accuracy with center-based PPF)**.** *Let $\pi : E \to \mathcal{M}$ be a vector bundle with connection ∇. Let $s = [v_0, \ldots, v_{\ell+1}] \subset \mathcal{M}$ be a region in $\mathcal{M}$ for which there exists a diffeomorphism to a $(\ell+1)-$simplex σ where each point v_i is mapped to an associated vertex w_i of σ, and let us call the "center" $c_s \in s$ the point of s being mapped to the barycenter of σ. For $\alpha \in \Omega^{\ell}(\mathcal{M}, E)$ it holds that*

$$\int_s (d^{\nabla}\alpha)^{\nabla,c_s} = \int_{\partial s} \alpha^{\nabla,c_s} + \mathcal{O}(h^{\ell+3})$$

(compare with Equation (3.2.7)).

Proof. It holds in the center-based PPF that

$$\int_s (d^\nabla \alpha)^{\nabla,c_s} = \int_{\partial s} \alpha^{\nabla,c_s} + \int_s \omega^{\nabla,c_s} \wedge \alpha^{\nabla,c_s}.$$

Additionally, one has

$$\int_s \omega^{\nabla,c_s} \wedge \alpha^{\nabla,c_s} = \mathcal{O}(h^{\ell+3})$$

since the integral of the linear part cancels out when the center verifies $\omega^{\nabla,c_s}(c_s) = 0$. To see this, we consider a Taylor expansion of ω^{∇,c_s} and α. It holds for $p \in s$

$$\left(\omega^{\nabla,c_s}\right)_p = \underbrace{\left(\omega^{\nabla,c_s}\right)_{c_s}}_{=0} + \left(\omega^{\nabla,c_s}\right)'_{c_s}(p - c_s) + \mathcal{O}(h^2),$$

where of $(\omega^{\nabla,c_s})'$ is to be understood as a derivative applied to the components of ω^{∇,c_s}. Assuming sufficient smoothness, we get that $(\omega^{\nabla,c_s})'$ is still a smooth $1-$form. Similarly, we obtain

$$\alpha_p^{\nabla,c_s} = \alpha_{c_s}^{\nabla,c_s} + (\alpha^{\nabla,c_s})'_{c_s}(p - c_s) + \mathcal{O}(h^2).$$

Hence

$$\begin{aligned} \left\| \int_s \omega^{\nabla,c_s} \wedge \alpha^{\nabla,c_s} \right\| \leq& \left\| \int_{p \in s} ((\omega^{\nabla,c_s})'_{c_s} \wedge \alpha_{c_s}^{\nabla,c_s})(c_s - p) dp \right\| \\ &+ \underbrace{\left\| \int_s ((\omega^{\nabla,c_s})'_{c_s} \wedge (\alpha^{\nabla,c_s})'_{c_s}) \right\|}_{=\mathcal{O}(h^{\ell+1})} \cdot \mathcal{O}(h^2) + \mathcal{O}(h^{\ell+3}). \end{aligned}$$

Since $(\omega^{\nabla,c_s})'_{c_s} \wedge \alpha_{c_s}^{\nabla,c_s}$ is constant over s, we get that

$$\int_{p \in s} ((\omega^{\nabla,c_s})'_{c_s} \wedge (\alpha^{\nabla,c_s})_{c_s})(c_s - p) dp = 0, \tag{3.3.4}$$

leaving us with $\left\| \int_s \omega^{\nabla,c_s} \wedge \alpha^{\nabla,c_s} \right\| = \mathcal{O}(h^{\ell+3})$. □

Remark 3.40. The argumentation shows that the key property of the barycenter based PPF is the cancellation of the linear term in Equation (3.3.4). Later in this work in Chapter 4 when we will extend the discrete exterior covariant derivative to non-simplicial cells, we cannot pick the centroid of the cell anymore to ensure the required cancellation. To ensure the cancellation in Equation (3.3.4), we will require a *center-of-mass-based PPF*. Generally the center of mass of a region s is defined as

$$c_s = \frac{1}{\mathrm{vol}(s)} \int_{p \in s} p dp.$$

Thus a center based PPF in the following is to be understood as a center of mass based PPF. For a simplicial cell the center of mass and the centroid are identical, but for general cells that is no longer true.

Theorem 3.41. *Let $\pi : E \to \mathcal{M}$ be a vector bundle with connection ∇. Let $s = [v_0, \ldots, v_{\ell+1}] \subset \mathcal{M}$ be a region in $\mathcal{M}$ for which there exists a diffeomorphism ψ to a $(\ell+1)$-simplex σ where each point v_i are mapped to an associated vertex w_i of σ. Further let $\alpha \in \Omega^\ell(\mathcal{M}, E)$ and $\boldsymbol{\alpha}$ be its discretization defined in Equation (3.2.8). In this case we have*

$$R_{v_0,c_s} \int_s (d^\nabla \alpha)^{\nabla,c_s} = \mathfrak{d}^\nabla \boldsymbol{\alpha}(s, v_0) + \mathcal{O}(h^{\ell+2}), \tag{3.3.5}$$

or expressed intrinsically,

$$\mathcal{R}_{v_0,c_s} {}_{\varphi_{c_s}}\!\overset{\nabla}{\int_s} d^\nabla \alpha = \mathfrak{d}^\nabla \boldsymbol{\alpha}(s, v_0) + \mathcal{O}(h^{\ell+2}). \tag{3.3.6}$$

Proof. We use the identifications stated in Remark 3.18. It holds in the center-based parallel-propagated frame that

$$R_{v_0,c_s} \int_s (d^\nabla \alpha)^{\nabla,c_s} = R_{v_0,c_s} \int_{\partial s} R_{c_s} \alpha + R_{v_0,c_s} \int_s \omega^{\nabla,c_s} \wedge R_{c_s} \alpha. \tag{3.3.7}$$

As discussed above, we know

$$\int_s \omega^{\nabla,c_s} \wedge \alpha^{\nabla,c_s} = \mathcal{O}(h^{\ell+3}).$$

In the following we denote $s_i = [v_0, \ldots, \hat{v}_i, \ldots, v_{\ell+1}]$ the ℓ–subsimplex of s without v_i. By m_i we will denote the ℓ–simplex opposite to v_i with *positive* orientation relative to that of s, i.e., $m_i = (-1)^i s_i$. Extending the discrete $\boldsymbol{\alpha}$ to m_i by $\boldsymbol{\alpha}(m_i, v_0) = (-1)^i\, \boldsymbol{\alpha}(s_i, v_0)$, we have

$$\mathfrak{d}^\nabla \boldsymbol{\alpha}(s, v_0) = R_{v_0,v_1}\, \boldsymbol{\alpha}(s_0, v_1) + \sum_{i=1}^{\ell+1} (-1)^i\, \boldsymbol{\alpha}(s_i, v_0) = R_{v_0,v_1}\, \boldsymbol{\alpha}(m_0, v_1) + \sum_{i=1}^{\ell+1} \boldsymbol{\alpha}(m_i, v_0).$$

For all faces containing v_0, we have by definition

$$\boldsymbol{\alpha}(m_i, v_0) = \int_{m_i} R^{\nabla,v_0} \alpha.$$

If we compare the contribution of the PPF-derivative to the contribution from the boundary integral in Equation (3.3.7) coming from m_0, we obtain

$$R_{v_0,c_s} \int_{m_0} R^{\nabla,c_s} \alpha - R_{v_0,v_1} \int_{m_0} R^{\nabla,v_1} \alpha = \int_{m_0} (R_{v_0,c_s} R^{\nabla,c_s} - R_{v_0,v_1} R^{\nabla,v_1}) \alpha. \tag{3.3.8}$$

If we consider the expression

$$R_{v_0,c_s} R_{c_s,p} - R_{v_0,v_1} R_{v_1,p} = (R_{v_0,c_s} R_{c_s,p} - R_{v_0,p}) - (R_{v_0,v_1} R_{v_1,p} - R_{v_0,p}),$$

we can express this, following Equation 3.2.14, as

$$(R_{v_0,c_s} R_{c_s,p} - R_{v_0,p}) - (R_{v_0,v_1} R_{v_1,p} - R_{v_0,p}) = \Omega^\nabla_{v_0}(v_0 - p, v_0 - c_s) - \Omega^\nabla_{v_0}(v_0 - p, v_0 - v_1) + \mathcal{O}(h^3),$$

where h is the triangle diameter.

We define the auxiliary function

$$g\colon \psi(m_0) \to \mathbb{R}^{r\times r}\colon p \mapsto \Omega^{\nabla}_{v_0}(v_0 - p, v_0 - c_s) - \Omega^{\nabla}_{v_0}(v_0 - p, v_0 - v_1)$$

Note that g is affine linear in p, thus the second order derivatives vanish. If we do a Taylor expansion of g at c_{m_0}, note that $c_s - v_0$ and $c_{m_0} - v_0$ are collinar. Hence,

$$\Omega^{\nabla}_{v_0}(v_0 - c_m, v_0 - c_s) = 0.$$

Further note that we have for the gradient

$$Dg_{c_m} = \Omega^{\nabla}(v_0 - v_1, \cdot) - \Omega^{\nabla}(v_0 - c_s, \cdot) = \Omega^{\nabla}(c_s - v_1, \cdot).$$

Since we always implicitly assume that the curvature is sufficiently regular and $(v_s - v_1) \in \mathcal{O}(h)$, it follows that $Dg \in \mathcal{O}(h)$. As in the proof of Definition 3.39 we can expand the differential form α as

$$\alpha_p = \alpha_{c_m} + (\alpha)'_{c_m}(p - c_{m_0}) + \mathcal{O}(h^2).$$

Therefore we have

$$\begin{aligned}
&\int_{m_0} (R_{v_0,c_s} R^{\nabla,c_s} - R_{v_0,v_1} R^{\nabla,v_1})\alpha = \int_{m_0} g\alpha + \mathcal{O}(h^{\ell+3}) \\
&= \int_{m_0} \Big(g_{c_{m_0}} + (g_{c_{m_0}})'(p - c_m)\Big) + \Big(\alpha_{c_{m_0}} + (\alpha_{c_{m_0}})'(p - c_{m_0}) +\Big) + \mathcal{O}(h^{\ell+3})
\end{aligned}$$

Let $\alpha_{c_{m_0}}[m_0]$ be the evaluation of α at c_{m_0} on the stencil spanning the tangent space of m_0 in the sense of Definition 1.2. Since $(\alpha_{c_{m_0}})'$ and $(g_{c_{m_0}})$ are constant, we can rewrite the integral as

$$\begin{aligned}
&\int_{m_0} (R_{v_0,c_s} R^{\nabla,c_s} - R_{v_0,v_1} R^{\nabla,v_1})\alpha = \int_{m_0} g\alpha + \mathcal{O}(h^{\ell+3}) \\
&= \int_{m_0} \Big(g_{c_{m_0}} + (g_{c_{m_0}})'(p - c_m)\Big) + \Big(\alpha_{c_{m_0}} + (\alpha_{c_{m_0}})'(p - c_{m_0})\Big) + \mathcal{O}(h^{\ell+3}) \\
&= g_{c_{m_0}} \alpha_{c_{m_0}}[m_0] + g_{c_{m_0}} (\alpha_{c_{m_0}})' \underbrace{\int_{m_0} (p - c_{m_0})}_{=0} + (g_{c_{m_0}})'(\alpha_{c_{m_0}}) \underbrace{\int_{m_0} (p - c_{m_0})}_{=0} \\
&\quad + \underbrace{(g_{c_{m_0}})'}_{\in\mathcal{O}(h)} \underbrace{\int_{m_0} (\alpha_{c_{m_0}})'(p - c_{m_0})(p - c_{m_0})}_{\in\mathcal{O}(h^{\ell+2})} + \mathcal{O}(h^{\ell+3}) \\
&= \Omega^{\nabla}_{v_0}(v_0 - c_{m_0}, v_0 - v_1)\alpha_{c_{m_0}}[m_0] + \mathcal{O}(h^{\ell+3})
\end{aligned}$$

For a positively oriented face $m \in \partial s$ that contains v_0, we obtain

$$\int_m \Big(R_{v_0,c_s} R^{\nabla,c_s} - R_{v_0,c_m} R^{\nabla,c_m}\Big)\alpha = \int_m \Big(\Big(R_{v_0,c_s} R^{\nabla,c_s} - R^{\nabla,v_0}\Big) - \Big(R_{v_0,c_m} R^{\nabla,c_m} - R^{\nabla,v_0}\Big)\Big)\alpha.$$

Using Equation 3.2.14, we obtain

$$\Big(\big(R_{v_0,c_s}R^{\nabla,c_s}-R^{\nabla,v_0}\big)-\big(R_{v_0,c_m}R^{\nabla,c_m}-R^{\nabla,v_0}\big)\Big)=\Omega^{\nabla}_{v_0}(v_0-p,v_0-c_s)-\Omega^{\nabla}_{v_0}(v_0-p,v_0-c_m)+\mathcal{O}(h^{\ell+3})$$

Using the auxiliary function

$$\tilde{g}\colon m\to\mathbb{R}^{r\times r}\colon p\mapsto\Omega^{\nabla}_{v_0}(v_0-p,v_0-c_s)-\Omega^{\nabla}_{v_0}(v_0-p,v_0-c_m),$$

we can argue parallely to the case of m_0 that

$$\int_m\big(R_{v_0,c_s}R^{\nabla,c_s}-R_{v_0,c_m}R^{\nabla,c_m}\big)\alpha=\Omega^{\nabla}_{v_0}(v_0-c_m,v_0-c_s)\alpha_{c_m}[m]+\mathcal{O}(h^{\ell+3}).\tag{3.3.9}$$

Since $\Omega^{\nabla}_{v_0}$ is evaluated on a stencil of order $\mathcal{O}(h^2)$, this yields with Equation (3.3.7) and Equation (3.3.8),

$$\mathfrak{d}^{\nabla}\alpha(s,v_0)=R_{v_0,v_1}\,\alpha(m_0,v_1)+\sum_{i=1}^{\ell+1}\alpha(m_i,v_0)=R_{v_0,c_s}\int_s R^{\nabla,c_s}d^{\nabla}\alpha+\mathcal{O}(h^{\ell+2}).$$

□

Remark 3.42 (Differences as tangent vectors)**.** Throughout this proof, and in the analogous proofs that follow, expressions such as v_0-v_i require clarification: their literal interpretation as differences of points on $\mathcal{M}$ is not well-defined. What we mean is the following. Fixing the base point v_0 and assuming $\mathcal{M}$ is sufficiently regular so that all relevant vertices lie in a normal neighbourhood of v_0, the inverse exponential map $\log_{v_0}:=\exp^{-1}_{v_0}$ provides a diffeomorphism between this neighbourhood and a star-shaped open subset of $T_{v_0}\mathcal{M}$. Writing

$$\xi_p:=\log_{v_0}(p)\in T_{v_0}\mathcal{M},$$

we interpret all affine operations between points—differences, sums, barycentres, integrals—as operations between their tangent-space representatives:

$$p-q:=\xi_p-\xi_q,\qquad \xi_{v_0}=0,\qquad v_0-p=-\xi_p.$$

With this convention, all such expressions are carried out in the vector space $T_{v_0}\mathcal{M}$, where they are well-defined, and $\Omega^{\nabla}_{v_0}$ is evaluated on the resulting tangent vectors.

In particular, we take each centroid to be the arithmetic mean of its vertex representatives in $T_{v_0}\mathcal{M}$:

$$\xi_{c_s}=\frac{1}{\ell+2}\sum_{i=0}^{\ell+1}\xi_{v_i},\qquad \xi_{c_m}=\frac{1}{|m|}\sum_{v_i\in m}\xi_{v_i},\qquad c_s:=\exp_{v_0}(\xi_{c_s}).$$

Two consequences are worth noting. First, the median identity $\xi_{c_s}=\frac{\ell+1}{\ell+2}\,\xi_{c_{m_0}}$ holds *exactly*, so v_0,c_{m_0},c_s are collinear in $T_{v_0}\mathcal{M}$, and $\Omega^{\nabla}_{v_0}(v_0-c_{m_0},v_0-c_s)=0$ by antisymmetry. Second, the first-moment identities $\int_m(p-c_m)=0$ and the affineness of the auxiliary maps $g,\tilde{g}$ used below all hold exactly, being statements about affine functions on a vector space.

This is an abuse of notation: writing v_0-v_i for tangent-space differences read through the inverse exponential map streamlines the exposition considerably, at the cost of conflating points on $\mathcal{M}$ with their representatives in $T_{v_0}\mathcal{M}$. With this convention in mind, the formulas below should be read accordingly.

Since the volume of the simplicial cell is of order $\mathcal{O}(h^{\ell+1})$, this shows that the operator $\mathfrak{d}^{\nabla}$ converges under refinement *if the input is obtained through integration in an appropriate PPF.* However, to ensure convergence of a second application of $\boldsymbol{d}^{\nabla}$, this is not sufficient since the error after division with the volume of a $(\ell+1)$-simple can remain arbitrarily large. This is where the alternation can improve the accuracy order.

Theorem 3.43 (Alternation increases accuracy)**.** *Let $\pi : E \to \mathcal{M}$ be a vector bundle with connection ∇. Let $s = [v_0, \dots, v_{\ell+1}] \subset \mathcal{M}$ be a region in $\mathcal{M}$ for which there exists a diffeomorphism to a $(\ell+1)$-simplex σ where each point v_i is mapped to an associated vertex w_i of σ. Further let $\alpha \in \Omega^{\ell}(\mathcal{M}, E)$ and $\boldsymbol{\alpha}$ be its discretization defined in Equation (3.2.8). In this case, we have*

$$R_{v_0,c_s} \int_s (d^{\nabla}\alpha)^{(\nabla,c_s)} = \mathrm{Alt}^{\nabla}\mathfrak{d}^{\nabla}\boldsymbol{\alpha}(s,v_0) + \mathcal{O}(h^{\ell+3}) = \boldsymbol{d}^{\nabla}\boldsymbol{\alpha}(s,v_0) + \mathcal{O}(h^{\ell+3}), \tag{3.3.10}$$

or expressed intrinsically,

$$\mathcal{R}_{v_0,c_s\varphi_{c_s}} \overset{\nabla}{\int_s} d^{\nabla}\alpha = \mathrm{Alt}^{\nabla}\mathfrak{d}^{\nabla}\boldsymbol{\alpha}(s,v_0) + \mathcal{O}(h^{\ell+3}) = \boldsymbol{d}^{\nabla}\boldsymbol{\alpha}(s,v_0) + \mathcal{O}(h^{\ell+3}). \tag{3.3.11}$$

Proof. It holds by Theorem 3.39

$$\int_s R_{v_0,c_s}(d^{\nabla}\alpha)^{\nabla,c_s} = R_{v_0,c_s}\int_{\partial s} \alpha^{\nabla,c_s} + \mathcal{O}(h^{\ell+3}). \tag{3.3.12}$$

Let $\{m_i\} \subset \partial s$ be the set of ℓ–cells with positive orientation forming the boundary of s where $v_i \notin m_i$. In the following, we will show that the contributions for every ℓ–face coming from Equation (3.3.12) and those of $\boldsymbol{d}^{\nabla}(s, v_0)$ differ by a term of order $\mathcal{O}(h^{\ell+3})$. To see this, we rewrite the exterior covariant derivative as

$$\begin{aligned} \boldsymbol{d}^{\nabla}\boldsymbol{\alpha}(s,v_0) &= \mathrm{Alt}^{\nabla}\mathfrak{d}^{\nabla}\boldsymbol{\alpha}(s,v_0) \\ &= \frac{1}{\ell+2}\sum_{j=0}^{\ell+1} R_{v_0,v_j}\Bigg(\frac{1}{(\ell+1)!}\sum_{\substack{\pi\in S_{\ell+2}\\ \pi(0)=j}} \mathrm{sgn}(\pi)\mathfrak{d}^{\nabla}\boldsymbol{\alpha}(\pi(s),v_j)\Bigg). \end{aligned} \tag{3.3.13}$$

Let

$$\mathrm{Alt}_j^{\nabla}\mathfrak{d}^{\nabla}\boldsymbol{\alpha}(s,v_j) := \frac{1}{(\ell+1)!}\sum_{\pi\in S_{\ell+2},\pi(0)=j} \mathrm{sgn}(\pi)\mathfrak{d}^{\nabla}\boldsymbol{\alpha}(\pi(s),v_j)$$

be the operator that uses an alternation on the face opposite to v_j only. For the boundary cell m_i we consider the contributions coming from $\mathrm{Alt}_j^{\nabla}\mathfrak{d}^{\nabla}\boldsymbol{\alpha}$ to Equation (3.3.13) for $i \neq j$ first. In this case the face m_i is not opposite to v_j. Hence, its contributions turn into

$$R_{v_0,v_j}\boldsymbol{\alpha}(m_i,v_j) = R_{v_0,v_j}\int_{m_i} R^{\nabla,v_j}\alpha.$$

For the case $j = i$, m_i is the face opposite to the evaluation vertex of $\mathrm{Alt}_j^{\nabla} \mathfrak{d}^{\nabla} \boldsymbol{\alpha}(s, v_j)$. In this case, we can rewrite

$$\mathrm{Alt}_i^{\nabla} \mathfrak{d}^{\nabla} \boldsymbol{\alpha}(s, v_i) = \frac{1}{\ell+1} \sum_{v_k \in m_i} \frac{1}{\ell!} \sum_{\substack{\pi \in S_{\ell+2} \\ \pi(0)=j \\ \pi(1)=k}} \mathrm{sgn}(\pi) \mathfrak{d}^{\nabla} \alpha(\pi(s), v_j).$$

This yields that the contributions coming from m_i are of the form

$$R_{v_0, v_i} \frac{1}{\ell+1} \sum_{k \neq i} R_{v_i, v_k} \int_{m_i} R^{\nabla, v_k} \alpha. \tag{3.3.14}$$

If we analyze the difference of this expression to the integral of α in the v_i−based parallel-propagated frame, we obtain

$$\frac{1}{\ell+1} \sum_{k \neq i} R_{v_i, v_k} \int_{m_i} R^{\nabla, v_k} \alpha - \int_{m_i} R^{\nabla, v_i} \alpha = \frac{1}{\ell+1} \sum_{k \neq i} \int_{m_i} (R_{v_i, v_k} R^{\nabla, v_k} - R^{\nabla, v_i}) \alpha. \tag{3.3.15}$$

Similar to the discussion in Theorem 3.39, we can argue that the integral of the center-based Taylor expansion yields

$$\begin{aligned} &\frac{1}{\ell+1} \sum_{k \neq i} \int_{m_i} (R_{v_i, v_k} R^{\nabla, v_k} - R^{\nabla, v_i}) \alpha \\ &= \frac{1}{\ell+1} \sum_{k \neq i} (R_{v_i, v_k} R_{v_k, c_{m_i}} - R_{v_i, c_{m_i}}) \alpha_{c_{m_i}}[m_i] + \mathcal{O}(h^{\ell+3}) \end{aligned}$$

As explained in Section 3.2.5 , it holds

$$\begin{aligned} &(R_{v_i, v_k} R_{v_k, c_{m_i}} - R_{v_i, c_{m_i}}) \\ &= \boldsymbol{\Omega}^{\nabla}([v_i, v_k, c_{m_i}], v_i, c_{m_i}) = \Omega_{v_i}^{\nabla}[v_k - v_i, c_{m_i} - v_i] + \mathcal{O}(h^3). \end{aligned} \tag{3.3.16}$$

Therefore,

$$\begin{aligned} &\frac{1}{\ell+1} \sum_{k \neq i} (R_{v_i, v_k} R_{v_k, c_{m_i}} - R_{v_i, c_{m_i}}) \alpha_{c_{m_i}}[m_i] \\ &= \frac{1}{\ell+1} \sum_{k \neq i} \Omega_{v_i}^{\nabla}[v_k - v_i, c_{m_i} - v_i] \alpha_{c_{m_i}}[m_i] + \mathcal{O}(h^{\ell+3}) \\ &= \underbrace{\Omega_{v_i}^{\nabla}\left[\frac{1}{\ell+1} \sum_{k \neq i} v_k - v_i, c_{m_i} - v_i\right]}_{=0} \alpha_{c_{m_i}}[m_i] + \mathcal{O}(h^{\ell+3}). \end{aligned}$$

Since $\frac{1}{\ell+1} \sum_{k \neq i} v_k = c_{m_i}$, we obtain

$$\frac{1}{\ell+1} \sum_{k \neq i} R_{v_i, v_k} \int_{m_i} R^{\nabla, v_k} \alpha - \int_{m_i} R^{\nabla, v_i} \alpha \in \mathcal{O}(h^{\ell+3}).$$

Therefore, we can deduce that the contribution of the face m_i for the difference $\boldsymbol{d}^\nabla \boldsymbol{\alpha}(s, v_0) - R_{v_0,c_s}\int_s (d^\nabla \alpha)^{\nabla,c_s}$ is, up to order $\mathcal{O}(h^{\ell+3})$, of the form

$$\begin{aligned}
&\frac{1}{\ell+2}\sum_{j=0}^{\ell+1} R_{v_0,v_j}\int_{m_i} R^{\nabla,v_j}\alpha - R_{v_0,c_s}\int_{m_i} R^{\nabla,c_s}\alpha \\
&= \frac{1}{\ell+2}\sum_{j=0}^{\ell+1}\int_{m_i}\left(R_{v_0,v_j}R^{\nabla,v_j} - R_{v_0,c_s}R^{\nabla,c_s}\right)\alpha.
\end{aligned}$$

Integration of the Taylor expansion at c_{m_i} yields

$$\begin{aligned}
&\frac{1}{\ell+2}\sum_{j=0}^{\ell+1} R_{v_0,v_j}\int_{m_i} R^{\nabla,v_j}\alpha - R_{v_0,c_s}\int_{m_i} R^{\nabla,c_s}\alpha \\
&= \frac{1}{\ell+2}\sum_{j=0}^{\ell+1}(R_{v_0,v_j}R_{v_j,c_{m_i}} - R_{v_0,c_s}R_{c_s,c_{m_i}})\alpha_{c_{m_i}}[m_i] + \mathcal{O}(h^{\ell+3}) \\
&= \frac{1}{\ell+2}\sum_{j=0}^{\ell+1}\left(R_{v_0,v_j}R_{v_j,c_{m_i}} - R_{v_0,c_{m_i}} - (R_{v_0,c_s}R_{c_s,c_{m_i}} - R_{v_0,c_{m_i}})\right)\alpha_{c_{m_i}}[m_i] + \mathcal{O}(h^{\ell+3}) \\
&= \frac{1}{\ell+2}\sum_{j=0}^{\ell+1}\Bigg(\Omega^\nabla_{v_0}[v_j - v_0, c_{m_i} - v_0]\alpha_{c_{m_i}}[m_i] \\
&\quad - \Omega^\nabla_{v_0}[c_s - v_0, c_{m_i} - v_0]\,\alpha_{c_{m_i}}[m_i]\Bigg) + \mathcal{O}(h^{\ell+3}) \\
&= \Omega^\nabla_{v_0}\Bigg[\underbrace{\frac{1}{\ell+2}\sum_{j=0}^{\ell+1} v_j}_{=c_s} - v_0, c_{m_i} - v_0\Bigg]\alpha_{c_{m_i}}[m_i] \\
&\quad - \Omega^\nabla_{v_0}[c_s - v_0, c_{m_i} - v_0]\,\alpha_{c_{m_i}}[m_i] + \mathcal{O}(h^{\ell+3}) \\
&= \mathcal{O}(h^{\ell+3}).
\end{aligned}$$

Since v_i was chosen arbitrarily, this result yields the claim. □

To conclude the convergence of $\boldsymbol{d}^\nabla\boldsymbol{d}^\nabla$ under refinement, we need another lemma.

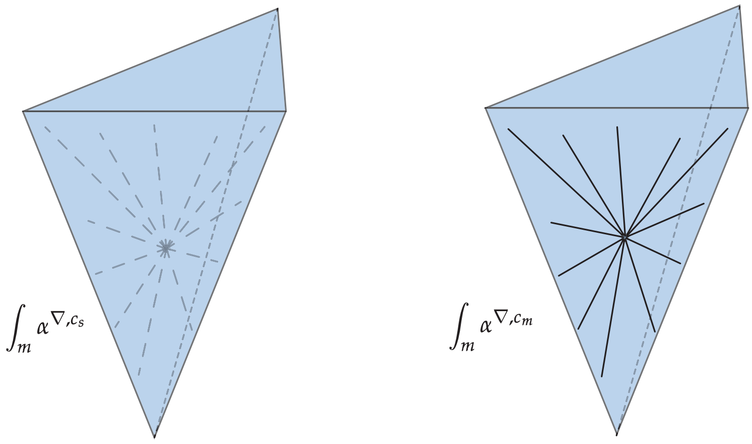

Figure 3.10: **Visualization** of the two parallel-propagated frame fields used in Lemma 3.44. It is noteworthy that the integral computed on the right-hand side involves a PPF whose source is not contained within the integration domain m.

Lemma 3.44. *Let $\pi : E \to \mathcal{M}$ be a vector bundle with connection ∇. Let $s = [v_0, \dots, v_{\ell+1}] \subset \mathcal{M}$ be a region in $\mathcal{M}$ for which there exists a diffeomorphism to a $(\ell+1)$-simplex σ where each point v_i are mapped to an associated vertex w_i of σ. Let $m \subset s$ be the image under ψ of a ℓ−subcell containing v_0. In this case, it holds that*

$$R_{v_0,c_m} \int_m \alpha^{\nabla,c_m} = R_{v_0,c_s} \int_m \alpha^{\nabla,c_s} + \mathcal{O}(h^{\ell+2}), \tag{3.3.17}$$

which can be expressed intrinsically as

$$\mathcal{R}_{v_0,c_m} \, {}_{\varphi_{c_m}}\!\!\overset{\nabla}{\int_m} \alpha = \mathcal{R}_{v_0,c_s} \, {}_{\varphi_{c_s}}\!\!\overset{\nabla}{\int_m} \alpha + \mathcal{O}(h^{\ell+2}) \tag{3.3.18}$$

where two PPFs (one from the center c_m of m, one from the center c_s of s) are used, see Figure 3.10.

Proof. It holds

$$\begin{aligned} R_{v_0,c_s} \int_m \alpha^{\nabla,c_s} - R_{v_0,c_m} \int_m \alpha^{\nabla,c_m} &= \int_m (R_{v_0,c_s} R^{\nabla,c_s} - R_{v_0,c_m} R^{\nabla,c_m})\alpha \\ &= (R_{v_0,c_s} R_{c_s,c_m} - R_{v_0,c_m})\alpha_{c_m}[m] + \mathcal{O}(h^{\ell+3}) \\ &= \underbrace{\mathbf{\Omega}^{\nabla}([v_0, c_s, c_m], v_0, c_m)}_{=\mathcal{O}(h^2)} \underbrace{\alpha_{c_m}[m]}_{=\mathcal{O}(h^{\ell})} = \mathcal{O}(h^{\ell+2}). \end{aligned}$$

□

This allows us to conclude the convergence of $\boldsymbol{d}^{\nabla}\boldsymbol{d}^{\nabla}$ under refinement, as explained next.

Corollary 3.45 (Convergence of $\boldsymbol{d}^{\nabla}\boldsymbol{d}^{\nabla}$)**.** *Let $\pi : E \to \mathcal{M}$ be a vector bundle with connection ∇. Let $s = [v_0, \ldots, v_{\ell+2}] \subset \mathcal{M}$ be a region in $\mathcal{M}$ for which there exists a diffeomorphism to a $(\ell+2)$-simplex σ where each point v_i are mapped to an associated vertex w_i of σ. Further, let $\alpha \in \Omega^{\ell}(M, E)$ and $\boldsymbol{\alpha}$ be its discretization defined in Equation (3.2.8). We have*

$$\boldsymbol{d}^{\nabla}\boldsymbol{d}^{\nabla}\boldsymbol{\alpha}(\sigma, v_0) = R_{v_0,c_s}\int_s (d^{\nabla}d^{\nabla}\alpha)^{\nabla,c_s} + \mathcal{O}(h^{\ell+3}). \tag{3.3.19}$$

or equivalently,

$$\boldsymbol{d}^{\nabla}\boldsymbol{d}^{\nabla}\boldsymbol{\alpha}(\sigma, v_0) = \mathcal{R}_{v_0,c_s}\varphi_{c_s}\overset{\nabla}{\int_s}(d^{\nabla}d^{\nabla}\alpha) + \mathcal{O}(h^{\ell+3}). \tag{3.3.20}$$

Proof. It holds

$$R_{v_0,c_s}\int_s (d^{\nabla}d^{\nabla}\alpha)^{\nabla,c_s} = R_{v_0,c_s}\int_{\partial s}(d^{\nabla}\alpha)^{\nabla,c_s} + \mathcal{O}(h^{\ell+4}),$$

by Theorem 3.39. Hence, by the previous lemma and since $d^{\nabla}\alpha \in \Omega^{\ell+1}(M; E)$, we obtain,

$$R_{v_0,c_s}\int_s (d^{\nabla}d^{\nabla}\alpha)^{\nabla,c_s} = \sum_{m\in\partial s} R_{v_0,c_s}\int_m (d^{\nabla}\alpha)^{\nabla,c_m} + \mathcal{O}(h^{\ell+3}).$$

As in the previous proof, let m_i be the $(\ell+1)$-subcell in ∂s opposite to v_i with positive orientation. Thus by Theorem 3.43 we obtain

$$R_{v_0,c_s}\int_s (d^{\nabla}d^{\nabla}\alpha)^{\nabla,c_s} = R_{v_0,c_{m_0}}\int_{m_0}(d^{\nabla}\alpha)^{\nabla,c_{m_0}} + \sum_{i=1}^{\ell+2}\boldsymbol{d}^{\nabla}\boldsymbol{\alpha}(m_i, v_0) + \mathcal{O}(h^{\ell+3}).$$

For the first term, note that

$$R_{v_0,c_{m_0}}\int_{m_0}(d^{\nabla}\alpha)^{\nabla,c_{m_0}} = R_{v_0,v_1}R_{v_1,c_{m_0}}\int_{m_0}(d^{\nabla}\alpha)^{\nabla,c_{m_0}} - \boldsymbol{\Omega}^{\nabla}([v_0,v_1,c_{m_0}],v_0,c_{m_0})\int_{m_0}(d^{\nabla}\alpha)^{\nabla,c_{m_0}}.$$

Since

$$\underbrace{\boldsymbol{\Omega}^{\nabla}([v_0,v_1,c_{m_0}],v_0,c_{m_0})}_{=\mathcal{O}(h^2)}\underbrace{\int_{m_0}(d^{\nabla}\alpha)^{\nabla,c_{m_0}}}_{=\mathcal{O}(h^{\ell+1})} = \mathcal{O}(h^{\ell+3})$$

and

$$R_{v_0,v_1}R_{v_1,c_{m_0}}\int_{m_0}(d^{\nabla}\alpha)^{\nabla,c_{m_0}} = R_{v_0,v_1}\boldsymbol{d}^{\nabla}\boldsymbol{\alpha}(m_0, v_1),$$

we obtain

$$\begin{aligned} R_{0,c_s}\int_s (d^{\nabla}d^{\nabla}\alpha)^{\nabla,c_s} &= R_{v_0,v_1}\boldsymbol{d}^{\nabla}\boldsymbol{\alpha}(m_0,v_1) + \sum_{j=1}^{\ell+2}\boldsymbol{d}^{\nabla}\boldsymbol{\alpha}(m_j,v_0) + \mathcal{O}(h^{\ell+3}) \\ &= \mathfrak{d}^{\nabla}\boldsymbol{d}^{\nabla}\boldsymbol{\alpha}(s, v_0) + \mathcal{O}(h^{\ell+3}). \end{aligned}$$

Furthermore,

$$\begin{aligned}
&\mathrm{Alt}^{\boldsymbol{\nabla}}\left(\mathfrak{d}^{\boldsymbol{\nabla}}\boldsymbol{d}^{\boldsymbol{\nabla}}\boldsymbol{\alpha}(s,v_0)\right) - R_{v_0,c_s}\int_s (d^\nabla d^\nabla \alpha)^{\nabla,c_s}\\
&= \mathrm{Alt}^{\boldsymbol{\nabla}}\left(R_{v_0,c_s}\int_s (d^\nabla d^\nabla \alpha)^{\nabla,c_s}\right) - R_{v_0,c_s}\int_s (d^\nabla d^\nabla \alpha)^{\nabla,c_s} + \mathcal{O}(h^{\ell+3})\\
&= \frac{1}{\ell+3}\sum_{j=0}^{\ell+2}\left(R_{v_0,v_j}R_{v_j,c_s} - R_{v_0,c_s}\right)\left(\int_s (d^\nabla d^\nabla \alpha)^{\nabla,c_s}\right) + \mathcal{O}(h^{\ell+3})\\
&= \Omega^\nabla\Big(v_0 - c_s, \underbrace{\frac{1}{\ell+3}\sum_{j=0}^{\ell+2} v_j - c_s}_{=0}\Big)\int_s (d^\nabla d^\nabla \alpha)^{\nabla,c_s} + \mathcal{O}(h^{\ell+3}) \in \mathcal{O}(h^{\ell+3}).
\end{aligned}$$

Hence $\boldsymbol{d}^{\boldsymbol{\nabla}}\boldsymbol{d}^{\boldsymbol{\nabla}}\boldsymbol{\alpha}(s,v_0) - R_{v_0,c_s}\int_s (d^\nabla d^\nabla \alpha)^{\nabla,c_s} \in \mathcal{O}(h^{\ell+3})$, which yields the claim. $\square$

In the proof, we only show that the operators $\boldsymbol{d}^{\boldsymbol{\nabla}}\boldsymbol{d}^{\boldsymbol{\nabla}}$ and $\mathfrak{d}^{\boldsymbol{\nabla}}\boldsymbol{d}^{\boldsymbol{\nabla}}$ are of the same convergence order, although one might expect that a novel alternation could augment the accuracy of the PPF-derivative. However, for a second application, the alternation cannot compensate for the lack of accuracy from the original input. Numerical tests will confirm that a novel application of the alternation operator to $\mathfrak{d}^{\boldsymbol{\nabla}}\boldsymbol{d}^{\boldsymbol{\nabla}}$ cannot augment the accuracy further, indicating that a numerical realization of a third application of the exterior covariant derivative will be, in this setup, impossible to achieve accurately.

Remark 3.46. This corollary confirms the convergence, under mesh refinement, of the implicitly defined wedge product between the curvature 2−form and a vector-valued form, as introduced in Theorem 3.36. It converges towards the smooth curvature wedge product in Equation (1.5.12). Thus, the discrete algebraic Bianchi Identity holds both conceptually and numerically in the limit under mesh refinement.

Remark 3.47. As discussed in the analysis preceding Def. 3.29, a noteworthy reduction in the number of terms for the alternation can be used and will still ensure enhanced convergence of the sided discrete exterior covariant derivative. Equation (3.3.14) shows that we can reduce the number of permutations from the full alternation group down to only $(\ell+1)$-terms, resulting in a substantial decrease in the computational cost of the alternation. However in this case the combinatorial properties of the discrete exterior covariant derivative are no longer satisfied.

Remark 3.48 (Convergence analysis for general endomorphism-valued forms)**.** In the vector-valued case, we have successfully established that the discrete exterior derivative converges under refinement and satisfies the Bianchi identities. These results hold great significance within the context of our study. We showed that the differential Bianchi Identity holds in an exact sense. In the definition of the exterior covariant derivative for $(1,1)$-tensor valued forms, we used an alternation of the PPF-derivative, although the differential Bianchi Identity is already enforced for the PPF-derivative exactly. However, for the analysis of convergence under refinement of general endomorphism-valued forms, it is necessary to use an alternation of the PPF-derivative as in the vector-valued case. It turns out that the convergence analysis for arbitrary endomorphism-valued forms can be carried out similarly to the vector-valued case. We saw that the alternated

PPF-derivative realizes a discrete notion of the identity

$$d^{\nabla^{\mathrm{End}}} d^{\nabla^{\mathrm{End}}} \beta = [\Omega^{\nabla} \wedge \beta],$$

for $\beta \in \Omega^{\ell}(M, \mathrm{End}(E))$. For the discretization of a general endomorphism-valued form through integration, we can, in contrast to the curvature form, not expect in general that the integration can be carried out as a boundary integral exactly. As in the case for vector-valued case, one can therefore use a discretization in a parallel-propagated frame for

$$d^{\nabla^{\mathrm{End}}} \beta = d\beta + \omega \wedge \beta + (-1)^{\deg(\beta)} \beta \wedge \omega.$$

However, in contrast to the vector-valued case it is necessary to use a PPF-for the integration for the output *and* input fiber. If we define the discretization through integration for an endomorphism-valued form through

$$\boldsymbol{\beta}(s, v, w) = \int_s \mathcal{R}^{\nabla, v} \beta (\mathcal{R}^{\nabla, w})^{-1}, \tag{3.3.21}$$

it is possible to show that for $\beta \in \Omega^{\ell}(M, \mathrm{End}(E))$ it holds

$$\mathfrak{d}^{\nabla} \boldsymbol{\beta}(s, v, w) = \int_s R_{v, c_s} (d^{\nabla^{\mathrm{End}}} \beta)^{\nabla, c_s, c_s} R_{c_s, w} + \mathcal{O}(h^{\ell+2})$$

and

$$\boldsymbol{d}^{\nabla} \boldsymbol{\beta}(s, v, w) = \int_s R_{v, c_s} (d^{\nabla^{\mathrm{End}}} \beta)^{\nabla, c_s, c_s} R_{c_s, w} + \mathcal{O}(h^{\ell+3}),$$

where $(d^{\nabla^{\mathrm{End}}} \beta)^{\nabla, c_s, c_s} = R^{\nabla, c_s} \, d^{\nabla^{\mathrm{End}}} \beta \, (R^{\nabla, c_s})^{-1}$ is the representation of the form $d^{\nabla^{\mathrm{End}}} \beta$ in the frame that uses a center based PPF for the input and the output of the form. This allows to conclude that for a simplicial $(\ell + 2)$-cell s' it holds

$$\boldsymbol{d}^{\nabla} \boldsymbol{d}^{\nabla} \boldsymbol{\beta}(s', v, w) = \int_{s'} R_{v, c_{s'}} (d^{\nabla^{\mathrm{End}}} d^{\nabla^{\mathrm{End}}} \beta)^{\nabla \, c_s, c_s} R_{c_{s'}, w} + \mathcal{O}(h^{\ell+3}),$$

ensuring convergence under refinement.

3.3.3 Numerical Testing

We now report on our tests of the numerical validity of the formulas we propose in this paper. For all examples, we start from a connection $1-$form ω and a differential form, both given in closed form, which we discretize on a sample mesh element. We then compare the smooth (closed-form) exterior derivative and curvature to the results obtained by our discrete operators when applied to the discrete 1-connection and the discrete form using increasingly fine meshes, in order to observe the convergence rates of our operators. Note that our Python code for all these tests is available at `https://gitlab.inria.fr/geomerix/public/fulldec`.

Setup

Computing discrete connection. For a given analytical connection $1-$form ω in the standard frame of $\mathbb{R}^3$ and an edge $[a, b]$ (where $a, b \in \mathbb{R}^3$) defined as the straight path $\gamma_{ab} \colon [0, 1] \to$

$\mathbb{R}^3 : t \mapsto (1-t)\cdot a + t \cdot b$, the discrete parallel transport R_{ab} induced by the connection is

$$R_{ab} = P\exp\left(\int_\gamma \omega\right).$$

We approximate this discrete path ordering by splitting the interval $[a,b]$ into N sub-intervals. If we define the i^{th} path segment via $\gamma_i : [i/N, (i+1)/N] \to \mathbb{R}^3 : t \mapsto (1-t)\cdot a + t\cdot b$, a discrete parallel transport is computed as

$$R_{ab} \approx \prod_{i=0}^{N-1} \exp\left(\int_{\gamma_i} \omega\right), \tag{3.3.22}$$

where the matrix exponential on the right is evaluated *without* path ordering.

Discretization of vector-valued forms. As described in Section 3.2.1, we enforce that the discretization of the forms is carried out in a parallel-propagated frame field. That is, given a smooth $T\mathbb{R}^3$−valued k−form α, a simplex $\sigma \subset \mathbb{R}^3$ with a vertex $v \in \sigma$ and a smooth connection 1−form ω, the discretization described in Equation (3.2.8) is

$$\boldsymbol{\alpha}(\sigma, v) := \int_S R^{\nabla,v}\alpha.$$

Here, we assume that the underlying chosen local frame field is the standard frame of $T\mathbb{R}^3$, and $R^{\nabla,v} : \sigma \to \mathrm{SO}(3)$ is the gauge field turning this standard frame into the PPF centered at v. In our numerical tests, we apply quadrature rules to approximate this integral. For instance, for the case of a one-form represented in the standard frame of $T\mathbb{R}^3$ via

$$\alpha = \begin{pmatrix}\alpha_1\\ \alpha_2\\ \alpha_3\end{pmatrix} \in \Omega^1(\mathbb{R}^3, T\mathbb{R}^3),$$

where $\alpha_1, \alpha_2, \alpha_3 \in \Omega^1(\mathbb{R}^3)$ are standard scalar-valued differential forms. For an edge $\gamma : [0,1] \to \mathbb{R}^3$, where $\gamma(0) = a$ and $\gamma(1) = b$, we denote the evaluation of the smooth differential form $\alpha \in \Omega^1(M, \mathbb{R}^3)$ at a point $p \in e = \gamma([0,1])$ for the vector $b - a \in T_p\mathbb{R}^3$ through $\alpha_p(b-a)$, where we use the canonical identification induced by the standard frame of $\mathbb{R}^3$ of $T_a\mathbb{R}^3$ with $T_p\mathbb{R}^3$. Writing the gauge field $R^{\nabla,a}$ as

$$R^{\nabla,a} = \begin{pmatrix} - & R_{a_1} & - \\ - & R_{a_2} & - \\ - & R_{a_3} & - \end{pmatrix} = (R_{a_i})_j \in SO(3) \text{ for } (i,j) \in \{1,2,3\},$$

it holds by definition that

$$\boldsymbol{\alpha}([a,b],a) = \int_\gamma R^{\nabla,a}\alpha = \int_{[0,1]} \gamma^*(R^{\nabla,a})\,\gamma^*\alpha = \int_{[0,1]} \begin{pmatrix} R_{a_1}(\gamma(t))\cdot\alpha_{\gamma(t)}(b-a)\\ R_{a_2}(\gamma(t))\cdot\alpha_{\gamma(t)}(b-a)\\ R_{a_3}(\gamma(t))\cdot\alpha_{\gamma(t)}(b-a)\end{pmatrix} dt, \tag{3.3.23}$$

where we use the standard matrix product for the multiplication of a row with a column vector. In this case, we get the integral of the first component, for instance:

$$\begin{aligned}
&\int_\gamma R_{a_{11}}\,\alpha_1 + R_{a_{12}}\,\alpha_2 + R_{a_{13}}\,\alpha_3\\
&= \int_0^1 R_{a_{11}}(\gamma(t))\,\alpha_{1_{\gamma(t)}}(\dot\gamma(t)) + R_{a_{12}}(\gamma(t))\,\alpha_{2_{\gamma(t)}}(\dot{\gamma(t)}) + R_{a_{13}}(\gamma(t))\,\alpha_{3_{\gamma(t)}}(\dot\gamma(t))\,dt,
\end{aligned}$$

and we use a 5^{th}−order Gauss-Legendre quadrature to evaluate this 1D integral numerically. The final expression of the discretization of α thus reads:

$$\boldsymbol{\alpha}(e,a) \approx \sum_{i=0}^{4} w_i \; R_{a,\gamma(t_i)} \; \alpha_{\gamma(t_i)}(b-a),$$

where w_i are the usual Gauss-Legendre quadrature weights.

Similarly, if we want to discretize a smooth $(1,1)$-tensor valued 1−form β over $e = [a,b]$ with evaluation at a and cut at b, we discretize the integral

$$\boldsymbol{\beta}([a,b],a,b) = \int_e R^{\nabla,a} \; \beta \; (R^{\nabla,b})^{-1}.$$

In this case, we approximate the integral through

$$\boldsymbol{\beta}(e,a,b) \approx \sum_{i=0}^{4} w_i \; R_{a,\gamma(x_i)} \; \beta_{\gamma(x_i)}(b-a) \; R_{\gamma(x_i),b}.$$

Now, if we are given a vector-valued 2−form α and we want to calculate its discretization over a triangle $\sigma = [a,b,c]$ evaluated at a, we discretize the 2D integral

$$\boldsymbol{\alpha}(\sigma,a) = \int_\sigma R^{\nabla,a}\alpha.$$

We thus use 2D quadrature rules (provided, for instance, in [Bur10]) to approximate this integral. Similarly, we use for $(1,1)$-tensor valued forms the integral

$$\boldsymbol{\beta}(\sigma,a,b) = \int_\sigma R^{\nabla,a}\beta(R^{\nabla,b})^{-1}$$

and apply 2D quadrature to obtain the discretization of the form over the triangle.

Convergence under element refinement. For each example, we evaluate the discrete operator on a given mesh element, then scale the element down while keeping the evaluation vertex fixed. At each scale we report the relative error, i.e. the norm of the difference between the discrete operator applied to the discretized form and the integral of the smooth ground-truth result, divided by the norm of that ground-truth integral. This yields a plot of the rate at which our discrete approximants converge to their continuous counterparts. Quantifying the error of a discrete differential operator generally requires a norm adapted to the function space in which the discrete object is expected to live, and the appropriate choice is far from obvious: the angle-defect definition of Gaussian curvature, for instance, fails to converge in the L^2 and H^{-1} norms yet converges in H^{-2} [Gaw20]. We therefore restrict ourselves to the pointwise relative error described above, which isolates the consistency of the operator at a fixed point; the function-space considerations become essential once the operators are used to solve a PDE.

Various numerical tests

For the connection $1-$form ω given as

$$\omega = \begin{pmatrix} 0 & 0 & 1 \\ 0 & 0 & 0 \\ -1 & 0 & 0 \end{pmatrix} x\,dz + \begin{pmatrix} 0 & 1 & 0 \\ -1 & 0 & 0 \\ 0 & 0 & 0 \end{pmatrix} (y\,dx + dz), \tag{3.3.24}$$

one can derive its torsion as

$$\Theta^\nabla = d^\nabla \theta = \begin{pmatrix} y\,dx \wedge dy - dy \wedge dz \\ dx \wedge\, dz \\ x\,dx \wedge dz \end{pmatrix},$$

where $\theta = (dx, dy, dz)^T$. Further, the exterior derivative of the torsion yields

$$d^\nabla \Theta^\nabla = d\Theta^\nabla + \omega \wedge \Theta^\nabla = \Omega^\nabla \wedge \begin{pmatrix} dx \\ dy \\ dz \end{pmatrix} = \begin{pmatrix} 0 \\ 0 \\ -xy \end{pmatrix} dx \wedge dy \wedge dz,$$

where

$$\Omega^\nabla = \begin{pmatrix} 0 & -dx \wedge dy & dx \wedge dz \\ dx \wedge dy & 0 & -xy\,dx \wedge dz \\ -dx \wedge dz & xy\,dx \wedge dz & 0 \end{pmatrix}.$$

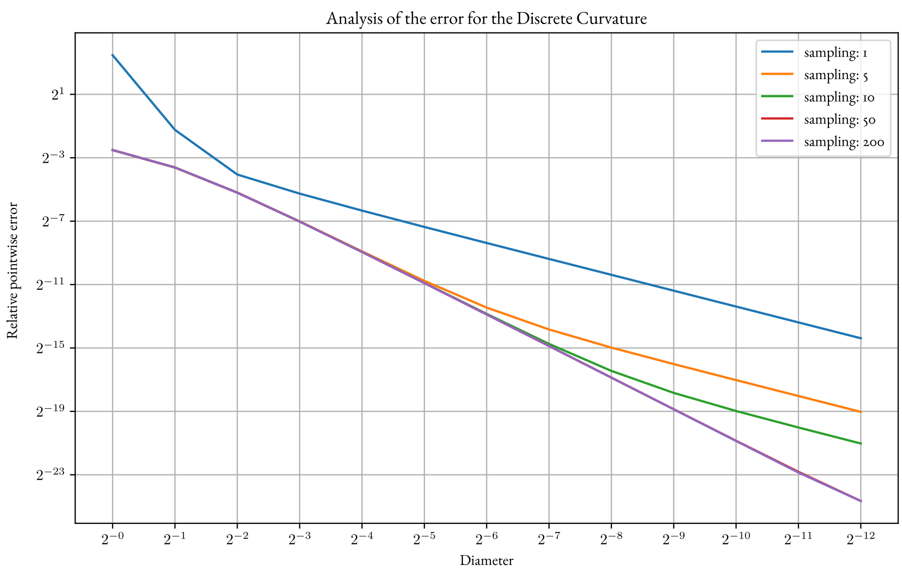

Figure 3.11: **Convergence of discrete curvature.** The discrete curvature converges to the integrated (continuous) curvature over a center-based parallel-propagated frame field; insufficient sampling for the integration of the smooth connection (Equation (3.3.22)) affects the convergence rate.

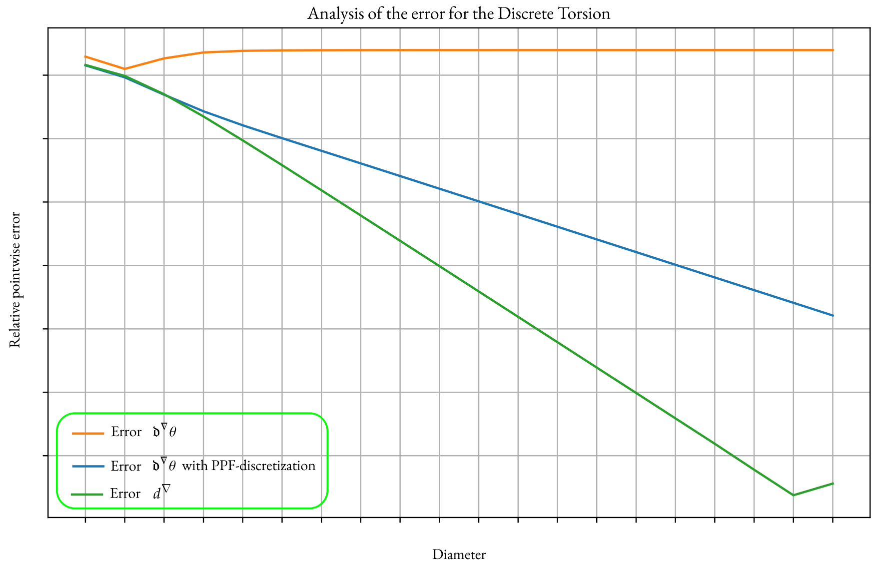

Figure 3.12: **Convergence of discrete torsion.** This graph illustrates that employing a non-parallel-propagated frame field for discretizing the solder form fails to yield convergence of the PPF-induced exterior covariant derivative. Utilizing a PPF for the discretization of a form and a subsequent use of the PPF derivative results in a linear decay of errors. Notably, the alternation process further enhances accuracy, leading to a quadratic decay in errors for our full discrete exterior covariant derivative.

Convergence of the Discrete Curvature. To verify the convergence of our discrete curvature, we construct a triangle from the three following points: $v_0 = \left(0,0,0\right)^T, \quad v_1 = \left(1,0,0\right)^T, \quad v_2 = \left(0.4,0.3,0\right)^T$, which we subsequently shift by the vector $v = \left(2.4,-1.3,2.9\right)^T$ and rotate using Euler angles $(30°, 45°, 27°)$ around the $X-,Y-,Z-$axes to ensure arbitrariness. We calculate the relative error of the discrete curvature compared to the integral of the smooth curvature form in a center-based PPF with pre- and post-composition to the corresponding evaluation and cut fiber. The resulting convergence plot is in Figure 3.11.

We note in passing here that the correct evaluation of the path ordering of the matrix exponential is essential to find the correct convergence order ($\mathcal{O}(h^2)$) for the discrete curvature compared to the integral of the smooth curvature in a center-based PPF.

Convergence of the Discrete Covariant Derivative of Bundle-valued $1-$Forms. To numerically test the validity of Theorem 3.43, we consider the triangle $[v_0, v_1, v_2]$ that we used above. We shift the triangle by a vector $v = (3.0, 4.1, -2.0)^T$ and use Euler angles $(10°, 15°, 5°)$ around the $X-,Y-,Z-$axes to ensure arbitrariness. We calculate the integral of the smooth torsion in a barycenter based PPF, transported to v_0. Subsequently we compute the sided PPF-induced discrete exterior covariant derivative $\mathfrak{d}^\nabla\theta$ and compute the relative error to the smooth ground truth (blue). Further, we calculate the discrete exterior covariant derivative and calculate the relative error with the smooth ground-truth integral (green). In addition, we illustrate that the discrete exterior covariant derivative operator presented in [BEHS21] does not converge under refinement if the input is obtained through discretization without the usage of a PPF (orange). In Figure 3.12, the size of the triangle is halved in each refinement step. As our theorems stated, we observe that the decay of the relative error for the PPF-derivative is indeed linear, with a quadratic convergence order when alternation is used, as can be seen in the different slopes in the logarithmic scale of the error plots. Additionally, the tests show that it is essential to use a parallel-propagated frame for the discretization of the differential forms, otherwise convergence cannot be achieved.

Since the case of the solder form is special, we also illustrate the convergence behavior proven in Theorems 3.41 and 3.43 for a more general differential form, which we pick to be:

$$\alpha = \begin{pmatrix} 2x\,dy \\ x\,dx \\ dz - z\,dy \end{pmatrix}, \tag{3.3.25}$$

with the connection introduced in Equation (3.3.24). In this test, the same test triangle is shifted by a vector $v = (2.4, -1.3, 2.9)$ and is rotated using Euler angles $(30°, 45°, 27°)$ for $X-$,$Y-$,$Z-$axes. The triangle size is each time reduced by a factor two, leading to the convergence plot in Figure 3.13: the alternation operator indeed improves the convergence order of the PPF-derivative.

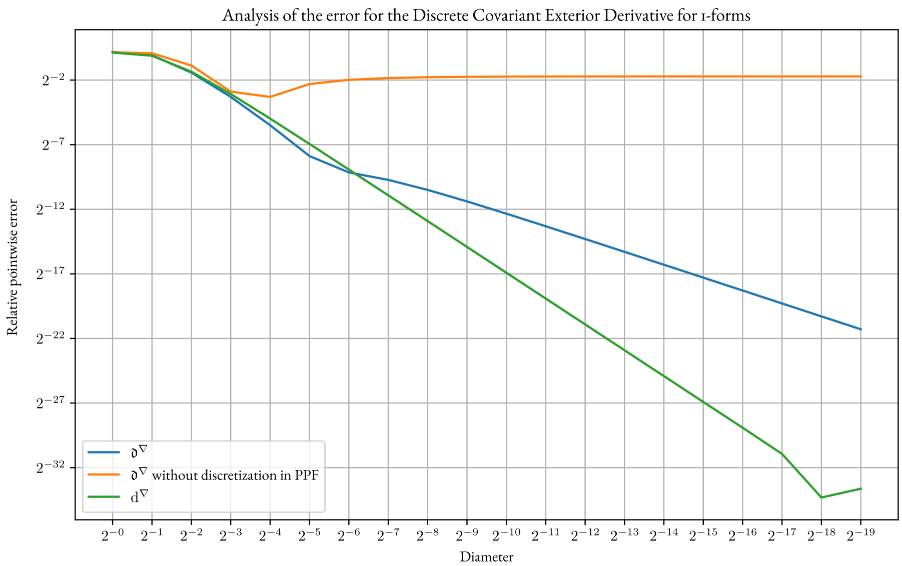

Figure 3.13: **Discrete exterior covariant derivative for vector-valued $1-$forms.** Comparison of the decay of the relative error for the PPF-derivative and the exterior covariant derivative for the $1-$form α given in Equation (3.3.25). A different slope in the logarithmic plot indicates a different convergence order (here, linear in blue vs. quadratic in orange).

Convergence of Discrete Covariant Derivative of Bundle-valued $2-$Forms. In order to check Theorems 3.41-3.43 for vector-valued $2-$forms as well, we construct a tetrahedron with points $p_0 = \left(0,0,0\right)^T, p_1 = \left(\sin(\frac{5\pi}{3}), \cos(\frac{5\pi}{3}), 1\right)^T, p_2 = \left(\sin(\frac{\pi}{3}), \cos(\frac{\pi}{3}), 1\right)^T, p_3 = \left(\sin(\pi), \cos(\pi), 1\right)^T$. We use Euler angles $(50°, 15°, 70°)$ to rotate the tetrahedron, and shift the tetrahedron by $v =$

$(3.4, -1.8, 3.9)$ for arbitrariness. For the vector-valued differential $2-$form

$$\alpha = \begin{pmatrix} 3y\, dy \wedge dz + x^2 dz \wedge dx \\ (xyz+1)\, dx \wedge dy \\ xy\, dy \wedge dz \end{pmatrix} \tag{3.3.26}$$

and the connection introduced in Equation (3.3.24), we illustrate convergence under mesh refinements for the discrete PPF-induced derivative and the discrete exterior covariant derivative in Figure 3.14.

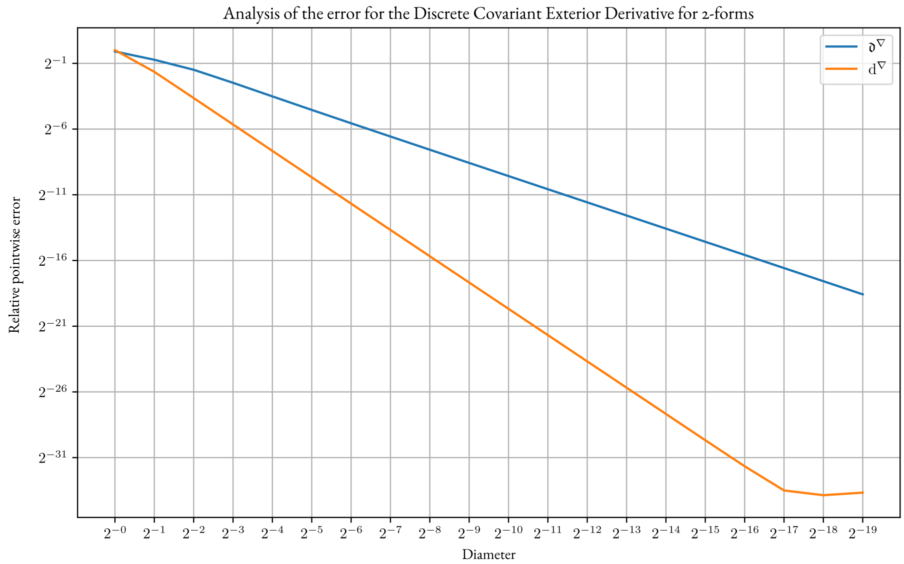

Figure 3.14: **Discrete exterior covariant derivative for vector-valued $2-$forms.** The alternation operator for discrete vector valued $2-$forms yields, as in the case for $1-$forms, an improved accuracy under refinement compared to the PPF-induced discrete exterior covariant derivative (orange vs. blue curve).

Algebraic Bianchi for Vector-valued Forms To check the convergence of the discrete algebraic Bianchi identity to its continuous counterpart, we consider the connection introduced in Equation (3.3.24). We compare the primal discrete exterior derivative $\mathfrak{d}^\nabla \boldsymbol{d}^\nabla$ for the solder form (orange) against the discrete exterior covariant derivative $\boldsymbol{d}^\nabla \boldsymbol{d}^\nabla$ (blue). We use the tetrahedron introduced above shifted by a vector $v = (3.4, -1.8, 3.9)^T$ and subsequently rotated by three matrices through the Euler angles $(50°, 15°, 70°)$. We observe in Figure 3.15 that the convergence is of the same order. Further, we illustrate that two consecutive applications of the operator $\mathfrak{d}^\nabla$ do not converge under refinement, even if the input form is obtained through discretization in a PPF. However note that the operator would have converged under refinement if it would have been applied to a discrete section.

Discrete Exterior Covariant Derivative for $(1,1)$-Tensor-valued One-Forms We also illustrate the numerical behavior of the discrete exterior covariant derivative for $(1,1)$-tensor valued

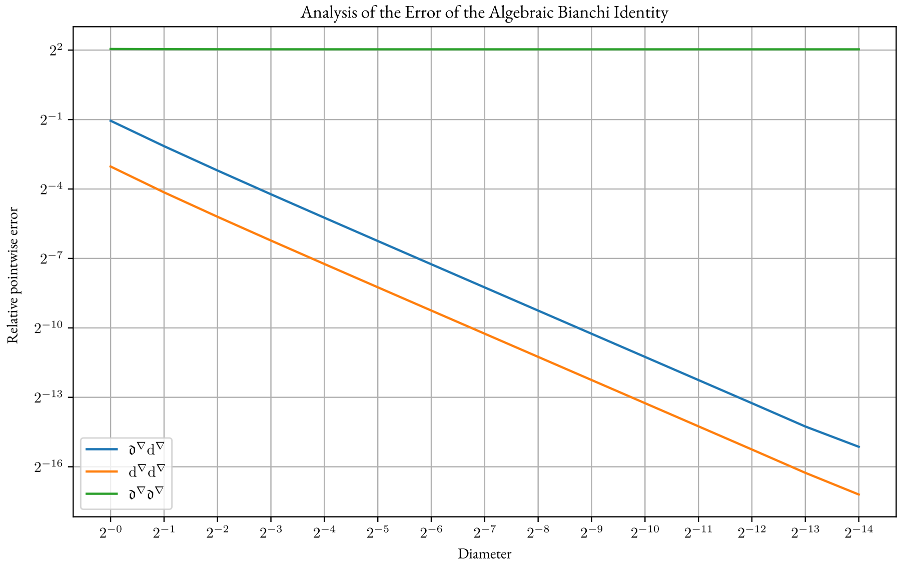

Figure 3.15: **Algebraic Bianchi identity under refinement for vector-valued $1-$forms** Using the PPF-Derivative of the alternated torsion or the discrete exterior covariant derivative of the alternated discrete torsion both lead under refinement to the same convergence order. However, two consecutive applications of the operator $\mathfrak{d}^\nabla$ without alternation in between to improve accuracy do not lead to convergence under refinement, even if the original form is discretized in a parallel-propagated frame field (green curve).

forms. Given a $(1,1)$-tensor-valued $1-$form

$$\beta = \begin{pmatrix} 0 & -xdy & 0 \\ xdy & 0 & dz \\ 0 & -dz & 0 \end{pmatrix} \in \Omega^1(\mathbb{R}^3, \mathrm{End}(T\mathbb{R}^3)) \tag{3.3.27}$$

and the connection $1-$form introduced in Equation (3.3.24), one can calculate that

$$d^{\nabla^{\mathrm{End}}}\beta = \begin{pmatrix} 0 & -\,dx \wedge dy & y\,dx \wedge dz \\ dx \wedge dy & 0 & x^2 dy \wedge dz \\ -y\,dx \wedge dz & -x^2\,dy \wedge dz & 0 \end{pmatrix}.$$

We translate the usual triangle we used previously with a vector $v = (3.5, 1.1, -1.2)^T$ and use Euler angles $(30°, 45°, 27°)$ to rotate the evaluation domain. We then calculate the discrete endomorphism-valued derivative and calculate the relative error against the smooth ground-truth value, resulting in Figure 3.16.

Discrete Exterior Covariant Derivative for $(1,1)$-Tensor-valued Two-Forms. For the endomorphism-valued $2-$form

$$\beta = \begin{pmatrix} 0 & x^2\,dy \wedge dz & 2z\,dx \wedge dy \\ -x^2\,dy \wedge dz & 0 & 0 \\ -2z\,dx \wedge\,dy & 0 & 0 \end{pmatrix},$$

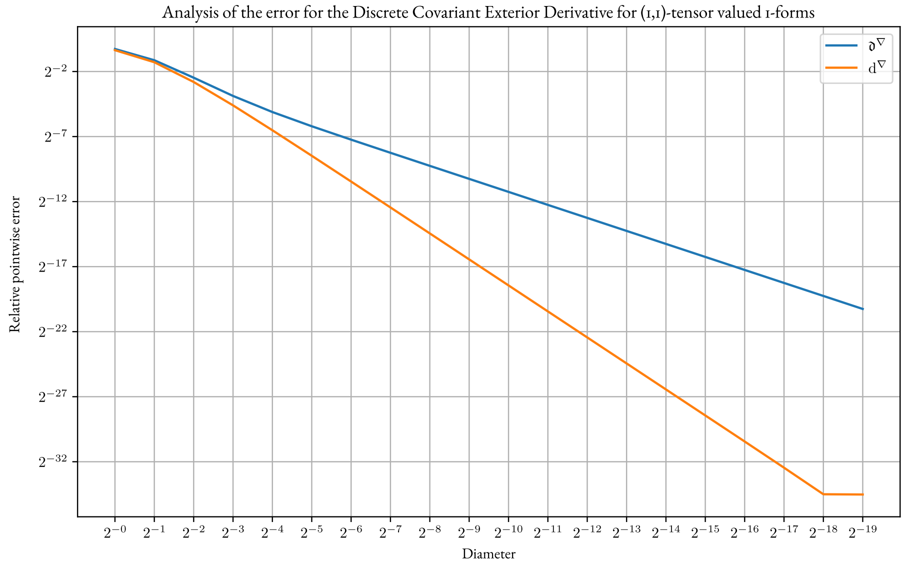

Figure 3.16: **Discrete exterior covariant derivative for $(1,1)$-tensor-valued forms** As in the $(1,0)$-tensor-valued case, we observe that the decay of the relative error for the PPF-derivative for $(1,1)$-tensor-valued forms is linear, and the endomorphism-valued alternation improves the accuracy of the PPF-derivative for a faster decay of the error.

the exterior covariant derivative can be calculated for the connection introduced in Equation (3.3.24) as

$$d^{\nabla^{\mathrm{End}}}\beta = \begin{pmatrix} 0 & 2x & 2 \\ -2x & 0 & -2z \\ -2 & 2z & 0 \end{pmatrix} dx \wedge dy \wedge dz.$$

Translating the tetrahedron introduced earlier with $v = \left(3, 3, 2\right)^T$ and using Euler angles $(30°, 10°, 190°)$ to rotate the tetrahedron, we can numerically verify in Figure 3.17 the convergence behavior explained in Remark 3.48.

Algebraic Bianchi for $(1,1)$-Tensor-valued One-Forms Using the aforementioned tetrahedron rotated with Euler angles $(60°, 50°, 120°)$ and shifted by a vector $v = (6.4, -3.8, 1.9)$, we obtain for the $(1,1)$-tensor valued form introduced in Equation (3.3.27) convergence of the algebraic Bianchi identity to its continuous counterpart under refinement as seen in Figure 3.18.

Conclusion. The numerical experiments confirm that our discrete exterior covariant derivative satisfies the properties established in this chapter, and that the convergence orders predicted by our analysis are sharp. These tests measure pointwise consistency. On each element we compare the discrete operator against the smooth ground truth at a fixed evaluation vertex under refinement. A natural and more demanding next step is a convergence analysis in the L^2 sense, where the discrete operator is assessed globally against a suitable Sobolev norm rather than at a single point. As the angle-defect example of [Gaw20] illustrates, identifying the norm in which a given discrete operator converges — and at what rate — is itself nontrivial, and it is exactly this question

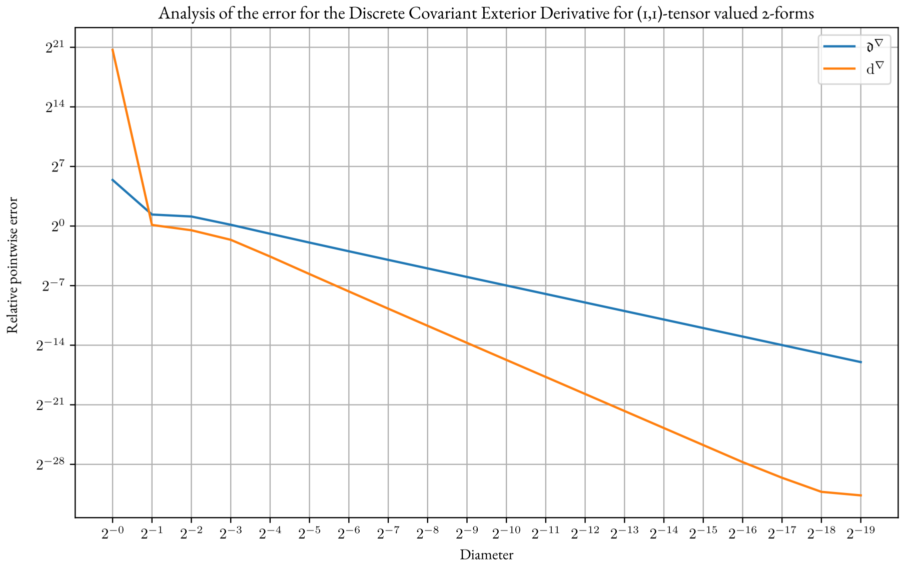

Figure 3.17: **Discrete exterior covariant derivative for $(1,1)$-tensor-valued 2–forms.** As in the $(1,0)$- tensor-valued case, we observe that the exterior covariant derivative for $(1,1)$-tensor-valued 2–forms converges faster under refinement compared to the PPF-induced discrete exterior covariant derivative.

that governs the operator's behaviour when used to discretize and solve PDEs.

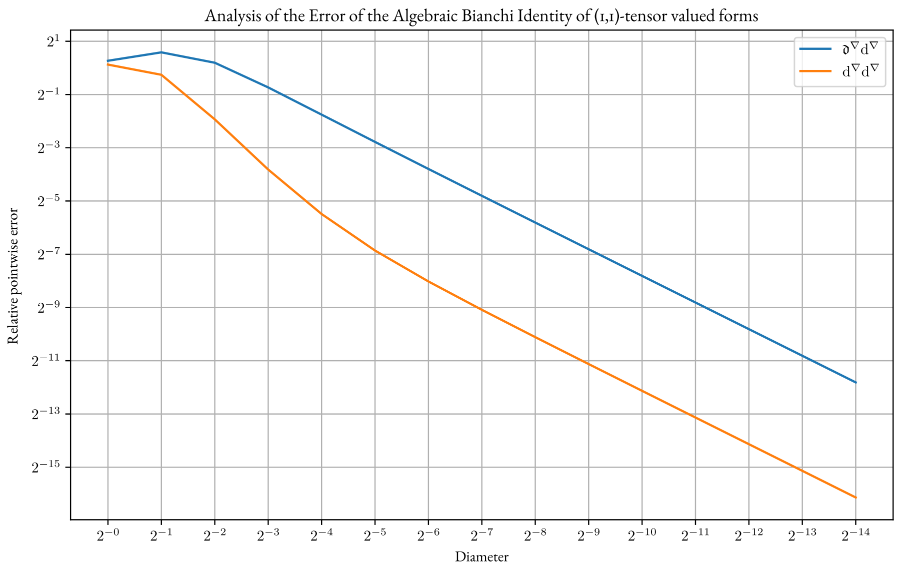

Figure 3.18: **Algebraic Bianchi identity for** $(1,1)$**-tensor-valued** $1-$**forms.** Calculating $\mathfrak{d}^{\nabla}\boldsymbol{d}^{\nabla}$ and $\boldsymbol{d}^{\nabla}\boldsymbol{d}^{\nabla}$ under refinement yields a linear decay under mesh refinement of the relative error compared to the integral of the smooth groundtruth. As in the $(1,0)$-tensor-valued case, another alternation cannot compensate for the lack of accuracy coming from the initial input.

4 Discrete Exterior Calculus of Bundle-Valued Forms on non-simplicial cells

Until this point, we showed that we can define a discrete exterior derivative for bundle-valued differential forms that satisfies the algebraic and the differential Bianchi identities. However, we limited our explanations to the case of simplicial cells. However, we show now that many of the presented concepts can be seamlessly carried over to the non-simplicial case.

4.1 Discrete Bundle-Valued Forms on non-simplicial cells

We have reviewed the definition of discrete bundle-valued forms in Definition 3.5 and Definition 3.6. It is important to note that these forms can similarly be defined for polytopal cells as a collection of maps. Additionally, the discretization scheme employing a parallel-propagated frame field to transform smooth bundle-valued forms into discrete bundle-valued forms can be adapted for retractable non-convex cells.

For retractable cells, we have introduced in Definition 3.16 the concept of a parallel-propagated frame field. This allows us to establish a retraction-dependent discretization scheme. When we restrict our focus to convex cells, we benefit from a canonical retraction map. Consequently, we also obtain a canonical parallel-propagated frame field, which can be utilized for the discretization of smooth bundle-valued forms.

4.2 Discrete Exterior Covariant Derivative on non-simplicial meshes

Let $\mathcal{M}$ be a smooth manifold and $E(\mathcal{M})$ be a smooth vector bundle with connection ∇. Further let M be a discrete manifold and $T \subset \mathcal{M}$ a domain for which there exists a diffeomorphism φ and a polytopal $(\ell + 1)$-dimensional cell $\mathcal{T}$ such that $\varphi(\mathcal{T}) = T$. Furthermore we assume that there exist pairwise disjoint polytopal (ℓ)-cells $\{\sigma_i\}_{i=1,\ldots,N}$ with $\mathcal{T} = \cup_i \sigma_i$. We denote by $s_i \subset T$ the image of σ_i under φ. We denote by $c_{\mathcal{T}}$ the center of mass of $\mathcal{T}$ and $c_T = \varphi(c_{\mathcal{T}})$ the image under φ.

We will in the following add the center of mass as an imaginary new vertex to the cell $\mathcal{T}$ to have a canonical evaluation fiber. The point $c_{\mathcal{T}}$ subdivides the cell into cones, consisting of the $\ell-$dimensional polytopal boundary faces and the center of mass. We denote by $\tilde{T}$ be the union of these cones.

Let ∇^{int} be a discrete connection on $\tilde{T}$ such that

$$\nabla^{\text{int}}|_T = \nabla,$$

which additionally contains parallel transport matrices between the primal vertices and the barycenter. We discuss the case that the transport matrices are given by an oracle first. This could be the case if ∇ arises through integration from a known smooth connection ∇ and can therefore be integrated between arbitrary points. Afterwards we explain how one can derive estimations for the parallel transport maps from the primal vertices to the barycenter solely from the data available on primal edges. The advantage of the introduced simplicialization is that all conical $(\ell+1)$-cells that form $\tilde{T}$ share a common evaluation fiber; the center of mass.

We have reviewed that the PPF-induced discrete exterior covariant derivative can be interpreted as a high order approximation of the discretization of the smooth exterior covariant derivative in a parallel-propagated frame field for bundle-valued $\ell-$forms. This motivates the following definition in the non-simplicial case:

Definition 4.1 (PPF-Induced exterior covariant derivative on non-simplicial cells)**.** *Let M be a discrete orientable manifold with a discrete vector bundle $\mathbf{E}$ with discrete connection $\nabla = \{R_{ij}\}_{e_{ij}\in\mathcal{E}}$ over it. Let T be an $(\ell+1)$-dimensional convex polytopal region with $\partial T = \bigcup_j s_j$, where $s_j \in M^\ell$ are polytopal $\ell-$cells forming the boundary of T and $v_j \in s_j$ one arbitrary vertex in s_j. Further let α be a discrete vector valued $\ell-$form and c_T be the center of mass of T. We denote*

$$\nabla^{\text{int}} := \nabla \cup \{R_{i,c_T}, R_{c_T,i} : i \in \mathcal{V}\}$$

the discrete connection that contains in addition the parallel transport maps from the primal vertices to the barycenter of the cell. The PPF-induced discrete exterior covariant derivative is then given by

$$\mathfrak{d}^{\nabla^{\text{int}}}\alpha(T, c_T) = \sum_{s_j\in T} R_{c_T,v_j}\alpha(s_j, v_j).$$

For a primal vertex $v \in T$ we define the PPF-induced discrete exterior covariant derivative through

$$\mathfrak{d}^{\nabla^{\text{int}}}\alpha(T, v) = R_{v,c_T}\mathfrak{d}^{\nabla^{\text{int}}}\alpha(T, c_T).$$

It should be noted that the operator depends on the particular choice of intermediate evaluation fiber v_j.

In the study of the simplicial case, we demonstrated the importance of averaging the output of the PPF-induced discrete exterior covariant derivative proposed by [BEHS21]. This averaging converts corner-based approximations of the integral of the smooth exterior covariant derivative into center-based integrals. This approach allowed us to show that the proposed averaged d^∇ satisfies the algebraic Bianchi identity numerically under mesh refinement.

In this chapter, we introduce an extended notion of the bundle-valued exterior derivative applicable to arbitrary convex cells and special star-shaped cells. The presented operator, $\mathfrak{d}^{\nabla^{\text{int}}}$, shares similarities with the side-based PPF-induced discrete exterior covariant derivative proposed in Chapter 3. Specifically, it approximates the integral in the corner-based PPF of the discrete exterior covariant derivative.

In the simplicial case, we employed the alternation operator to mitigate bias and enhance the accuracy of the discrete exterior covariant derivative. For the non-simplicial case, we will apply a similar strategy. However, unlike many of the previously mentioned concepts, the alternation does not seamlessly transfer to the polytopal case. Consequently, we need to adapt the definition of the discrete exterior covariant derivative for non-simplicial cells.

Generalized Barycentric Coordinates. Given a convex simplicial $\ell-$cell, we can define Whitney basis functions, i.e zero forms as the barycentric coordinate functions of the primal vertices. In the simplicial case the barycentric coordinate functions can be simply computed through a volume ratio. In the non-simplicial case, this is not possible anymore.

Given a convex $\ell-$cell s with vertices $v_0 \ldots, v_n$, we call a set of functions $\phi_i \colon s \to [0, 1]$, $i = 0, \ldots, n$ *generalized barycentric coordinates* if for all $x \in s$

1. $\sum_{i=0}^{n} \phi_i \equiv 1$
2. $x = \sum_{i=0}^{n} \phi_i(x) \cdot v_i$

In [WSHD07], they propose a way to define such a set of generalize barycentric coordinates for convex cells.

Definition 4.2 (Weight function of a simple vertex, [WSHD07]). *Given a convex cell C of dimension n, whose faces are pairwise not colinear, we call a vertex $v \in C$ simple, if its valence is n. For a simple vertex let $\{n_{\mathrm{ind}(v)}\}$ be the set of normals of the faces that contain v. For $x \in C \backslash \partial C$ the weight function of dimension n for vertex v is given by*

$$w_n^v(x) = \frac{\left|\det(\mathrm{n}_{\mathrm{ind(v)}})\right|}{\prod_{j \in \mathrm{ind}(v)} n_j \cdot (v - x)}.$$

For $x \in \partial C$ we define

$$w_n^v(x) = w_{n-1}^v(x).$$

For a vertex v whose valence is $k \neq n$, we follow the idea of [WSHD07] to infinitesimally perturb the vertex, to create new artificial vertices in the mesh, that are each simple, for which we can use the above definition, see Figure 4.1. The weight for v is subsequently calculated as the sum of the weights of each of the artificial new vertices.

We calculate the normal via the shoelace formula presented in [DGBD20]. This allows to attribute a normal also to faces that are not necessarily planar anymore.

Definition 4.3 (Generalized Barycentric Coordinates.[WSHD07]). *Given a convex n-cell C,*

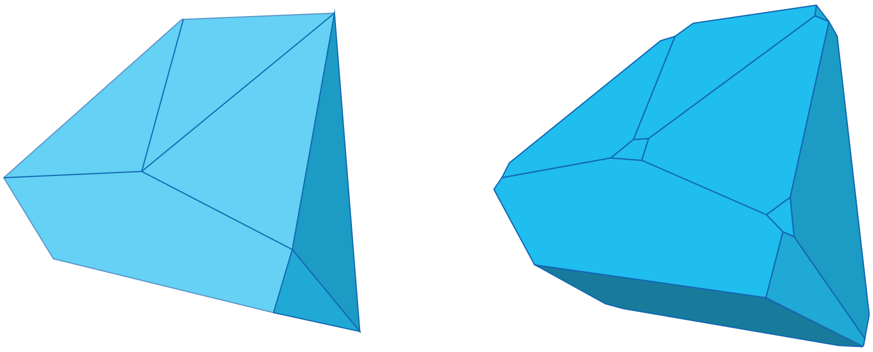

Irregular Simplex | Perturbation into simple Vertices

Figure 4.1: **Perturbation into simple vertices:** Any non simple vertex can be perturbed into an infinitesimal $k-$ gon whose vertices are all simple

the generalized $n-$dimensional barycentric coordinate function of vertex $v \in C$ is defined as

$$\phi_v(x) = \frac{w_n^v(x)}{\sum_{v_i \in C} w_n^{v_i}(x)}$$

In their Appendix B, [WSHD07] prove that the coordinates functions ϕ_v are linear accurate and that they form a partition of unity.

Remark 4.4. In contrast to the simplicial case the aforementioned generalized barycentric coordinates are in general not linear functions along a straight path, but rational polynomials.

With this at our disposal we can define the discrete exterior covariant derivative on non simplicial cells.

Definition 4.5 (Discrete exterior derivative for convex non-simplicial cells)**.** *Let M be a discrete orientable manifold with a discrete vector bundle $\mathbf{E}$ with discrete connection $\boldsymbol{\nabla} = \{R_{ij}\}_{e_{ij} \in \mathcal{E}}$ on it. Let T be an $(\ell + 1)$-dimensional convex polytopal region with $\partial T = \bigcup_j s_j$, where $s_j \in C^\ell(T)$ are convex polytopal $\ell-$cells forming the boundary of T. Further let $\boldsymbol{\alpha}$ be a discrete vector valued $\ell-$form and c_T be the center of mass of T. We denote*

$$\boldsymbol{\nabla}^{\text{int}} := \boldsymbol{\nabla} \cup \{R_{i,c_T}, R_{c_T,i} : i \in \mathcal{V}\}$$

the discrete connection that contains in addition parallel transport maps from the primal vertices to the barycenter of the cell. In addition, let $\left\{\phi_i^{s_j} \middle| i \in T\right\}$ be a set of generalized barycentric coordinate functions for every $\ell-$cell $s_j \in \partial T$.

We define the discrete exterior covariant derivative in this case as

$$\boldsymbol{d}^{\boldsymbol{\nabla}^{\text{int}}} \boldsymbol{\alpha}(T, c_T) = \sum_{s_j \in \partial T} \left(\sum_{w \in s_j} \phi_w^{s_j}(c_{s_j}) R_{c_T,w} \boldsymbol{\alpha}(s_j, w) \right),$$

where c_{s_j} is the center of mass of s_j. For a primal vertex $v \in T$ we define the PPF-induced discrete exterior covariant derivative as

$$\boldsymbol{d}^{\nabla^{\text{int}}}\boldsymbol{\alpha}(T,v) = R_{v,c_T}\boldsymbol{d}^{\nabla^{\text{int}}}\boldsymbol{\alpha}(T,c_T).$$

Remark 4.6. It is noteworthy that unlike in the simplicial case, we cannot generally define the discrete exterior covariant derivative solely in terms of the PPF-induced derivative. In the simplicial scenario, to exploit the sidedness of the PPF-Derivative, we could uniformly apply weights to convert integrals in vertex-based PPF into integrals in center-based PPF. However, in the non-simplicial case, this approach is generally no longer feasible. Nonetheless, under the additional assumption that the $(\ell+1)$-cell solely consists of $\ell-$simplices, we demonstrate below a correlation between the operators $\mathfrak{d}^{\nabla}$ and $\boldsymbol{d}^{\nabla}$.

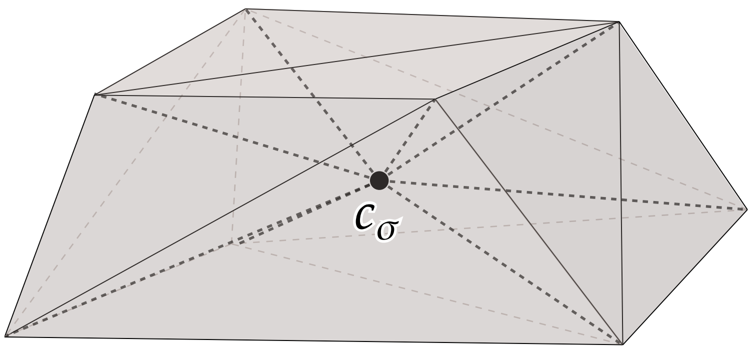

Figure 4.2: The choice of the center of mass as evaluation vertex implicitly subdivides the cell into cones.

We can now prove that the discrete exterior covariant derivative evaluated on the barycenter converges under refinement.

Theorem 4.7. *Let $\mathcal{M}$ be a smooth manifold and $E(\mathcal{M})$ a smooth vector bundle with connection ∇. Further let $T \subset \mathcal{M}$ be domain for which there exists a diffeomorphism φ and a polytopal convex $(\ell+1)$-dimensional cell $\mathcal{T}$ such that $\varphi(\mathcal{T}) = T$. Furthermore we assume that there exist convex polytopal (ℓ)-cells $\{\sigma_i\}_{i=1,\dots,N}$ with $\partial\mathcal{T} = \bigcup_i \sigma_i$. We denote by $s_i \subset T$ the image of σ_i under φ. Let $\boldsymbol{\alpha}$ be an $\mathbf{E}-$valued $\ell-$form arising through integration from a smooth form $\alpha \in \Omega^\ell(M,E)$. Let $\boldsymbol{\nabla}^{\text{int}}$ be the discrete connection containing the parallel transport maps along the primal edges of T and the joining paths from the primal vertices to c_T, obtained through integration of ∇. In this case, it holds*

$$\int_T R^{\nabla,c_T} d^\nabla \alpha = \mathfrak{d}^{\boldsymbol{\nabla}^{\text{int}}} \boldsymbol{\alpha}(T, c_T) + \mathcal{O}(h^{\ell+2}) \tag{4.2.1}$$

$$\int_T R^{\nabla,c_T} d^\nabla \alpha = \boldsymbol{d}^{\boldsymbol{\nabla}^{\text{int}}} \boldsymbol{\alpha}(T, c_T) + \mathcal{O}(h^{\ell+3}) \tag{4.2.2}$$

or equivalently intrinsically

$$\underset{T}{{}^{\nabla}_{\varphi c_T}\!\!\int} d^\nabla \alpha = \mathfrak{d}^{\boldsymbol{\nabla}^{\text{int}}} \boldsymbol{\alpha}(T, c_T) + \mathcal{O}(h^{\ell+2}) \tag{4.2.3}$$

$$\underset{T}{{}^{\nabla}_{\varphi c_T}\!\!\int} d^\nabla \alpha = \boldsymbol{d}^{\boldsymbol{\nabla}^{\text{int}}} \boldsymbol{\alpha}(T, c_T) + \mathcal{O}(h^{\ell+3}). \tag{4.2.4}$$

Proof. It holds for the integral in a center of mass based parallel-propagated frame

$$\int_T R^{\nabla,c_T} d^\nabla \alpha = \int_{\partial T} R^{\nabla,c_T} \alpha + \mathcal{O}(h^{\ell+3}).$$

This result was shown in Definition 3.43 for the simplicial case. However, the same argumentation can be used to show this statement also for the case of more general convex polytopal cells as long as we base the PPF in the center of mass, see Remark 3.40.

Therefore

$$\int_T R^{\nabla,c_T} d^\nabla \alpha = \sum_{s_i \in \partial T} \int_{s_i} R^{\nabla,c_T} \alpha + \mathcal{O}(h^{\ell+3}).$$

By definition, the contributions for $\boldsymbol{d}^{\boldsymbol{\nabla}^{\text{int}}} \boldsymbol{\alpha}(T, c_T)$ coming from s_i can be expressed as

$$\sum_{v \in s_i} R_{c_T,v} \phi_v(c_{s_i}) \boldsymbol{\alpha}(s_i, v).$$

Thus, this means that the contributions for the error of Equation (4.2.2) coming from s_i are of the form

$$\begin{aligned}
\sum_{v\in s_i} R_{c_T,v}\phi_v(c_{s_i})\boldsymbol{\alpha}(s_i,v) - \int_{s_i} R^{\nabla,c_T}\alpha - &= \sum_{v\in s_i}\phi_v(c_{s_i})\left(R_{c_T,v}\int_{s_i} R^{\nabla,v}\alpha - \int_{s_i} R^{\nabla,c_T}\alpha\right)\\
&= \sum_{v\in s_i}\phi_v(c_{s_i})\int_{s_i}\left(R_{c_T,v}R^{\nabla,v} - R^{\nabla,c_T}\right)\alpha\\
&= \sum_{v\in s_i}\phi_v(c_{s_i})\underbrace{\int_{s_i}\Omega^{\nabla}_{c_T}(v-c_T,c_{s_i}-c_T)\alpha}_{*} + \mathcal{O}(h^{\ell+3})\\
&= \Omega^{\nabla}_{c_T}\Bigg(\underbrace{\sum_{v\in s_i}\phi_v(c_{s_i})(v-c_T)}_{=c_{s_i}-c_T}, c_{s_i}-c_T\Bigg)\int_{s_i}\alpha + \mathcal{O}(h^{\ell+3})\\
&= \mathcal{O}(h^{\ell+3})
\end{aligned}$$

The contribution in $*$ is of order $\mathcal{O}(h^{\ell+2})$ and is the contribution to the error for face s_i in Equation Equation (4.2.1) and does not cancel for the operator $\mathfrak{d}^{\nabla^{\text{int}}}$, which yields the claim. $\square$

The key insight of the alternation operator in the simplicial case is its ability to convert corner-based integrals into center-of-mass-based integrals. In the simplicial case, considering the centroid or the center of mass is equivalent, allowing the use of uniform weights. However, in the non-simplicial case, this equivalence does not hold, as the center of mass and the centroid are not identical. Consequently, non-uniform weights must be applied.

We provide in Section 4.2.1 a numerical verification of the theorems presented in this chapter.

Using the properties of the simplicial exterior derivative, we get the following result for the operator acting on non-simplicial cells whose boundary consists of simplicial cells.

Theorem 4.8 (Relationship between the simplicial and non-simplicial discrete exterior covariant derivative)**.** *Let M be a discrete manifold and $\mathbf{E}$ a discrete vector bundle over M with connection $\boldsymbol{\nabla}$. Let $\boldsymbol{\alpha}$ be an $\mathbf{E}$−valued ℓ−form. Further let $T = \bigcup_i s_i$ be an $(\ell+1)$-cell whose boundary consists of simplicial ℓ−cells. Let $c_T \in \mathbb{R}^n$ be the center of mass of T and $\boldsymbol{\nabla}^{\text{int}}$ the connection extending $\boldsymbol{\nabla}$ to the joining paths from the primal vertices to c_T. We denote by $[c_T, s_i]$ the simplicial $\ell+1$−cell formed by the center of mass and the ℓ−cell s_i. In this case we have*

$$\boldsymbol{d}^{\boldsymbol{\nabla}^{\text{int}}}\boldsymbol{\alpha}(T,c_T) = \sum_{s_i\in\partial T}\boldsymbol{d}^{\boldsymbol{\nabla}}\boldsymbol{\alpha}([c_T,s_i],c_T). \tag{4.2.5}$$

Proof. In the following we will denote by s_i^j the j−th vertex of the i−th simplicial cell in the boundary of T. It holds

$$\sum_{s_i \in \partial T} \boldsymbol{d}^{\nabla^{\text{int}}} \boldsymbol{\alpha}([c_T, s_i], c_T) = \sum_{s_i \in \partial T} \text{Alt}^{\nabla^{\text{int}}} \mathfrak{d}^{\nabla^{\text{int}}} \boldsymbol{\alpha}([c_T, s_i], c_T)$$

$$= \sum_{s_i \in \partial T} \text{Alt}^{\nabla^{\text{int}}} \left(R_{c_T, s_i^0}\, \boldsymbol{\alpha}(s_i, s_i^0) + \sum_{j=0}^{\ell} (-1)^j\, \boldsymbol{\alpha}([c_T, s_i^0, \ldots, \widehat{s_i^j}, \ldots, s_i^\ell]) \right).$$

Note that all non-boundary faces appear exactly twice in this summation. But in the two cases each time with opposite orientation. Therefore, as in the theory of scalar valued DEC, we can argue that their contributions cancel. We are therefore left with the contributions on the boundary. Using the definition of the alternation, we can deduce that every vertex in the simplicial cell serves as intermediate evaluation fiber to transport the quantities to the barycenter. Hence

$$\sum_i \boldsymbol{d}^{\nabla^{\text{int}}} \boldsymbol{\alpha}([c_T, s_i], c_T) = \sum_i \left(\frac{1}{\ell+1} \sum_{j=0}^{\ell} R_{c_T, s_i^j}\, \boldsymbol{\alpha}(s_i, s_i^j) \right) = \boldsymbol{d}^{\nabla^{\text{int}}} \boldsymbol{\alpha}(T, c_T),$$

which means that in this particular setting we can reproduce the discrete exterior covariant derivative with the simplical discrete exterior covariant derivative. □

Discrete Exterior Covariant Derivative for $(1,1)$-Tensor Valued Forms In the vector valued case, in order to define the sided PPF induced discrete exterior covariant derivative we made use of the center of mass as an auxiliary evaluation fiber to have a common evaluation fiber. For the case of $(1,1)$-tensor valued forms, we need to use a canonical fiber for input and output for which we will both use the center of mass. We define therefore the sided discrete exterior covariant derivative for $(1,1)$-tensor valued forms through the following

Definition 4.9 (PPF-induced Discrete Exterior Covariant Derivative for $(1,1)$-Tensor Valued Forms)**.** *Let M be a discrete orientable manifold with a discrete vector bundle $\mathbf{E}$ with discrete connection $\nabla = \{R_{ij}\}_{e_{ij} \in \mathcal{E}}$ over it. Let T be an $(\ell+1)$-dimensional convex polytopal region with $\partial T = \bigcup_j s_j$, where $s_j \in C^\ell(T)$ are polytopal pairwise disjoint ℓ–cells forming the boundary of T. For each $s_j \in \partial s$ let $v_0^j, v_1^j \in s_j$ be two arbitrary vertices in s_j. Further let $\boldsymbol{\beta}$ be a discrete $(1,1)$-tensor valued ℓ–form and c_T be the center of mass of T. We denote*

$$\nabla^{\text{int}} := \nabla \cup \{R_{i,c_T}, R_{c_T,i} : i \in \mathcal{V}\}$$

the discrete connection that contains in addition the parallel transport maps from the primal vertices to the barycenter of the cell. We define the PPF-induced discrete exterior covariant derivative through

$$\mathfrak{d}^{\nabla^{\text{int}}} \boldsymbol{\beta}(T, c_T, c_T) = \sum_{s_j \in T} R_{c_T, v_0^j}\, \boldsymbol{\beta}\left(s_j, v_0^j, v_1^j\right) R_{v_1^j, c_T}.$$

It should be noted that the operator depends on the particular choice of intermediate input and evaluation fiber v_0^j, v_1^j.

If we are in the setup of Theorem 4.7 it is possible to show that

$$\mathfrak{d}^{\nabla}\beta(T,c_T,c_T) = \int_T R^{\nabla,c_T}\, d^{\nabla^{\text{End}}}\beta \left(R^{\nabla,c_T}\right)^{-1} + \mathcal{O}(h^{\ell+2}). \tag{4.2.6}$$

The definition of the sided discrete exterior covariant derivative depends on an arbitrarily chosen input and evaluation fiber, introducing some sidedness. We aim to introduce an alternation operator that addresses this sidedness and converts corner-based integrals into center-based integrals up to higher order. Unlike the vector-valued case, a consistent averaging over both the input and evaluation fibers is necessary. This motivates the following definition.

Definition 4.10 (Discrete Exterior Covariant Derivative for $(1,1)$-Tensor Valued Forms on non Simplicial Cells)**.** *Let M be a discrete orientable manifold with a discrete vector bundle* $\mathbf{E}$ *with discrete connection $\boldsymbol{\nabla} = \{R_{ij}\}_{e_{ij}\in\mathcal{E}}$ over it. Let T be an $(\ell+1)$-dimensional convex polytopal region with $\partial T = \bigcup_j s_j$, where $s_j \in C^{\ell}(T)$ are convex polytopal disjoint $\ell-$cells forming the boundary of T. Further let $\boldsymbol{\beta}$ be a discrete $(1,1)$-tensor valued $\ell-$form and c_T be the center of mass of T. We denote*

$$\boldsymbol{\nabla}^{\text{int}} := \boldsymbol{\nabla} \cup \{R_{i,c_T}, R_{c_T,i} : i \in \mathcal{V}\}$$

the discrete connection that contains in addition the parallel transport maps from the primal vertices to the barycenter of the cell. In addition, let $\{\phi_i | i \in T\}$ be a set of generalized barycentric coordinate functions in T.

We define the discrete exterior covariant derivative in this case as

$$\boldsymbol{d}^{\nabla^{\text{int}}}\boldsymbol{\beta}(T,c_T,c_T) = \sum_{s_j\in T}\left(\sum_{(v,w)\in s_j\times s_j} \phi_w(c_{s_j})\,\phi_v(c_{s_j})\,R_{c_T,w}\,\boldsymbol{\beta}(s_j,w,v)\,R_{v,c_T}\right),$$

where c_{s_j} is the center of mass of s_j.

We observe that we have to do a nested alternation for the input and the output fiber in order to improve the accuracy of the discrete exterior covariant derivative under refinement. With this discrete operator in place it holds

$$\boldsymbol{d}^{\nabla}\boldsymbol{\beta}(T,c_T,c_T) = \int_T R^{\nabla,c_T}\, d^{\nabla^{\text{End}}}\beta \left(R^{\nabla,c_T}\right)^{-1} + \mathcal{O}(h^{\ell+3}). \tag{4.2.7}$$

We provide in Section 4.2.1 a numerical verification of the convergence results and the derivation can be carried out similarly to the simiplicial endomorphism valued case, see Chapter E.

Comparison with [BEHS21] and [CH23]. An alternative methodology for describing discrete vector bundles at the cellular level is presented in [CH23]. Their approach involves assigning one fiber per cell, considering per cell only one fiber on one inner point, which stands in contrast to our method of one fiber per vertex. They define a connection by means of linear maps between the chosen fibers per cell. This differs from our simplicial approach where a discrete connection is established as a parallel transport map per primal edge. Unlike our method, their notion requires additional information for parallel transport along the paths connecting the centers of $\ell-$ and

$(\ell + 1)$-cells. This is in some sense closer to the ∇^{int} defined above. In their framework, given a discrete connection and a differential $\ell-$form, the definition of a discrete exterior covariant derivative on a $(\ell+1)$-cell involves summing the evaluations of discrete bundle-valued differential forms on the $\ell-$faces, transported to the dedicated fiber of the $(\ell + 1)$-cell.

Our approach to defining a discrete exterior derivative on non-simplicial cells shares some similarities with the methodology introduced in [BEHS21, Chapter 11]. We select a dedicated 'artificial' fiber situated at the center of the $(\ell+1)$-cell, serving as a point where summation is performed, and the choice of transport paths is clearer. However, we currently assume that these transport paths to the fiber in the center are provided. In addressing these limitations, we will elaborate below on how our methodology resolves these issues. While our discrete exterior covariant derivative on simplicial cells bears some resemblance to the approach presented in [BEHS21], the key distinction lies in the incorporation of the alternation operator.

Notably, in Proposition 11.1 of [BEHS21], it was demonstrated that the sided discrete exterior covariant derivative can reproduce the exterior covariant derivative introduced in [CH23]. This Proposition 11.1 shares similarities with the presented Theorem 4.8 above.

Examining the right-hand side of Equation (4.2.5), we find a sum over all $\ell-$cells transported to a dedicated fiber in the center, resembling the exterior covariant derivative presented in [CH23] and our presented notion of discrete exterior covariant derivative. On the right-hand side in theorem 4.8, we observe a sum of exterior covariant derivatives on simplicial cells, defining $\boldsymbol{d}^{\nabla}$ for non-simplicial cells, similar to the right-hand side of Proposition 11.1 in [BEHS21].

Estimation of the Connection $1-$form. While we achieve convergence using the operator $\boldsymbol{d}^{\nabla^{\text{int}}}$ with parallel transport matrices from primal vertices to the barycenter, it necessitates data not initially available on the primal complex. If we had knowledge of the underlying smooth connection, integration would be possible. However, adopting a discrete perspective where information is limited to the connection on primal edges, this approach falls short.
In our numerical tests, we empirically observed that Definition 4.7 can be reproduced by fitting a linear connection $1-$form ω to the integrated data available on primal edges. By integrating the fitted differential form along arbitrary paths within the interior of the domain, we are able to determine the parallel transport along these paths.
This approach worked well for the cells tested in our numerical experiments. The downside of this approach is that the linearly fitted connection $1-$form does not interpolate the values on the boundary edges. If we were given linear accurate cellular basis 1-forms on non simplicial cells that interpolate the connection $1-$form on the boundary edges, we could use these to integrate the connection $1-$form along the joining paths from the primal vertices to the barycenter. This would yield an exact reproduction of the connection $1-$form on the boundary edges. However, as we will explain in the following remark, constructing such basis forms is not straightforward.

Remark 4.11. In our experiments, we also conducted an estimation of the integral of the connection $1-$form by integrating Whitney basis forms derived from the aforementioned Whitney basis 0-forms. However, in contrast to the simplicial case, a limitation arises. As demonstrated in [GRB16] to reconstruct an accurately linear connection $1-$form through Whitney basis forms that are derived from Wachspress coordinates for 0-forms[Wac75, WSHD07], it is necessary to possess information about the connection $1-$form on segments connecting two vertices, even when they do not constitute an edge. If ϕ_i denotes the Whitney $0-$form for vertex v_i, we obtain

$$dx = \sum_{i\in\mathcal{V}} d\phi_i x_i = \sum_{i\in\mathcal{V}}\left(\sum_{j\in\mathcal{V}}\phi_j\right) d\phi_i x_i = \sum_{(i,j)\in\mathcal{V}\times\mathcal{V}, i\neq j} \phi_j d\phi_i x_i + \sum_{i\in\mathcal{V}} \phi_i d\phi_i x_i.$$

Since the functions ϕ_i form a partition of unity, it holds $0 = \sum_{i\in\mathcal{V}} d\phi_i$, thus

$$\begin{aligned} dx &= \sum_{(i,j)\in\mathcal{V}\times\mathcal{V}, i\neq j} \phi_j d\phi_i x_i + \sum_{i\in\mathcal{V}} \phi_i \left(-\sum_{j\in\mathcal{V}, i\neq j} d\phi_j\right) x_i \\ &= \sum_{(i,j)\in\mathcal{V}\times\mathcal{V}, i\neq j} (\phi_j d\phi_i - \phi_i d\phi_j) x_i. \end{aligned}$$

Equivalently

$$dx = \sum_{(i,j)\in\mathcal{V}\times\mathcal{V}, i\neq j} (\phi_i d\phi_j - \phi_j d\phi_i) x_j,$$

thus

$$dx = \sum_{(i,j)\in\mathcal{V}\times\mathcal{V}, i\neq j} (\phi_i d\phi_j - \phi_j d\phi_i)(x_j - x_i) = 2\sum_{i<j} (\phi_i d\phi_j - \phi_j d\phi_i)(x_j - x_i).$$

By using the forms $\{\phi_i d\phi_j - \phi_j d\phi_j \mid (i,j) \in \mathcal{V}\times\mathcal{V}, i \neq j\}$, we can re express the form dx in an exact sense.

The derivation underscores a key challenge: achieving linear accuracy for the approximation of the connection $1-$form with Whitney forms necessitates knowledge of the differential form along segments connecting vertices, even if they don't constitute a primal edge. Despite employing various strategies to estimate the connection $1-$form on these non-primal edges, numerical tests revealed that these techniques lack the required accuracy. While these estimates ensure the convergence under refinement for a single application of $\boldsymbol{d}^{\nabla}$, they fall short of achieving enhanced accuracy through alternation compared to $\mathfrak{d}^{\nabla}$. Notably, only through a direct integral of the connection $1-$form along these non-primal segments can we managed to attain improved accuracy for the exterior covariant derivative under refinement when compared to the sided PPF-induced discrete exterior covariant derivative.
Furthermore, this underscores a challenge for the construction of a Whitney map on non simplicial cells.

Numerically we are nevertheless able to reproduce the convergence under mesh refinement using just the data available on the boundary edges. In practice we can use a least square fit of the connection 1-form on the discrete data on the boundary.

Extension onto more general cells The argumentation in the convergence proof of Theorem 4.7 reveals that the requirement of convexity is somewhat more stringent than strictly necessary. In cases where the $(\ell+1)-$dimensional region is star-shaped and the barycenter is accessible from every point within the cell, we can maintain convergence up to $\mathcal{O}(h^{\ell+3})$. This would require to use a set of generalized barycentric coordinates, like mean value coordinates to define the averaging in the discrete exterior covariant derivative. Even if the star-shaped domain does not allow reaching the center of mass from every point, we can establish the parallel-propagated frame based on the reachable point. However, under such circumstances, the reduction to the boundary integral is only of order $\mathcal{O}(h^{\ell+2})$.

4.2.1 Numerical Verification

In the following we will illustrate for sample cases the convergence of the discrete exterior covariant derivative. The python verification code can be found under the following link `https://gitlab.inria.fr/geomerix/public/fulldec-non-simplicial/`.
For the numerical test we will consider a given connection $1-$form ω and integrate it on segments to use the discrete exterior covariant derivative. We use the connection $1-$forms

$$\omega_1 = \begin{pmatrix} 0 & ydx+dz & xdz \\ -ydx-dz & 0 & 0 \\ -xdz & 0 & 0 \end{pmatrix}, \quad \text{and} \quad \omega_2 = \begin{pmatrix} 0 & xydz+dx & x^2dz \\ -xydz-dx & 0 & 0 \\ -x^2dz & 0 & 0 \end{pmatrix} \tag{4.2.8}$$

to conduct the tests.
We use the approximation and quadrature schemes described in Section 3.3.3 to calculate the path ordered matrix exponential. Further we will use for the discretization of $1-$forms a $5^{\text{th}}-$order Gauß-Legendre quadrature scheme to approximate the integral of the differential form α in a PPF. For the discretization of $2-$forms, we use 2D-quadrature rules (provided, for instance, in [Bur10]) to approximate the integral in a PPF on the polytopal cells.
We illustrate the convergence under refinement when we use the direct integral of the connection $1-$form on arbitrary paths to obtain the parallel transport and if we use an integral of a linear least square fit with the data of the integrated connection $1-$form on the primal edges to approximate the parallel transport on arbitrary paths.

Verification of Theorem 4.7 for bundle-valued $1-$forms. We consider a convex non-simplicial domain defined through the points shown in Figure 4.3.

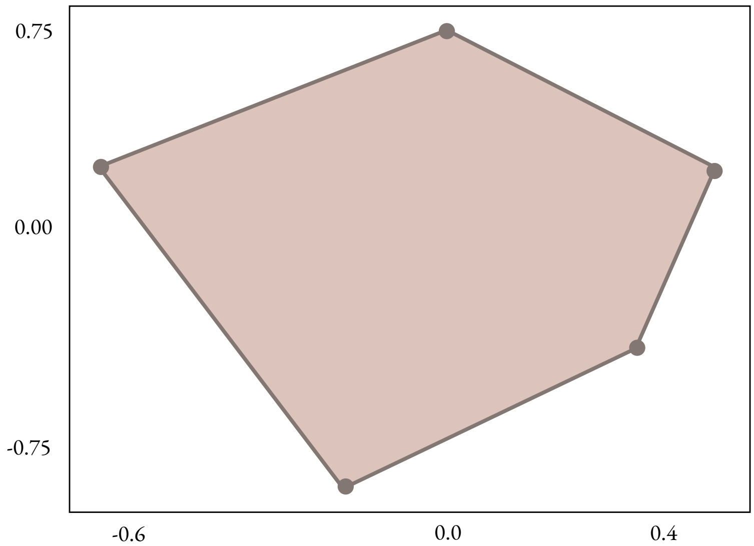

Figure 4.3: **Sample non simplicial test domain:** We consider a convex, non simplicial test domain to carry out the convergence tests of the discrete exterior covariant derivative under mesh refinement.

Subsequently we rotate by the angles $(50°, 25°, 5°)$. and shift these points by a vector $v =$

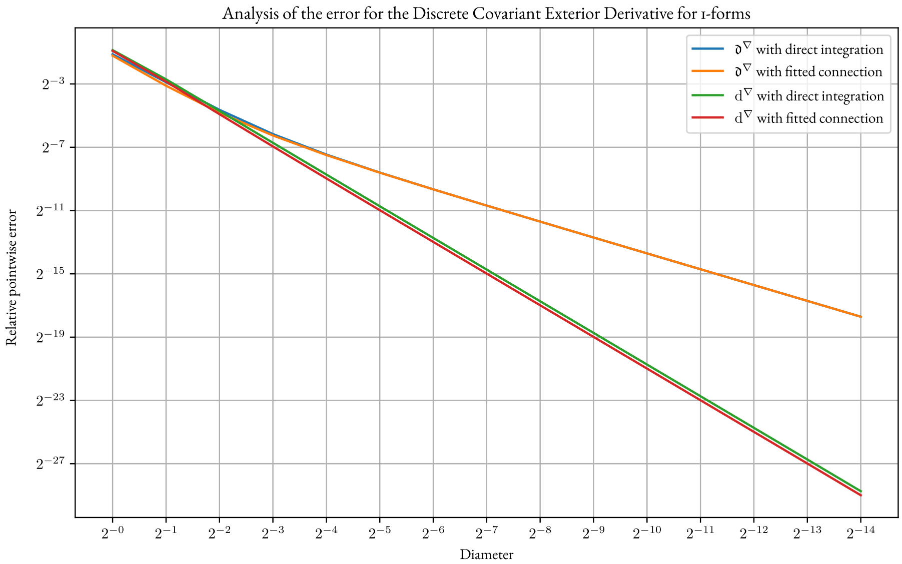

Figure 4.4: **Decay of the error for bundle-valued one-forms:** We observe that if we use a direct integral of a known smooth connection or fit linearly a connection $1-$form on the data available on primal edges to calculate parallel transport, the discrete exterior covariant derivative converges with quadratic order under refinement; to the PPF-induced sided discrete exterior covariant derivative with linear order.

$(2.0, 2.1, -2.0)$ and For this particular test we use the solder form and the quadratic connection presented in Equation (4.2.8). In this case we obtain the following convergence behaviour illustrated in Figure. 4.4.

Algebraic Bianchi identity under refinement for vector-valued $1-$forms For the verification of the convergence of two consecutive applications of the discrete exterior covariant derivative we consider a sample cell consisting of a pentagon and a parallelogram, see Figure. We use the differential form

$$\alpha = \begin{pmatrix} 2x dx \\ x dx \\ dz - z dy \end{pmatrix} \in \Omega^1(M, \mathbb{R}^3)$$

and the linear connection presented in Equation (4.2.8). We rotate the test domain by the angles $(150°, 25°, 55°)$ and shift it subsequently by the vector $v = (-2.9, 1.1, -2.5)$. In this case the convergence behavior can be seen in Figure 4.5

Convergence for bundle-valued $2-$forms To test the validity of Theorem 4.7 for bundle-valued $2-$forms on non simplicial cells, we use the cell illustrated in Figure 4.6. We use the differential form

$$\alpha = \begin{pmatrix} 3y\, dy \wedge dz + x^2 dz \wedge dx \\ (xyz + 1)\, dx \wedge dy \\ xy\, dy \wedge dz \end{pmatrix}$$

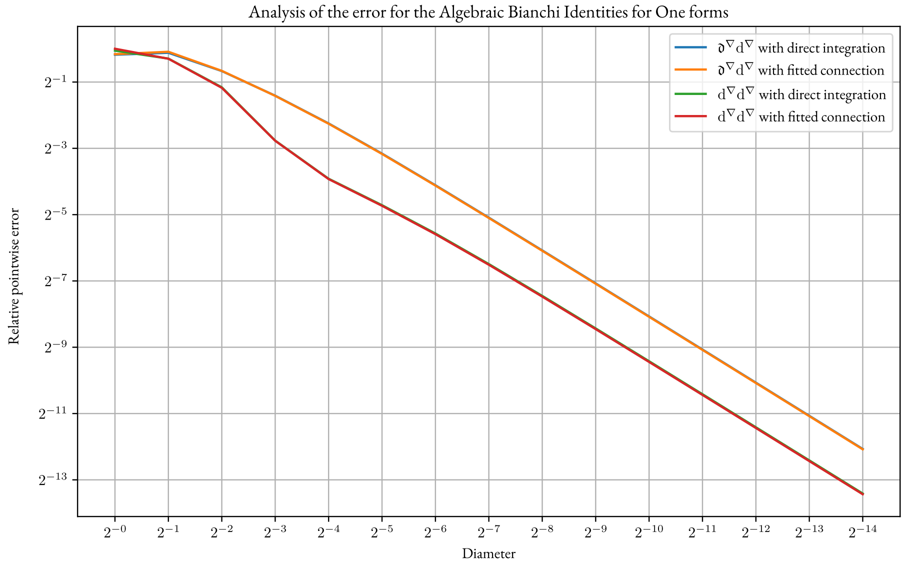

Figure 4.5: **Decay of the error for the algebraic Bianchi identity of bundle-valued one-forms:** We observe that if we use a direct integral of a known smooth connection or fit linearly a connection $1-$form on the data available on primal edges to calculate parallel transport to calculate two consecutive applications of the discrete exterior covariant derivative converge under refinement. As in the simplicial case, the operator $\boldsymbol{d}^{\nabla}\boldsymbol{d}^{\nabla}$ has the same convergence order as the operator $\mathfrak{d}^{\nabla}\boldsymbol{d}^{\nabla}$ under mesh refinement.

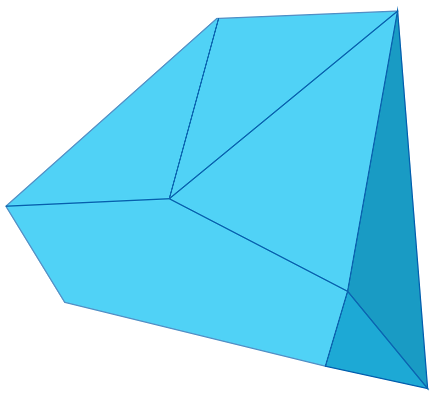

Figure 4.6: **Non simplicial test cell:** For the verification of the results, we use a convex non simplicial $3-$cell to verify the convergence results under refinement

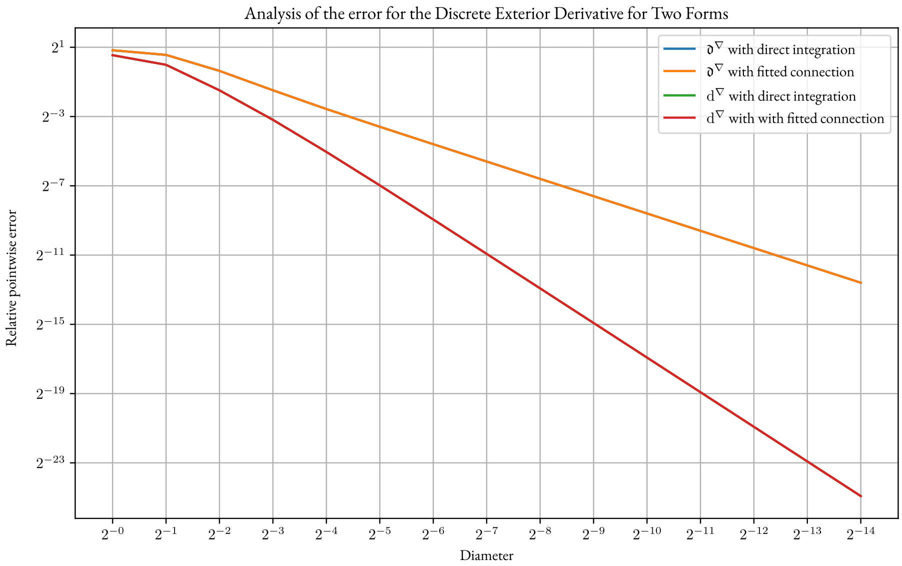

Figure 4.7: **Decay of the error for bundle-valued** $2-$**forms** In the described setup, we observe that the relative error of the discrete exterior covariant derivative is of quadratic order under mesh refinement, even if we use a least square fit of a connection $1-$form to approximate the parallel transport. For the sided discrete exterior covariant derivative we observe that the relative error compared to the smooth ground truth is of linear order.

Given the quadratic connection presented in Equation (4.2.8), we rotate the test domain with the Euler angles $(110°, 335°, 15°)$ and shift it with the vector $v = (-6.9, 1.4, -2.5)$. As in the previous tests we compare the convergence under refinement using for the computation of the parallel transport the direct integral of the connection $1-$form and an integral of a least square approximation of a connection $1-$form fitted on the integrated connection $1-$form on primal edges. We illustrate the convergence behaviour in Figure 4.7.

Convergence for $(1,1)$**-tensor valued one–forms under refinement** To verify the convergence results that we described for $(1,1)$-tensor valued forms in Equations Equation (4.2.6) and Equation (4.2.7), we consider the $(1,1)$-tensor valued $1-$form

$$\beta = \begin{pmatrix} 0 & y^2 dx & 0 \\ x dy & dz & 0 \\ 0 & 0 & 0 \end{pmatrix}.$$

We consider as a sample domain for the convergence the cell presented in Figure 4.3. Further, we use the linear connection presented in Equation Equation (4.2.8). We rotate the cell by the angles $(50°, 125°, 35°)$ and shift the cell by the vector $v = (-3.6, 1.1, -2.5)$. We illustrate the convergence behaviour under refinement in Figure 4.8.

Convergence of the Algebraic Bianchi Identity for $(1,1)$**-tensor valued forms under refinement** To test the convergence under refinement of the algebraic Bianchi identity towards

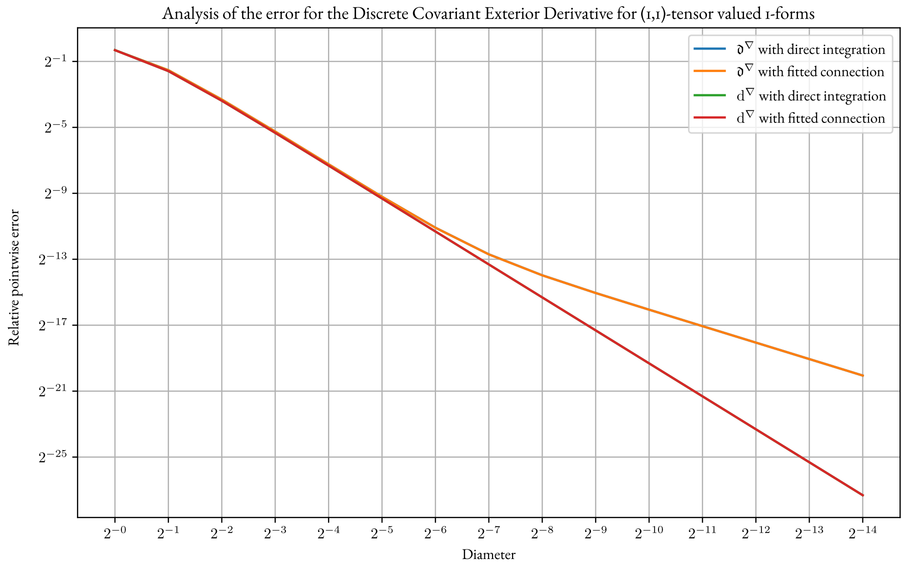

Figure 4.8: **Decay of the relative error for $(1,1)$-tensor valued $1-$forms** In the described setup, we observe that the relative error of the discrete exterior covariant derivative for $(1,1)$-tensor valued $1-$forms is of quadratic order under mesh refinement, even if we use a least square fit of a connection $1-$form to approximate the parallel transport. For the sided discrete exterior covariant derivative we observe that the relative error compared to the smooth ground truth is of linear order.

its smooth counterpart, we use the 3D cell illustrated in Figure 4.6. Further, we use the differential form

$$\beta = \begin{pmatrix} 0 & -xdy & 0 \\ xdy & 0 & dz \\ 0 & -dz & 0 \end{pmatrix} \in \Omega^1(\mathbb{R}^3, \mathrm{End}(T\mathbb{R}^3)) \tag{4.2.9}$$

and the quadratic connection described in Equation Equation (4.2.8). We rotate the cell by the angles $(10°, 15°, 5°)$ and shift the cell by the vector $(2.3, -2.1, -1.2)$. We illustrate the convergence under refinement in Figure 4.9.

Convergence Analysis for the Discrete Exterior Covariant Derivative for $(1,1)$-tensor valued $2-$forms To illustrate that the discrete exterior covariant derivative has a better convergence rate then the sided PPF-induced discrete exterior covariant derivative, we will use a distorted cube as a testing domain, where we slice off a corner. Subsequently we rotate the domain by the angles $(50°, 135°, 65°)$ and shift the domain by the vector $v = (0.3, -1.6, 0.5)$. We illustrate the convergence behaviour under refinement in Figure 4.10.

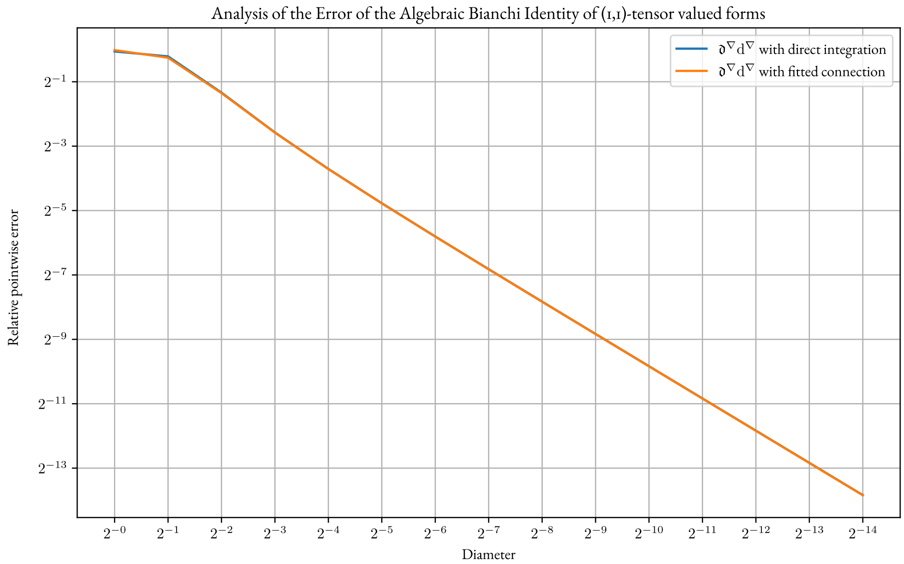

Figure 4.9: **Decay of the relative error for the algebraic Bianchi Identity of** $(1,1)$**-tensor valued** $1-$**forms** In the described setup, we observe that the relative error of the operator $\mathfrak{d}^\nabla \boldsymbol{d}^\nabla$ converges linearly towards the smooth ground truth.

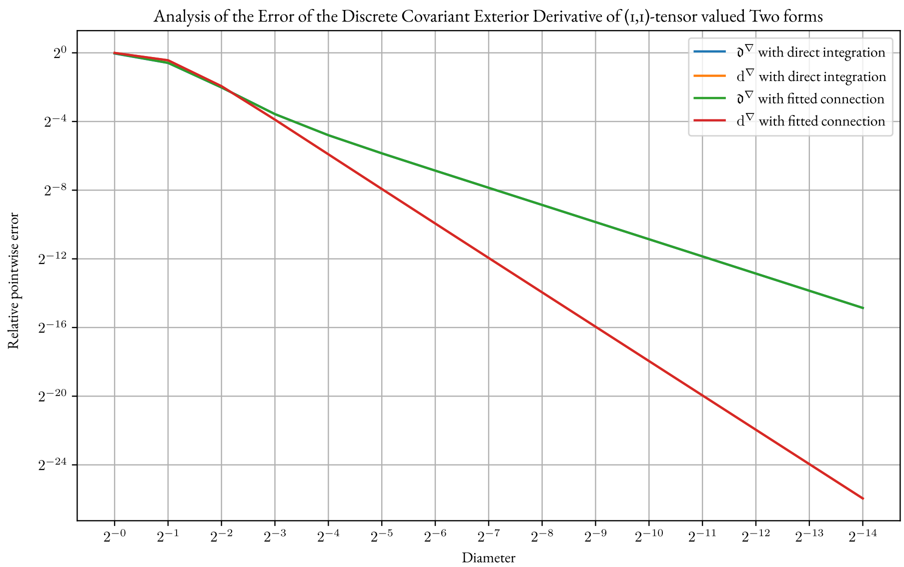

Figure 4.10: **Decay of the relative error for the Discrete Exterior Covariant Derivative of** $(1,1)$**-tensor valued** $2-$**forms** In the described setup, we observe that the relative error of the operator $\boldsymbol{d}^\nabla$ compared to the smooth ground truth converges quadratically, whereas the relative error for the PPF-induced sided discrete exterior covariant derivative decays linearly. As in the previous tests, we observe that the relative error still decays order when we use a linearly fitted connection $1-$form to estimate the parallel transport.

5 | Conclusion

5.1 Summary

This thesis develops a structure-preserving discretization of Cartan's exterior calculus that extends classical scalar-valued discrete exterior calculus to the setting of vector-bundle–valued differential forms. The principal goal is to preserve the geometric and algebraic structure of the smooth theory—connections, torsion, curvature, and their identities—while enabling accurate and robust computation on discrete meshes. To this end, we first reviewed the differential-geometric foundations underlying Cartan's calculus, with particular emphasis on the interplay between vector bundles, differential forms, and connections. This perspective clarifies which structures are essential to preserve under discretization and guides the design of discrete analogues that preserve the structures of the smooth theory. As a first concrete application, we studied the discretization of torsion in a geometry-processing context. Focusing initially on surface meshes, we leveraged the isomorphism between vector-valued 2-forms, tangent vector fields, and differential 1-forms to construct a discrete notion of torsion that is compatible with the underlying geometry. Along the way, we introduced a new discrete Levi–Civita connection that more accurately approximates its smooth counterpart under mesh refinement. This construction enriches the geometry-processing toolbox and was validated in applications such as vector field and cross-field generation. The thesis then presents a general and unified framework for a discrete exterior calculus of bundle-valued differential forms. A key conceptual difference from the scalar-valued setting is that discrete bundle-valued forms must be associated not only with a simplicial cell, but also with a choice of evaluation fiber. This additional structure is unavoidable and plays a central role in the formulation of discrete operators. A major challenge in this setting is the strong frame dependence of bundle-valued quantities. To address this, we introduced the notion of parallel-propagated frames, which provide a canonical discretization frame for bundle-valued forms. When discrete bundle-valued differential forms arise from discretization of a smooth differential form in such a frame, the resulting discrete exterior covariant derivative converges to its smooth counterpart under mesh refinement. We further showed that the accuracy and structural fidelity of the discrete exterior covariant derivative can be improved by incorporating an additional alternation operator. This operator is essential to ensure that the algebraic Bianchi identities are satisfied in a combinatorial sense, and that these identities remain valid in the limit of mesh refinement. Finally, we demonstrated that the proposed construction extends beyond simplicial meshes to more general cellular complexes, while retaining improved accuracy and convergence properties. Together, these results establish a principled and extensible framework for discretizing Cartan's exterior calculus on vector bundles, bridging differential geometry, numerical analysis, and geometry processing, and opening the door to structure-preserving discretizations of a wide range of geometric and physical theories.

5.2 Discussion of alternative discretization strategies

In the preceding chapters, we described two approaches for discretizing bundle-valued differential forms. In the course of this work, we also investigated several alternative discretization strategies. While each of these approaches was conceptually consistent, they presented distinct structural or practical challenges. We briefly review these directions below, as they offer valuable insight and suggest constructive ideas for future research.

5.2.1 Direct Optimization of the Connection with the Parallel-Propagated Frame

Conceptually, in the development of this dissertation, we started to develop the mathematics of discrete exterior calculus for bundle-valued forms presented in Chapter 3 and Chapter 4. We subsequenty tried to turn this framework directly into a geometry processing application. Our initial aim was to control a connection with a given torsion on a discrete surface. A natural first attempt was to formulate an optimization problem based on a PPF-boundary integral definition of discrete torsion. Although this is conceptually appealing, this approach proved impractical in practice for a number of reasons. In this section we will document this attempt and explain where the difficulties lay with this formulation.

Discrete Torsion via Parallel-Propagated frames

In the same spirit as in Chapter 2 we tried to define the torsion of a connection on dual 2-cells of a surface. Within this formulation, we could still maintain the identification (for a metric preserving connection) of a connection 1-form with its angle valued component as seen in Equation 2.1.4.

We began by defining discrete torsion on dual 2-cells. For each dual face, we selected a primal face as an evaluation fiber and used a parallel-propagated frame to transport vectors across the one-ring of the corresponding vertex. Given a discrete connection, this construction yields a PPF in the one-ring of each vertex.

Using this frame, the discrete torsion was defined by integrating the solder form along the boundary of the dual face. Concretely, we consider a dual face $(f_0, \dots, f_n)$ with evaluation in the fiber of f_0. We denote as in Chapter 2 by E_{f_i} the chosen frame in this face.

Discrete Solder Form

To finalize the discretization of the discrete torsion, we need to describe how the solder form described in Section 1.5 can be realized discretely in a parallel-propagated frame. For us, we discretized the solder form on dual halfedges in the PPF associated to the one ring with origin in the evaluation fiber f_0. Given a dual halfedge $*\overrightarrow{ij}$ oriented from face f_i to face f_j, we note that the parallel-propagated frame in face f_i is given by

$$E_{f_i}^{\mathrm{PPF}} = R_{f_0,f_1} \cdots R_{f_{i-1},f_i} E_{f_i},$$

where $R_{f_k,f_{k+1}}$ denotes the rotation matrix associated to the discrete connection on the dual (half)edge $*\overrightarrow{f_i, f_{i+1}}$ expressed in the initially chosen base frame E. We denote by $\theta_{f_i, e_{f_i,f_{i+1}}}$ the integral of the solder form from the dual vertex in face f_i to the intersection point of the dual halfedge with the associated primal edge. We calculate the discrete solder form on the dual halfedge $*\overrightarrow{ij}$ expressed in the base frame as

$$\theta_{*\overrightarrow{i,i+1}} := E_{f_i}\theta_{f_i,e_{i,i+1}} + E_{f_{i+1}}\theta_{f_{i+1},e_{i,i+1}},$$

The solder form in the parallel-propagated frame is subsequently defined as

$$\theta^{\mathrm{PPF}}_{*\overrightarrow{i,i+1}} := E^{\mathrm{PPF}}_{f_i}\theta_{f_i,e_{i,i+1}} + E^{\mathrm{PPF}}_{f_{i+1}}\theta_{f_{i+1},e_{i,i+1}}$$

In this case the torsion takes the form

$$\Theta(f_0,\dots,f_n), f_0 := \left(\theta^{PPF}_{*\overrightarrow{f_0,f_1}} + \theta^{PPF}_{*\overrightarrow{f_1,f_2}} + \cdots + \theta^{PPF}_{*\overrightarrow{f_n,f_0}}\right). \tag{5.2.1}$$

As a result the torsion depends nonlinearly on the connection.

Formulation of the Optimization Problem

In order to control the discrete torsion, we need to formulate an optimization problem. The goal was to find a connection that steers towars a given target torsion, while preserving the curvature of the initial connection.

Inspired by the curvature control strategy of [CDS10], we considered a base connection α defined on dual edges and introduced a closed angle-valued 1-form β on dual edges. The modified connection $\alpha + \beta$ preserves curvature by construction, while β is intended to control torsion. Stacking the torsion vectors at all vertices yields

$$\Theta_\alpha(\beta) \in \mathbb{R}^{2|V|}.$$

For a prescribed target torsion Θ_{target}, we defined the energy

$$E_\alpha(\beta) = (\Theta_\alpha(\beta) - \Theta_{\mathrm{target}})^\top(\Theta_\alpha(\beta) - \Theta_{\mathrm{target}}). \tag{5.2.2}$$

This energy is highly nonlinear and non-convex in β, making direct minimization impossible. For the case of a genus zero surface, we can express the closedness constraint of β through the existence of a potential function ϕ on dual faces such that $\beta = d\phi$. This allows us to reformulate the energy as an optimization over the potential ϕ.

Direct Nonlinear Optimization. We tried to minimize this energy using standard nonlinear optimization techniques. Similar problems have been addressed using Levenberg–Marquardt methods, for instance in [CC19].

We derived analytical expressions for the gradient of the torsion with respect to β. Despite this analytic access, the optimization landscape was extremely ill-conditioned. The torsion depends on the connection through nested products of rotations, leading to strong nonlinear coupling across edges and faces. In practice, standard nonlinear solvers consistently failed to converge to meaningful solutions.

5.2.2 Torsion of Connections on Surfaces Through a Linear System

We presented in Chapter 2 a framework that allows us to control connections and their curvature. Prior to this study, we worked on a different approach, where we tried to analyze torsion similar to curvature via a linear construction, similar to the construction of [CDS10], where the curvature of a connection is controlled via a linear system. We tried to discretize the equation

$$d^{\nabla}\theta = d\theta + \omega \wedge \theta$$

in a fashion that depends linearly on the connection. We followed the idea that torsion is a tangent vector valued 2−form. Just as the curvature is defined as a quantity on dual 2-cells, we tried to introduce torsion as a tangent vector on dual 2−cells. However in order to do that, we first need to describe a special local frame field in which the torsion vector can be expressed.

Local One-ring Frames

We defined in Section 2.2.2 to derive the modified Levi-Civita connection a local one-ring frame inside the one ring of a vertex.

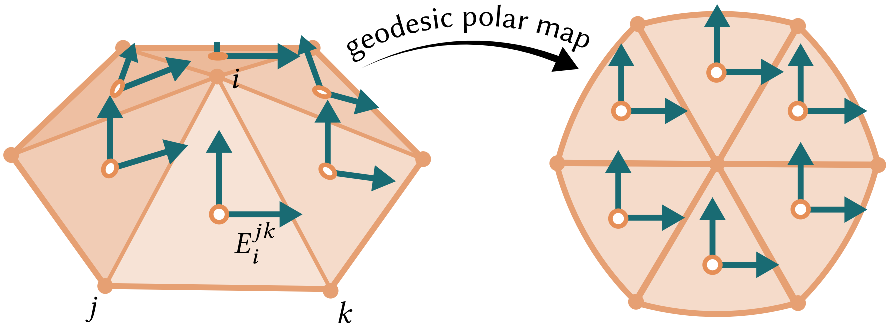

Figure 5.1: **Local One-ring Frame.** We construct for every one-ring neighborhood a parallel-propagated frame field which is constant per each face *(left)*. This frame is constructed from a geodesic polar map of the 1-ring, *i.e.*, a planar parameterization where radial edge lengths are unchanged and the tip angles around vertex i are scaled by a constant to sum to 2π *(right)*.

Following the formulas derived in Section 2.2.2, we could write down a direct analytic expression for the frame in the one ring neighborhood. Using this frame, we aimed to discretize the wedge product arising in the definition of torsion directly. Given a vertex $i \in \mathcal{V}$ and a face $ijk \in \mathcal{F}$ seen in the one ring neighborhood of i, denote this constant frame per face by E_i^{jk}.

Discrete Wedge Product

In order to guarantee convergence under mesh refinement, we also introduce a weighted version of the discrete dual-dual wedge product of [Hiro3]. Our wedge product between two discrete 1-forms β and γ on dual face $*i$ is given by

$$(\beta \wedge \gamma)_{*i} = \sum_{ijk \succ i} \lambda_i \left(\beta_{*ij}\gamma_{*ik} - \beta_{*ik}\gamma_{*ij}\right), \tag{5.2.3}$$

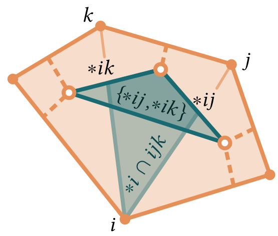

where $\lambda_i \in \mathbb{R}$ are weights to ensure convergence of the wedge product. While the original wedge product uses $\lambda_i = 1$, it cannot even be exact for constant forms. For general duals, λ_i should be set instead to the ratio between the areas of two regions depicted in the inset: quadrilateral $*i \cap ijk$ consisting of the subset of dual cell $*i$ which belongs to face ijk, and the triangle spanned by the two dual edges $*ij, *ik$. Explicitly,

$$\lambda_i = \frac{\sum_{ijk>i} \mathrm{Area}(*i \cap ijk)}{2\sum_{ijk>i} \mathrm{Area}(\{*ij, *ik\})}.$$

We thus define the weight λ_i accordingly, through:

$$\lambda_i := \frac{1}{2} \frac{A_{*i}}{\sum_{ijk>i} A_{ijk} \star_{ij} \star_{ik}}. \tag{5.2.4}$$

Discrete Solder Form

The last ingredient required for our discretization of torsion is a solder form $\theta_{*\vec{ij}}$, discretizing the smooth form θ introduced in Section 2.1.2. Our discrete solder form associates values to dual halfedges: the value $\theta_{*\vec{ij}}$ is a two-dimensional vector encoding the dual halfedge $*\vec{ij}$ in the frame field associated to vertex i. Note that the discrete solder form $\theta_{*\vec{ij}}$ is *not* a discrete 1-form in the sense of DEC, *i.e.* $\theta_{*\vec{ij}} \neq \theta_{*\vec{ji}}$, because $\theta_{*\vec{ij}}$ represents a vector in the frame associated to vertex i while $\theta_{*\vec{ji}}$ represents a vector in the frame associated to vertex j.

To compute $\theta_{*\vec{ij}}$, we begin by breaking the dual edge $*ij$ up into two segments: one running from the dual vertex c_{jil} of face jil to the midpoint c_{ij} on edge ij, and one continuing on from that intersection point onto the dual vertex c_{ijk} of face ijk. We then sum up the expressions for each segment in its face's frame:

$$\theta_{*\vec{ij}} := \left(E_i^{jk}\right)^T (c_{ijk} - c_{ij}) + \left(E_i^{lj}\right)^T (c_{ij} - c_{jil}) \in \mathbb{R}^2. \tag{5.2.5}$$

Discrete Torsion

From the discrete solder form $\theta_{*\vec{ij}}$, computing its exterior derivative over the dual face $*i$ amounts to simply summing these dual-edge values around vertex i. Similarly, with the weights introduced above, we can evaluate the discrete wedge product between the matrix-valued connection values $\omega_{*\vec{ij}}$ and the vector-valued solder values $\theta_{*\vec{ij}}$

$$(\omega \wedge \theta)_{*i} = \sum_{ijk>i} \lambda_{ijk} \left(\omega_{*\vec{ij}} \theta_{*\vec{ik}} - \omega_{*\vec{ik}} \theta_{*\vec{ij}}\right), \tag{5.2.6}$$

Discrete torsion expression With all of these definitions in place, our discrete torsion is simply defined by the exact same equation defining the *smooth* torsion, *i.e.*,

$$\boxed{\Theta^{\nabla}_{*i} = (d\theta)_{*i} + (\omega \wedge \theta)_{*i}\,,} \tag{5.2.7}$$

where the term $d\theta$ is interpreted as the ordinary discrete exterior derivative applied separately to the two coordinates of θ. We note that as in Chapter 2, there exists the angle valued 1−form $\alpha_{*\vec{ij}}$ and we have the relationship

$$\omega_{*\vec{ij}} = \begin{pmatrix} 0 & -\alpha_{*\vec{ij}} \\ \alpha_{*\vec{ij}} & 0 \end{pmatrix},$$

hence the discrete torsion per dual face depends in a linear fashion on the values of $\alpha_{*\vec{ij}}$ on the dual halfedges.

Change of frame formula The discrete torsion we just defined depends linearly on the choice of connection ω as Eq. 5.2.7 explicitly states. However, note that we use the discrete connection expressed in the local frame around each vertex; so two nearby vertices will use different values for the same connection. Yet, for implementation purposes, we need to only rely on $|\mathcal{E}|$ values to define our connection. Notice that our connection $\omega = \mathbb{J}\alpha$ represents by a scalar rotation angle $\alpha_{*\vec{ij}}$ associated to each halfedge $\vec{ij}$; but the values $\alpha_{*\vec{ij}}$ and $\alpha_{*\vec{ji}}$ on the two sides of edge ij are not independent since $\alpha_{*\vec{ij}}$ measures a rotation in the local frame field of vertex i, while $-\alpha_{*\vec{ji}}$ measures a rotation in the local frame field of vertex j. Therefore, the two values are in fact related through

$$\alpha_{*\vec{ji}} = -\alpha_{*\vec{ij}} + \rho_{*\vec{ij}} \tag{5.2.8}$$

where the scalar shift $\rho_{*\vec{ij}}$ accounts for the difference between the local frame fields associated to vertices i and j. Note that this amounts to a special case of the gauge transformation for the connection 1−form in Equation 1.5.3.

Angle shifts Conceptually, a rotation by $\alpha_{*\vec{ji}}$ maps vectors from basis E_j^{ki} to basis E_j^{il}, whereas a rotation by $-\alpha_{*\vec{ij}}$ maps from basis E_i^{jk} to basis E_i^{lj}. So to convert between the two, we must account for the rotation from basis E_j^{ki} to E_i^{jk}, and the rotation from basis E_i^{lj} to basis E_j^{il}. If $\psi_{\vec{ij}}$ denotes the angle needed to rotate from E_i^{jk} to E_j^{ki} and $\psi_{\vec{ji}}$ denotes the angle required to rotate from E_j^{il} to E_i^{lj}, then the shift $\rho_{*\vec{ij}}$ is given by

$$\rho_{*\vec{ij}} := \psi_{\vec{ij}} + \psi_{\vec{ji}}. \tag{5.2.9}$$

With these shifts, Eq. 5.2.7 can be properly evaluated for any discrete dual connection as intended.

Issues with this formulation

This formulation seems at first glance to be directly in line with the work done in [CDS10] for the curvature. But we realized in our experiments that this formulation is extremely sensitive to mesh quality. In our experiments, we noticed that the trivial connection algorithm is extremely robust, even on the worst meshes. In our experiements, we tried for instance to design the curvature of a connection with the trivial connection algorithm, subsequently even if we prescribed an admissable torsion in the sense of Chapter 2, we could only recover a connection on meshes that were perfectly Delaunay. Even slight and local deteriorations of the mesh quality were sufficient in order to introduce large noise in the final connection, such that the recovered field had no resemblance with the fields that we presented in Chapter 2.

However, this presented formulation has the advantage that it is not directly dependent on the isomorphism of vector fields and vector valued 2-forms. Therefore, this formulation could serve as a starting point for analyzing the torsion of a connection on a 3−dimensional manifold. In this context, it may serve as a helpful tool for the analysis of 3D frame fields as used in the generation of hexahedral meshes.

5.3 Future Work

Building on the framework developed in this thesis, several natural directions for further investigation emerge. The structure-preserving discretization of bundle-valued exterior calculus opens new perspectives both in differential geometry and in geometry processing. In the following, we outline three research directions in mathematics and computational geometry where the ideas developed here may serve as a foundation. Each of these directions builds on the core principles of discrete connections, torsion, and parallel transport, while extending them toward new theoretical or practical applications.

5.3.1 Torsion Guided 3D Frame Generation

Hex meshing remains one of the central challenges in geometry processing, largely because a high-quality hex mesh is tightly linked to the existence of a globally consistent *3D guidance frame field*. A common conceptual pipeline is to (i) compute a frame field in the volume that aligns with prescribed boundary frames and exhibits low distortion, and then (ii) extract a hexahedral mesh by tracing iso-surfaces / separatrices of the induced coordinate directions and fitting a combinatorial grid to this structure [PCS+22]. A key difficulty is therefore to characterize and enforce when a frame field is *meshable*, i.e. when it can be interpreted as a coordinate frame of an (approximately) grid-like parameterization.

Frame fields come with an additional source of ambiguity: In three dimensions, a cube has 24 rotational symmetries, so a choice of three orthogonal axes is only defined up to the action of the octahedral group. Consequently, directly storing a frame as an ordered triple of vectors is numerically and conceptually challenging, since neighboring frames may differ by a rotation in the octahedral group. In an optimization context this would lead to a difficult mixed-integer problem.

This motivates *implicit* frame representations, where a frame is encoded not by explicit axes, but by an invariant object that attains extrema at those axes.

A particularly successful strategy is to represent a frame through a scalar function on the sphere, whose maxima occur at the (unsigned) axis directions of the frame. One convenient construction uses a homogeneous polynomial of degree four:

$$f : S^2 \to \mathbb{R}, \qquad f(x) = \sum_{i=1}^{3} \lambda_i \, (v_i^\top x)^4, \tag{5.3.1}$$

where (v_1, v_2, v_3) is an orthonormal basis representing the frame and $\lambda_i > 0$ encode anisotropic weights. Since f is a polynomial restricted to the sphere, it can be expanded in spherical harmonics, i.e. as a finite sum of Laplace–Beltrami eigenfunctions on S^2 [HTWB11, PBS20]. In the isotropic case $\lambda_1 = \lambda_2 = \lambda_3$, the signal can be captured purely by the band-4 subspace. If Y_4^i,

$i \in \{-4, \ldots, 4\}$ denotes a basis of the band 4 spherical harmonics, we can expand

$$f : S^2 \to \mathbb{R} : x \mapsto \sum_{i=-4}^{4} Y_4^i q_i,$$

yielding a coefficient vector in $\mathbb{R}^9$. If we allow for distinct λ_i, it was shown by [PBS20] that this introduces band-2 components (in addition to band-4). In this case, the frame is still represented by 3 orthogonal axes (unless the $\lambda_i = 0$), thus these tensors are referred to as orthogonally decomposable tensors (Odeco). However now the frame may have differently scaled axis. In this case the frame may be represented by an $\mathbb{R}^{15}$ coefficient vector. These implicit representations are attractive because they avoid mixed integer programming in the optimization due to 24-fold symmetry.

Most practical methods prescribe boundary alignment, extend the field to the interior (e.g. by harmonic or Poisson-type smoothing), and then optimize an energy combining smoothness, alignment, and regularization. Depending on the representation, this is done either directly in coefficient space or via manifold-based optimization to better respect the underlying quotient geometry. However, even when a field is smooth in this sense, it does not need to be meshable: smoothness controls variation but does not, by itself, enforce the commutativity constraints that would make the frame behave like a coordinate system.

This observation connects to the viewpoint developed in Chapter 2. There we saw that torsion of a trivial connection induces twists in the arising field. In the present setting, a frame field may likewise be interpreted as the outcome of some (implicit) parallel transport rule: if neighboring frames are aligned by a discrete transport map (e.g. the nearest symmetry element relating their implicit representations), this alignment can be viewed as defining a connection.

In two dimensions, the situation is conceptually cleaner and the literature typically phrases integrability in terms of *commutativity* rather than torsion. Given two guiding directions U, V (e.g. the two directions of a cross field after choosing a local branch), the existence of a local parameterization whose coordinate lines follow U and V is equivalent to the vanishing Lie bracket $[U, V] = 0$. Using the torsion-free Levi–Civita connection, this condition can be rewritten as $\nabla_U V - \nabla_V U = 0$, which is the form most directly exploited in "integrable cross field" methods [CCR26, SFCBCV19].

We conducted several experiments in two dimensions. In particular, we considered a spiral vector field exhibiting a slight closure defect: the streamline fails to close consistently after transport around a loop, resulting in a small "near miss." We then interpreted the resulting displacement vector as an interior torsion contribution and prescribed the exact component of the target torsion accordingly. After re-propagating the field with this torsion corrected connection, the closure defect was eliminated, effectively resolving the near miss.

Extending these ideas to 3D remains challenging. While local integrability conditions for frame fields are understood [LB23], globally meshable configurations involve topology, singularity structure, and discrete symmetry choices. Hence, meshability in 3D is far less settled than in 2D. Nevertheless, the torsion viewpoint suggests an interesting avenue for future research: Can we augment frame-field optimization with an additional term that controls the torsion of the connection induced by a frame alignment rule. In principle, such a term would penalize the failure of infinitesimal cells to close under the induced transport and could bias the solution toward integrable, grid-like structure. In practice, defining and differentiating such a torsion energy in 3D (in

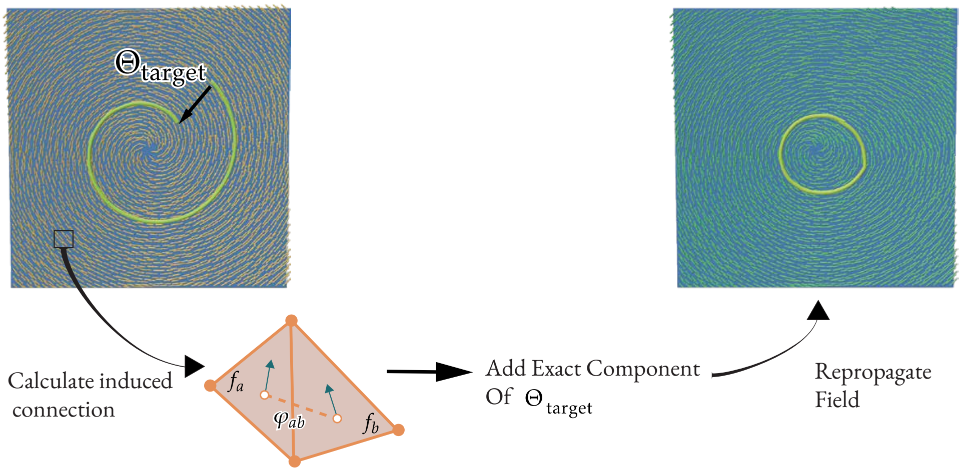

Figure 5.2: **Torsion guided field design.** We start with a spiral vector field (left) which has a near miss and does not close up. We then take the displacement vector between the start and end of the spiral and prescribe it as torsion in the interior of the spiral. Repropagating the field with this torsion yields a closed spiral field (right).

the presence of octahedral symmetry and singularities) is nontrivial. We would need to find a differentiable way to encode torsion on a mesh in terms of the $\mathbb{R}^{15}$ Odeco coefficients. We therefore regard this as an interesting direction for future work.

5.4 Discrete Ricci Tensor and Contracted Bianchi Identities

The central theme of this thesis is the development of *exact, structure-preserving discretizations* of geometric objects and differential operators. Rather than aiming solely at asymptotic convergence, our focus lies on discretizations that inherit fundamental identities and invariances of the smooth theory by construction, independently of mesh resolution or approximation order.

A particularly compelling application of bundle-valued exterior calculus and the Bianchi identities lies in *general relativity*.

In the smooth setting, spacetime is modeled as a four-dimensional Lorentzian manifold $(\mathcal{M}, g)$ equipped with a Levi–Civita connection ∇. From this connection one derives the Riemann curvature tensor, its contraction to the Ricci tensor Ric, the scalar curvature R, and finally the Einstein tensor

$$G := \mathrm{Ric} - \tfrac{1}{2}Rg.$$

The Einstein tensor encodes the geometric response of spacetime curvature to matter and energy, represented by the stress-energy tensor T through the Einstein field equations [MTW73, Ein16]

$$G = 8\pi T.$$

Solutions of these equations include flat Minkowski spacetime, as well as curved spacetimes describing physically observable phenomena such as the precession of planetary orbits, famously exemplified by the anomalous perihelion advance of Mercury [Ein06]. Beyond the field equations themselves, general relativity is governed by a fundamental conservation law: the *contracted*

Bianchi identity, stating that the Einstein tensor is divergence free

$$\operatorname{div} G = 0,$$

which ensures local conservation of energy and momentum. This identity can be derived from the differential Bianchi identity for the Riemann curvature tensor. In the book "Gravitation" by Misner, Thorne and Wheeler [MTW73, page 364], the importance of this geometric structure for the physical theory is motivated as follows:

> **§15.1. BIANCHI IDENTITIES IN BRIEF**
>
> Geometry gives instructions to matter, but how does matter manage to give instructions to geometry? Geometry conveys its instructions to matter by a simple handle: "pursue a world line of extremal lapse of proper time (geodesic)." What is the handle by which matter can act back on geometry? How can one identify the right handle when the metric geometry of Riemann and Einstein has scores of interesting features? Physics tells one what to look for: *a machinery of coupling between gravitation (spacetime curvature) and source* (matter; stress-energy tensor $\boldsymbol{T}$) *that will guarantee the automatic conservation of the source* ($\boldsymbol{\nabla} \cdot \boldsymbol{T} = 0$). Physics therefore asks mathematics: "What tensor-like feature of the geometry is automatically conserved?" Mathematics comes back with the answer: "The Einstein tensor." Physics queries, "How does this conservation come about?" Mathematics, in the person of Élie Cartan, replies, "Through the principle that 'the boundary of a boundary is zero'" (Box 15.1).

In recent years, several works have explored discretizations of scalar curvature and Einstein-type quantities [GN23b, GN23a]. In their work, they use finite-element formulations of Regge calculus [Reg61, Li18] that give rise to definitions of scalar curvature and Einstein tensors in a distributional sense, together with convergence results. Within this variational framework, the contracted Bianchi identity is recovered *in a weak sense*, meaning that the discrete Einstein tensor satisfies the appropriate conservation law when paired against admissible test fields, reflecting the underlying variational and symmetry structure of the continuous theory.

While this weak formulation is fully consistent with the geometric origin of the identity and sufficient for many analytical purposes, it differs conceptually from the type of exactness encountered in discrete exterior calculus. For instance, identities such as Stokes' theorem or discrete Bianchi identities for exterior derivatives hold *exactly* at the cochain level, independently of polynomial degree or mesh resolution, as a direct consequence of the nature of the discretization.

This opens an important direction for future research. An interesting question is whether one can develop a discretization of the Ricci tensor, scalar curvature, and Einstein tensor that is geometric and structure-preserving in the same strong sense, such that identities like the contracted Bianchi identity hold *by construction* at the discrete level, like we have seen for the discrete Bianchi identities (Theorem 3.36, Theorem 3.35) or Stokes' theorem c.f. Section 1.3 . Achieving such a formulation would require a deeper synthesis of discrete connections, curvature, and the discrete Bianchi identities, and remains an open challenge.

5.5 Discrete Elasticity with Bundle-Valued Forms

Classical formulations of nonlinear elasticity are most commonly expressed in terms of the deformation gradient $F = D\varphi$, from which strain measures, stresses, and equations of motion are derived. While highly effective in practice, this representation is not intrinsic: it depends on the choice of coordinates, reference frames, and Piola-type transformations between reference and current configurations.

An alternative, geometric viewpoint has been developed in a series of works on bundle-valued differential forms, most notably by [KAT$^+$07, RBC$^+$23], where stress is interpreted as a covector-valued differential form and balance laws are expressed in terms of exterior calculus. This perspective provides a coordinate-free and structure-preserving formulation of continuum mechanics.

Metric-based description of deformation. Let $\mathcal{M}$ denote the reference configuration of an elastic body, modeled as a three-dimensional Riemannian manifold endowed with a reference metric g_0. A time-dependent deformation is given by a smooth embedding $\varphi_t : \mathcal{M} \to \mathbb{R}^3$. Pulling back the Euclidean metric of the ambient space yields a Riemannian metric

$$g_t := \varphi_t^* g_{\mathrm{eucl}}$$

on $\mathcal{M}$, which encodes the elastic deformation. In contrast to the deformation gradient, the metric g_t is an intrinsic object, independent of coordinates or frames, and captures all local changes of length and angle.

The metric g_t induces a Levi–Civita connection ∇^{g_t} on the tangent bundle $T\mathcal{M}$, which in general differs from the reference connection associated with g_0. Elastic strain may therefore be interpreted geometrically as a discrepancy between the current and reference metrics. A particularly natural measure of this discrepancy is given by the Riemannian logarithmic strain

$$W_t := \log_{g_0}(g_t),$$

which represents the tangent vector at g_0 corresponding to the shortest geodesic (in the manifold of symmetric positive-definite metrics) connecting g_0 and g_t. This strain measure is the intrinsic analogue of the classical Hencky (logarithmic) strain and reduces to the linearized strain tensor in the infinitesimal limit.

Elastic energy and Doyle–Ericksen stress. Based on the logarithmic strain, one may define an elastic energy density of Hencky type,

$$e(g_t) = \mu \|W_t\|_{g_0}^2 + \frac{\lambda}{2}\left(\mathrm{tr}_{g_0} W_t\right)^2,$$

where μ and λ are Lamé parameters. This energy density is quadratic in the intrinsic strain, isotropic, objective, and recovers classical linear elasticity for small deformations. Integrating $e(g_t)$ over the reference configuration yields a global elastic energy functional.

For hyperelastic materials, the stress is obtained variationally by differentiating the energy with respect to the metric. In the geometric formulation of elasticity, this relation is known as the Doyle–Ericksen formula [KAT$^+$07],

$$\sigma = \frac{\partial e}{\partial g},$$

where σ is a symmetric contravariant 2-tensor, often referred to as the *metric stress*. This definition is intrinsic and avoids reference to Piola transformations or mixed two-point tensors.

Following the geometric reformulation of continuum mechanics proposed by [KAT+07], the metric stress σ can be canonically converted into a covector-valued differential two-form

$$\tau := \iota_{(\cdot)}\sigma \;\in\; \Omega^2(M; T^*M),$$

referred to as the *traction stress form*. This object represents force flux across oriented surface elements and is the natural quantity to integrate over faces. In particular, pairing τ with a velocity field and integrating over a surface yields the rate of work done by elastic forces, without the need to introduce surface normals explicitly. If v denotes the spatial velocity field and b denotes a body force per unit mass. Using Cartan's exterior calculus for bundle-valued forms, the balance of linear momentum can be written compactly as

$$\dot{v}^\flat \otimes \rho\, \mu = d^{\nabla^{g_t}} \tau + b^\flat \otimes \rho\, \mu, \tag{5.5.1}$$

where ρ is the mass density, μ the volume form associated with g_t, and $d^{\nabla^{g_t}}$ denotes the exterior covariant derivative induced by the Levi-Civita connection of the current metric, c.f. [KAT+07]. This equation is the intrinsic, form-based analogue of the classical elastodynamic equations and expresses force balance as a geometric conservation law. In particular, equilibrium corresponds to the condition $d^{\nabla^{g_t}} \tau = 0$.

Outlook toward discretization. While the continuous formulation above is fully intrinsic, to this day there does not exist a similar intrinsic discrete description of elastodynamics. A central contribution of this thesis is the introduction of a discrete analogue of the exterior covariant derivative d^∇ for bundle-valued forms, which opens, a concrete pathway toward discretizing Equation 5.5.1 in a structure-preserving manner. In this setting, the traction stress τ may be interpreted as a discrete covector-valued two-form associated with (possibly dual) faces of a tetrahedral mesh, while the discrete operator d^∇ naturally maps such quantities to (dual) volumes, encoding force balance through an exact combinatorial relation.

This perspective suggests a novel route to elasticity simulation in which stresses are treated as fluxes and equilibrium arises from a discrete Stokes-type theorem, rather than from assembled element-wise force vectors. Whether such a formulation leads to improved numerical properties, such as enhanced stability, robustness under large deformations, or reduced sensitivity to locking, remains an open question. Nonetheless, the availability of a discrete exterior covariant derivative for bundle-valued quantities provides a previously missing geometric ingredient and motivates further investigation into form-based, metric-driven discretizations of elasticity.

Bibliography

[AMR88] Ralph Abraham, Jerrold E. Marsden, and Tudor Ratiu. *Manifolds, Tensor Analysis, and Applications*, volume 75 of *Applied Mathematical Sciences*. Springer, New York, NY, 2 edition, 1988. Originally published by Addison–Wesley, 1983.

[Arn18] Douglas N. Arnold. *Finite Element Exterior Calculus*, volume 93 of *CBMS-NSF Regional Conference Series in Applied Mathematics*. SIAM, 2018.

[AS53] Warren Ambrose and Isadore Manuel Singer. A theorem of holonomy. *Transactions of the American Mathematical Society*, 75(3):428–443, 1953.

[BEHS21] Daniel Berwick-Evans, Anil N. Hirani, and Mark D. Schubel. Discrete vector bundles with connection and the Bianchi identity, 2021.

[BGTD25] Theo Braune, Mark Gillespie, Yiying Tong, and Mathieu Desbrun. Discrete torsion of connection forms on simplicial meshes. *ACM Trans. Graph.*, 44(4), aug 2025.

[Bos98] Alain Bossavit. *Computational Electromagnetism*. Academic Press, 1998.

[BTGBD25] Theo Braune, Yiying Tong, François Gay-Balmaz, and Mathieu Desbrun. A discrete exterior calculus of bundle-valued forms, 2025.

[Bur10] John Burkardt. Quadrature_rules_tri dataset. `https://people.sc.fsu.edu/~jburkardt/datasets/quadrature_rules_tri/quadrature_rules_tri.html`, 2010. Last revised on 28 September 2010.

[Car23] Elie Cartan. Sur les variétés à connexion affine et la théorie de la relativité généralisée (première partie). *Annales scientifiques de l'École Normale Supérieure*, 40(3):325–412, 1923.

[CC19] Etienne Corman and Keenan Crane. Symmetric moving frames. *ACM Transactions on Graphics*, 38(4), 2019.

[CC23] Guillaume Coiffier and Etienne Corman. The method of moving frames for surface global parametrization. *ACM Transactions on Graphics*, 42(5), 2023.

[CCL99] S. S. Chern, W. Chen, and K. S. Lam. *Lectures on Differential Geometry*. Series on university mathematics. World Scientific, 1999.

[CCR26] Mattéo Couplet, Alexandre Chemin, and Jean-François Remacle. Size-controlled quadrilateral meshing using integrable odeco fields. *Computer-Aided Design*, 190:103974, 2026.

[CdGDS13] Keenan Crane, Fernando de Goes, Mathieu Desbrun, and Peter Schröder. Digital geometry processing with discrete exterior calculus. In *ACM SIGGRAPH 2013 Courses*, 2013.

[CDS10] Keenan Crane, Mathieu Desbrun, and Peter Schröder. Trivial connections on discrete surfaces. *Computer Graphics Forum*, 29(5):1525–1533, 2010.

[CH23] Snorre H. Christiansen and Kaibo Hu. Finite element systems for vector bundles: Elasticity and curvature. *Foundations of Computational Mathematics*, 23(2):545–596, 4 2023. Published on 2023/04/01.

[Cor24] Etienne Corman. Curvature-driven conformal deformations. *ACM Transactions on Graphics*, 43(4), 2024.

[DGBD20] Fernando De Goes, Andrew Butts, and Mathieu Desbrun. Discrete differential operators on polygonal meshes. *ACM Trans. Graph.*, 39(4), 7 2020.

[dGDT16] Fernando de Goes, Mathieu Desbrun, and Yiying Tong. Vector field processing on triangle meshes. In *ACM SIGGRAPH 2016 Courses*, 2016.

[DHLM05] Mathieu Desbrun, Anil N. Hirani, Melvin Leok, and Jerrold E. Marsden. Discrete exterior calculus, 2005.

[DKT08] Mathieu Desbrun, Eva Kanso, and Yiying Tong. *Discrete Differential Forms for Computational Modeling*, pages 287–324. Birkhäuser Basel, 2008.

[Ein16] A. Einstein. Die grundlage der allgemeinen relativitätstheorie. *Annalen der Physik*, 354(7):769–822, 1916.

[Ein06] A. Einstein. *Erklärung der Perihelbewegung des Merkur aus der allgemeinen Relativitätstheorie*, volume 47, pages 78 – 87. 08 2006.

[FHTB23] Xianzhong Fang, Jin Huang, Yiying Tong, and Hujun Bao. Metric-driven 3d frame field generation. *IEEE Transactions on Visualization and Computer Graphics*, 29(4):1964–1976, 2023.

[Fra11] Theodore Frankel. *The Geometry of Physics: An Introduction*. Cambridge University Press, 3 edition, 2011.

[Gaw20] Evan S. Gawlik. High-order approximation of gaussian curvature with regge finite elements. *SIAM Journal on Numerical Analysis*, 58(3):1801–1821, 2020.

[GHB+23] Olga Guțan, Shreya Hegde, Erick Jimenez Berumen, Mikhail Bessmeltsev, and Edward Chien. Singularity-free frame fields for line drawing vectorization. *Computer Graphics Forum*, 42:e14901, 2023.

[GN23a] Evan S. Gawlik and Michael Neunteufel. Finite element approximation of scalar curvature in arbitrary dimension, 2023.

[GN23b] Evan S. Gawlik and Michael Neunteufel. Finite element approximation of the Einstein tensor, 2023.

[GRB16] Andrew Gillette, Alexander Rand, and Chandrajit Bajaj. Construction of scalar and vector finite element families on polygonal and polyhedral meshes. *Computational Methods in Applied Mathematics*, 16(4):667–683, 2016.

[HDOS10] J. William Helton, Mauricío De Oliveira, and Mark Stankus. NCAlgebra — non commutative algebra package for mathematica, 2010.

[Hir03] Anil N. Hirani. *Discrete Exterior Calculus*. PhD thesis, California Institute of Technology, 2003.

[HTWB11] Jin Huang, Yiying Tong, Hongyu Wei, and Hujun Bao. Boundary aligned smooth 3d cross-frame field. *ACM Trans. Graph.*, 30(6):1–8, December 2011.

[KAT+07] E. Kanso, M. Arroyo, Y. Tong, A. Yavari, J. E. Marsden, and M. Desbrun. On the geometric character of stress in continuum mechanics. *Z. angew. Math. Phys.*, 58:843–856, 2007.

[KCPS13] Felix Knöppel, Keenan Crane, Ulrich Pinkall, and Peter Schröder. Globally optimal direction fields. *ACM Transactions on Graphics*, 32(4), 2013.

[KCPS15] Felix Knöppel, Keenan Crane, Ulrich Pinkall, and Peter Schröder. Stripe patterns on surfaces. *ACM Transactions on Graphics*, 34(4), 2015.

[Koc97] Anders Kock. Combinatorics of curvature, and the Bianchi identity. *Theory and Applications of Categories [electronic only]*, 2:69–89, 1997.

[Kot08] P. Robert Kotiuga. Theoretical limitations of discrete exterior calculus in the context of computational electromagnetics. *IEEE Transactions on Magnetics*, 44(6):1162–1165, 2008.

[LB23] Heng Liu and David Bommes. Locally meshable frame fields. *ACM Trans. Graph.*, 42(4), July 2023.

[Li18] Lizao Li. *Regge Finite Elements with Applications in Solid Mechanics and Relativity*. Ph.d. dissertation, University of Minnesota, May 2018. Advisor: Douglas N. Arnold.

[LTGD16] Beibei Liu, Yiying Tong, Fernando De Goes, and Mathieu Desbrun. Discrete connection and covariant derivative for vector field analysis and design. *ACM Transactions on Graphics*, 35(3), 2016.

[Mar18] A. Marsh. *Mathematics for Physics: An Illustrated Handbook*. World Scientific Publishing Company Pte. Limited, 2018.

[MDSB03] Mark Meyer, Mathieu Desbrun, Peter Schröder, and Alan H. Barr. Discrete differential-geometry operators for triangulated 2-manifolds. In *Visualization and Mathematics III*, pages 35–57. Springer, 2003.

[MJBHC24] Rahul Mitra, Erick Jimenez Berumen, Megan Hofmann, and Edward Chien. Singular foliations for knit graph design. In *ACM SIGGRAPH 2024 Conference Papers*, 2024.

[MMDH+23] Juan Sebastian Montes Maestre, Yinwei Du, Ronan Hinchet, Stelian Coros, and Bernhard Thomaszewski. Differentiable stripe patterns for inverse design of structured surfaces. *ACM Transactions on Graphics*, 42(4), 2023.

[MMWC23] Rahul Mitra, Liane Makatura, Emily Whiting, and Edward Chien. Helix-free stripes for knit graph design. In *ACM SIGGRAPH 2023 Conference Proceedings*, 2023.

[MR02] J.E. Marsden and T. Ratiu. *Introduction to Mechanics and Symmetry: A Basic Exposition of Classical Mechanical Systems*. Texts in Applied Mathematics. Springer New York, 2002.

[MS74] J.W. Milnor and J.D. Stasheff. *Characteristic Classes*. Annals of mathematics studies. Princeton University Press, 1974.

[MTW73] Charles W. Misner, K. S. Thorne, and J. A. Wheeler. *Gravitation*. W. H. Freeman, San Francisco, 1973.

[PBS20] David Palmer, David Bommes, and Justin Solomon. Algebraic representations for volumetric frame fields. *ACM Trans. Graph.*, 39(2), April 2020.

[PCS+22] Nico Pietroni, Marcel Campen, Alla Sheffer, Gianmarco Cherchi, David Bommes, Xifeng Gao, Riccardo Scateni, Franck Ledoux, Jean Remacle, and Marco Livesu. Hex-mesh generation and processing: A survey. *ACM Trans. Graph.*, 42(2), October 2022.

[RBC+23] Ramy Rashad, Andrea Brugnoli, Federico Califano, Erwin Luesink, and Stefano Stramigioli. Intrinsic nonlinear elasticity: An exterior calculus formulation. *Journal of Nonlinear Science*, 33(5):84, 2023.

[Reg61] T. Regge. General relativity without coordinates. *Il Nuovo Cimento (1955-1965)*, 19(3):558–571, 1961.

[Sch18] Mark D. Schubel. *Discretization of Differential Geometry for Computational Gauge Theory*. PhD thesis, University of Illinois at Urbana-Champaign, 2018.

[SFCBCV19] Andrew O. Sageman-Furnas, Albert Chern, Mirela Ben-Chen, and Amir Vaxman. Chebyshev nets from commuting polyvector fields. *ACM Trans. Graph.*, 38(6), November 2019.

[Sha97] Richard W. Sharpe. *Differential Geometry: Cartan's Generalization of Klein's Erlangen Program*. Springer-Verlag, 1997.

[SSC19] Nicholas Sharp, Yousuf Soliman, and Keenan Crane. The vector heat method. *ACM Transactions on Graphics*, 38(3), 2019.

[TKB99] T. Tarhasaari, L. Kettunen, and A. Bossavit. Some realizations of a discrete hodge operator: a reinterpretation of finite element techniques [for em field analysis]. *IEEE Transactions on Magnetics*, 35(3):1494–1497, 1999.

[VCD+17] Amir Vaxman, Marcel Campen, Olga Diamanti, David Bommes, Klaus Hildebrandt, Mirela Ben-Chen Technion, and Daniele Panozzo. Directional field synthesis, design, and processing. In *ACM SIGGRAPH 2017 Courses*, 2017.

[Wac75] Eugene L. Wachspress. A rational finite element basis. volume 114 of *Mathematics in Science and Engineering*, pages 1–31. Elsevier, 1975.

[Whi57] Hassler Whitney. *Geometric Integration Theory*. Series on university mathematics. Princeton University Press, 1957.

[WNC23] Stephanie Wang, Mohammad Sina Nabizadeh, and Albert Chern. Exterior calculus in graphics. 2023.

[WSHD07] Joe Warren, Scott Schaefer, Anil Hirani, and Mathieu Desbrun. Barycentric coordinates for convex sets. *Adv. Comput. Math.*, 27:319–338, 10 2007.

[WW94] William Welch and Andrew Witkin. Free-form shape design using triangulated surfaces. In *Proceedings of the 21st Annual Conference on Computer Graphics and Interactive Techniques*, pages 247–256, 1994.

[YS25] Nicholas Sharp Yousuf Soliman. The affine heat method. 44(5), 2025.

A | Analytic Minimal-Torsion Trivial Connections

We obtain closed-form expressions for minimal-torsion trivial connections on the sphere by first deriving closed-form expressions on the plane, and then showing that minimal-torsion connections map to minimal-torsion connections by conformal maps. We can thus apply stereographic projection to obtain minimal-torsion trivial connections on the sphere, at which point we can easily achieve any other torsion by adding a given 1-form to our connection.

The planar case Suppose we have singularities located at positions $\left\{\mathbf{s}_i = \left(s_i^x, s_i^y\right)\right\}_i$ with target indices $n_i \in \mathbb{Z}$. In the standard frame e_1, e_2 of $\mathbb{R}^2$, the connection 1-form for the Levi-Civita connection is zero. So we can write any metric connection using a real 1-form $\alpha \in \Omega^1(\mathbb{R}^2)$, and it will capture these singularities if its curvature is

$$d\alpha|_{(x,y)} = -\sum_i 2\pi\, n_i \delta\left(x - s_i^x, y - s_i^y\right), \tag{A.0.1}$$

where δ is the Dirac δ function. This equation is solved by

$$\alpha^{\text{opt}} = -\sum_i n_i\, d\varphi|_{\left(x - s_i^x, y - s_i^y\right)}, \tag{A.0.2}$$

where $d\varphi$ is the angle 1-form

$$d\varphi|_{(x,y)} = \tfrac{1}{x^2+y^2}(-y\,dx + x\,dy). \tag{A.0.3}$$

We can always add a gradient to α^{opt} to get another solution, but α^{opt} is the minimum-norm solution, and hence describes the minimal-torsion connection with this curvature.

Finally, we can easily integrate α^{opt} along any line segment by observing that the integral of $d\varphi$ along a line segment measures the angle between the endpoints when viewed from the origin. Using the integral of α^{opt}, we obtain parallel vector fields from our minimal-torsion trivial connection.

Transformation under conformal maps Let $\mathcal{M}$ be a surface with metric g, and fix an orthonormal frame E and with solder form θ. If $\widetilde{g} := e^{2u} g$ is a conformally rescaled metric, then the frame $\widetilde{E} := e^{-u} E$ is orthonormal with respect to $\widetilde{g}$, and the dual frame is $\widetilde{\theta} := e^{u}\theta$.

Now, suppose we have a connection 1-form $\widetilde{\omega}$ compatible with metric $\widetilde{g}$ written with respect to frame $\widetilde{E}$. So $\widetilde{\omega}$ has the form $\widetilde{\omega} = \mathbb{J}\widetilde{\alpha}$.

We can apply a change of frame to $\widetilde{\omega}$ to express our connection in frame E. Intuitively, when seen from E, parallel transport by $\widetilde{\omega}$ rotates vectors by $-\alpha$ the same way it did in frame $\widetilde{E}$ but now scales them by $-du$ as well. If we ignore the scaling and "project" $\widetilde{\omega}^E$ to be compatible with our original metric g, we get a new g-compatible connection

$$\text{Proj}\left(\widetilde{\omega}^{(E)}\right) = \mathbb{J}\widetilde{\alpha}, \tag{A.0.4}$$

which is just our original expression for $\widetilde{\omega}$. Note that $\widetilde{\omega}^{(E)}$ and $\text{Proj}(\widetilde{\omega}^{(E)})$ have the same curvature, since they differ by a du term whose exterior derivative is zero.

Now, we can look at how torsion changes under our change of frame. The torsion of $\widetilde{\omega}$ in frame $\widetilde{E}$ is given by

$$\widetilde{\Theta} := d\widetilde{\theta} + \widetilde{\omega} \wedge \widetilde{\theta}. \tag{A.0.5}$$

If we expand out the definitions, we find that

$$\widetilde{\Theta} = e^u \left(du \wedge \theta + d\theta + \widetilde{\omega} \wedge \theta\right), \tag{A.0.6}$$

and therefore,

$$d\theta + \widetilde{\omega} \wedge \theta = e^{-u}\widetilde{\Theta} - du \wedge \theta. \tag{A.0.7}$$

Applying Equation A.0.4 reveals that

$$d\theta + \text{Proj}\left(\widetilde{\omega}^{(E)}\right) \wedge \theta = e^{-u}\widetilde{\Theta} - du \wedge \theta, \tag{A.0.8}$$

or equivalently, the torsion of $\text{Proj}(\widetilde{\omega}^{(E)})$ is equal to $e^{-u}\widetilde{\Theta} - du \wedge \theta$. Finally, one can check that $du \wedge \theta$ is exactly equal to $(\star du)^\sharp dA$, where the sharp operator and area form come from the original metric g. In summary, if we start with a connection $\widetilde{\omega}$ with torsion $\widetilde{\Theta}$, then applying a conformal transformation and projecting the resulting 1-form to be compatible with the new metric yields a connection with the desired curvature and torsion equal to $e^{-u}\widetilde{\Theta} - (\star du)^\sharp dA$.

Since we are interested in the case of the sphere, and we know that $\text{Proj}(\widetilde{\omega}^{(E)})$ has the correct curvature, it suffices to check that the divergence of its torsion is zero whenever the divergence of $\widetilde{\Theta}$ is zero. More formally, let $\widetilde{T}$ be the vector field such that $\widetilde{\Theta} = \widetilde{T} d\widetilde{A}$, and similarly let T be the vector field such that $e^{-u}\widetilde{\Theta} - (\star du)^\sharp dA = T dA$. We wish to show that $\text{div}_{\tilde{g}}\, \widetilde{T} = 0$ if and only if $\text{div}_g\, T = 0$. Since $d\widetilde{A} = e^{2u} dA$, we have $\widetilde{\Theta} = e^{-u} e^{2u} \widetilde{T} dA$, and therefore $T = e^u \widetilde{T} - (\star du)^\sharp$.

$$\begin{aligned}
\text{div}_g\, T &= \text{div}_g\left(e^u \widetilde{T} - (\star du)^\sharp\right) && \text{(A.0.9)}\\
&= \text{div}_g\left(e^u \widetilde{T}\right) && \text{(A.0.10)}\\
&= e^u\, \text{div}_{\tilde{g}}\left(\widetilde{T}\right), && \text{(A.0.11)}
\end{aligned}$$

the first step uses the fact that $(\star du)^\sharp$ is divergence-free (since it is a rotated gradient), and the second fact uses the transformation rule for the divergence of a vector field under a conformal change of metric. Since e^u is nonzero, we conclude that $\text{div}_g\, T = 0$ if and only if $\text{div}_{\tilde{g}}\, \widetilde{T} = 0$. So our projected connection has minimal torsion if and only if our original did, as desired.

B | Proof of Theorem. Definition 3.36

Proof. By definition,

$$\boldsymbol{d}^{\nabla}\boldsymbol{d}^{\nabla}\boldsymbol{\alpha}(\sigma, v_0) = \mathrm{Alt}^{\nabla}\,\mathfrak{d}^{\nabla}\,\mathrm{Alt}\,\mathfrak{d}^{\nabla}\boldsymbol{\alpha}([v_0,\dots,v_{\ell+2}], v_0).$$

We will show that the discrete map $\mathfrak{d}^{\nabla}\,\mathrm{Alt}\,\mathfrak{d}^{\nabla}\boldsymbol{\alpha}$ can be brought in the desired form. We will argue below that a novel application of the alternation operator does not violate this and will still be of the required form in Definition 3.36. In this case, we have

$$\begin{aligned}
&\mathfrak{d}^{\nabla}\,\mathrm{Alt}\,\mathfrak{d}^{\nabla}\boldsymbol{\alpha}([v_0,\dots,v_{\ell+2}], v_0)\\
&= \mathcal{R}_{01}\,\mathrm{Alt}\,\mathfrak{d}^{\nabla}\,\boldsymbol{\alpha}([v_1,\dots,v_{\ell+2}], v_1) + \sum_{i=1}^{\ell+2}(-1)^i \mathrm{Alt}\,\mathfrak{d}^{\nabla}\,\boldsymbol{\alpha}([v_0,\dots,\hat{v}_i,\dots,v_{\ell+2}], v_0)\\
&= \mathcal{R}_{01}\frac{1}{|S_{\ell+2}|}\sum_{\pi\in S_{\ell+2}}\mathcal{R}_{1\pi(1)}\,\mathrm{sgn}(\pi)\mathfrak{d}^{\nabla}\boldsymbol{\alpha}(\pi([v_1,\dots,v_{\ell+2}]), v_{\pi(1)})\\
&\quad + \sum_{i=1}^{\ell+1}(-1)^i\frac{1}{|S_{\ell+2}|}\sum_{\pi\in S_{\ell+2}}\mathrm{sgn}(\pi)\mathcal{R}_{0\pi(0)}\,\mathfrak{d}^{\nabla}\boldsymbol{\alpha}(\pi([v_0,\dots,\hat{v}_i,\dots,v_{\ell+2}]), v_{\pi(0)}).
\end{aligned}$$

In the following, we will use the notation $\sigma^i := [v_0,\dots,\widehat{v_i},\dots,v_{\ell+2}]$, and with it,

$$(\pi(\sigma^i))^j = [\pi(\sigma^i)_0,\dots,\widehat{\pi(\sigma^i)}_j,\dots,\pi(\sigma^i)_{\ell+2}],$$

to mean that we first omit the i^{th} vertex, then permute the $(\ell+1)$-simplex with a permutation and then, out of the induced ordering, omit the j^{th} vertex to obtain an $\ell-$simplex. This yields

$$\begin{aligned}
&\mathfrak{d}^{\nabla}\,\mathrm{Alt}\,\mathfrak{d}^{\nabla}\boldsymbol{\alpha}([v_0,\dots,v_{\ell+2}], v_0) =\\
&\mathcal{R}_{01}\frac{1}{|S_{\ell+2}|}\sum_{\pi\in S_{\ell+2}}\mathrm{sgn}(\pi)\mathcal{R}_{1\pi(\sigma)_1}\left(\mathcal{R}_{\pi(s)_1\pi(\sigma^0)_1}\boldsymbol{\alpha}(\pi(\sigma^0)^0, v_{\pi(2)}) + \sum_{j=1}^{\ell+1}(-1)^j\boldsymbol{\alpha}(\pi(\sigma^0)^j, v_{\pi(\sigma)_1})\right) \quad \text{(B.0.1)}\\
&+\sum_{i=1}^{\ell+2}\frac{(-1)^i}{|S_{\ell+2}|}\sum_{\pi\in S_{\ell+2}}\mathrm{sgn}(\pi)\mathcal{R}_{0\pi(\sigma)_0}\left(\mathcal{R}_{\pi(0),\pi(\sigma^i)_1}\boldsymbol{\alpha}(\pi(\sigma^i)^0, v_{\pi(\sigma^i)_1}) + \sum_{j=1}^{\ell+1}(-1)^j\boldsymbol{\alpha}(\pi(\sigma^i)^j, v_{\pi(\sigma)_0})\right).
\end{aligned}$$

Each of the parts of the sum consists of a sign, the evaluation of the differential form $\boldsymbol{\alpha}$ over a permuted subsimplex with two missing vertices and a parallel transport map to the common evaluation fiber. It thus remains to show that for a given permutation $\tau\in S_{\ell+1}$, the subsimplex $\tau(\sigma^{ij})$

is used twice for the evaluation of $\boldsymbol{\alpha}$, but with a different sign. In this case, in Equation (B.0.1), the evaluation of $\boldsymbol{\alpha}$ on $\tau(\sigma^{ij})$ appears twice, with two potentially different parallel transport paths to v_0 and with opposite sign, leading to a discrete curvature expression to which we apply the evaluation of $\boldsymbol{\alpha}$ on the permuted sub-simplex.

Without loss of generality we can assume that $i < j$. In order to create the permuted simplices, we distinguish two cases. For the first application $\mathfrak{d}^{\nabla}$ we omit v_i, leading to a sign of $(-1)^i$.

Starting with σ^i, since we assumed that $i < j$, we can now apply $(j-2)$ transpositions to bring v_j in the first slot of the simplex. Next, we can apply the permutation τ on the last $(\ell+1)$ vertices. This leads to a sign of $(-1)^{j-2} \cdot \operatorname{sgn}(\tau)$. Now, for the second application of $\mathfrak{d}$, the vertex v_j is in the 0^{th} slot — thus the sign does not change. The sign of evaluation will then be $(-1)^{i+j-2+\operatorname{sgn}(\tau)}$.

On the other hand, consider the case where we omit first the j^{th} vertex in the first application of $\mathfrak{d}$. This leads to a sign of $(-1)^j$. On the simplex σ^j, there are now $(i-1)$ transpositions needed to transport v_i to the 0^{th} slot. We can now again apply the permutation τ on the last $(\ell+1)$ vertices. Subsequently, when applying $\mathfrak{d}$ a second time we will omit v_i in the 0^{th} slot, leading to a total sign of $(-1)^{j+i-1+\operatorname{sgn}(\tau)}$.

This implies that for each evaluation of $\boldsymbol{\alpha}$ over $\tau(\sigma^{ij})$, there exists an evaluation of $\boldsymbol{\alpha}$ over $\tau(\sigma^{ij})$, with a possibly different transport path to the common evaluation fiber over v_0, and more importantly a different sign for the parallel transport path, turning the expression of Equation (B.0.1) into a sum of curvatures, to which we apply evaluations of $\boldsymbol{\alpha}$.

Since the alternation of a discrete bundle-valued differential form takes care of consistent signing and transporting to common fibers, we can conclude that there exists a $K \subseteq C^2(\sigma) \times C^{\ell}(\sigma)$ such that

$$\boldsymbol{d}^{\nabla}\boldsymbol{d}^{\nabla}\boldsymbol{\alpha}(\sigma) = \frac{1}{(\ell+3)! \cdot (\ell+2)!} \sum_{(m,\kappa)\in K} \boldsymbol{\Omega}^{\nabla}(f)\,\boldsymbol{\alpha}(\kappa) =: \boldsymbol{\Omega}^{\nabla} \wedge \boldsymbol{\alpha}.$$

□

C | Simplification of non-commmutative expressions.

In various parts of this paper, we used the NCAlgebra library [HDOS10] to simplify expressions from our operators, where connection matrices and discrete 1-forms are non-commutative variables. A notebook is available at `https://gitlab.inria.fr/geomerix/public/fulldec`, structured in the following way: first, as illustrated in Figure C.1, we initialize the symbolic parallel transport matrices; then we show in Figure C.2 how to initialize a symbolic vector-valued differential 1-form; finally, we see in Figure C.3 how the PPF-induced sided discrete exterior covariant derivative and discrete exterior covariant derivative can be implemented with simplified expressions.

```
In[1]:= << NC`
        ••• NC: You are using the version of NCAlgebra which is found in: "C:\Users\tbraune\NC\".
In[2]:= << NCAlgebra`
        ••• NCAlgebra: All lower cap single letter symbols (e.g. a,b,c,...) were set as noncommutative.
In[3]:= SetOptions[inv, Distribute → True]
In[4]:= SNC[r12, r13, r14, r23, r24, r34]
In[5]:= r21 = inv[r12]; r31 = inv[r13]; r32 = inv[r23]; r42 = inv[r24]; r43 = inv[r34]; r41 = inv[r14];
In[6]:= r44 = Id; r33 = Id; r22 = Id; r11 = Id;

In[7]:= rot = {{r11, r12, r13, r14}, {r21, r22, r23, r24}, {r31, r32, r33, r34}, {r41, r42, r43, r44}}
Out[7]= {{1, r12, r13, r14}, {r12^-1, 1, r23, r24}, {r13^-1, r23^-1, 1, r34}, {r14^-1, r24^-1, r34^-1, 1}}

In[8]:= MatrixForm[rot]
Out[8]//MatrixForm=
```

$$\begin{pmatrix} 1 & r12 & r13 & r14 \\ r12^{-1} & 1 & r23 & r24 \\ r13^{-1} & r23^{-1} & 1 & r34 \\ r14^{-1} & r24^{-1} & r34^{-1} & 1 \end{pmatrix}$$

Figure C.1: Definition of the symbolic variables for the connection

```
In[9]:= SNC[alpha11, alpha12, alpha13, alpha14, alpha21, alpha22, alpha23, alpha24, alpha31, alpha32, alpha33, alpha34, alpha41, alpha42, alpha43, alpha44]

In[10]:= alpha = {{alpha11, alpha12, alpha13, alpha14}, {alpha21, alpha22, alpha23, alpha24}, {alpha31, alpha32, alpha33, alpha34}, {alpha41, alpha42, alpha43, alpha44}}
Out[10]= {{alpha11, alpha12, alpha13, alpha14}, {alpha21, alpha22, alpha23, alpha24}, {alpha31, alpha32, alpha33, alpha34}, {alpha41, alpha42, alpha43, alpha44}}
```

Implement the formula for the exterior derivative of the 1-form

```
In[11]:= dalpha[{a_Integer, b_Integer, c_Integer}] := (alpha[[a]][[b]] + (rot[[a]][[b]]) ** alpha[[b]][[c]] - alpha[[a]][[c]])

In[12]:= dalpha[{1, 2, 3}]
Out[12]= alpha12 - alpha13 + r12 ** alpha23

In[13]:= dalphaBar[{a_Integer, b_Integer, c_Integer}] := (avg = 0; G = Permutations[{a, b, c}]; Alp = Map[dalpha, Permutations[{a, b, c}]]; len = Length[G];
  (* Do not forget to pre and post multiply with the matrices to the start and end fiber !!! *)
  Do[sigma = G[[i]]; sgn = Signature[sigma];
   transport = Alp[[i]];
   start = sigma[[1]];
   transport = rot[[a]][[ start ]] ** transport ;
   avg += (sgn / len) * transport, {i, 1, len}];
  avg)

In[14]:= NCSimplifyRational[dalphaBar[{1, 2, 3}]]
Out[14]= alpha12/2 - alpha13/2 - (r12 ** alpha21)/3 + (r12 ** alpha23)/2 + (r13 ** alpha31)/3 - (r13 ** alpha32)/2 + (r12 ** r23 ** alpha31)/6 - 1/6 r13 ** r23^-1 ** alpha21

In[15]:= ddalpha[{a_Integer, b_Integer, c_Integer, d_Integer}] := rot[[a]][[b]] ** dalpha[{b, c, d}] - dalpha[{a, c, d}] + dalpha[{a, b, d}] - dalpha[{a, b, c}]

In[ ]:= NCSimplifyRational[ddalpha[{1, 2, 3, 4}]]
Out[ ]= -r13 ** alpha34 + r12 ** r23 ** alpha34

In[16]:= ddalphaBar[{a_Integer, b_Integer, c_Integer, d_Integer}] := rot[[a]][[b]] ** dalphaBar[{b, c, d}] - dalphaBar[{a, c, d}] + dalphaBar[{a, b, d}] - dalphaBar[{a, b, c}]

In[17]:= NCSimplifyRational[ddalphaBar[{1, 2, 3, 4}]]
 (r13 ** alpha32)/2 - (r13 ** alpha34)/2 - (r14 ** alpha42)/2 + (r14 ** alpha43)/2 - (r12 ** r23 ** alpha31)/6 - (r12 ** r23 ** alpha32)/3 + (r12 ** r23 ** alpha34)/2 + (r12 ** r24 ** alpha41)/6 +
 (r12 ** r24 ** alpha42)/3 - (r12 ** r24 ** alpha43)/2 - (r13 ** r34 ** alpha41)/6
 + 1/6 r13 ** r23^-1 ** alpha21 - 1/6 r14 ** r24^-1 ** alpha21 + 1/6 r14 ** r34^-1 ** alpha31 + 1/6 r12 ** r23 ** r34 ** alpha42
 - 1/6 r12 ** r24 ** r34^-1 ** alpha32
```

Figure C.2: Setup for the symbolic discrete 1-forms

We try averaging with the odd and even permutations

```
In[ ]:= dalphaBarOdd[{a_Integer, b_Integer, c_Integer}] := (avg = 0; G = Permutations[{a, b, c}]; Alp = Map[dalpha, Permutations[{a, b, c}]]; len = Length[G];
  (* Do not forget to pre and post multiply with the matrices to the start and end fiber !!! *)
  Do[sigma = G[[i]]; sgn = Signature[sigma];
   transport = Alp[[i]];
   start = sigma[[1]];
   transport = rot[[a]][[ start ]] ** transport ;
   avg += ((sgn - 1) / (len)) * transport, {i, 1, len}];
  avg)

In[ ]:= dalphaBarEven[{a_Integer, b_Integer, c_Integer}] := (avg = 0; G = Permutations[{a, b, c}]; Alp = Map[dalpha, Permutations[{a, b, c}]]; len = Length[G];
  (* Do not forget to pre and post multiply with the matrices to the start and end fiber !!! *)
  Do[sigma = G[[i]]; sgn = Signature[sigma];
   transport = Alp[[i]];
   start = sigma[[1]];
   transport = rot[[a]][[ start ]] ** transport ;
   avg += ((sgn + 1) / (len)) * transport, {i, 1, len}];
  avg)

In[ ]:= NCSimplifyRational[dalphaBarEven[{1, 2, 3}]]
Out[ ]= (2 alpha12)/3 - alpha13/3 - (r12 ** alpha21)/3 + (2 r12 ** alpha23)/3 + (r13 ** alpha31)/3 - (r13 ** alpha32)/3 + (r12 ** r23 ** alpha31)/3

In[ ]:= NCSimplifyRational[dalphaBarOdd[{1, 2, 3}]]
Out[ ]= alpha12/3 - (2 alpha13)/3 - (r12 ** alpha21)/3 + (r12 ** alpha23)/3 + (r13 ** alpha31)/3 - (2 r13 ** alpha32)/3 - 1/3 r13 ** r23^-1 ** alpha21

In[ ]:= ddalphaBarOdd[{a_Integer, b_Integer, c_Integer, d_Integer}] := rot[[a]][[b]] ** dalphaBarOdd[{b, c, d}] - dalphaBarOdd[{a, c, d}] + dalphaBarOdd[{a, b, d}] - dalphaBarOdd[{a, b, c}]

In[ ]:= ddalphaBarEven[{a_Integer, b_Integer, c_Integer, d_Integer}] := rot[[a]][[b]] ** dalphaBarEven[{b, c, d}] - dalphaBarEven[{a, c, d}] + dalphaBarEven[{a, b, d}] - dalphaBarEven[{a, b, c}]

In[ ]:= NCSimplifyRational[ddalphaBarEven[{1, 2, 3, 4}]]
 -alpha13/3 + (r12 ** alpha24)/3 + (r13 ** alpha32)/3 - (2 r13 ** alpha34)/3 - (r14 ** alpha42)/3 + (r14 ** alpha43)/3 - (r12 ** r23 ** alpha31)/3 - (r12 ** r23 ** alpha32)/3 +
 (2 r12 ** r23 ** alpha34)/3 + (r12 ** r24 ** alpha41)/3 + (r12 ** r24 ** alpha42)/3 - (r12 ** r24 ** alpha43)/3 - (r13 ** r34 ** alpha41)/3 + 1/3 r12 ** r23 ** r34 ** alpha42

In[ ]:= NCSimplifyRational[ddalphaBarOdd[{1, 2, 3, 4}]]
 alpha13/3 - (r12 ** alpha24)/3 + (2 r13 ** alpha32)/3 - (r13 ** alpha34)/3 - (2 r14 ** alpha42)/3 + (2 r14 ** alpha43)/3 - (r12 ** r23 ** alpha32)/3 + (r12 ** r23 ** alpha34)/3 +
 (r12 ** r24 ** alpha42)/3 - (2 r12 ** r24 ** alpha43)/3 + 1/3 r13 ** r23^-1 ** alpha21 - 1/3 r14 ** r24^-1 ** alpha21 + 1/3 r14 ** r34^-1 ** alpha31 - 1/3 r12 ** r24 ** r34^-1 ** alpha32
```

Figure C.3: Implementation of the symbolic discrete exterior covariant derivative.

D | Direct Calculation for the Discrete Exterior Covariant Derivative of Bundle-Valued $1-$Forms

We want to illustrate here through a direct calculation that the discrete exterior derivative of a discretized $1-$form in the limit converges to the value of the smooth exterior derivative of the continuous $1-$form if the discretization of the differential form was carried out in a parallel-propagated frame field.

In the following, let $\mathcal{M}$ be a smooth manifold and $\pi\colon E \to \mathcal{M}$ a smooth vector bundle with connection ∇ over $\mathcal{M}$. Let $\alpha \in \Omega^1(\mathcal{M}, E)$ be an $E-$valued differential $1-$form. Let $\sigma_2 = [abc]$ be a triangle diffeomorphic to a triangular region $s_2 \subset M$. Further let $\sigma_3 = [abcd]$ an arbitrary tetrahedron diffeomorphic to a region $s_3 \subset \mathcal{M}$. As explained in Section 3.3.2, we will use the image of the simplicial cells in $\mathcal{M}$ to carry out the discretization of α. Once this is done, we will just regard this as discrete data available on the simplicial cells. As before, we denote by $\boldsymbol{\alpha}_{ab}$ the integral in a parallel-propagated frame of α on $[ab]$ based in a. We also denote by α_{ab} the integral in an arbitrary local frame of α on $[ab]$ based at a.

Convergence of the PPF-induced Sided Discrete Exterior Covariant Derivative. It holds for the second-order approximation of the integral in the parallel-propagated frame that $\boldsymbol{\alpha}_{ab} = \left(I + \frac{\omega_{ab}}{2}\right)\alpha_{ab} + \mathcal{O}(h^3)$. Therefore,

$$\begin{aligned}
\mathfrak{d}^\nabla \boldsymbol{\alpha}([abc], a) &= \boldsymbol{\alpha}_{ab} + R_{ab}\boldsymbol{\alpha}_{bc} - \boldsymbol{\alpha}_{ac} \\
&= \left(I + \frac{\omega_{ab}}{2}\right)\alpha_{ab} + (I + \omega_{ab})\left(I + \frac{\omega_{bc}}{2}\right)\alpha_{bc} - \left(I + \frac{\omega_{ac}}{2}\right)\alpha_{ac} + \mathcal{O}(h^3) \\
&= (\alpha_{ab} + \alpha_{bc} - \alpha_{ac}) + \frac{\omega_{ab}\alpha_{ab}}{2} + \omega_{ab}\alpha_{bc} + \frac{\omega_{bc}\alpha_{bc}}{2} - \frac{\omega_{ac}\alpha_{ac}}{2} + \mathcal{O}(h^3).
\end{aligned}$$

Thus, we obtain

$$\begin{aligned}
&\mathfrak{d}^{\boldsymbol{\nabla}} \boldsymbol{\alpha}([abc], a) \\
&= (\boldsymbol{d}\alpha)_{abc} + \frac{\omega_{ab}}{2}\alpha_{ab} + \omega_{ab}(\alpha_{ac} - \alpha_{ab}) + \frac{1}{2}(\omega_{ac} - \omega_{ab})(\alpha_{ac} - \alpha_{ab}) - \frac{\omega_{ac}}{2}\alpha_{ac} + \mathcal{O}(h^3) \\
&= (\boldsymbol{d}\alpha)_{abc} + \frac{\omega_{ab}}{2}\alpha_{ab} - \frac{\omega_{ac}}{2}\alpha_{ac} + \omega_{ab}\alpha_{ac} - \omega_{ab}\alpha_{ab} + \frac{\omega_{ac}}{2}\alpha_{ac} - \frac{\omega_{ac}}{2}\alpha_{ab} - \frac{\omega_{ab}}{2}\alpha_{ac} + \frac{\omega_{ab}}{2}\alpha_{ab} \\
&= (\boldsymbol{d}\alpha)_{abc} + \frac{\omega_{ab}\alpha_{ac}}{2} - \frac{\omega_{ac}\alpha_{ab}}{2} + \mathcal{O}(h^3) \\
&= (\boldsymbol{d}\alpha)_{abc} + (\omega \wedge \alpha)(e_{ab}, e_{ac}) + \mathcal{O}(h^3).
\end{aligned}$$

Direct Calculation for the Discrete Exterior Covariant Derivative of Bundle-Valued 1–Forms

In the notation $(\omega \wedge \alpha)(e_{ab}, e_{ac})$, we refer to the discretization on edges $[ab]$ and $[ac]$, respectively. This notation highlights the link to the smooth wedge product: it is as if we evaluate the smooth wedge product $\omega \wedge \alpha$ at the point a on the outgoing vectors e_{ab} and e_{ac}. This calculation emphasizes the crucial role of discretization in a parallel-propagated frame. Without this frame, only the term $\boldsymbol{d}\alpha$ would remain. However, with the employed parallel-propagated frame, we can demonstrate that this approach precisely yields the terms we would expect from the smooth counterpart.

Convergence of the Discrete Algebraic Bianchi Identity. It was shown in [BEHS21] that

$$\mathfrak{d}^{\nabla}\mathfrak{d}^{\nabla}\boldsymbol{\alpha}([abcd], a) = \boldsymbol{\Omega}^{\nabla}([abc], a, c)\boldsymbol{\alpha}_{cd}.$$

Thus, two consecutive applications of the sided discrete exterior covariant derivative rely on a single stencil for curvature evaluation. As demonstrated in Section 3.3.3, even when the form α is obtained through integration in a PPF, convergence to the smooth algebraic Bianchi identity under mesh refinement is not achieved. In the following, we will illustrate through a direct calculation for 1–forms that the alternation operator provides a remedy. This operator transforms the resulting discrete expression into a form that closely resembles the smooth wedge product between the curvature form and the vector-valued 1–form, up to higher-order terms.

We saw in our numerical tests that we can achieve convergence if we reduce the alternation Alt of the PPF-induced sided discrete exterior covariant derivative to a subset of the full permutation group that consists only of the even — or the odd — permutations τ_k. In this case, the alternation becomes:

$$\widetilde{\mathrm{Alt}}(\alpha)[x_0, \dots, x_k] = \frac{2}{|S_k|}\sum_{\sigma\in\tau_k} R_{0,\sigma(0)}\cdot\alpha[x_{\sigma(0)}, \dots, x_{\sigma(k)}].$$

This yields for a 1–form, after simplification with NCAlgebra [HDOS10] on Mathematica,

$$\begin{aligned}\mathfrak{d}^{\nabla}(\widetilde{\mathrm{Alt}})\, \mathfrak{d}^{\nabla}\boldsymbol{\alpha}([abcd], a) = \frac{1}{3}&((R_{ac} - R_{ab}R_{bc})(\boldsymbol{\alpha}_{ca} + \boldsymbol{\alpha}_{cb} - 2\boldsymbol{\alpha}_{cd})\\ &+ (R_{ab}R_{bc}R_{cd} - R_{ad})\,\boldsymbol{\alpha}_{db} - (R_{ab}R_{bd} - R_{ad})\,\boldsymbol{\alpha}_{dc} + (R_{ab}R_{bd} - R_{ac}R_{cd})\boldsymbol{\alpha}_{da}).\end{aligned}$$

If we expand this formula, we obtain

$$\begin{aligned}&\mathfrak{d}^{\nabla}(\widetilde{\mathrm{Alt}})\, \mathfrak{d}^{\nabla}\boldsymbol{\alpha}([abcd], a)\\ &= -\frac{1}{3}(\boldsymbol{\Omega}^{\nabla}([abc], a, c)(\boldsymbol{\alpha}_{ca} - \boldsymbol{\alpha}_{cd} + \boldsymbol{\alpha}_{cb} - \boldsymbol{\alpha}_{cd}) + \boldsymbol{\Omega}^{\nabla}([abd], a, d)\boldsymbol{\alpha}_{dc}\\ &\quad + (R_{ab}R_{bc} - R_{ad}R_{dc})R_{cd}\boldsymbol{\alpha}_{db} - \boldsymbol{\Omega}^{\nabla}([abd], a, d)\boldsymbol{\alpha}_{dc} + (R_{ab}R_{bd} - R_{ac}R_{cd})\boldsymbol{\alpha}_{da})\\ &= -\frac{1}{3}\boldsymbol{\Omega}^{\nabla}([abc], a, c)(\boldsymbol{\alpha}_{ca} + \boldsymbol{\alpha}_{cb} - \boldsymbol{\alpha}_{cd}) + \frac{1}{3}\boldsymbol{\Omega}^{\nabla}, ([abc], a, c)R_{cd}\boldsymbol{\alpha}_{db} - \frac{1}{3}\boldsymbol{\Omega}^{\nabla}([adc], a, c)R_{cd}\boldsymbol{\alpha}_{db}\\ &\quad - \frac{1}{3}\boldsymbol{\Omega}^{\nabla}([abd], a, d)\boldsymbol{\alpha}_{dc} + \frac{1}{3}\boldsymbol{\Omega}^{\nabla}([abd], a, d)\boldsymbol{\alpha}_{da} - \frac{1}{3}\boldsymbol{\Omega}^{\nabla}([acd], a, d)\boldsymbol{\alpha}_{da}.\end{aligned}$$

We have seen that the discrete exterior derivative for 1–forms (arising from discretization in a parallel-propagated frame of a smooth differential form α) generates terms that are of order $\mathcal{O}(h^2)$, therefore, they can be ignored to first order. It holds, for instance, that

$$\boldsymbol{\alpha}_{ca} - \boldsymbol{\alpha}_{cd} = -R_{ca}\boldsymbol{\alpha}_{ad} + \underbrace{\mathfrak{d}^{\nabla}\boldsymbol{\alpha}([cad], c)}_{\in\mathcal{O}(h^2)}.$$

We obtain

$$
\begin{aligned}
\mathfrak{d}^{\nabla}(\widetilde{\mathrm{Alt}})\,\mathfrak{d}^{\nabla}\boldsymbol{\alpha}([abcd],a) &= \frac{1}{3}\boldsymbol{\Omega}^{\nabla}([abc],a,c)R_{ca}\boldsymbol{\alpha}_{ad} + \frac{1}{3}\boldsymbol{\Omega}^{\nabla}([abc],a,c)R_{cd}\boldsymbol{\alpha}_{db} \\
&\quad - \frac{1}{3}\boldsymbol{\Omega}^{\nabla}([adc],a,c)R_{cd}\boldsymbol{\alpha}_{db} - \frac{1}{3}\boldsymbol{\Omega}^{\nabla}([abd],a,d)\boldsymbol{\alpha}_{dc} \\
&\quad + \frac{1}{3}\boldsymbol{\Omega}^{\nabla}([abd],a,d)\boldsymbol{\alpha}_{da} - \frac{1}{3}\boldsymbol{\Omega}^{\nabla}([acd],a,d)\boldsymbol{\alpha}_{da} + \mathcal{O}(h^4) \\
&= \frac{1}{3}\boldsymbol{\Omega}^{\nabla}([abc],a,c)R_{ca}\boldsymbol{\alpha}_{ad} + \frac{1}{3}\boldsymbol{\Omega}^{\nabla}([abc],a,c)R_{cb}\boldsymbol{\alpha}_{bd} + \frac{1}{3}\boldsymbol{\Omega}^{\nabla}([abc],a,c)R_{cd}\boldsymbol{\alpha}_{db} \\
&\quad - \frac{1}{3}\boldsymbol{\Omega}^{\nabla}([acd],a,d)\underbrace{(\boldsymbol{\alpha}_{db} - \boldsymbol{\alpha}_{da})}_{=-R_{da}\boldsymbol{\alpha}_{ab}} + \frac{1}{3}\boldsymbol{\Omega}^{\nabla}([abd],a,d)\underbrace{(\boldsymbol{\alpha}_{da} - \boldsymbol{\alpha}_{dc})}_{-R_{da}\boldsymbol{\alpha}_{ac}} + \mathcal{O}(h^4) \\
&= \frac{1}{3}\boldsymbol{\Omega}^{\nabla}([abc],a,a)\boldsymbol{\alpha}_{ad} + \frac{1}{3}\boldsymbol{\Omega}^{\nabla}([acd],a,a)\boldsymbol{\alpha}_{ab} - \frac{1}{3}\boldsymbol{\Omega}^{\nabla}([abd],a,a)\boldsymbol{\alpha}_{ac} \\
&\quad + \frac{1}{3}\boldsymbol{\Omega}^{\nabla}([abc],a,c)\underbrace{(R_{cb}\boldsymbol{\alpha}_{bd} + R_{cd}\boldsymbol{\alpha}_{db})}_{-\boldsymbol{\Omega}^{\nabla}([cdb],c,b)\boldsymbol{\alpha}_{bd}} + \mathcal{O}(h^4).
\end{aligned}
$$

Since the curvature form is a 2−form, we can neglect the last term of the calculation for the convergence analysis since their product is of order $\mathcal{O}(h^4)$. We are then left with:

$$
\mathfrak{d}^{\nabla}(\widetilde{\mathrm{Alt}})\,\mathfrak{d}^{\nabla}\boldsymbol{\alpha}([abcd],a) = \frac{1}{3}\left(\boldsymbol{\Omega}^{\nabla}([abc],a,a)\boldsymbol{\alpha}_{ad} + \boldsymbol{\Omega}^{\nabla}([acd],a,a)\boldsymbol{\alpha}_{ab} - \boldsymbol{\Omega}^{\nabla}([abd],a,a)\boldsymbol{\alpha}_{ac}\right) + \mathcal{O}(h^4)
$$

If we use instead the odd permutations

$$
\wr_k = \{\sigma \in S_n \quad \mathrm{sgn}(\sigma) = -1\}
$$

for the alternation of the discrete form, we denote the alternation operator as:

$$
\mathrm{Alt}^{\wr}(\alpha)[x_0,\ldots,x_k] = \frac{2}{|S_k|}\sum_{\sigma\in\wr_k} -R_{0,\sigma(0)} \cdot \alpha[x_{\sigma(0)},\ldots,x_{\sigma(k)}].
$$

Using Mathematica, NCAlgebra [HDOS10] simplifies this expression to

$$
\begin{aligned}
&\mathfrak{d}^{\nabla}(\mathrm{Alt}^{\wr})\,\mathfrak{d}^{\nabla}\boldsymbol{\alpha}([abcd],a) \\
&= \frac{1}{3}\Big((R_{ad}R_{dc} - R_{ac})\boldsymbol{\alpha}_{ca} + (R_{ad}R_{db} - R_{ab})\boldsymbol{\alpha}_{bd} + (R_{ab}R_{bd} - R_{ad})\boldsymbol{\alpha}_{db} \\
&\quad - (R_{ab}R_{bc} - R_{ac})\boldsymbol{\alpha}_{bc} - (R_{ab}R_{bd}R_{dc} - R_{ac})\boldsymbol{\alpha}_{cb} + (R_{ab}R_{bc} - R_{ac})\boldsymbol{\alpha}_{cd} \\
&\quad - 2(R_{ab}R_{bd} - R_{ad})\boldsymbol{\alpha}_{dc} + (R_{ac}R_{cb} - R_{ad}R_{db})\boldsymbol{\alpha}_{ba}\Big)
\end{aligned}
$$

$$= \frac{1}{3}\Bigg(\boldsymbol{\Omega}^{\nabla}([adc],a,c)\boldsymbol{\alpha}_{ca} + \boldsymbol{\Omega}^{\nabla}([adb],a,b)\boldsymbol{\alpha}_{bd} + \boldsymbol{\Omega}^{\nabla}([abd],a,d)\boldsymbol{\alpha}_{db}$$

$$- \boldsymbol{\Omega}^{\nabla}([abc],a,c)\boldsymbol{\alpha}_{cb} - \boldsymbol{\Omega}^{\nabla}([abd],a,d)R_{dc}\boldsymbol{\alpha}_{cb} - \boldsymbol{\Omega}^{\nabla}([adc],a,c)\boldsymbol{\alpha}_{cb}$$

$$+ \boldsymbol{\Omega}^{\nabla}([abc],a,c)\boldsymbol{\alpha}_{cd} - 2\boldsymbol{\Omega}^{\nabla}([abd],a,d)\boldsymbol{\alpha}_{dc} + \boldsymbol{\Omega}^{\nabla}([acb],a,b)\boldsymbol{\alpha}_{ba} - \boldsymbol{\Omega}^{\nabla}([adb],a,b)\boldsymbol{\alpha}_{ba}\Bigg)$$

$$= \frac{1}{3}\Bigg(\boldsymbol{\Omega}^{\nabla}([adc],a,c)(\boldsymbol{\alpha}_{ca} - \boldsymbol{\alpha}_{cb}) + \boldsymbol{\Omega}^{\nabla}([abc],a,b)(\boldsymbol{\alpha}_{cd} - \boldsymbol{\alpha}_{cb} - R_{cb}\boldsymbol{\alpha}_{ba})$$

$$+ \boldsymbol{\Omega}^{\nabla}([abd],a,d)(-R_{db}\boldsymbol{\alpha}_{bd} + \boldsymbol{\alpha}_{db} - R_{dc}\boldsymbol{\alpha}_{cb} - 2\boldsymbol{\alpha}_{dc} + R_{db}\boldsymbol{\alpha}_{ba})\Bigg).$$

We again take advantage of the fact that the product of the curvature 2–form and $\boldsymbol{d}^{\nabla}\alpha$ is of order $\mathcal{O}(h^4)$ and therefore can be neglected for the analysis of convergence, leading to:

$$\begin{aligned}
&\mathfrak{d}^{\nabla}(\mathrm{Alt}^{2})\,\mathfrak{d}^{\nabla}\boldsymbol{\alpha}([abcd],a)\\
&= -\frac{1}{3}\boldsymbol{\Omega}^{\nabla}([adc],a,c)R_{ca}\boldsymbol{\alpha}_{ab} + \frac{1}{3}\boldsymbol{\Omega}^{\nabla}([abc],a,c)(\underbrace{\boldsymbol{\alpha}_{cd} - \boldsymbol{\alpha}_{ca}}_{-R_{cd}\boldsymbol{\alpha}_{da}+\mathcal{O}(h^2)})\\
&\quad + \frac{1}{3}\boldsymbol{\Omega}^{\nabla}([abd],a,d)(-R_{db}\boldsymbol{\alpha}_{db} + \boldsymbol{\alpha}_{db} - R_{dc}\boldsymbol{\alpha}_{cb} - 2\boldsymbol{\alpha}_{dc} + R_{db}\boldsymbol{\alpha}_{ba}) + \mathcal{O}(h^4)\\
&= -\frac{1}{3}\boldsymbol{\Omega}^{\nabla}([adc],a,c)R_{ca}(\boldsymbol{\alpha}_{ab}) + \frac{1}{3}\boldsymbol{\Omega}^{\nabla}([acb],a,b)\underbrace{R_{bc}R_{cd}\boldsymbol{\alpha}_{da}}_{-R_{ba}\boldsymbol{\alpha}_{ad}+\mathcal{O}(h^4)}\\
&\quad - \frac{1}{3}\boldsymbol{\Omega}^{\nabla}([abd],a,d)R_{da}\boldsymbol{\alpha}_{ac} + \frac{1}{3}\boldsymbol{\Omega}^{\nabla}([abd],a,d)(-\mathfrak{d}^{\nabla}\boldsymbol{\alpha}([dcb],d) + \mathcal{O}(h^4)\\
&= -\frac{1}{3}\boldsymbol{\Omega}^{\nabla}([adc],a,a)\boldsymbol{\alpha}_{ab} - \boldsymbol{\Omega}^{\nabla}([acb],a,a)\boldsymbol{\alpha}_{ad} + \boldsymbol{\Omega}^{\nabla}([adb],a,a)\boldsymbol{\alpha}_{ac} + \mathcal{O}(h^4).
\end{aligned}$$

We can now take the mean over both subsets of the group. We denote e_{ab}, e_{ac}, e_{ad} the edges coming out a and by (e_{ab}, e_{ac}, e_{ad}) the tetrahedron that is formed by this edges. Any selection of two edges denotes the triangle formed by these two edges. With this notation, we have

$$\mathfrak{d}^{\boldsymbol{\nabla}}\boldsymbol{d}^{\boldsymbol{\nabla}}\boldsymbol{\alpha}((e_{ab}, e_{ac}, e_{ad}), a) = \frac{1}{6}\sum_{\sigma\in S_3}\mathrm{sgn}(\sigma)\boldsymbol{\Omega}^{\nabla}[\sigma(e_{ab}), \sigma(e_{ac})]\boldsymbol{\alpha}(\sigma(e_{ad})) + \mathcal{O}(h^4). \tag{D.0.1}$$

This is the counterpart to the smooth wedge product between the curvature form and a vector-valued form. It highlights the importance of the alternation operator in achieving convergence under refinement. The calculation demonstrates that, with the use of the alternation operator, the form $\mathfrak{d}^{\boldsymbol{\nabla}}\boldsymbol{d}^{\boldsymbol{\nabla}}\boldsymbol{\alpha}$ can be brought to a higher order, in the form of a smooth wedge product between the curvature and a vector-valued form. Without the alternation operator, this simply is not the case.

E | Convergence Analysis for Endomorphism Valued Forms

In this chapter we will demonstrate the convergence proof for the exterior covariant derivative under refinement. As in the case of discrete **E**-valued differential forms we will begin to show the convergence behavior of $\mathfrak{d}^{\nabla}$ under refinement. Subsequently we demonstrate that the alternation can improve the accuracy and finally we will demonstrate that this allows to conclude that $\boldsymbol{d}^{\nabla}\boldsymbol{d}^{\nabla}$ converges under refinement.

Theorem E.1. *Let $\pi : E \to \mathcal{M}$ be a vector bundle with connection ∇. Let $s = [v_0, \dots, v_{\ell+1}] \subset \mathcal{M}$ be a region in $\mathcal{M}$ for which there exists a diffeomorphism to a $(\ell+1)$-simplex σ where each point v_i are mapped to an associated vertex w_i of σ. Further let $\beta \in \Omega^{\ell}(\mathcal{M}, \mathrm{End}(E))$ and $\boldsymbol{\beta}$ be its discretization defined in Equation 3.3.21. In this case we have*

$$R_{v_0,c_s} \int_s (d^{\nabla^{\mathrm{End}}} \beta)^{\nabla, c_s, c_s} R_{c_s, v_{\ell+1}} - \mathfrak{d}^{\nabla} \boldsymbol{\beta}(\sigma, w_0, w_{\ell+1}) = \mathcal{O}(h^{\ell+2}) \tag{E.0.1}$$

Proof. As in Section 3.3.2 we are going to denote in the following by σ_i the ℓ–subsimplex $\sigma_i = [v_0, \dots, \widehat{v_i}, \dots, v_{\ell+1}]$, where the i–th vertex is omitted. We denote by $s_i \subset \mathcal{M}$ the image of σ_i under the diffeomorphism. Further let $m_i \subset \mathcal{M}$ be the image of $(-1)^i \sigma_i$, i.e the subsimplex of σ without v_i with positive orientation.
If we consider the integral of the covariant exterior derivative in the center based parallel-propagated frame, we obtain

$$\begin{aligned}
&R_{v_0,c_s} \int_s (d^{\nabla^{\mathrm{End}}} \beta)^{\nabla, c_s, c_s} R_{c_s, v_{\ell+1}} = R_{v_0,c_s} \int_s \Big((d\beta)^{\nabla, c_s, c_s} + (\omega \wedge \beta)^{\nabla, c_s, c_s} + (-1)^{\deg(\beta)} \beta \wedge \omega \Big) R_{c_s, v_{\ell+1}} \\
&= R_{v_0,c_s} \int_s (d\beta)^{\nabla, c_s, c_s} R_{c_s, v_{\ell+1}} + \mathcal{O}(h^{\ell+3}) = \sum_{i=0}^{\ell+1} R_{v_0,c_s} \int_{m_i} R^{\nabla, c_s} \beta (R^{\nabla, c_s})^{-1} \, R_{c_s, v_{\ell+1}} + \mathcal{O}(h^{\ell+3}) \\
&= R_{v_0,c_s} \int_{m_0} R^{\nabla, c_s} \beta (R^{\nabla, c_s})^{-1} \, R_{c_s, v_{\ell+1}} + \sum_{i=1}^{\ell} R_{v_0,c_s} \int_{m_i} R^{\nabla, c_s} \beta (R^{\nabla, c_s})^{-1} \, R_{c_s, v_{\ell+1}} \\
&\quad + R_{v_0,c_s} \int_{m_{\ell+1}} R^{\nabla, c_s} \beta (R^{\nabla, c_s})^{-1} \, R_{c_s, v_{\ell+1}} + \mathcal{O}(h^{\ell+3})
\end{aligned}$$

If we consider the first term, we can analyze the difference

$$
\begin{aligned}
&R_{v_0,v_1}\beta(\sigma_i,v_1,v_{\ell+1}) - R_{v_0,c_s}\int_{m_0} R^{\nabla,c_s}\beta(R^{\nabla,c_s})^{-1}\,R_{c_s,v_{\ell+1}}\\
&= \int_{m_0} R^{\nabla,v_0}\beta R^{\nabla,v_{\ell+1}} - R_{v_0,c_s}\int_{m_0} R^{\nabla,c_s}\beta(R^{\nabla,c_s})^{-1}\,R_{c_s,v_{\ell+1}}\\
&= \int_{m_0}(R_{v_0,v_1}R^{\nabla,v_1} - R_{v_0,c_s}R^{\nabla,c_s})\beta(R^{\nabla,v_{\ell+1}})^{-1} + \int_{m_0}(R_{v_0,c_s}R^{\nabla,c_s})\beta\left(\left(R^{\nabla,v_{\ell+1}}\right)^{-1} - \left(R^{\nabla,c_s}\right)^{-1}R_{c_s,v_{\ell+1}}\right)
\end{aligned}
$$

We can now apply the argumentation presented in Theorem 3.41 and argue that

$$
\begin{aligned}
&R_{v_0,v_1}\beta(\sigma_0,v_1,v_{\ell+1}) - R_{v_0,c_s}\int_{m_0} R^{\nabla,c_s}\beta(R^{\nabla,c_s})^{-1}\,R_{c_s,v_{\ell+1}}\\
&= \underbrace{\Omega^{\nabla}_{v_0}(v_0-c_m,v_0-c_s)\beta_{c_{m_0}}[m_0]}_{\in\mathcal{O}(h^{\ell+2})}R_{c_{m_0},v_{\ell+1}} + R_{v_0,c_{m_0}}\underbrace{\Omega^{\nabla}_{c_{m_0}}(c_{m_0}-c_s,c_{m_0}-c_s)\beta_{c_{m_0}}[m_0]}_{\in\mathcal{O}(h^{\ell+2})}+\mathcal{O}(h^{\ell+3})\\
&= \mathcal{O}(h^{\ell+2}).
\end{aligned}
$$

We can argue in the same manner that we have for the last term that

$$
\begin{aligned}
&\beta(\sigma_{\ell+1},v_0,v_\ell)R_{v_\ell,v_{\ell+1}} - R_{v_0,c_s}\int_{m_{\ell+1}} R^{\nabla,c_s}\beta(R^{\nabla,c_s})^{-1}\,R_{c_s,v_{\ell+1}}\\
&= \underbrace{\Omega^{\nabla}_{v_0}(v_0-c_{m_{\ell+1}},v_0-c_s)\beta_{c_{m_{\ell+1}}}[m_{\ell+1}]}_{\in\mathcal{O}(h^{\ell+2})}R_{c_{m_{\ell+1}},c_s}R_{c_s,v_{\ell+1}}\\
&\quad + R_{v_0,c_{m_{\ell+1}}}\beta_{c_{m_{\ell+1}}}[m_{\ell+1}]\Omega^{\nabla}_{c_{m_{\ell+1}}}(c_{m_{\ell+1}}-v_{\ell+1},c_s-v_{\ell+1}) + \mathcal{O}(h^{\ell+3})\\
&= \mathcal{O}(h^{\ell+2}).
\end{aligned}
$$

For the terms in the middle we obtain

$$
\begin{aligned}
&\beta(\sigma_i,v_0,v_{\ell+1}) - R_{v_0,c_s}\int_{m_i} R^{\nabla,c_s}\beta(R^{\nabla,c_s})^{-1}\,R_{c_s,v_{\ell+1}}\\
&= \Omega^{\nabla}_{v_0}(v_0-c_s,v_0-c_{m_i})\beta_{c_{m_i}}R_{c_{m_i},v_{\ell+1}} - R_{v_0,c_s}R_{c_s,c_{m_i}}\beta_{c_{m_i}}[m_i]\Omega^{\nabla}_{c_{m_i}}(c_{m_i}-v_{\ell+1},c_{m_i}-c_s) + \mathcal{O}(h^{\ell+2}).
\end{aligned}
$$

Altogether we obtain

$$
R_{v_0,c_s}\int_s R^{\nabla,c_s}d^{\nabla^{\mathrm{End}}}\beta(R^{\nabla,c_s})^{-1}R_{c_s,v_{\ell+1}} = \mathfrak{d}^{\nabla}\beta(\sigma,v_0,v_{\ell+1}) + \mathcal{O}(h^{\ell+2})
$$

$\square$

Theorem E.2 (Alternation increases accuracy). *Let $\pi : E \to \mathcal{M}$ be a vector bundle with connection ∇. Let $s = [v_0, \ldots, v_{\ell+1}] \subset \mathcal{M}$ be a region in $\mathcal{M}$ for which there exists a diffeomorphism to a $(\ell+1)$-simplex σ where each point v_i is mapped to an associated vertex w_i of σ. Further let $\beta \in \Omega^\ell(\mathcal{M}, \mathrm{End}(E))$ and $\boldsymbol{\beta}$ be its discretization defined in Equation (3.3.21). In this case, we have*

$$R_{v_0,c_s} \int_s (d^\nabla \beta)^{(\nabla, c_s, c_s)} R_{c_s, v_{\ell+1}} = \mathrm{Alt}^\nabla \mathfrak{d}^\nabla \boldsymbol{\beta}(\sigma, v_0, v_{\ell+1}) + \mathcal{O}(h^{\ell+3}) = \boldsymbol{d}^\nabla \boldsymbol{\beta}(\sigma, v_0, v_{\ell+1}) + \mathcal{O}(h^{\ell+3}). \tag{E.0.2}$$

Proof. We follow the ideas of Theorem 3.43 and adapt them to the endomorphism-valued setting.

Recall that the discrete exterior covariant derivative is defined by

$$\begin{aligned}
&\boldsymbol{d}^\nabla \boldsymbol{\beta}([v_0, \ldots, v_{\ell+1}], v_0, v_{\ell+1}) \\
&= \frac{1}{(\ell+2)!} \sum_{\pi \in S_{\ell+2}} \Bigg(\frac{1+\mathrm{sgn}(\pi)}{2} \mathcal{R}_{v_0, v_{\pi(0)}} \mathfrak{d}^\nabla \boldsymbol{\beta}(\pi(\sigma), v_{\pi(0)}, v_{\pi(\ell+1)}) \mathcal{R}_{v_{\pi(\ell+1)}, v_{\ell+1}} \\
&\qquad + \frac{\mathrm{sgn}(\pi)-1}{2} \mathcal{R}_{v_0, v_{\pi(0)}} \mathfrak{d}^\nabla \boldsymbol{\beta}(\pi(\sigma), v_{\pi(0)}, v_{\pi(\ell+1)}) \mathcal{R}_{v_{\pi(\ell+1)}, v_{\pi(\ell)}} \mathcal{R}_{v_{\pi(\ell)}, v_{\ell+1}} \Bigg).
\end{aligned}$$

The additional transport in the second term is required to preserve the discrete Bianchi identity exactly. For the convergence analysis, however, we compare this expression with the simpler alternation

$$\frac{1}{(\ell+2)!} \sum_{\pi \in S_{\ell+2}} \mathcal{R}_{v_0, v_{\pi(0)}} \mathfrak{d}^\nabla \boldsymbol{\beta}(\pi(\sigma), v_{\pi(0)}, v_{\pi(\ell+1)}) \mathcal{R}_{v_{\pi(\ell+1)}, v_{\ell+1}}.$$

Their difference is

$$\frac{1}{(\ell+2)!} \sum_{\pi \in S_{\ell+2}} \frac{\mathrm{sgn}(\pi)-1}{2} \mathcal{R}_{v_0, v_{\pi(0)}} \underbrace{\mathfrak{d}^\nabla \boldsymbol{\beta}(\pi(\sigma), v_{\pi(0)}, v_{\pi(\ell)})}_{\mathcal{O}(h^{\ell+1})} \underbrace{\left(\mathcal{R}_{v_{\pi(\ell)}, v_{\pi(\ell-1)}} \mathcal{R}_{v_{\pi(\ell-1)}, v_{\ell+1}} - \mathcal{R}_{v_{\pi(\ell+1)}, v_{\ell+1}} \right)}_{\mathcal{O}(h^2)}.$$

Since the discrete derivative is of order $\mathcal{O}(h^{\ell+1})$ and the curvature term that arises as mismatch of transports is $\mathcal{O}(h^2)$, the total difference is $\mathcal{O}(h^{\ell+3})$.

Hence for the accuracy estimate it suffices to analyze the simplified alternation.

Explicit decoupling of the permutation sum.

We now decompose the alternation over the full permutation group by fixing the first and last vertex.

As in Theorem 3.43, we write

$$
\begin{aligned}
&\boldsymbol{d}^{\nabla}\beta(\sigma, v_0, v_{\ell+1}) = \mathrm{Alt}^{\nabla}\mathfrak{d}^{\nabla}\beta(\sigma, v_0, v_{\ell+1}) \\
&= \frac{1}{\ell+2}\frac{1}{\ell+1}\frac{1}{\ell}\frac{1}{\ell-1}\sum_j\sum_{k\neq j} R_{v_0,v_j}\left(\sum_{m\neq j,k}\sum_{n\neq j,k,m}\frac{1}{(\ell-2)!}\sum_{\substack{\pi\in S_{\ell+2}\\ \pi(0)=j,\\ \pi(1)=m,\\ \pi(\ell+1)=k,\\ \pi(\ell)=n}} \mathrm{sgn}(\pi)\mathfrak{d}^{\nabla}\beta(\pi(\sigma), v_j, v_k)\right) R_{v_k,v_{\ell+1}}.
\end{aligned}
\tag{E.0.3}
$$

For a fixed permutation π, denote by $\pi(\sigma)^i$ the simplex obtained by omitting the i-th vertex in the permuted ordering. Then

$$
\begin{aligned}
\mathfrak{d}^{\nabla}\beta(\pi(\sigma), v_j, v_k) &= R_{v_j,v_m}\beta(\pi(\sigma)^0, v_m, v_k) \\
&\quad + \sum_{i=1}^{\ell}(-1)^i\beta(\pi(\sigma)^i, v_j, v_k) \\
&\quad + (-1)^{\ell+1}\beta(\pi(\sigma)^{\ell+1}, v_j, v_n)R_{v_n,v_k}.
\end{aligned}
$$

Substituting the discretization (cf. Equation (3.3.21)) yields

$$
\begin{aligned}
\mathfrak{d}^{\nabla}\beta(\pi(\sigma), v_j, v_k) &= R_{v_j,v_m}\int_{m_j} R^{\nabla,v_m}\beta(R^{\nabla,v_k})^{-1} \\
&\quad + \ldots + \int_{m_{\ell+1}} R^{\nabla,v_j}\beta(R^{\nabla,v_n})^{-1}R_{v_n,v_k}.
\end{aligned}
$$

Crucially, after this substitution the expression no longer depends on the particular permutation π, but only on the indices j,k. Therefore the inner permutation sum in Equation (E.0.3) reduces to a purely combinatorial factor.

Therefore it holds

$$
\begin{aligned}
&\boldsymbol{d}^{\nabla}\beta(\sigma, v_0, v_{\ell+1}) = \mathrm{Alt}^{\nabla}\mathfrak{d}^{\nabla}\beta(\sigma, v_0, v_{\ell+1}) \\
&= \frac{1}{\ell+2}\frac{1}{\ell+1}\frac{1}{\ell}\frac{1}{\ell-1}\sum_j\sum_{k\neq j} R_{v_0,v_j}\Bigg(\\
&\left.\underbrace{\sum_{m\neq j,k}\sum_{n\neq j,k,m} R_{v_j,v_m}\int_{m_j} R^{\nabla,v_m}\beta(R^{\nabla,v_k})^{-1} + \ldots + \int_{m_{\ell+1}} R^{\nabla,v_j}\beta(R^{\nabla,v_n})^{-1}R_{v_n,v_k}}_{*}\right) R_{v_k,v_{\ell+1}} + \mathcal{O}(h^{\ell+3}).
\end{aligned}
\tag{E.0.4}
$$

The integral of the continuous exterior covariant derivative amounts to

$$R_{v_0,c_s}\int_s (d^{\nabla^{\mathrm{End}}}\beta)^{\nabla,c_s,c_s} R_{c_s,v_{\ell+1}} = \sum_{i=0}^{\ell+1} R_{v_0,c_s}\int_{m_i} R^{\nabla,c_s}\beta(R^{\nabla,c_s})^{-1}\, R_{c_s,v_{\ell+1}} + \mathcal{O}(h^{\ell+3})$$

As in the proof of Theorem 3.43, for a vertex v_i we will analyze all contributions for the face opposite to v_i of the continuous integral and the discrete expression. We will denote this face (or more precisely the image of the face in $\mathcal{M}$ under the diffeomeorphism) as m_i.

We will now analyze the contributions to the error in Equation E.0.2 stemming from $(*)$ in Equation E.0.4 that come from integration over m_i.

Case $i \neq j,k$:

In this case the contributions in $(*)$ are of the form

$$\int_{m_i} R^{\nabla,v_j}\beta(R^{\nabla,v_k})^{-1}.$$

Therefore the contributions to the error in Equation E.0.2 are of the form

$$\begin{aligned}
&\frac{1}{\ell+2}\frac{1}{\ell+1}\sum_{j=0}^{\ell+1}\sum_{k\neq j}\left(R_{v_0,v_j}\int_{m_i} R^{\nabla,v_j}\beta(R^{\nabla,v_k})^{-1}R_{v_k,v_{\ell+1}} - R_{v_0,c_s}\int_{m_i} R^{\nabla,c_s}\beta(R^{\nabla,c_s})^{-1}R_{c_s,v_{\ell+1}}\right)\\
&= \frac{1}{\ell+2}\frac{1}{\ell+1}\sum_{j=0}^{\ell+1}\sum_{k\neq j}\left(R_{v_0,v_j}\int_{m_i} R^{\nabla,v_j}\beta(R^{\nabla,v_k})^{-1}R_{v_k,v_{\ell+1}} - R_{v_0,c_s}\int_{m_i} R^{\nabla,c_s}\beta(R^{\nabla,c_s})^{-1}R_{c_s,v_{\ell+1}}\right)\\
&= \frac{1}{\ell+2}\frac{1}{\ell+1}\sum_{j=0}^{\ell+1}\sum_{k\neq j}\left(R_{v_0,v_j}\int_{m_i} R^{\nabla,v_j}\beta(R^{\nabla,v_k})^{-1}R_{v_k,v_{\ell+1}} - R_{v_0,c_s}R^{\nabla,c_s}\beta(R^{\nabla,c_s})^{-1}R_{c_s,v_{\ell+1}}\right)\\
&= \frac{1}{\ell+2}\frac{1}{\ell+1}\sum_{j=0}^{\ell+1}\sum_{k\neq j}\left(\int_{m_i}(R_{v_0,v_j}R^{\nabla,v_j} - R_{v_0,c_s}R^{\nabla,c_s})\beta(R^{\nabla,c_s})^{-1}R_{c_s,v_{\ell+1}}\right)\\
&\quad+\frac{1}{\ell+2}\frac{1}{\ell+1}\sum_{j=0}^{\ell+1}\sum_{k\neq j}\left(\int_{m_i}(R_{v_0,v_j}R^{\nabla,v_j})\beta\left((R^{\nabla,v_k})^{-1}R_{v_k,v_{\ell+1}} - (R^{\nabla,c_s})^{-1}R_{c_s,v_{\ell+1}}\right)\right)\\
&= \underbrace{\frac{1}{\ell+2}\sum_{j=0}^{\ell+1}\left(\int_{m_i}(R_{v_0,v_j}R^{\nabla,v_j} - R_{v_0,c_s}R^{\nabla,c_s})\beta(R^{\nabla,c_s})^{-1}R_{c_s,v_{\ell+1}}\right)}_{(1)}\\
&\quad\underbrace{+\frac{1}{\ell+2}\frac{1}{\ell+1}\sum_{j=0}^{\ell+1}\sum_{k\neq j}\int_{m_i}R_{v_0,v_j}R^{\nabla,v_j}\beta\left((R^{\nabla,v_k})^{-1}R_{v_k,v_{\ell+1}} - (R^{\nabla,c_s})^{-1}R_{c_s,v_{\ell+1}}\right)}_{(2)}
\end{aligned}$$

To simplify (1), we follow the argumentation of the proof of Theorem 3.41 and can deduce,

$$
\begin{aligned}
&\frac{1}{\ell+2}\sum_{j=0}^{\ell+1}\left(\int_{m_i}(R_{v_0,v_j}R^{\nabla,v_j}-R_{v_0,c_s}R^{\nabla,c_s})\beta(R^{\nabla,c_s})^{-1}R_{c_s,v_{\ell+1}}\right)\\
&=\frac{1}{\ell+2}\sum_{j=0}^{\ell+1}\left(\int_{m_i}((R_{v_0,v_j}R^{\nabla,v_j}-R^{\nabla,v_0})-(R_{v_0,c_s}R^{\nabla,c_s}-R^{\nabla,v_0}))\beta(R^{\nabla,c_s})^{-1}R_{c_s,v_{\ell+1}}\right)\\
&=\frac{1}{\ell+2}\sum_{j=0}^{\ell+1}\Big(((R_{v_0,v_j}R_{v_j,c_{m_i}}-R_{v_0,c_{m_i}})-(R_{v_0,c_s}R_{c_s,c_{m_i}}-R_{v_0,c_{m_i}}))\beta_{c_{m_i}}[m_i]R_{c_{m_i},c_s}R_{c_s,v_{\ell+1}}\Big)+\mathcal{O}(h^{\ell+3})\\
&=\frac{1}{\ell+2}\sum_{j=0}^{\ell+1}\Big((\Omega^{\nabla}_{v_0}(v_j-v_0,c_{m_i}-v_0)-\Omega^{\nabla}_{v_0}(c_s-v_0,c_{m_i-v_0}))\beta_{c_{m_i}}[m_i]R_{c_{m_i},c_s}R_{c_s,v_{\ell+1}}\Big)+\mathcal{O}(h^{\ell+3})\\
&=\frac{1}{\ell+2}\sum_{j=0}^{\ell+1}\Big(\Omega^{\nabla}_{v_0}(v_j-c_s,c_{m_i}-v_0)\beta_{c_{m_i}}[m_i]R_{c_{m_i},c_s}R_{c_s,v_{\ell+1}}\Big)+\mathcal{O}(h^{\ell+3})\\
&=\Omega^{\nabla}_{v_0}\left(\frac{1}{\ell+2}\sum_{j=0}^{\ell+1}v_j-c_s,c_{m_i}-v_0\right)\beta_{c_{m_i}}[m_i]R_{c_{m_i},c_s}R_{c_s,v_{\ell+1}}+\mathcal{O}(h^{\ell+3})\\
&=\Omega^{\nabla}_{v_0}\Big(c_s-c_s,c_{m_i}-v_0\Big)\beta_{c_{m_i}}[m_i]R_{c_{m_i},c_s}R_{c_s,v_{\ell+1}}+\mathcal{O}(h^{\ell+3})\\
&=\mathcal{O}(h^{\ell+3})
\end{aligned}
$$

Furthermore, we can simplify (2) to

$$
\begin{aligned}
&\frac{1}{\ell+2}\frac{1}{\ell+1}\sum_{j=0}^{\ell+1}\sum_{k\neq j}\int_{m_i}R_{v_0,v_j}R^{\nabla,v_j}\beta\Big((R^{\nabla,v_k})^{-1}R_{v_k,v_{\ell+1}}-(R^{\nabla,c_s})^{-1}R_{c_s,v_{\ell+1}})\Big)\\
&=\frac{1}{\ell+2}\frac{1}{\ell+1}\sum_{j=0}^{\ell+1}\sum_{k\neq j}\int_{m_i}(R_{v_0,v_j}R^{\nabla,v_j}-R^{\nabla,v_0})\beta\Big((R^{\nabla,v_k})^{-1}R_{v_k,v_{\ell+1}}-(R^{\nabla,c_s})^{-1}R_{c_s,v_{\ell+1}})\Big)\\
&\quad+\frac{1}{\ell+2}\frac{1}{\ell+1}\sum_{j=0}^{\ell+1}\sum_{k\neq j}\int_{m_i}R^{\nabla,v_0}\beta\Big((R^{\nabla,v_k})^{-1}R_{v_k,v_{\ell+1}}-(R^{\nabla,c_s})^{-1}R_{c_s,v_{\ell+1}})\Big)\\
&=\frac{1}{\ell+2}\frac{1}{\ell+1}\sum_{j=0}^{\ell+1}\sum_{k\neq j}\underbrace{(R_{v_0,v_j}R_{v_j,c_{m_i}}-R_{v_0,c_{m_i}})}_{\in\mathcal{O}(h^2)}\underbrace{\beta_{c_{m_i}}[m_i]}_{\in\mathcal{O}(h^\ell)}\underbrace{\Big(R_{c_{m_i},v_k}R_{v_k,v_{\ell+1}}-R_{c_{m_i},c_s}R_{c_s,v_{\ell+1}})\Big)}_{\in\mathcal{O}(h^2)}\\
&\quad+\frac{1}{\ell+2}\frac{1}{\ell+1}\sum_{j=0}^{\ell+1}\sum_{k\neq j}R^{v_0,c_{m_i}}\beta_{c_{m_i}}[m_i]\Big(R_{c_{m_i},v_k}R_{v_k,v_{\ell+1}}-R_{c_{m_i},c_s}R_{c_s,v_{\ell+1}})\Big)+\mathcal{O}(h^{\ell+3})\\
&=\frac{1}{\ell+2}\frac{1}{\ell+1}\sum_{j=0}^{\ell+1}\sum_{k\neq j}R_{v_0,c_{m_i}}\beta_{c_{m_i}}[m_i]\Big(R_{c_{m_i},v_k}R_{v_k,v_{\ell+1}}-R_{c_{m_i},v_{\ell+1}}-(R_{c_{m_i},c_s}R_{c_s,v_{\ell+1}}-R_{c_{m_i},v_{\ell+1}})\Big)+\mathcal{O}(h^{\ell+3})
\end{aligned}
$$

$$
\begin{aligned}
&= \frac{1}{\ell+2}\frac{1}{\ell+1}\sum_{j=0}^{\ell+1}\sum_{k\neq j} R_{v_0,c_{m_i}}\beta_{c_{m_i}}[m_i]\Big(\Omega^{\nabla}_{c_{m_i}}(v_k - c_{m_i}, v_{\ell+1}-c_{m_i}) \\
&\qquad\qquad - \Omega^{\nabla}_{c_{m_i}}(c_s - c_{m_i}, v_{\ell+1}-c_{m_i})\Big) + \mathcal{O}(h^{\ell+3}) \\
&= \frac{1}{\ell+2}\sum_{j=0}^{\ell+1} R_{v_0,c_{m_i}}\beta_{c_{m_i}}[m_i]\left(\Omega^{\nabla}_{c_{m_i}}\left(\frac{1}{\ell+1}\sum_{k\neq j} v_k - c_s, v_{\ell+1}-c_{m_i}\right)\right) + \mathcal{O}(h^{\ell+3}) \\
&= \frac{1}{\ell+2}\sum_{j=0}^{\ell+1} R_{v_0,c_{m_i}}\beta_{c_{m_i}}[m_i]\Big(\Omega^{\nabla}_{c_{m_i}}\big(c_{m_j} - c_s, v_{\ell+1}-c_{m_i}\big)\Big) + \mathcal{O}(h^{\ell+3}) \\
&= R_{v_0,c_{m_i}}\beta_{c_{m_i}}[m_i]\left(\Omega^{\nabla}_{c_{m_i}}\left(\frac{1}{\ell+2}\sum_{j=0}^{\ell+1} c_{m_j} - c_s, v_{\ell+1}-c_{m_i}\right)\right) + \mathcal{O}(h^{\ell+3}) \\
&= R_{v_0,c_{m_i}}\beta_{c_{m_i}}[m_i]\Big(\Omega^{\nabla}_{c_{m_i}}\big(c_s - c_s, v_{\ell+1}-c_{m_i}\big)\Big) + \mathcal{O}(h^{\ell+3}) \\
&= \mathcal{O}(h^{\ell+3}),
\end{aligned}
$$

where the last equality is due to the fact that in a simplicial $(\ell+1)$cell, if we take the average of all centers of all faces, we obtain the center of the cell itself.
Next we analyze the contributions to the error in Equation E.0.2 stemming from $(*)$ in Equation E.0.4 that come from integration over m_i for the case that $i = j$.
In this case the contributions coming from the face m_i are of the form

$$
\frac{1}{\ell+2}\frac{1}{\ell+1}\sum_{j}\sum_{k\neq j} R_{v_0,v_j}\left(\frac{1}{\ell}\sum_{m\neq j,k} R_{v_j,v_m}\int_{m_i} R^{\nabla,v_m}\beta(R^{\nabla,v_k})^{-1}\right) R_{v_k,v_{\ell+1}}
$$

We denote in the following $\tilde{\ell} := (\ell+2)(\ell+1)\ell$. The contributions to the error turn into

$$
\begin{aligned}
&\frac{1}{\tilde{\ell}}\sum_{j}\sum_{k\neq j}\sum_{m\neq j,k}\left(R_{v_0,v_j}R_{v_j,v_m}\int_{m_i} R^{\nabla,v_m}\beta(R^{\nabla,v_k})^{-1}R_{v_k,v_{\ell+1}} - R_{v_0,c_s}\int_{m_i} R^{\nabla,c_s}\beta(R^{\nabla,c_s})^{-1}R_{c_s,v_{\ell+1}}\right) \\
=\quad &\frac{1}{\tilde{\ell}}\sum_{j}\sum_{k\neq j}\sum_{m\neq j,k}\left(R_{v_0,v_j}R_{v_j,v_m}\int_{m_i} R^{\nabla,v_m}\beta(R^{\nabla,v_k})^{-1}R_{v_k,v_{\ell+1}} - R_{v_0,c_s}R^{\nabla,c_s}\beta(R^{\nabla,c_s})^{-1}R_{c_s,v_{\ell+1}}\right)
\end{aligned}
$$

$$
\begin{aligned}
&= \frac{1}{\tilde{\ell}} \sum_j \sum_{k\neq j} \sum_{m\neq j,k} \left(\int_{m_i} (R_{v_0,v_j} R_{v_j,v_m} R^{\nabla,v_m} - R_{v_0,c_s} R^{\nabla,c_s}) \beta (R^{\nabla,c_s})^{-1} R_{c_s,v_{\ell+1}} \right) \\
&\quad + \frac{1}{\tilde{\ell}} \sum_j \sum_{k\neq j} \sum_{m\neq j,k} \left(\int_{m_i} (R_{v_0,v_j} R_{v_j,v_m} R^{\nabla,v_m}) \beta ((R^{\nabla,v_k})^{-1} R_{v_k,v_{\ell+1}} - (R^{\nabla,c_s})^{-1} R_{c_s,v_{\ell+1}}) \right) \\
&= \frac{1}{\tilde{\ell}} \sum_j \sum_{k\neq j} \sum_{m\neq j,k} \left(\int_{m_i} (R_{v_0,v_j} R_{v_j,v_m} R^{\nabla,v_m} - R_{v_0,v_j} R^{\nabla,v_j}) \beta (R^{\nabla,c_s})^{-1} R_{c_s,v_{\ell+1}} \right) \\
&\quad - \frac{1}{\tilde{\ell}} \sum_j \sum_{k\neq j} \sum_{m\neq j,k} \left(\int_{m_i} (R_{v_0,c_s} R^{\nabla,c_s} - R_{v_0,v_j} R^{\nabla,v_j}) \beta (R^{\nabla,c_s})^{-1} R_{c_s,v_{\ell+1}} \right) \\
&\quad + \frac{1}{\tilde{\ell}} \sum_j \sum_{k\neq j} \sum_{m\neq j,k} \left(\int_{m_i} (R_{v_0,v_j} R_{v_j,v_m} R^{\nabla,v_m}) \beta ((R^{\nabla,v_k})^{-1} R_{v_k,v_{\ell+1}} - (R^{\nabla,c_s})^{-1} R_{c_s,v_{\ell+1}}) \right)
\end{aligned}
$$

If we use again the midpoint development, we obtain

$$
\begin{aligned}
&\frac{1}{\tilde{\ell}} \sum_j \sum_{k\neq j} \sum_{m\neq j,k} \left(R_{v_0,v_j} R_{v_j,v_m} \int_{m_i} R^{\nabla,v_m} \beta (R^{\nabla,v_k})^{-1} R_{v_k,v_{\ell+1}} - R_{v_0,c_s} R^{\nabla,c_s} \beta (R^{\nabla,c_s})^{-1} R_{c_s,v_{\ell+1}} \right) \\
&= \frac{1}{\tilde{\ell}} \sum_j \sum_{k\neq j} \sum_{m\neq j,k} \left((R_{v_0,v_j} R_{v_j,v_m} R_{v_m,c_{m_i}} - R_{v_0,v_j} R_{v_j,c_{m_i}}) \beta_{c_{m_i}} [m_i] R_{c_{m_i},c_s} R_{c_s,v_{\ell+1}} \right) \qquad \text{(E.0.5)} \\
&\quad - \frac{1}{\tilde{\ell}} \sum_j \sum_{k\neq j} \sum_{m\neq j,k} \left((R_{v_0,c_s} R_{c_s,c_{m_i}} - R_{v_0,v_j} R_{v_j,c_{m_i}}) \beta_{c_{m_i}} [m_i] R_{c_{m_i},c_s} R_{c_s,v_{\ell+1}} \right) \qquad \text{(E.0.6)} \\
&\quad + \frac{1}{\tilde{\ell}} \sum_j \sum_{k\neq j} \sum_{m\neq j,k} \left((R_{v_0,v_j} R_{v_j,v_m} R_{v_m,c_{m_i}}) \beta_{c_{m_i}} [m_i] (R_{c_{m_i},v_k} R_{v_k,v_{\ell+1}} - R_{c_{m_i},c_s} R_{c_s,v_{\ell+1}}) \right) + \mathcal{O}(h^{\ell+3}) \\
&\qquad \text{(E.0.7)}
\end{aligned}
$$

Let us analyze the first term E.0.5. First, notice that

$$
\begin{aligned}
&\frac{1}{\tilde{\ell}} \sum_j \sum_{k\neq j} \sum_{m\neq j,k} \left((R_{v_0,v_j} R_{v_j,v_m} R_{v_m,c_{m_i}} - R_{v_0,v_j} R_{v_j,c_{m_i}}) \beta_{c_{m_i}} [m_i] (R_{c_{m_i},c_s} R_{c_s,v_{\ell+1}} \right) \\
&= \frac{1}{\tilde{\ell}} \sum_j \sum_{k\neq j} \sum_{m\neq j,k} \left(\underbrace{(R_{v_0,v_j} R_{v_j,v_m} R_{v_m,c_{m_i}} - R_{v_0,v_j} R_{v_j,c_{m_i}})}_{\in \mathcal{O}(h^2)} \underbrace{\beta_{c_{m_i}} [m_i]}_{\in \mathcal{O}(h^\ell)} \underbrace{(R_{c_{m_i},c_s} R_{c_s,v_{\ell+1}} - R_{c_{m_i},v_{\ell+1}})}_{\in \mathcal{O}(h^2)} \right) \\
&\quad + \frac{1}{\tilde{\ell}} \sum_j \sum_{k\neq j} \sum_{m\neq j,k} \left((R_{v_0,v_j} R_{v_j,v_m} R_{v_m,c_{m_i}} - R_{v_0,v_j} R_{v_j,c_{m_i}}) \beta_{c_{m_i}} [m_i] (R_{c_{m_i},v_{\ell+1}}) \right) \\
&= \frac{1}{\tilde{\ell}} \sum_j \sum_{k\neq j} \sum_{m\neq j,k} \left((R_{v_0,v_j} R_{v_j,v_m} R_{v_m,c_{m_i}} - R_{v_0,v_j} R_{v_j,c_{m_i}}) \beta_{c_{m_i}} [m_i] (R_{c_{m_i},v_{\ell+1}}) \right) + \mathcal{O}(h^{\ell+3})
\end{aligned}
$$

We are going to use this kind of simplification in the following repeatedly. Since we are in the case of $i = j$, the first term turns into

$$\begin{aligned}
&\frac{1}{\tilde{\ell}}\sum_{j} R_{v_0,v_j}\sum_{k\neq j}\sum_{m\neq j,k}\Big((R_{v_j,v_m}R_{v_m,c_{m_i}} - R_{v_j,c_{m_i}})\beta_{c_{m_i}}[m_i](R_{c_{m_i},v_{\ell+1}})\Big)\\
&= \frac{1}{\tilde{\ell}}\sum_{j}\sum_{k\neq j}\sum_{m\neq j,k}\Big(\Omega^{\nabla}_{v_j}(v_m - v_j, c_{m_i} - v_j)\beta_{c_{m_i}}[m_i](R_{c_{m_i},v_{\ell+1}})\Big) + \mathcal{O}(h^{\ell+3})\\
&= \frac{1}{\ell+2}\sum_{j}\left(\Omega^{\nabla}_{v_j}\left(\frac{1}{\ell+1}\frac{1}{\ell}\sum_{k\neq j}\sum_{m\neq jk} v_m - v_j, c_{m_i} - v_j\right)\right) + \mathcal{O}(h^{\ell+3})\\
&= \frac{1}{\ell+2}\sum_{j}\Omega^{\nabla}_{v_j}(c_{m_i} - v_j, c_{m_i} - v_j) + \mathcal{O}(h^{\ell+3}) = \mathcal{O}(h^{\ell+3})
\end{aligned}$$

If we analyze the contributions coming from the second term E.0.6, we obtain

$$\begin{aligned}
&\frac{1}{\tilde{\ell}}\sum_{j}\sum_{k\neq j}\sum_{m\neq j,k}\Big((R_{v_0,c_s}R_{c_s,c_{m_i}} - R_{v_0,v_j}R_{v_j,c_{m_i}})\beta_{c_{m_i}}[m_i]R_{c_{m_i},c_s}R_{c_s,v_{\ell+1}}\Big)\\
&= \frac{1}{\ell+2}\sum_{j}\Big((R_{v_0,c_s}R_{c_s,c_{m_i}} - R_{v_0,v_j}R_{v_j,c_{m_i}})\beta_{c_{m_i}}[m_i]R_{c_{m_i},c_s}R_{c_s,v_{\ell+1}}\Big)\\
&= \frac{1}{\ell+2}\sum_{j}\Big(R_{v_0,c_s}R_{c_s,c_{m_i}} - R_{v_0,c_{m_i}} - (R_{v_0,v_j}R_{v_j,c_{m_i}} - R_{v_0,c_{m_i}})\Big)\beta_{c_{m_i}}[m_i]R_{c_{m_i},c_s}R_{c_s,v_{\ell+1}}\\
&= \frac{1}{\ell+2}\sum_{j}\Big(\Omega^{\nabla}_{v_0}(c_s - v_0, c_{m_i} - v_0) - \Omega^{\nabla}_{v_0}(v_j - v_0, c_{m_i} - v_0)\Big)\beta_{c_{m_i}}[m_i]R_{c_{m_i},c_s}R_{c_s,v_{\ell+1}} + \mathcal{O}(h^{\ell+3})\\
&= \frac{1}{\ell+2}\sum_{j}\Big(\Omega^{\nabla}_{v_0}(c_s - v_j, c_{m_i} - v_0)\Big)\beta_{c_{m_i}}[m_i]R_{c_{m_i},c_s}R_{c_s,v_{\ell+1}} + \mathcal{O}(h^{\ell+3})\\
&= \Omega^{\nabla}_{v_0}\left(c_s - \underbrace{\frac{1}{\ell+2}\sum_{j} v_j}_{=c_s}, c_{m_i} - v_0\right)\beta_{c_{m_i}}[m_i]R_{c_{m_i},c_s}R_{c_s,v_{\ell+1}} + \mathcal{O}(h^{\ell+3})\\
&= \mathcal{O}(h^{\ell+3})
\end{aligned}$$

For the third term E.0.7, note that in a first step we can again reduce the sum to an average in the right multiplication argument. We obtain

$$\begin{aligned}
&\frac{1}{\tilde{\ell}}\sum_{j}\sum_{k\neq j}\sum_{m\neq j,k}\Big((R_{v_0,v_j}R_{v_j,v_m}R_{v_m,c_{m_i}})\beta_{c_{m_i}}[m_i](R_{c_{m_i},v_k}R_{v_k,v_{\ell+1}} - R_{c_{m_i},c_s}R_{c_s,v_{\ell+1}})\Big)\\
&= \frac{1}{\tilde{\ell}}\sum_{j}\sum_{k\neq j}\sum_{m\neq j,k}\Big((R_{v_0,v_j}R_{v_j,v_m}R_{v_m,c_{m_i}} - R_{v_0,c_{m_i}})\beta_{c_{m_i}}[m_i](R_{c_{m_i},v_k}R_{v_k,v_{\ell+1}} - R_{c_{m_i},c_s}R_{c_s,v_{\ell+1}})\Big)\\
&\quad + \frac{1}{\tilde{\ell}}\sum_{j}\sum_{k\neq j}\sum_{m\neq j,k}\Big(R_{v_0,c_{m_i}}\beta_{c_{m_i}}[m_i](R_{c_{m_i},v_k}R_{v_k,v_{\ell+1}} - R_{c_{m_i},c_s}R_{c_s,v_{\ell+1}})\Big)
\end{aligned}$$

Again, we observe that the first term is of order $\mathcal{O}(h^{\ell+4})$. The second term can be simplified to

$$
\begin{aligned}
&\frac{1}{\tilde{\ell}}\sum_{j}\sum_{k\neq j}\sum_{m\neq j,k}\Big((R_{v_0,v_j}R_{v_j,v_m}R_{v_m,c_{m_i}})\beta_{c_{m_i}}[m_i](R_{c_{m_i},v_k}R_{v_k,v_{\ell+1}}-R_{c_{m_i},c_s}R_{c_s,v_{\ell+1}})\Big)\\
&=\frac{1}{\tilde{\ell}}\sum_{j}\sum_{k\neq j}\sum_{m\neq j,k}\Big(R_{v_0,c_{m_i}}\beta_{c_{m_i}}[m_i](R_{c_{m_i},v_k}R_{v_k,v_{\ell+1}}-R_{c_{m_i},c_s}R_{c_s,v_{\ell+1}})\Big)+\mathcal{O}(h^{\ell+3})\\
&=\frac{1}{\tilde{\ell}}\sum_{j}\sum_{k\neq j}\sum_{m\neq j,k}\Big(R_{v_0,c_{m_i}}\beta_{c_{m_i}}[m_i](R_{c_{m_i},v_k}R_{v_k,v_{\ell+1}}-R_{c_{m_i},v_{\ell+1}}-(R_{c_{m_i},c_s}R_{c_s,v_{\ell+1}}-R_{c_{m_i},v_{\ell+1}}))\Big)+\mathcal{O}(h^{\ell+3})\\
&=\frac{1}{\tilde{\ell}}\sum_{j}\sum_{k\neq j}\sum_{m\neq j,k}\Big(R_{v_0,c_{m_i}}\beta_{c_{m_i}}[m_i](\Omega^{\nabla}_{c_{m_i}}(v_k-c_{m_i},v_{\ell+1}-c_{m_i})-\Omega^{\nabla}_{c_{m_i}}(c_s-c_{m_i},v_{\ell+1}-c_{m_i}))\Big)+\mathcal{O}(h^{\ell+3})\\
&=\frac{1}{(\ell+2)(\ell+1)}\sum_{j}\sum_{k\neq j}\Big(R_{v_0,c_{m_i}}\beta_{c_{m_i}}[m_i](\Omega^{\nabla}_{c_{m_i}}(v_k-c_s,v_{\ell+1}-c_{m_i})))\Big)+\mathcal{O}(h^{\ell+3})\\
&=\frac{1}{(\ell+2)}\sum_{j}\left(R_{v_0,c_{m_i}}\beta_{c_{m_i}}[m_i]\left(\Omega^{\nabla}_{c_{m_i}}\left(\frac{1}{\ell+1}\sum_{k\neq j}v_k-c_s,v_{\ell+1}-c_{m_i}\right)\right)\right)+\mathcal{O}(h^{\ell+3})\\
&=\frac{1}{(\ell+2)}\sum_{j}\Big(R_{v_0,c_{m_i}}\beta_{c_{m_i}}[m_i]\big(\Omega^{\nabla}_{c_{m_i}}\left(c_{m_j}-c_s,v_{\ell+1}-c_{m_i}\right)\big)\Big)+\mathcal{O}(h^{\ell+3})
\end{aligned}
$$

Again, using the argument that the average of all centers of all codimension 1 faces of a simplex is the center of the simplex itself, we obtain that the last term is also of order $\mathcal{O}(h^{\ell+3})$. The third case of $i=k$ can be analyzed in the same way and also yields an error of $\mathcal{O}(h^{\ell+3})$.

Combining all cases, we conclude that the total error is $\mathcal{O}(h^{\ell+3})$. $\square$

Theorem E.3 (Convergence of $\boldsymbol{d}^{\nabla}\boldsymbol{d}^{\nabla}$)**.** *Let $\pi : E \to \mathcal{M}$ be a vector bundle with connection ∇. Let $s=[v_0,\dots,v_{\ell+2}]\subset\mathcal{M}$ be a region in $\mathcal{M}$ for which there exists a diffeomorphism to a ℓ–simplex σ where each point v_i are mapped to an associated vertex w_i of σ. Further, let $\beta\in\Omega^{\ell}(M,\mathrm{End}(E))$ and $\boldsymbol{\beta}$ be its discretization defined in Equation (3.2.8). We have*

$$
\boldsymbol{d}^{\nabla}\boldsymbol{d}^{\nabla}\boldsymbol{\beta}(\sigma,v_0,v_{\ell+1})=R_{v_0,c_s}\int_s(d^{\nabla}d^{\nabla}\beta)^{\nabla,c_s,c_s}R_{c_s,v_{\ell+2}}+\mathcal{O}(h^{\ell+3}). \tag{E.0.8}
$$

Proof. We begin by using the peoperties of the center based PPF. As in the previous proof, we denote by m_i the codimension 1-cell opposite to the vertex v_i. We rewrite the right hand side as

$$
\begin{aligned}
&R_{v_0,c_s}\int_s(d^{\nabla}d^{\nabla}\beta)^{\nabla,c_s,c_s}R_{c_s,v_{\ell+2}}=R_{v_0,c_s}\int_{\partial s}(d^{\nabla}\beta)^{\nabla,c_s,c_s}R_{c_s,v_{\ell+2}}+\mathcal{O}(h^{\ell+4})\\
&=\sum_{i=0}^{\ell+2}R_{v_0,c_s}\int_{m_i}(d^{\nabla}\beta)^{\nabla,c_s,c_s}R_{c_s,v_{\ell+2}}+\mathcal{O}(h^{\ell+4})
\end{aligned}
$$

Now, for a face m_i note that the integral of $d^\nabla\beta$ taken in a center of s based PPF or in a center of m_i based PPF only differ by an error of order $\mathcal{O}(h^{\ell+3})$. To see that this is the case note that

$$\begin{aligned}
&\int_{m_i} R_{v_0,c_s} R^{\nabla,c_s}(d^\nabla\beta)\left(R^{\nabla,c_s}\right)^{-1} R_{c_s,v_{\ell+2}} - \int_{m_i} R_{v_0,c_s} R^{\nabla,c_s} \underbrace{(d^\nabla\beta)}_{\in\mathcal{O}(h^{\ell+1})} \left(R^{\nabla,c_s}\right)^{-1} R_{c_s,v_{\ell+2}} \\
&= \int_{m_i} \underbrace{\left(R_{v_0,c_s} R^{\nabla,c_s} - R_{v_0,c_{m_i}} R^{\nabla,c_{m_i}}\right)}_{\in\mathcal{O}(h^2)} (d^\nabla\beta)\left(R^{\nabla,c_s}\right)^{-1} R_{c_s,v_{\ell+2}} \\
&\quad + \int_{m_i} R_{v_0,c_{m_i}} R^{\nabla,c_{m_i}} \underbrace{(d^\nabla\beta)}_{\in\mathcal{O}(h^{\ell+1})} \underbrace{\left(\left(R^{\nabla,c_s}\right)^{-1} R_{c_s,v_{\ell+2}} - \left(R^{\nabla,c_{m_i}}\right)^{-1} R_{c_{m_i},v_{\ell+2}}\right)}_{\in\mathcal{O}(h^2)} \\
&= \mathcal{O}(h^{\ell+3})
\end{aligned}$$

Furthermore note that for the face m_0 it holds

$$\begin{aligned}
&R_{v_0,c_{m_0}} \int_{m_0} R^{\nabla,c_{m_0}}\left(d^\nabla\beta\right)(R^{\nabla,c_{m_0}})^{-1} R_{c_{m_0},v_{\ell+2}} \\
&- R_{v_0,v_1} R_{v_1,c_{m_0}} \int_{m_0} R^{\nabla,c_{m_0}}\left(d^\nabla\beta\right)(R^{\nabla,c_{m_0}})^{-1} R_{c_{m_0},v_{\ell+2}} \\
&= \int_{m_0} \underbrace{\left(R_{v_0,c_{m_0}} - R_{v_0,v_1} R_{v_1,c_{m_0}}\right)}_{\in\mathcal{O}(h^2)} R^{\nabla,c_{m_0}}\left(d^\nabla\beta\right)(R^{\nabla,c_{m_0}})^{-1} R_{c_{m_0},v_{\ell+2}} \in \mathcal{O}(h^{\ell+3}).
\end{aligned}$$

In the same way, for the face $m_{\ell+2}$, we can show that

$$\begin{aligned}
&\int_{m_{\ell+2}} R^{\nabla,c_{m_{\ell+2}}}\left(d^\nabla\beta\right)(R^{\nabla,c_{m_{\ell+2}}})^{-1} R_{c_{m_{\ell+2}},v_{\ell+2}} \\
&- \int_{m_{\ell+2}} R^{\nabla,c_{m_{\ell+2}}}\left(d^\nabla\beta\right)(R^{\nabla,c_{m_{\ell+2}}})^{-1} R_{c_{m_{\ell+2}},v_{\ell+1}} R_{v_{\ell+1},v_{\ell+2}} \in \mathcal{O}(h^{\ell+3})
\end{aligned}$$

Thus, using the previous theorem, we obtain

$$
\begin{aligned}
&R_{v_0,c_s}\int_s (d^\nabla d^\nabla \beta)^{\nabla,c_s,c_s} R_{c_s,v_{\ell+2}} \\
&= \sum_{i=0}^{\ell+2} R_{v_0,c_s}\int_{m_i} (d^\nabla \beta)^{\nabla,c_s,c_s} R_{c_s,v_{\ell+2}} + \mathcal{O}(h^{\ell+4}) \\
&= \sum_{i=0}^{\ell+2} R_{v_0,c_{m_i}}\int_{m_i} R^{\nabla,c_{m_i}}\left(d^\nabla \beta\right)(R^{\nabla,c_{m_i}})^{-1} R_{c_{m_i},v_{\ell+2}} + \mathcal{O}(h^{\ell+3}) \\
&= R_{v_0,v_1}R_{v_1,c_{m_0}}\int_{m_0} R^{\nabla,c_{m_0}}\left(d^\nabla \beta\right)(R^{\nabla,c_{m_0}})^{-1} R_{c_{m_0},v_{\ell+2}} \\
&\quad + \sum_{i=1}^{\ell+1} R_{v_0,c_{m_i}}\int_{m_i} R^{\nabla,c_{m_i}}\left(d^\nabla \beta\right)(R^{\nabla,c_{m_i}})^{-1} R_{c_{m_i},v_{\ell+2}} \\
&\quad + R_{v_0,c_{m_{\ell+2}}}\int_{m_{\ell+2}} R^{\nabla,c_{m_{\ell+2}}}\left(d^\nabla \beta\right)(R^{\nabla,c_{m_{\ell+2}}})^{-1} R_{c_{m_{\ell+2}},v_{\ell+1}} R_{v_{\ell+1},v_{\ell+2}} + \mathcal{O}(h^{\ell+3}) \\
&= R_{v_0,v_1}\boldsymbol{d}^{\boldsymbol{\nabla}}\boldsymbol{\beta}(\sigma_0,v_1,v_{\ell+2}) + \sum_{i=1}^{\ell+1}(-1)^i \boldsymbol{d}^{\boldsymbol{\nabla}}\boldsymbol{\beta}(\sigma_i,v_0,v_{\ell+2}) \\
&\quad + (-1)^{\ell+2}\boldsymbol{d}^{\boldsymbol{\nabla}}\boldsymbol{\beta}(\sigma_{\ell+2},v_0,v_{\ell+1})R_{v_{\ell+1},v_{\ell+2}} + \mathcal{O}(h^{\ell+3}) \\
&= \mathfrak{d}^{\boldsymbol{\nabla}}\boldsymbol{d}^{\boldsymbol{\nabla}}\boldsymbol{\beta}(\sigma,v_0,v_{\ell+1}) + \mathcal{O}(h^{\ell+3})
\end{aligned}
$$

Since the alternation operator does not decrease the order of accuracy, this yields the claim. Note that as in the vector valued case, we cannot expect that a novel alternation operator would yield a better order of accuracy then $\mathcal{O}(h^{\ell+3})$. □

ECOLE DOCTORALE

Titre : Discrétisation d'Opérateurs Différentielles basée sur la Géometrie

Mots clés : calcul extérieur discret ; fibrés vectoriels ; connexions discrètes ; torsion ; courbure ; géométrie computationnelle

Résumé : Le calcul extérieur discret (DEC) fournit un cadre structure-préservant pour la discrétisation des formes différentielles, en conservant au niveau combinatoire des identités fondamentales telles que $d^2 = 0$ et le théorème de Stokes. Toutefois, le DEC classique se limite aux formes à valeurs scalaires, alors que de nombreuses théories géométriques et physiques reposent sur des formes à valeurs dans un fibré vectoriel muni d'une connexion.
Cette thèse étend le DEC au cadre des fibrés vectoriels. Dans une première partie, nous étudions les connexions sur les surfaces simpliciales et proposons une version discrète modifiée de la connexion de Levi-Civita, ainsi qu'une représentation discrète de la torsion. En exploitant les isomorphismes spécifiques à la dimension deux entre 2-formes à valeurs tangentes, champs de vecteurs et 1-formes scalaires, nous développons une approche cohérente pour analyser torsion et courbure sur maillage, avec des applications en conception de champs de directions et en traitement géométrique.
La seconde partie introduit un cadre général pour les formes différentielles discrètes à valeurs dans un fibré. Nous formalisons une notion d'intégration adaptée aux formes fibrées à l'aide des connexions et des rétractions, ce qui permet d'induire des cochaînes discrètes à partir de formes lisses. Nous définissons ensuite une dérivée extérieure covariante discrète convergente sous raffinement du maillage, établissons la compatibilité de la courbure discrète avec la courbure lisse, et montrons que les identités de Bianchi sont satisfaites exactement au niveau combinatoire.

Title : Geometry Driven Discretization of Differential Operators

Keywords : discrete exterior calculus; vector bundles; discrete connections; torsion; curvature; geometric computation

Abstract : Discrete Exterior Calculus (DEC) provides a structure-preserving framework for discretizing differential forms while maintaining fundamental identities such as $d^2 = 0$ and Stokes' theorem at the combinatorial level. However, classical DEC is restricted to scalar-valued forms, whereas many fundamental geometric and physical theories rely on differential forms valued in vector bundles equipped with a connection.
This thesis extends DEC to the setting of vector bundles. In the first part, we study connections on simplicial surfaces and introduce a modified discrete Levi-Civita connection together with a discrete representation of torsion. Exploiting the dimension-two isomorphisms between tangent-valued 2-forms, vector fields, and scalar 1-forms, we develop a coherent framework to analyze torsion and curvature on meshes, with applications to direction field design and geometric processing.
The second part develops a general framework for discrete bundle-valued differential forms. We formalize an integration procedure adapted to bundle-valued forms using connections and retractions, allowing discrete cochains to be induced directly from smooth forms. Based on this construction, we define a discrete covariant exterior derivative that converges under mesh refinement, establish compatibility between discrete and smooth curvature, and prove that the Bianchi identities hold exactly at the combinatorial level.

Institut Polytechnique de Paris
91120 Palaiseau, France